Facies and sequence stratigraphic implications of the Statfjord formation (upper triassic-lower Jurassic), northern north sea, UK

Khaeri Segayer Tawengi

FACIES AND SEQUENCE STRATIGRAPHIC IMPLICATIONS OF THE STATFJORD FORMATION (UPPER TRIASSIC-LOWER JURASSIC), NORTHERN NORTH SEA, UK

By
Khaeri Segayer A. Tawengi
A thesis submitted to the University of Durham in the fulfillment of the requirement of Master of Science

Department of Geological Sciences, University of Durham

DECLARATION

This is to certify that this work is submitted for the degree of master of science under the title of 'Facies and sequence stratigraphic implications of the Statfjord Formation (Upper Triassic-Lower Jurassic), northern North Sea, UK' is the result of original work of the author. No quotation from this thesis should be published without prior permission. No part of it has been accepted in substance for any other degree and is not currently being submitted in candidature for any other degree.

Candidate:.....

Khaeri S. Tawengi

Director of research:.....

Dr. Brian R. Turner

ACKNOWLEDGMENTS

Thanks be to Allah (God Almighty), the Creator, the Wise, for his guidance, blessing and mercy.

My deepest gratitude goes to my supervisor Dr. Brian R. Turner who with his open thoughtful mind and endless patience has helped me throughout the period of the research with his comments and valuable suggestions. Thanks are also due to all the staff, postgraduates and secretaries at the Geology Department. Their assistance and support are gratefully acknowledged.

Thanks are also extended to Dr. A. Messallati, head of the Exploration Department, Agip Oil Company, Libya, for his efforts and valuable advice. Special thanks are due to the staff at the training department of Agip Oil Company and Al-Jawaby Oil Services Company for their efforts and sponsorship.

I am particularly grateful to Shell Oil Company, UK, for granting permission to use the data which forms the basis of this study.

I am also grateful to my parents and my wife for the encouragement, patience and sympathy which I received throughout the period of study.

CONTENTS

LIST OF FIGURES

Chapter 4

LIST OF TABLES

Page

LIST OF APPENDICES

ABSTRACT

Detailed sedimentological logging of core, and interpretation of wireline logs from the Brent Oil Field, northern North Sea, have allowed for the identification of sedimentary facies and environments of the Upper Triassic-Lower Jurassic Statfjord Formation.

The Statfjord Formation is interpreted to have been deposited within a diversity of sedimentary environments. These include delta plain, meandering rivers, braided rivers, tidally influenced fluvial systems and a shallow, high energy transgressive marine environment.

Within the fluvially-dominated part, which is by far the most important volumetrically, two distinct facies associations were recognized: channel and overbank. The channel facies association is in turn divided into three discrete end members: low sinuosity, high sinuosity and minor/crevasse channel facies. Similarly, the overbank facies association comprises a variety of sedimentary facies including levee, crevasse splay, swamp, flood plain and rare lacustrine and lacustrine deltas.

Low sinuosity channel facies are divided on the basis of their architectural style, into three different types. Type 1 low sinuosity channel facies dominates the northern part of the study area and resembles the sandy Platte River model of Miall (1977). Type 2 low sinuosity channel facies dominates the southern part of the study area and is characterized by numerous internal scour surfaces. This channel type is interpreted to have been deposited within a relatively proximal braided river system. Type 3 low sinuosity channel facies is a transitional facies between the proceeding two low sinuosity channel types and is similar in character to the South Saskatchewan and the Battery Point River models of Cant and Walker (1978). Documented point bar sediments within the high sinuosity channel facies association indicate that channel bankfull depths may have reached as much as 4.5 m. The lack of evidence of exposure of the in-channel sediments in addition to the thick, consistent bedforms suggest that the rivers were probably of a perennial nature. Palaeoflow indicators obtained form HDT log analysis reveal that the Statfjord Formation in the Brent Field has been deposited by a north to northwest flowing drainage systems.

Thorium/potassium cross-plots from NGS logs indicate an upward reduction in sandstone mineralogical maturity which may imply an upward reduction in the degree of reworking of sediments and a least sediment transport. The overall spatial and temporal consistency of the palaeocurrent indicators coupled with the upward decrease of sandstone maturity further indicate that no flow reversal occurred throughout the geological evolution of the Statfjord Formation.

Sequence stratigraphic concepts applied in conjunction with detailed facies analysis indicate that sedimentary facies of the Statfjord Formation are arranged within two successive depositional sequences. Although the sequences are incomplete they possess all the attributes of the depositional sequences described by Posamentier and Vail (1988) and Van Wagoner *et al.* (1990). The lower sequence comprises sediments deposited within a highstand systems tract. The lowermost part is characterised by low net/gross ratio and is interpreted to have been deposited within early highstand systems tract most likely in an upper delta plain setting. As the rate of additional subaerial accommodation space approaches zero during a stillstand and eventually reverses, high sinuosity rivers are thought to have migrated laterally during a late highstand combing the previously deposited fine-grained sediments. The upper sequence overlies a regional sequence boundary unconformity and comprises an early lowstand wedge systems tract which is characterised by braided river sediments deposited during a slightly rising base level. As the rate of additional subaerial accommodation space increases isolated high sinuosity river sediments are interpreted to have been deposited during a late lowstand wedge systems tract. Cyclic rhythmites reflecting neap-spring-neap tidal cyclicity of a diurnal palaeotidal regime represent the first 'local' major marine flooding. These are probably equivalent to a condensed section in the coeval marine realm and mark the onset of a transgressive systems tract. Continued marine transgression is documented by the deposition of the overlying high energy, transgressive marine sandstone which is probably separated from the underlying tidally influenced strata by the occurrence of a ravinement surface indicating a progressively landward migrating shore line.

In considering the relative tectonic quiescence of the area during the deposition of the formation which occurred during a post-rift thermal subsidence phase, the close link between variations in the stacking patterns of facies tracts and the eustatic curve reveal that the stratigraphy and deposition of the Statfjord Formation were largely controlled by processes of sea level fluctuations in a near-shore setting.

Chapter 1

Introduction and geological history of the northern North Sea Basin

1.1 Aim of thesis

The Statfjord Formation in SHELL's Brent Oil Field, northern North Sea, comprises an Upper Triassic-Lower Jurassic fluvial and shallow transgressive marine system. During the appraisal and field development, the reservoir sandstones and associated sediments were extensively cored. This provides an ideal opportunity for studying the sedimentology and stratigraphy from within a mainly fluvial hydrocarbon-bearing depositional system.

The main objective of part 1 of this thesis is to review the depositional history of the study area and the previous sedimentological work on the Statfjord Formation. Part 2 investigates individual depositional facies and associated environments based on core data. Part 3 provides a comprehensive analysis of the depositional facies and environments, based on sedimentological interpretation of well-log data, augmented by sandstone petrography interpreted from available wireline logs. Part 4 considers the effects of base level change on depositional patterns and facies architecture, and integrates the facies and sedimentary environments into a comprehensive sequence stratigraphically based depositional model.

1.2 Data sources

The database for this thesis comprises core material, including core photographs from three deviated, partially-cored wells (Wells BA/22, BD/36, and BD/44). Cored intervals and angles of deviation of these wells are illustrated in Fig. 1.1.

A complete set of conventional wireline logs including gamma-ray, sonic, neutron and density logs for wells 3/4-11, BA/22, 211/29-6, BC/16, BD/41, BD/44, BD/36, BD/03 and 24-1 were selected along the axis of the field Fig. 1.4. The NGS log (Natural Gamma-Ray Spectrometry) of well BD/44 in addition to the HDT log (High Resolution Dipmeter Tool) of well 211/29-6 were also taken for interpretation of

sandstone petrography and palaeoflow pattern investigation. Shell depth data are given in feet, in accordance with standard oil company practice. Thus, all depths referred to in this study, unless otherwise stated, are given in feet.

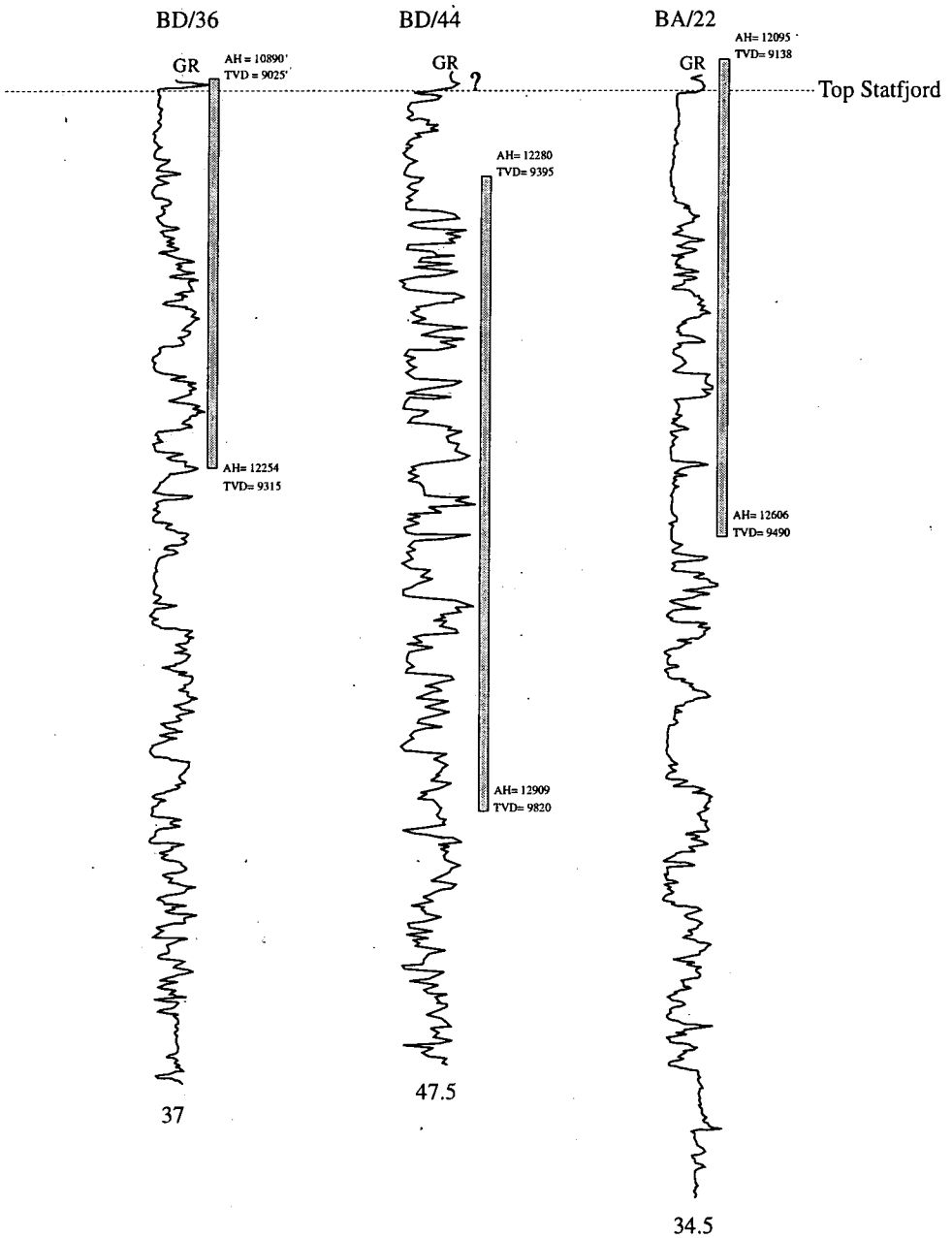

Fig. 1.1 Relative position of cored intervals in each study well. The number below each log is the well deviation angle.

1.3 Location and Background information

The Brent Oil Field is located in the extreme northern part of the UK sector of the North Sea, about 140 Km northeast of the Shetland Isles, and some 5-10 Km west of the median line between the UK and Norwegian sectors, slightly north of latitude 61° (Fig. 1.2). It lies in Shell/Esso licence block 211/29. In terms of the regional tectonic picture, it is centrally situated in the northern, wider part of the Viking Graben/East Shetland Basin. The field, which was first discovered in July 1971 and declared commercial in the following year (Bowen, 1975), is the first and largest discovery of hydrocarbon accumulations in the northern North Sea (Johnson and Krol, 1984). There are two main reservoirs in the Brent Province, one of Middle Jurassic age and the other of Late Triassic to Early Jurassic age separated by Liassic shales and siltstones. The Statfjord Formation, which is the focus of this study, is buried between 3.5 to 3.7 Km in the wells studied in the Brent Field. A gross reservoir thickness of 473 m is found on the crestal parts of the structure described below. The original reserves of the field are estimated to be in order of 2×10^9 bbls of oil, and some 10^{12} scf of associated gas. The Middle Jurassic Brent reservoir contains approximately two-thirds of the total reserves. The Statfjord sandstone reservoir, because of the geometry of the field lies to the east of the Brent sandstone reservoir. The porosity of the Statfjord sandstone ranges from 10 to 26% with permeabilities up to 5500 md (Bowen, 1975).

1.4 Structure and trap development

The Brent Field is structurally simple, comprising a major fault-block dipping at about 7° to the west, with a relief of about 910 m above the structurally deeper area to the west, overlain unconformably by sealing shales (Fig. 1.3). The trap is of the combination structural/stratigraphic truncation type comprising a westerly tilted and partially eroded fault-block. A major eastward dipping fault, with a throw of many thousands of feet (Bowen, 1975), bounds the Brent block to the east (Fig. 1.4). Dip slip faulting is almost absent in the main part of the Brent structure, but is more common in the southerly plunging part of the structure, while a southeast-northwest trending normal faults occur in the saddle which separates the Brent from the Statfjord

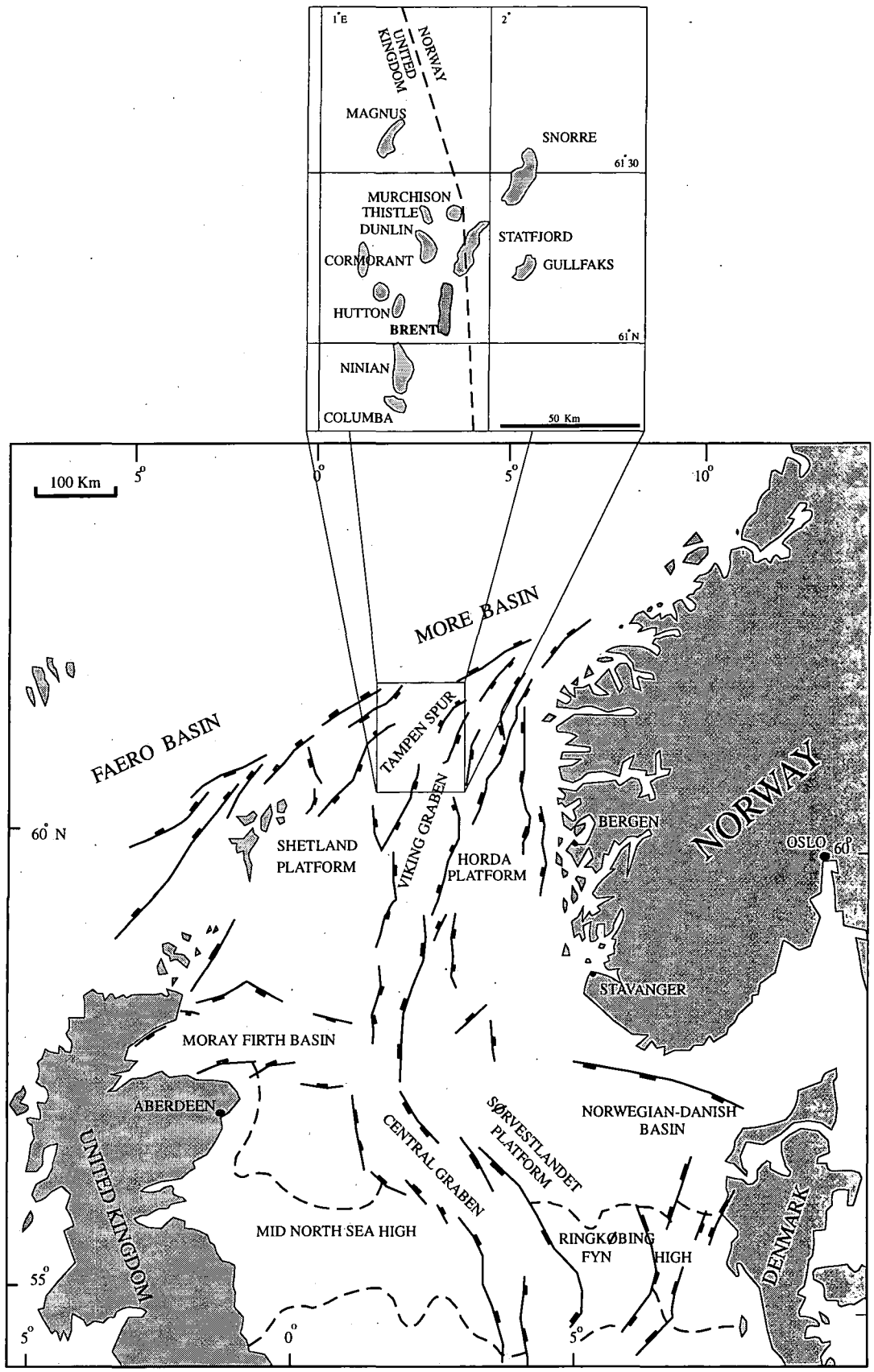

Fig. 1.2 Index map showing the location of the Brent Field in the North Sea, and the major tectonic elements. Modified after Høimyr *et al.* (1993).

structure to the northeast (Kirk, 1980). At the level of the Statfjord Formation the rectangular-shaped field outline is dip-closed to the west (Fig. 1.4). To the south, the closure is provided by the plunge of the structure as a whole, whereas to the north, the structure is closed by a north-northeasterly hading fault system (Bowen, 1975). The crestal part of the structure is partly eroded by a major late Jurassic unconformity (Johnson and Krol, 1984). To the west, the Statfjord sandstones are sealed by the Dunlin Formation, whilst to the east it is sealed by more than 1500 m of Lower Cretaceous and Tertiary sediments (Fig. 1.3). The trap is thought to have evolved as a result of a series of tilted and truncated fault-blocks which were established in the Late Triassic if not earlier. This continued during deposition of the Kimmeridge Clay, which was draped on the pre-existing, now drowned relief (Bowen, 1975). Movement between fault-blocks essentially ceased by Lower Cretaceous times after which basin subsidence became the major factor controlling sedimentation in the area (Kirk, 1980; Gibbs, 1990). The remaining relief was then engulfed by the onlap of flat-lying Lower Cretaceous clays and marls giving rise to the structural/stratigraphic combination trap type. The source of the oil reserves is thought to be the Kimmeridge Clay Formation (Fisher and Mudge, 1990; Richards, 1993). Oil generation, which is still in progress, probably commenced in the latest Cretaceous to Late Tertiary (Goff, 1983).

1.5 Geological setting and lithostratigraphy

The Stratigraphic nomenclature used in this study follows the scheme of Gabrielsen *et al.* (1990) and Richards (1993).

1.5.1 Basement

The Caledonian basement, which is overlain unconformably by Triassic sediments, is detected in many cases with uncertainty because of inadequate borehole penetration in the area (Gabrielsen *et al.* 1990). It consists, over most of the northern North Sea Basin, of high-grade metamorphic rocks and some deformed plutonic rocks of later igneous bodies (Johnson, 1993). Gabrielsen *et al.* (1990) claimed that the basement consisted of high-grade gneisses tentatively assigned to the late Palaeozoic, with a transitional unconformity into the overlying Triassic sediments being the most

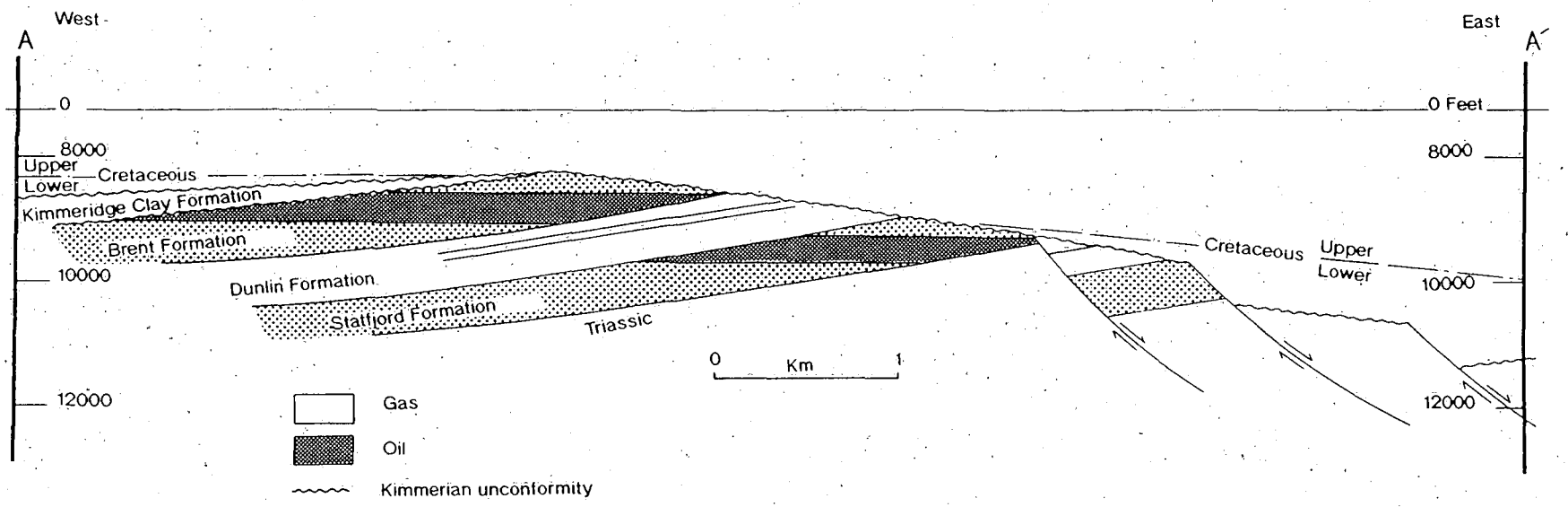

Fig. 1.3 Cross-section through the Brent Field. Modified from Bowen (1975). Line of section is illustrated in Fig. 1.4.

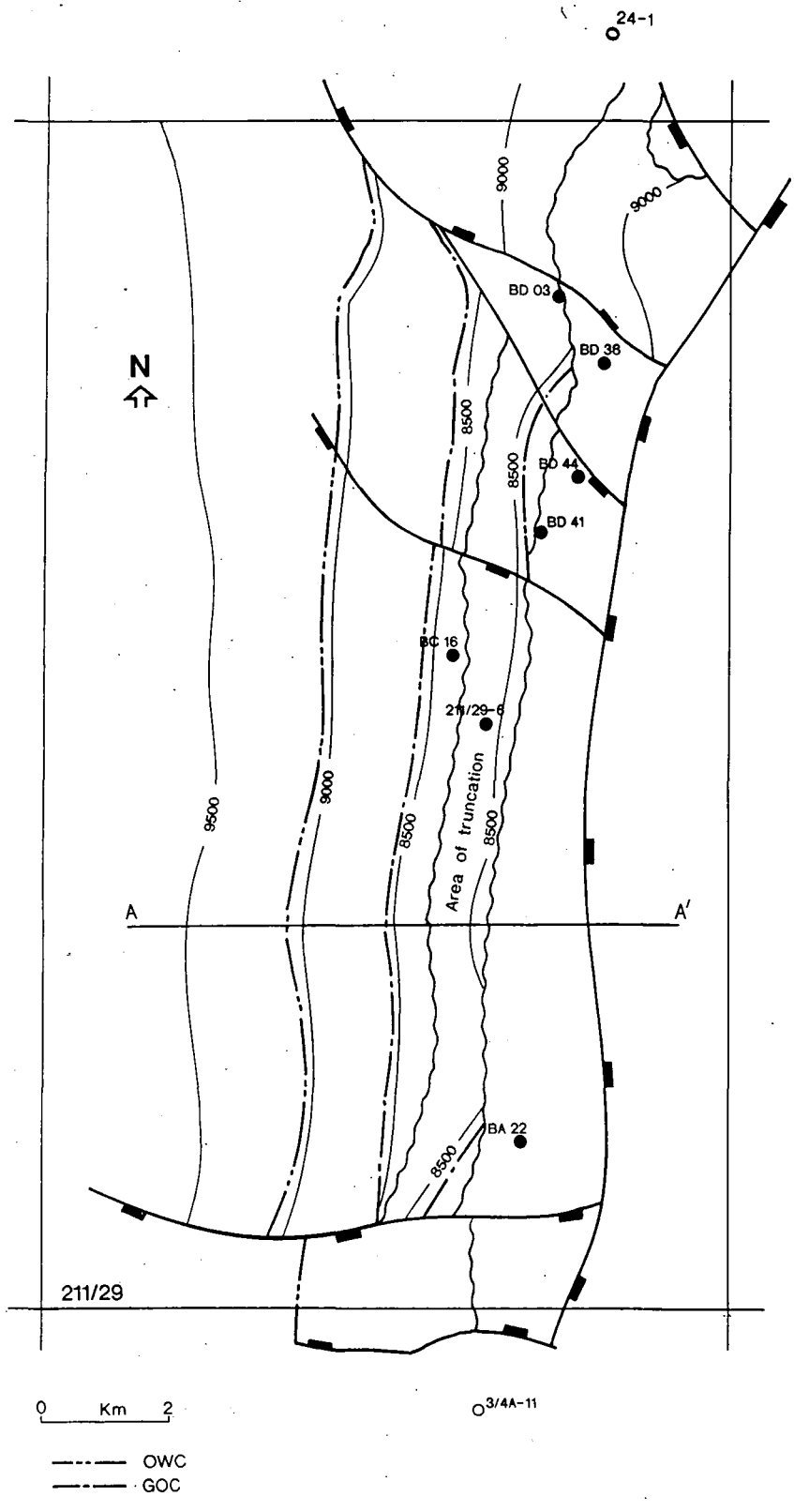

Fig. 1.4 Structural map of top Statfjord Formation in the Brent Oil Field showing location of wells used in this study. After Fisher and Mudge (1990). A-A` section is shown in Fig. 1.3 at a different scale.

prominent unconformity in the northern North Sea. In the Ninian Field (Fig. 1.2), a basement core recovered a dioritic gneiss with a minimum age determined by potassium-argon techniques, of 350 m.y. (Albright *et al.* 1980). It is thought that this dating may reflect a Late Palaeozoic tectonic overprinting, rather than the original age of emplacement of these rocks.

1.5.2 Hegre Group (Cormorant Formation)

The Cormorant Formation which conformably underlies the Statfjord Formation ranges in age from Scythian to Rhaetian (Gabrielsen *et al.* 1990). Deegan and Scull (1977) consider the Cormorant Formation to have been deposited in a continental setting. It comprises a sequence of alternating fine-grained, argillaceous, white to reddish brown sandstones and siltstones with some sandy claystones. The sandstones are usually poorly sorted with an argillaceous matrix (Fisher and Mudge, 1990). Vollset and Dore′ (1984) introduced the term "Hegre Group" for the Triassic sediments over much of the northern North Sea Region (Fig. 1.5) in an attempt to unify the Norwegian and UK Triassic and Jurassic nomenclature. According to Vollset and Dore′ (1984) the Teist Formation at the base of the Triassic succession is composed of interbedded fine to coarse-grained, reddish-brown fluvial sediments with gray to red lacustrine claystones. The overlying Lomvi Formation consists of fine to coarse-grained kaolinitic sandstones with subordinate red marls and claystones. The Lunde Formation at the top of the sequence comprises interbedded, white, pink or gray, fine to coarse-grained fluvial sandstones, with reddish brown lacustrine/flood plain mudstones, siltstones and shales with some caliche deposits (Richards, 1993). Because of the paucity of palynomorphs within the sequence it is difficult to subdivide the sequence on the basis of biostratigraphy (Richards, 1993). Lervik *et al.* (1989) showed that palynomorphs from the Teist, Lomvi and Lunde Formations suggest Scythian to Landinian ages, with the greater part of the Lunde Formation containing palynomorphs of Late Triassic age. Fisher and Mudge (1990) suggested that the palynological evidence indicates a Late Norian to Early Rhaetian age for a relatively widespread argillaceous horizon near the top of the Cormorant Formation, and a Rhaetian age for the higher beds.

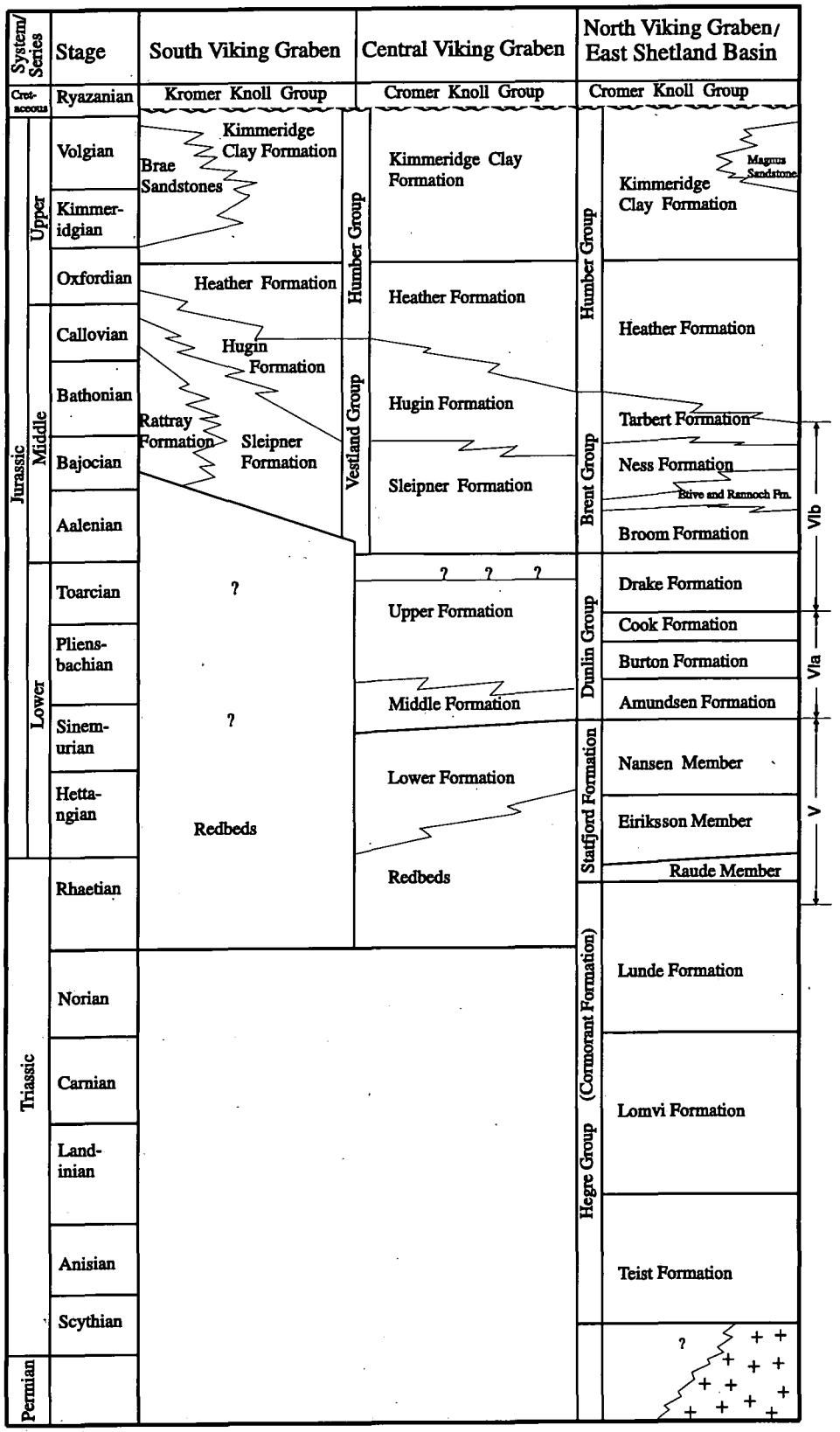

Fig. 1.5 Summary of Triassic-Jurassic lithostratigraphy of the northern North Sea. Modified from Richards (1993) and Gabrielsen *et al.* (1990).

1.5.3 Statfjord Formation

The Statfjord Formation forms the uppermost part of a 2-Km-thick continental rift and post rift basin-fill sequence (Hegre Group and Statfjord Formation) (Steel and Ryseth, 1990). Deposition of the Statfjord Formation occurred mostly within a fluvial environment throughout much of the north Viking Graben, between the East Shetland Platform to the west and the Horda Platform to the east (MacDonald and Halland, 1993). The Statfjord Formation ranges in age from Rhaetian to Sinemurian, spanning the transitional boundary between Triassic and Jurassic strata (Bowen, 1975; Deegan and Scull, 1977; Gabrielsen *et al.* 1990; Ziegler, 1990; Richards, 1993). Regionally, it appears to unconformably overlie or onlap Triassic sediments (Kirk, 1980).

The Statfjord Formation has been regarded as sequence "V" (Fig. 1.5) according to the classification of Gabrielsen *et al.* (1990), which also includes a shaly/silty unit below the Statfjord Formation. This is regarded as the uppermost part of the underlying Lunde Formation (Upper Cormorant Formation) in some classifications, or as the Raude Member of the Statfjord Formation in others (Deegan and Scull, 1977; Vollset and Doré, 1984) (Fig. 1.5). Further details about previous sedimentological studies of the Statfjord Formation will be introduced later in this chapter.

1.5.4 Dunlin Group

The conformably overlying Dunlin Group shales (Fig. 1.5) were deposited under open marine conditions during Sinemurian times (Ziegler, 1990). The subdivision of the Dunlin Group into four formations is based on the silt/sand ratio and log character (Kirk, 1980). The base of the Dunlin Group is normally conformable, but shows disconformity to the west, whilst the contact with the overlying Brent Group shows local disconformity (Deegan and Scull, 1977). The Amundsen, Burton and Cook Formations are regarded as part of the sequence "VIa" (Fig. 1.5) in the classification depicted by Gabrielsen *et al.* (1990). This is thought to be some 200 to 300 m thick on the eastern edge of the Viking Graben and the Horda Platform. It consists mainly of alternating shaly and sandy units, interpreted as representing mainly off-shore and prograding shelf conditions formed during periods of basin subsidence or eustatic sea-level rise (Gabrielsen *et al.* 1990). The Drake Formation forms the lower part of the

overlying sequence "VIb" (Fig. 1.5) which also includes the overlying Brent Group. In the shale-dominated Drake Formation, there occurs a number of basin margin attached sandstones indicating basin subsidence or eustatic sea-level fall (Gabrielsen *et al.* 1990)

1.5.5 Brent Group

The overlying Brent Group is the primary oil reservoir in the northern North Sea (Kirk, 1980). It represents sediments deposited within a fluvio-deltaic environments (Bowen, 1975) with sediment supply from a source area to the south from the basin margin. According to Deegan and Scull (1977), the lower part of the Brent Group is of fluvial origin while the upper part is deltaic dominated.

1.5.6 Humber Group

The overlying Humber Group includes both the Middle to Upper Jurassic Heather Formation and the Upper Jurassic Kimmeridge Clay Formation. Increasing sea-level rise/increased subsidence rate are interpreted to have led to a southward retreat of the Brent Group deltaic system and deposition of the Heather Formation Shales (Gabrielsen *et al.* 1990). These shallow marine deposits normally unconformably overlie Brent Sandstones, with a lithology consisting primarily of gray to dark gray silty claystone and shales (Kirk, 1980).

Syndepositional fault-block rotation and gradual basin filling are interpreted as the main factors controlling distribution and progressive onlap of the organically-rich, Upper Jurassic Kimmeridge Clay Formation (Kirk, 1980).

1.5.7 Cromer Knoll Group

The Lower Cretaceous Cromer Knoll sediments onlap and/or thin over older topographic highs. This unit is primarily represented by a basal, shallow marine, time-transgressive, white to gray argillaceous limestone (Kirk, 1980).

1.6 Review of previous sedimentological work

Although the Statfjord Formation is an important reservoir unit in the northern North Sea, and it contributes significantly to the hydrocarbon production in fields such as the Brent, Snorre, Statfjord and Gullfaks (Fig. 1.2), relatively little is known about its sedimentology in the UK sector (Purvis, 1995). This reflects the fact that the Triassic-Early Jurassic succession of the northern North Sea received relatively little attention largely because of the poor resolution of available seismic data, the apparently monotonous non-marine succession and poor biostratigraphic control (Steel and Ryseth, 1990).

The Statfjord Formation was first named by Bowen (1975), namely in the Brent Province in well 211/29-1. Kirk (1980) indicated that the base of the Statfjord Formation appears to be conformable with the underlying Triassic sediments, whereas in the western and northwestern parts of the basin it seems to unconformably overly or onlap Triassic sediments where only the thin upper calcareous member is present (Fig. 1.6). Kirk (1980) described the sediments of the Statfjord Formation as predominantly gray, and in part reddish-coloured shales, claystones, and siltstones interbeded with thin sands at the base, which tend to coarsen upward into thicker, cleaner, more massive sandstones in the upper section. These upper sandstones are white to gray, fine to very coarse and conglomeratic. Mineralogically, the sandstones are feldspathic to arkosic and contain both a kaolinitic matrix and calcite cement. The uppermost part may represent a shallow marine environment, as suggested by occasional glauconite and marine fossils. The base of the formation according to Kirk (1980) is difficult to determine due to the paucity of fauna and flora, and poor correlation because of non-diagnostic lithological changes. Chauvin and Valachi (1980) described the depositional environment of the Raude Member (lower Statfjord Formation) as floodplain with some meandering stream channels. However, Rϕe and Steel (1985) suggested that the fine-grained units of the Raude Member represent coastal plain rather than overbank deposits. The age of the Raude Member according to Rϕe and Steel (1985) is generally accepted as Rhaetian, most probably late Rhaetian, but the paucity of diagnostic palynofloras does not allow accurate dating of the upper member boundary.

In the Brent Field, the Statfjord Formation was classified by Johnson and Krol (1984)

as comprising two major facies associations, each with its distinctive sedimentological properties. The first facies is a transgressive shallow marine sandstone, comprising sheet-like sand-bodies. The sandstone is well-sorted, mainly coarse-grained and locally pebbly, predominantly massive to weakly stratified. The second facies comprises fluvial sandstones and shales, making up the bulk of the formation, and it comprises four main genetic bodies: (a) active fluvial channel fills containing mainly coarse-grained to pebbly sandstones, dominated internally by horizontal to low angle stratification; (b) inactive channel fills; (c) floodplain sheet sandstones; and (d) floodplain shales.

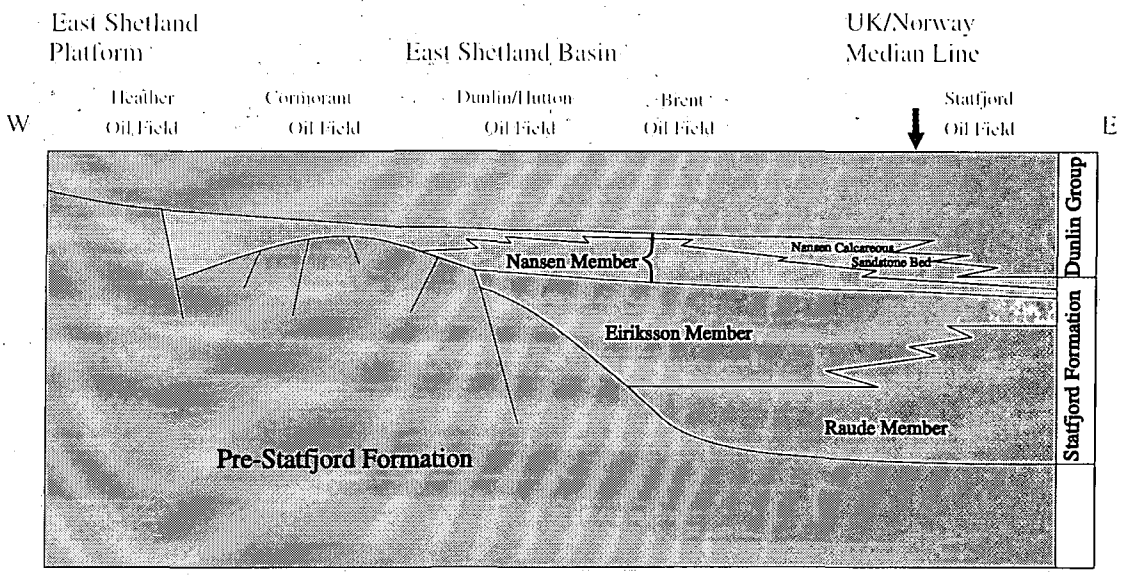

Fig. 1.6 Schematic cross-section through the East Shetland Basin, illustrating the distribution of the subdivisions of the Statfjord Formation. Modified from Richards (1993).

According to Johnson and Krol (1984) the channel sand bodies occur in three main geometric packages: (1) single channels (3-8 m thick); (2) moderately multistory channels comprising 2-6 stacked channels either coalesced or separated by inactive channel fills; and (3) strongly multistory channels comprising numerous stacked channels 24-40 m thick without significant intervening shales.

Fisher and Mudge (1990) indicated that the transition from the underlying fluvially-dominated Cormorant Formation to the Statfjord Formation is marked by an upward

coarsening succession of variegated gray, green and red shales interbedded with thin siltstones, sandstones and dolomites which is the Raude Member. They added that the continental pattern of deposition of the formation was established from the south, while the Statfjord Formation slowly onlapped from the north with pronounced diachroneity. Brown (1990) described the Statfjord Formation in the Viking Graben/East Shetland Basin as the oldest Jurassic deposits. He considered the Statfjord Formation at the type section in the Statfjord Field (Fig. 1.2), as recording a transition from non-marine to marginal marine conditions, with a sequence of floodplain, sinuous stream, braided stream, and coastal plain sediments at the top. The Statfjord sands which were thought to have been derived from the Fenno-Scandian Shield, the Scottish Highs and the Shetland Platform, represent continental sedimentation in the subsiding Viking Graben during Rhaetian to Hettangian times (Ziegler, 1990).

Purvis (1995) postulated that deposition of the Statfjord Formation was initiated after early Rhaetian tectonic activity elevated many of the major source areas around the North Sea Basin. It comprises a variety of fluvial sediments deposited in a semi-arid environment, followed by a high energy marine transgressive sandstone of the Nansen Member.

Gabrielsen *et al.* (1990) described the Raude member as being deposited within lacustrine, floodbasin, and local brackish lagoonal environments. They further reported that the sandstones of the Statfjord Formation were deposited by braided streams and by shoreline process in the uppermost part.

In the Statfjord Field, within the Norwegian sector, the sedimentology of the Statfjord Formation has been studied by MacDonald and Halland (1993). They noticed that the lower part of the sequence was characterized by a well-developed trend of upward increasing sandstone. Isolated fluvial channel sandstones embedded in a mudstone matrix occur towards the base, whereas the upper part has interstratified amalgamated fluvial channel sandstones and mudstones. An upward reduction in caliche formation and reddening of the mudstone throughout the Statfjord Formation was attributed by MacDonald and Halland (1993) to climatic changes from semi-arid during the Triassic to more humid during the Jurassic which may have resulted in floodplain areas becoming gradually less well-drained and more vegetated than during deposition of the

formation. The change may also be partly related to the encroaching early Jurassic transgression, which caused a regional change in the general depositional setting from well-drained alluvial plain to low-lying swamp nearer to the coastline characterised by a high water-table, abundant vegetation and reducing conditions.

Høimyr *et al.* (1993) studied the Statfjord Formation in the Snorre Field of the Norwegian sector where the formation attains a thickness of 85-105 m, and comprises an upward-coarsening and thickening sequence interpreted to be of braided stream origin. They postulated that the dominance of trough cross-bedding, moderate to poor sorting, coarse-grain size and the stacked multistory character of the sandbodies are characteristic elements of sandy braided river systems.

1.7 Structural framework

The north-northeasterly trending Viking Graben and the East Shetland Basin (Fig. 1.7) are potentially the most important structural elements of the northern North Sea. They are predominantly Mesozoic structural features, and contain upto 11000 m of Triassic to Quaternary sediments (Johnson, 1993; Hospers and Ediriweera, 1991 and Fig. 1.8).

The 500 Km long, narrow Viking Graben straddles the median line between the UK and Norwegian sectors of the northern North Sea. It is defined as an asymmetric structure with a well defined graben floor, which is delineated by systems of rotational or non-rotational normal faults (Ziegler, 1982; Gabrielsen *et al.* 1990). The East Shetland Platform with Tertiary strata resting directly on Devonian Redbeds (Brown, 1990) lies to the west of the central and southern parts of the Viking Graben. In the north, the axis of the Viking Graben swings north-northeast to south-southwest, separated from the edge of the East Shetland Platform by the development of an intermediate area of Mesozoic sedimentation termed the East Shetland Basin (Brown, 1990). To the east the Viking Graben is bounded by the partially fault-bounded Utsira High, Bergen High and the Horda Platform. In the extreme south the Viking Graben terminates in a structurally complex region at its intersection with the Central Graben, Moray Firth and the Ling Graben.

The Viking Graben has a general asymmetric, half-graben geometry, with thicker

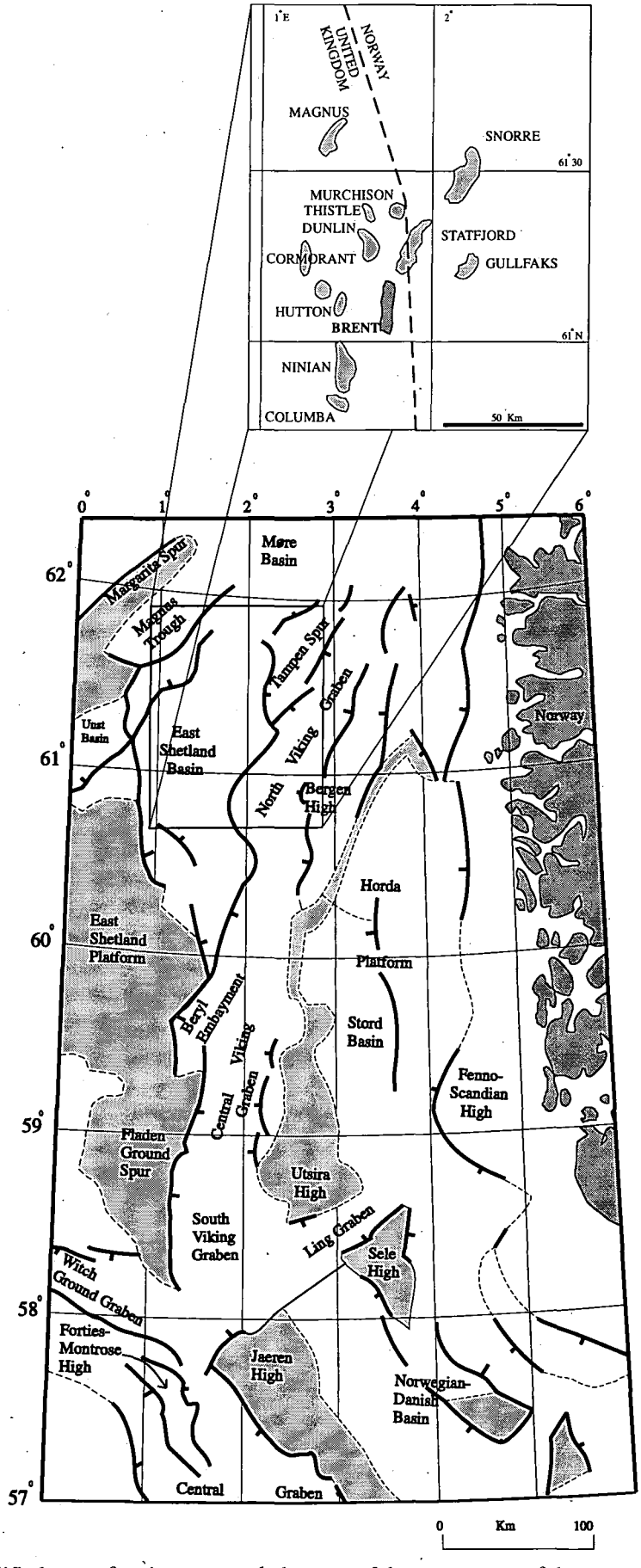

Fig. 1.7 Simplified map of major structural elements of the eastern part of the northern North Sea and surrounding areas. Modified from Johnson (1993).

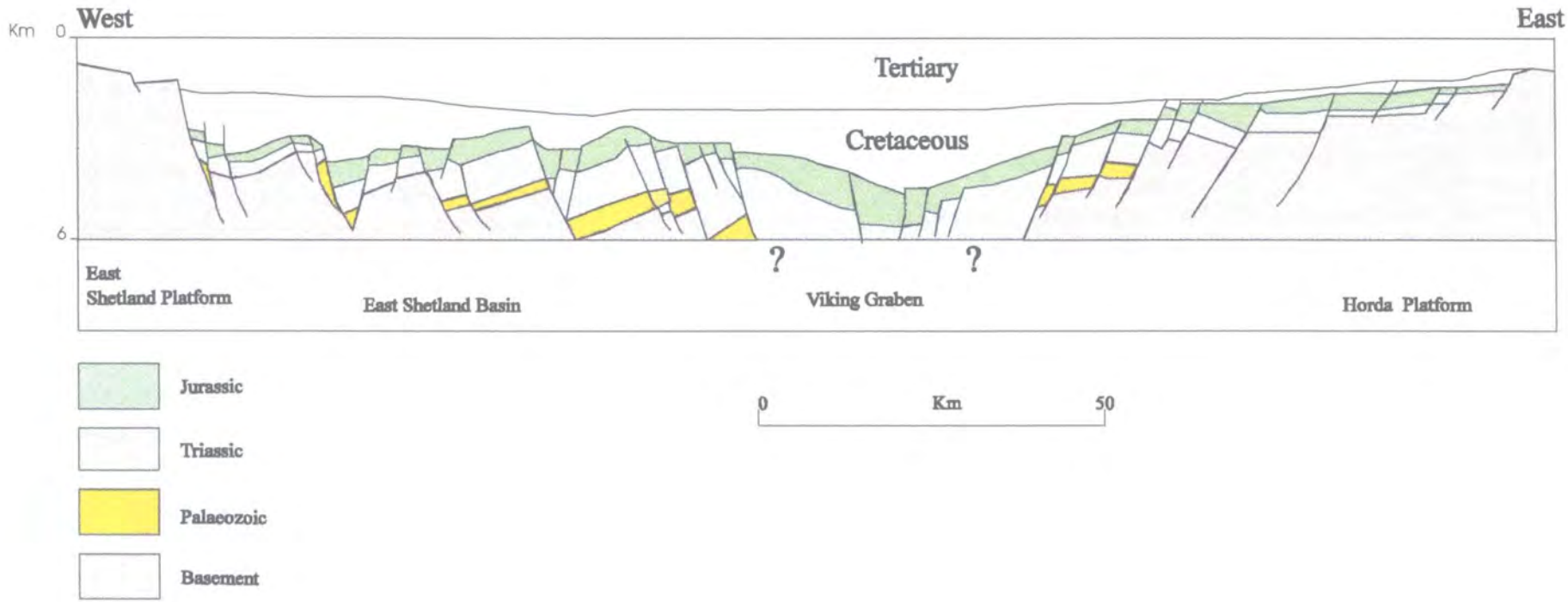

Fig. 1.8 Geological sketch section across the northern North Sea. Modified from Fisher and Mudge (1990).

sediments and larger faults developed along its western margin. Most of the Viking Graben lies within the Norwegian sector, and at about 60° 30′ it is offset to the north-west by a major fault forming a structural nose (Fig. 1.7). From about 60° 50′ the Graben margin trends north-northeastwards into the Norwegian sector where it is bounded by the Tampen Spur. The later element is a structural high consisting of a series of large, rotated fault-blocks (Høimyr *et al.* 1993).

The East Shetland Basin, containing a series of tilted fault-blocks, is characterized by two prominent and economically important, subparallel, north-trending structural blocks, whereas north-easterly trending faults are mainly developed in the northern part (Johnson, 1993). The area of the East Shetland Basin to the south is structurally simple, being dominated by a north-south or north-northeast to south-southwest trend, with most faults down throwing to the east, and blocks dipping to the west (Brown, 1990).

1.8 Structural development of the Viking Graben/East Shetland Basin

Between the Late Paleozoic to Cainozoic, North Sea tectonism has been divided into several discrete phases, namely Devonian-Carboniferous, Permo-Triassic, Middle-Late Jurassic and Late Cretaceous-Early Tertiary. The Devonian-Carboniferous part is not well understood mainly due to lack of data (Gabrielsen *et al.* 1990). However, the exact timing for the tectonic events in the northern North Sea is obscured in such a temporarily variable multiple rift system.

Devonian sedimentary basins containing over 5000 m of continental Old Red Sandstone developed following the Caledonian orogeny, and extended from the Moray Firth to the eastern coast of Norway (Johnson, 1993). During the Carboniferous the northern North Sea Basin was an area of non-deposition and erosion (Ziegler, 1982). Regional studies suggest that during Carboniferous to Early Permian times north-west Europe was transected by a postorogenic system of conjugate shears which reactivated older basement, and that regional uplift in the North Sea at this time was accompanied by erosion of Carboniferous and Devonian fault controlled sediments (Johnson, 1993). Early Permian subsidence formed the broad east-west trending north and south Permian Basins (Glennie, 1990).

Although the age of rift initiation is much debated (Johnson, 1993), the northerly-trending Viking and Central Grabens in the northern North Sea are dominantly Mesozoic structures. Ziegler (1990) claimed that Mesozoic rift activity in the North Sea commenced during the earliest Triassic, intensified during the Middle Jurassic-early Cretaceous and ceased during the Palaeocene. The Viking Graben/East Shetland Basin makes up part of this Mesozoic rift system. In the Viking Graben the first stage of rifting is tentatively dated as Permian-Triassic, but because the rocks have not been penetrated by sufficient wells data is sparce and timing is poorly dated (Scott and Rosendahl, 1989). Overall, it appears that during the Late Permian rifting propagated from the Norwegian-Greenland Sea area southward into the Faero-Rockall Trough and that the northern and southern basins continued to subside in response to thermal contraction of the lithosphere and loading by water and sediments (Ziegler, 1990). Rift-induced subsidence in the Viking Graben appears to have reached a maximum during Late Jurassic and Early Cretaceous when up to 3000 m of marine sediments accumulated in the Graben, following which a substantial decrease in the amount of fault-controlled subsidence of the Northern North Sea occurred (Johnson, 1993).

The mechanism by which continental lithosphere is thinned to produce sedimentary basins, however, has been a matter of debate. Early models of the North Sea rift system suggest that there had been a mantle plume-generated uplift centered on the middle Jurassic basaltic volcanic pile that lies at the intersection of the Viking Graben, Moray Firth Basin and the Central Graben (Johnson, 1993). These rifts were regarded as failed arms of a triple junction (Ziegler, 1975). Another model proposed by McKenzie (1978) include the uniform stretching and thinning of the lithosphere causing an isostatically driven fault-controlled subsidence of the crust accommodated by fault block rotation. However, Ziegler (1990) supported the later pure shear and stretching model. In general, these models have in common a two-stage development, namely the crustal stretching and thermal subsidence stages (Mckenzie, 1978).

It is found that during active stretching stages sand was more locally deposited because of topographic trapping, and the distribution of sandbodies was independent of the local drainage pattern. During stages of thermal cooling, the actual basin was more extensive and basin floor topography less pronounced which tends to cause more widespread sand distribution, except for periods of relatively rapid thermal subsidence.

Under these conditions the basin was mud-dominated, with sands restricted to the basin margin area and to lensoid tracts in the basin (Gabrielsen *et al.* 1990).

Ziegler (1988) postulated that by earliest Triassic times, north-west and central Europe as a whole were subjected to regional tensional stresses causing the differential subsidence of a complex set of multi-directional grabens such as the Central and the Viking Grabens. Major erosion of the Lower Jurassic and older sequences in the Central North Sea is thus attributed to the structural relief of the early extensive rift dome at the confluence of the grabens (Johnson, 1993). In the early Triassic there is evidence of movement along fault zones. Although the Rotliegendes continental redbed sedimentary sequences are considered to be pre-rift, Scott and Rosendahl (1989) showed that diverging early Triassic reflectors in many areas indicate that tectonic activity was active in at least the later stages of deposition. Stratigraphic evidence indicates that during the Earliest Triassic, differential subsidence of the Viking Graben took place, with evidence that the Viking Graben clearly cross-cuts the Caledonian basement trends.

Rifting activity continued throughout Triassic times into the Jurassic with little evidence for discrete rifting pulses (Ziegler, 1990). During the Rhaetian and Hettangian open marine conditions were established in the southern and south-central North Sea, whereas continental sandstones (Statfjord Sands) accumulated in the subsiding Viking Graben/East Shetland Basin and in the Horda Platform (Ziegler, 1990). During the Sinemurian the Arctic and Tethys Seas linked up via the Viking Graben and the Horda Basin as evidenced by deposition of the marine shales of the Dunlin Group. Evidence for continued Middle Jurassic crustal stretching across the North Sea rift system is provided by the subsidence pattern of individual fault-blocks in the northern Viking Graben (Brown *et al.* 1987).

Lower to Middle Jurassic sequences in the East Shetland Basin are generally interpreted to have been deposited during a time of relative tectonic quiescence, which is related to a thermal subsidence phase following a ? Permo-Triassic rifting episode (Badley *et al.* 1988). This has also been supported by Scott and Rosendahl (1989) who indicated that during the Early to Middle Jurassic, thermal subsidence dominated basin tectonics which is documented in deposition of the Dunlin and Brent sedimentary groups with an overall thickening of both sequences. However, Steel and Ryseth

(1990) insisted that there are clear signs of intrabasinal tectonics during the Rhaetian to Sinemurian stage of basinal post-rift history.

The northern Viking Graben which continued to subside during the Late-Middle Jurassic (Aalian to Bathonian), coincided with uplift of the Central North Sea which resulted in the development of major sandstone reservoirs in the Viking Graben (Ziegler, 1990). Badley *et al.* (1988) recognized two stages of Late Jurassic rifting represented by the Heather Formation (Lower Bathonian to Lower Kimmeridgian) and the Kimmeridge Clay Formation (Kimmeridgian to Ryazanian). Gibbs (1990) postulated that towards the end of the Jurassic, marked rift-controlled sedimentation ceased and the basin broadened markedly as thermal subsidence took over as the dominant process. At the end of the late Jurassic to earliest Cretaceous rifting episode, most of the Viking Graben was probably submerged (Johnson, 1993). Badley *et al.* (1988) showed that only crests of major fault-blocks such as the Brent structure may have been emergent, after which the rift topography became progressively infilled to produced a broadly asymmetric, westerly thickening wedge of Cretaceous deposits. In the Northern Viking Graben, substantial subsidence continued throughout the Lower to Middle Cretaceous along the western boundary fault of the Viking Graben rather than on the Shetland Terrace (Gibbs, 1990). Ziegler (1990) claimed that rifting activity abated during the Cretaceous and ended in the earliest Eocene, with the total rifting span of the North Sea covering a period of 175 m.y.

The Mesozoic North Sea thus forms an integral part of the Arctic-North Atlantic mega-rift system (Ziegler, 1990). Gibbs (1990) showed that regional maps of the North Sea rift system clearly show that the Viking Graben is bounded by continuous fault-zones along both margins forming part of the major tectonic lineament system of northwest Europe. The North Sea rift formed a more or less continuously subsiding basin throughout the Triassic and Jurassic (Gibbs, 1990).

The palaeogeographic picture proposed by Gabrielsen *et al.* (1990) (Fig. 1.9) suggests that the northern Viking Graben was dominated by alluvial fans, lakes, ephemeral streams and terminal flood basin environments during the Scythian to Hettangian. From Hettangian to Sinemurian times alluvial fans, through-flowing river systems with an encroaching low-energy shoreline were the dominant depositional

environments, following which shallow marine, basin margin-attached sands were deposited which include the Nansen Member of the Statfjord Formation.

A combination of extensional faulting, uplift and tilting of individual horst blocks, erosional truncation or non-deposition and subsidence in the Viking Graben/East Shetland Basin led to the formation of the prolific oil and gas fields in the northern North Sea (Gibbs, 1990). During the Permo-Triassic and Early Jurassic, sediments up to 4000 to 6000 m thick accumulated along the eastern bounding faults of the Viking Graben as opposed to 500 to 1500 m on the western side of the graben (Scott and Rosendahl, 1989).

Paleocene to Early Eocene thermal uplift of areas bordering the Rockall-Faero-West Shetland Trough gave rise to the accumulation of deeper water fan deposits in the Viking and Central Grabens (Ziegler, 1990).

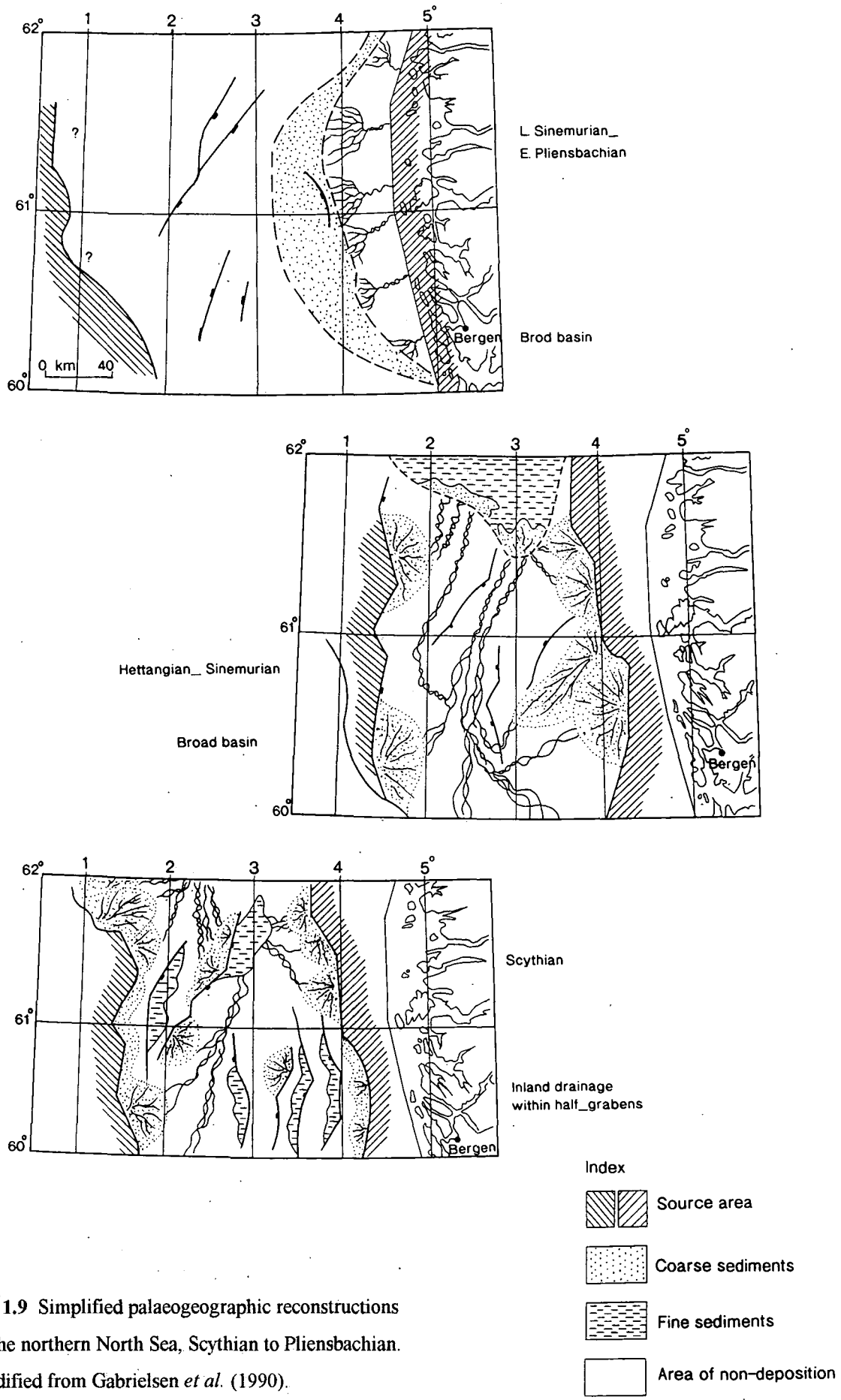

Fig. 1.9 Simplified palaeogeographic reconstructions in the northern North Sea, Scythian to Pliensbachian. Modified from Gabrielsen *et al.* (1990).

Chapter 2

Sedimentary facies analysis from conventional core

2.1 Introduction

Based on conventional core data, two distinct fluvial facies associations have been identified within the Statfjord Formation. These facies associations have been interpreted in terms of channel and overbank/floodbasin geometry and the mode of channel migration. However, in some instances facies identification is ambiguous because of the lack of two-dimensional data and palaeoflow indicators, a problem compounded by the similarity of these facies within a fluvial environment of deposition.

In this chapter a basic facies interpretation has been made in order to reconstruct the processes responsible for their deposition and distribution which may serve later as a basis for devoloping depositional models.

2.2 Hierarchy of bounding surfaces

A hierarchy of stratal bounding surfaces, based on the numerical ordering of Allen (1983) and Miall (1988a, b) (Fig. 2.1) have been recognised in this study. A first order bounding surface is described as a surface representing cross-bed set boundaries, with little or no apparent erosion. These resemble the first order surfaces introduced by Allen (1983) and Miall (1988a) claimed that these first order surfaces are very prominent in cores.

Second order surfaces are those marked by a significant change in lithofacies (Miall, 1988a, b) and indicate variation in flow conditions and direction with no significant erosion break.

Third and fourth order bounding surfaces are characterised by significant erosional breaks and are normally marked by a lag breccia above and mud drape below indicating change in flow stage (Miall, 1988a, b). Hence, both are erosional markers

cutting into the underlying lower rank surfaces and consequently sometimes they are difficult to differentiate in core. However, third order surfaces normally suggest reactivation with no apparent variation in lithofacies above and below (Miall, 1988a), whereas fourth order surfaces indicate basal scour surfaces of minor channels such as chute channels.

Fifth order surfaces are somewhat easier to recognise in core in that they bound major segments such as channel fills (Miall, 1988a, b) and resemble Allen's (1983) third order surface. Sixth order surfaces are difficult to recognise (Miall, 1988a) as they indicate the boundaries of meander belt deposits or palaeovalley fills.

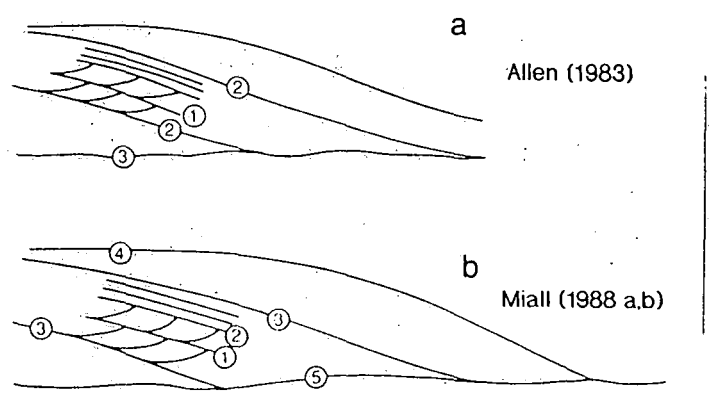

Fig. 2.1 Numerical ordering of stratal bounding surfaces, (a) classification of Allen (1983) and (b) hierarchy of stratal bounding surfaces modified from Miall (1988a, b). In Miall's classification, fifth and sixth order surfaces are amalgamated.

2.3 Channel facies association

Within this facies association, two channel facies were recognised on the basis of their facies architecture, textural attributes and pedogenic and biogenic characteristics. These attributes enable the channels to be assigned to low sinuosity and high sinuosity channel types, broadly corresponding to what Jackson (1978) referred to as braided and meandering.

2.3.1 Low sinuosity channel facies

Three types of low sinuosity channel facies have been identified in the study area, as described below.

2.3.1.1 Type 1 low sinuosity channel facies

Description: This facies type is represented by the cored interval from 12490 ft to 12457 ft in well BD/44 (Appendix 1). and is reproduced in detail in Fig. 2.2a. The facies typically commences with an irregular scour surface cutting into the underlying dark grey mudstone. This scour surface is overlain by a conglomeratic unit consisting of well-rounded pebble size quartzitic clasts up 2 cm in diameter associated with intraformational mudstone rip-up clasts 1 to 2 cm long set in a very coarse-grained sandstone matrix. The basal part of the facies consists of brown, poorly sorted very coarse-grained sandstone with crude horizontal stratification marked by variation in both sediment colour and grain size, overlain by high angle (25° ±) tabular cross-bedding in sets 20 to 30 cm thick. The horizontally stratified and high angle tabular cross-bedded sandstone is represented by unit A from 12490 ft to 12469 ft. A similar very coarse-grained sandstone with low angle (10° ±) tabular cross-bedding (Unit B from 12469 ft to 12457 ft) gradationally overlies unit A. The low angle tabular cross-bedding of unit B sometimes displays tangential lower boundaries and shows an overall upward reduction in set thickness (from about 20 to 10 cm), changing in the uppermost part into light grey, ripple cross-laminated fine-grained sandstone. The sequence is capped by a 3 m thick brownish-grey mudstone (Unit C) containing abundant coalified plant roots and debris.

Interpretation: The sequence described above resembles the sandy braided Platte River facies model of Miall (1977) (Fig. 2.3), where tabular cross-bedding is the most common stratification type laid down probably by straight to slightly sinuous-crested transverse tabular bars (Cant and Walker, 1976, 1978; Cant, 1992).

These channel bars are thought to have had relatively low amplitudes judging by the preserved thickness of the tabular cross-bedded sets, which must be a minimum value because of the effects of erosion. These bars correspond to Miall's (1988b)

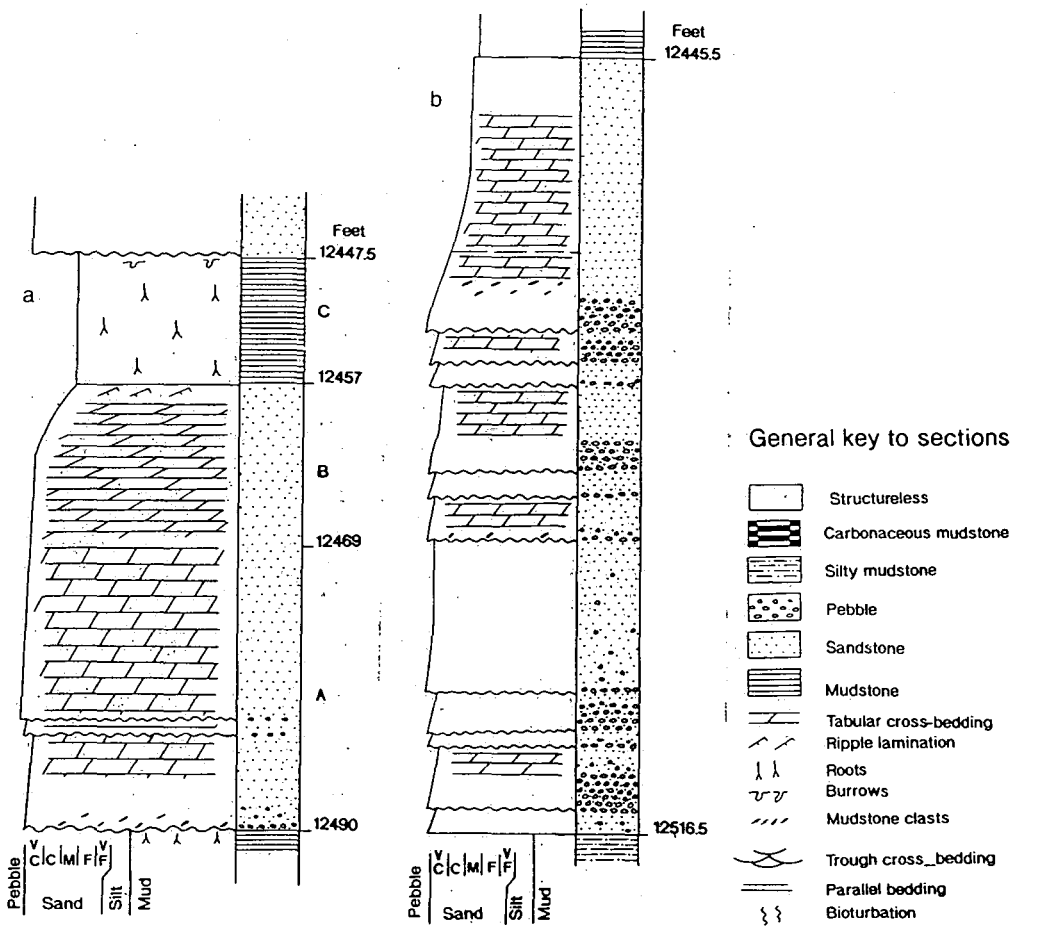

Fig. 2.2 a. Detail of section between 12490 ft and 12447.5 ft in well BD/44 representing type 1 low sinuosity channel facies of Platte River type and the overlying flood plain deposits. b. Detail of section from 12516.5 ft to 12445.5 ft in well BA/22 representing type 2 low sinuosity channel facies of Donjek River type.

macroforms who suggested that they are comparable in height to the depth of the channel in which they formed. The sequence is interpreted to result from lateral and vertical accretion of a bedload-dominated low sinuosity stream, characterised by wide, shallow channels floored by straight to slightly sinuous-crested bars of the transverse type. Bridge (1985) claimed that rivers which transport a large proportion of bed load relative to suspended load tend to have a relatively low sinuosity. Furthermore, the uniformity of sedimentary structures through several metres of this facies type,

without significant internal erosion surfaces, may indicate that the channel was perennial and not subjected to extreme variations in flow discharge (Davies *et al.* 1993).

The basal scour surface and the associated clasts are interpreted as a channel lag deposit. The rounded, resistant nature of the clasts suggests that they were transported under relatively high energy conditions (Rust and Jones, 1987). The associated mudstone rip-up clasts can be interpreted to have been either derived from flood plain or channel banks and bar tops, and may reflect significant incision of the channel. The horizontal stratification in the lower part of the channel fill is interpreted to be a result of upper flow regime conditions and the development of plane beds (Singh and Bhardwaj, 1991). The low angle tabular cross-stratification higher in the section (Unit B) is interpreted to have resulted from downstream accretion of transverse type bars or DA elements of Miall (1988b). The ripple-laminated, fine-grained sandstone at the top of the unit records falling water stage and decelerating flows over the shallowly submerged bar top. The overlying mudstone is interpreted as flood plain sediment deposited following channel shifting and abandonment, possibly in response to a major flood event.

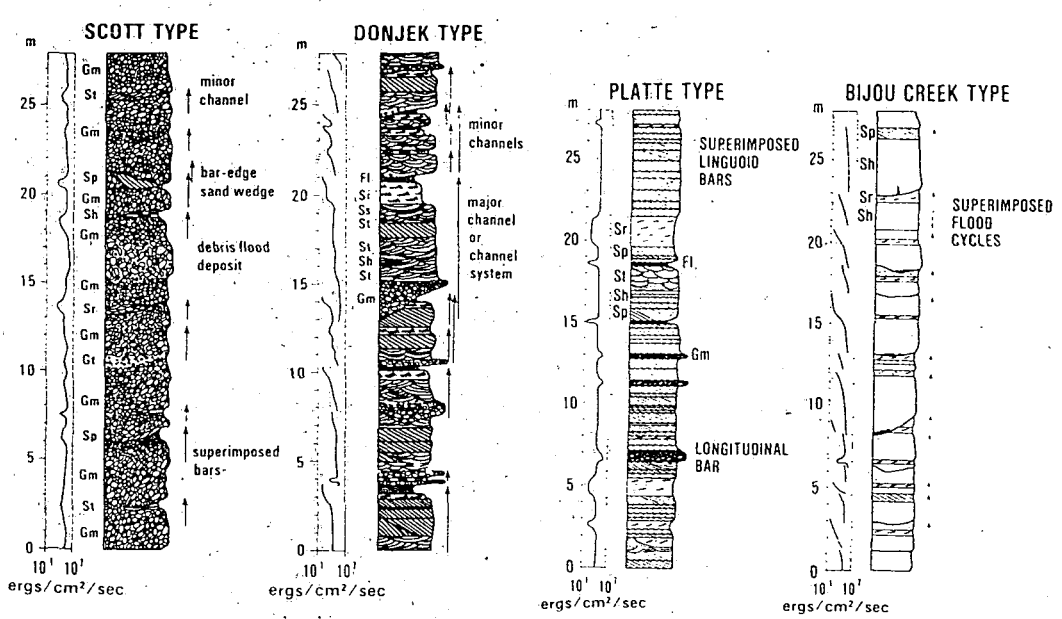

Fig. 2.3 Four generalised braided river depositional profiles representing the four models of braided river systems related to the energy involved during deposition. (From Miall, 1977).

2.3.1.2 Type 2 low sinuosity channel facies

Description: The thick interval from 12516.5 ft to 12445.5 ft (Fig. 2.2b) in the cored section of well BA/22 in the southern part of the field illustrates a good example of this low sinuosity channel type. The facies is lithologically similar throughout and it forms a discrete unit, part of which is illustrated in Appendix 2.

A crude cyclicity can be seen throughout the entire facies comprising several vertically stacked incomplete fining-upward cycles bounded by several prominent scour surfaces. Individual cycles vary in thickness and are composed of matrix-supported conglomerate overlain by very coarse-grained structureless or occasionally cross-bedded sandstone. The facies consists mainly of a matrix-supported conglomerate consisting of pebble size clasts (1 to 5 cm long) set within a very coarse-grained sandstone matrix. The clasts are typically poorly sorted, whitish-grey in colour and rounded to subrounded. Crude horizontal bedding is the dominant stratification type within the conglomerate which occasionally shows a poorly defined clast imbrication.

The sandstone above the conglomerate is dark brown in colour, poorly sorted and often displays flat bedding, medium to large-scale tabular cross-bedding; locally it appears structureless. Higher in the sequence a coarse-grained sandstone showing low angle (~10°) tabular cross-bedding, with sets averaging 10 cm thick, occurs. The stratification disappears at the top.

Interpretation: The sequence is interpreted to have been deposited by a mixed sand and gravel bedload dominated channel system. The abundant scour surfaces and paucity of *in situ* mudstone is consistent with a braided channel system (Rust and Jones, 1987), in which the prominent internal erosional surfaces at the base of fining-upward cycles represent scoured channel floors. Stacking of the cycles records shifting of channels characterised by dominant transverse channel bars (Cant, 1992; Davies *et al.* 1993).

The fining-upward cycles resemble those described by Cant (1992) in which each fining-upward cycle begins with horizontally stratified gravel which fines up into crudely cross-stratified gravelly sandstone. Hein and Walker (1977) emphasized that bar evolution and the development of stratification in gravelly braided streams is a result of the emplacement at maximum flow stages, of a diffuse gravel sheet with crude

horizontal stratification developed, in part, due to gravel clast imbrication. The cycles are commonly incomplete owing to their erosional truncation by the succeeding cycle. Mixed sand and gravel rivers, as described by Cant (1992), commonly develop some degree of vertical zonation but cyclicity is poorly developed because of erratically fluctuating discharge. The variation in cycle thickness may indicate migration of bedforms of variable size, or erosion prior to deposition of the succeeding cycle (Dawson and Bryant, 1987).

The overall textures, stratification, sand-shale ratio and internal erosional surfaces suggest a river system that was probably more proximal in location than type 1 channels. The high angle tabular cross-bedding which frequently appears at the top of some fining-upward cycles suggests a high ratio of bedload to suspension load and possibly a rate of aggradation which was relatively high compared to down stream slip face migration (Hein and Walker, 1977).

The low angle tabular cross-bedding higher in the sequence probably records straight-crested dune bedforms deposited close to the dune plane-bed transition possibly forming on top of a partially emergent sand flat complex (Cant and Walker, 1978; Røe, 1987).

Massive sandstone which frequently appears within the succession either above scour surfaces or within the cycles suggests rapid dumping of sediment at a rate too rapid to allow for sorting and traction currents. Turner and Monro (1987) attributed the lack of stratification to the rate of deposition and sediment concentration probably as a result of hyperconcentrated flood flows. They further considered that the presence of stratified strata within the same succession indicates that the structureless nature of sandstone is more likely to be related to the original depositional conditions rather than post depositional liquifaction.

2.3.1.3 Type 3 low sinuosity channel facies

Description: This channel facies, which is represented by the cored interval from 12532 ft to 12495.5 ft in well BD/44 (Appendix 3), is reproduced in detail in Fig. 2.4a. The section consists mainly of three lithological units. The basal unit A, from 12532 ft to 12520 ft, consists of an erosively-based, light brown to brown, very

coarse-grained pebbly sandstone overlying pale grey silty mudstone. The scour surface is overlain by a 20 cm thick extraformational matrix-supported conglomerate, containing poorly sorted, well rounded, pale grey quartzitic clasts from 1 to 2 cm long. Large-scale tabular cross-bedding is the dominant stratification type within unit A, with individual sets up to 1 m thick (Appendix 3 arrows). Internal, small local scour surfaces also occur within lower unit A which is sharply overlain by a light brown, very coarse-grained pebbly sandstone (Unit B from 12520 ft to 12502 ft). Unit B makes up most of the facies sequence and is characterised by small to medium-scale (10 to 20 cm) trough cross-bedding with pebble-size clasts defining the base of foresets. Unit C, from 12502 ft to 12495.5 ft, gradationally overlies unit B and consists predominantly of light brown, coarse-grained sandstone displaying disturbed and diffuse tabular cross-bedding, with set thickness varying from about 20 to 30 cm. The entire sequence is abruptly capped by a thick, dark grey, carbonaceous mottled mudstone.

Interpretation: The basal erosional surface and associated lag deposits at the bottom of the sequence record channel incision and initiation. The succeeding coarse, large-scale tabular cross-bedded sandstone (Unit A), characterised by solitary large sets up to 1 m thick, represents deposition as mid channel lingoid or transverse bars with downstream migrating slip faces (Miall, 1978). Cant (1992) has also attributed such deposits in a similar succession to large, flat-topped, oblique in-channel bars which probably formed where flow expands and velocity decreases such as at channel junctions. Unit B, which comprises trough cross-bedded sandstone is attributed to deposition by in-channel aggradation of migrating three-dimensional sinuous-crested dunes, probably within deeper parts of the channel (Cant, 1978). Thick successions of trough cross-bedded strata implies that cross-channel bars were probably inactive for prolonged periods of time during channel aggradation. Cosets of small to medium-scale tabular cross-bedding higher in the sequence (Unit C) are believed to represent a sand flat complex (Cant and Walker, 1978). The thin medium-grained parallel laminated sandstone in unit A and the dark grey, organic rich mudstone in unit B. may be the slumped banks of channel islands and adjacent flood plain deposits eroded during high river stages (Cant, 1978). This channel facies seems to be closely related in character to the Battery Point River facies model proposed by Cant and Walker

(1976) (Fig. 2.4b) which in turn resembles the South Saskatchewan channel type model of Cant and Walker (1978) and Cant (1978) (Fig. 2.4c). By analogy, Miall (1978) has termed deposits of this river type as sandy braided, characterised by cyclic deposits dominated by trough cross-bedding. It is recorded as an intermediate type between the proximal gravelly Donjek River and the non cyclic sandy braided Platte River models according to the classification adopted by Miall (1977). Cant (1992) suggested that the characteristics of the South Saskatchewan river system were steady discharge, high degree of topographic differentiation and in many instances sand flat accumulation. This type of river system commonly yields facies sequences similar to that produced by sand and gravel point bar deposits in high sinuosity systems, and consequently can be easily confused in vertical sequences. For this reason Cant (1978) highlighted criteria which may be helpful to distinguish these two closely related channel facies models. He emphasized that in low sinuosity channels tabular cross-bedding may develop at any level within the channel deposits. In contrast scroll bars always develop tabular cross-bed sets at the top of a point bar and are usually orientated in one direction relative to the main channel flow whereas cross-channel bars in low sinuosity system may show greater variability (Fig. 2.4b).

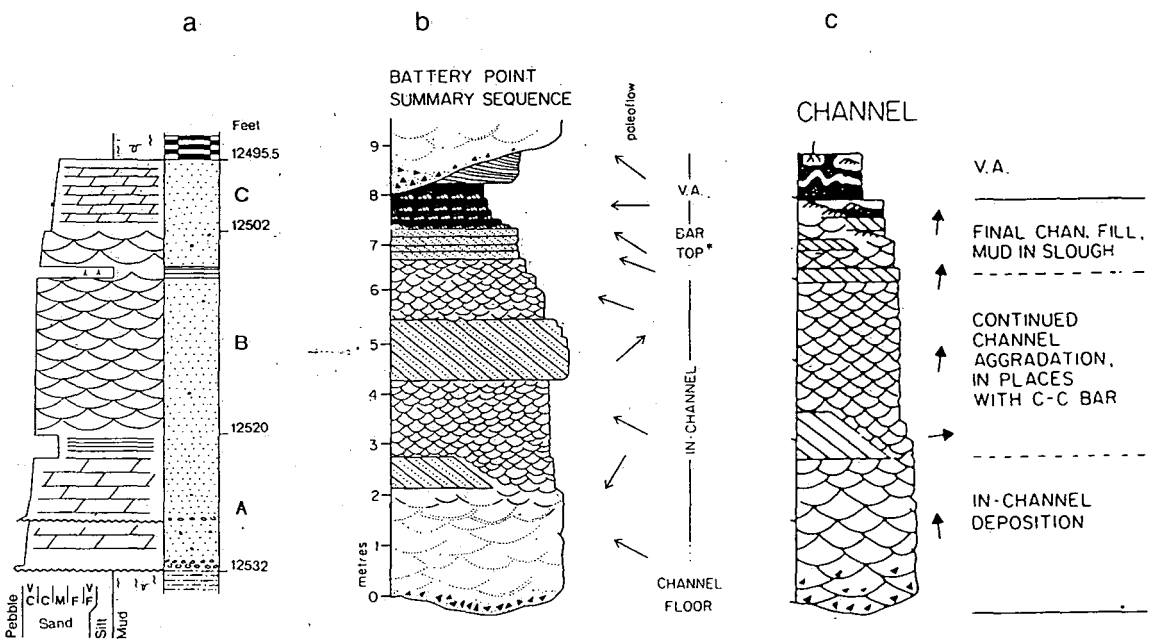

Fig. 2.4 a. Detail of section between 12532 ft and 12495.5 ft in well BD/44 illustrating type 3 low sinuosity channel facies. b. The Battery Point River type summary sequence Modified from Cant (1978). c. Channel sequence of the South Saskatchewan River type. After Cant (1992). See Fig. 2.2 for legend.

2.3.2 High sinuosity channel facies

Description: The sequence which represents this facies occurs in the cored interval between 12704.7 ft and 12674 ft in well BD/44 and is illustrated in Appendix 4. The sequence erosively overlies a thick, grey to dark grey mudstone package of poorly drained flood plain deposits. The scour surface is characterised by local variation in relief of up to 1 cm (Appendix 4 arrow). The scoured surface is followed by a 20 cm thick, internally scoured (Unit A from 12704.7 ft to 12703.9 ft), matrix supported conglomerate consisting of poorly imbricated, subrounded to rounded pebble-size clasts ranging from 1 to 2 cm long composed predominantly of grey to light grey quartzite and mudstone. The mudstone clasts are predominantly angular to subangular, and identical in composition to the underlying mudstone. Sharply overlying unit A is a thick sandstone package (Unit B from 12703.9 ft to 12685.5 ft) consisting of reddish-brown, moderately sorted, coarse to very coarse-grained pebbly sandstone. The pebbles are predominantly subrounded to rounded and composed of quartzite and mudstone. The quartzitic pebbles tend to concentrate at certain levels and may be up to 1 cm long. The sandstone is mainly structureless in the lower part of the unit with poorly defined large-scale trough cross-bedding, with individual sets up to 40 cm thick in the upper part. Gravel lags are sometimes present, possibly marking set boundaries, or concentrated along foresets. This trough cross-bedded sandstone grades upwards into poorly defined low angle tabular cross-bedding of uncertain set thickness. Frequent pebbly sandstone intervals are also present probably overlie randomly distributed local, scour surfaces. Very thin mudstone drapes can be seen within unit B marked by a slight variation in grain size (Appendix 4 arrows).

Unit B is sharply overlain by fine to very fine-grained, grey to light grey sandstone (Unit C from 12685.5 ft to 12682 ft), although the contact with Unit B is poorly preserved in the core section. Unit C is characterised by ripple cross-lamination in the lower part and lenses of light grey mudstone 2 to 3 mm thick, which are horizontally burrowed, in the upper part. This is in turn gradationally overlain by coarse-grained, brown to light brown sandstone (Unit D from 12682 ft to 12678.3 ft). The lower part of unit D displays small to medium-scale tabular cross-bedding in sets approximately 10 to 15 cm thick. The cross-bedding passes up into ripple cross-laminated, light grey argillaceous sandstone concomitant with an overall upward decrease in grain size.

A thin (< 5 cm thick) pebbly sandstone (Unit E from 12678.3 ft to 12678.2 ft) erosively overlies unit D. The erosion surface is characterized by a slight variation in its topographic relief (1 to 2 cm). Clasts concentrate along the scour surface and are subrounded to rounded, grey to light grey mudstone up to 1 cm in diameter. Unit E is sharply overlain by a fine-grained, reddish-brown structureless sandstone (Unit F from 12678.2 ft to 12674 ft) with occasional light grey thin mudstone layers.

The whole sequence lacks well preserved macroscopic biogenic and pedogenic features, apart from the possibly burrowed section in the upper part of unit C.

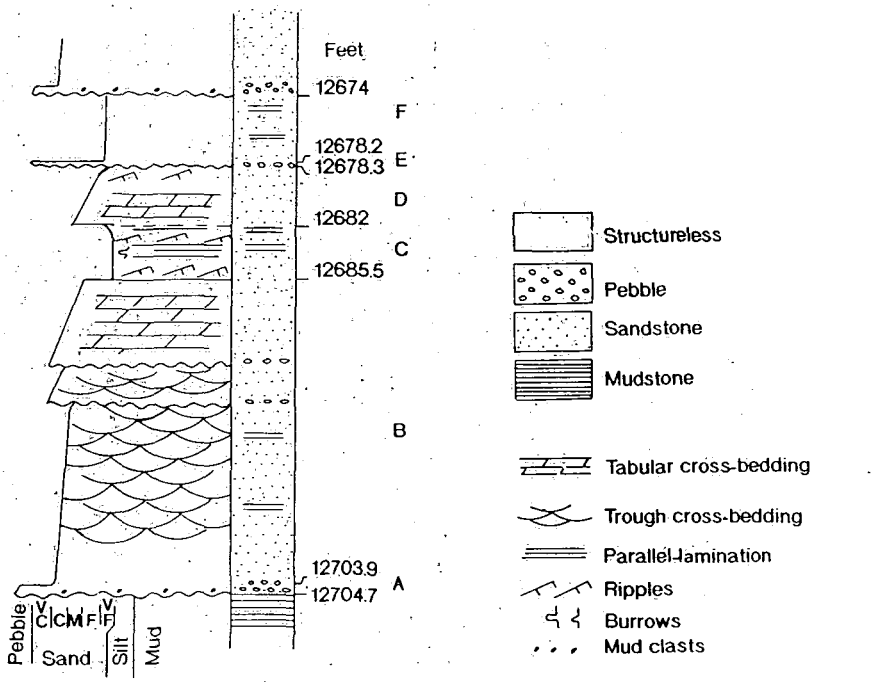

Fig. 2.5 Reproduced section of the cored interval from 12704.7 ft to 12674 ft in well BD/44 representing lateral accretion deposits in a high sinuosity channel, possibly associated with overbank deposits from 12678.2 ft to 12674 ft (See text for details).

Local evidence of synsedimentary faulting is confined to the trough cross-bedded sandstone unit. The entire sequence displays an upward overall decrease in grain size and cross-stratification set thickness together with the presence of flat bedding and ripple cross-lamination in the upper part. The sequence is terminated by an erosional surface at the base of the succeeding thick sandstone package.

Fig. 2.5 shows a detailed section for the interval between 12704.7 ft and 12674 ft in well DB/44.

Interpretation: For interpretive purposes this facies has been divided into four subfacies.

2.3.2.1 Channel lag subfacies

The basal conglomeratic unit (A) overlying the lower scour surface, is interpreted as a channel lag deposit produced by scouring of channel floor and banks (Collinson, 1991). This lag deposit represents the coarsest sediments transported by the channel during flood generated maximum velocities (Galloway, 1985). The mudstone clasts are interpreted to have been eroded from channel banks and floor as they have identical compositions to the underlying mudstone substrate. The angular shape of these clasts reflects the short distance of transport and the rapid rate of deposition with little reworking (Yinan *et al.* 1987).

2.3.2.2 Point bar subfacies

The two successive units B and C are interpreted as a point bar within the laterally migrating meander bend of a high sinuosity channel system. This interpretation is tentatively based on the fining-upward trend in the core associated with the overall upward decrease in scale of the cross-beds overlain at the top by rippled and wavy to parallel laminated sandstone representing decreasing depths and discharge (Friend, 1978; Collinson, 1991; Cant, 1992). The presence of trough cross-beds is interpreted to have originated from sand deposited as sinuous crested three-dimensional dunes (Bridge, 1993). Although trough cross-bedding is most common in point bars tabular cross-bedding may also form (Cant and Walker, 1978; Bridge, 1985). Kirschbaum and McCabe (1982) suggested that the lower point bar is commonly covered by sinuous crested dunes and upper parts are characterised most commonly by small-scale ripples. Walker and Cant (1984) suggested that during average discharge sinuous crested dunes are the dominant bedforms, and are preserved as trough cross-bedding.

The multiple scour surfaces within the lower sandy unit suggests cut and fill processes possibly resulting from fluctuating discharge (Warwick and Flores, 1987). Campbell and Hendry (1987) consider such scour surfaces to have originated during large floods when clasts were transported further down stream. These scour lags also

suggest complex histories of channel scour, fill and reactivation, and may indicate abrupt changes in river stage (Galloway, 1981). The apparent multistorey character is interpreted to be the result of superposition of different point bars within the meander belt as lateral migration and cut-off proceeded in concert with aggradation. In this case only the lower part of the point bar was preserved beneath the topmost part which was left intact (Gordon and Bridge, 1987). The fine mud drapes locally associated with the trough cross-bedded sandstone (Unit B Appendix 4 arrows) marked by contrasting grain size and intersected by minor syndepositional faults may indicate low stage flow and deposition on lateral accretion surfaces. Lateral accretion surfaces usually result from lateral point bar migration during flood events in a high sinuosity channel (Collinson, 1978, 1991). Bridge (1985) suggested that lateral accretion surfaces are usually highlighted by contrasting grain size due to deposition at different flow stages. However, this criteria is not essential for its recognition. The minor faults marking the trough cross-bedded unit may indicate penecontemporaneous soft sediments deformation process common to many point bars (Collinson, 1991) and are comparable to those induced in the sediments of a laterally migrating point bar in a tidal channel documented by Reineck and Singh (1980) (Fig. 2.6). Such small-scale features are reported to have been formed by movement and slumping of unconsolidated sediments of oversteeped slopes, and are characteristic of environments with rapid sedimentation rates (Potter and Pettijohn, 1977; Boggs, 1987). The tabular cross-bedded sandstone at the top of unit B may represent sand moving as straight crested dunes during lower flow velocities and depths (Collinson, 1978; Bridge, 1985). Local evidence of horizontal burrowing in the mud drapes of the upper unit C, may indicate modification of the upper point bar surface during periods of exposure (Galloway, 1985).

Point bar sediments can not exceed the bankfull depth of the palaeochannel (Miall, 1985a) Thus, bankfull depth can be estimated using the combined preserved thickness of unit B and C as follows:

(12703.9 ft - 12682 ft) = 21.9 ft apparent thickness (1)

True thickness of point bar is 21.9 ft $\times$ cos 47.5° = 14.8 ft (4.5 m) (2)

Where 47.5° is the well deviation angle.

Perennial flow is expected in this case as evidenced by the lack of desiccation and the absence of *in situ* plant remains in the lower parts of the point bar (Gordon and Bridge, 1987).

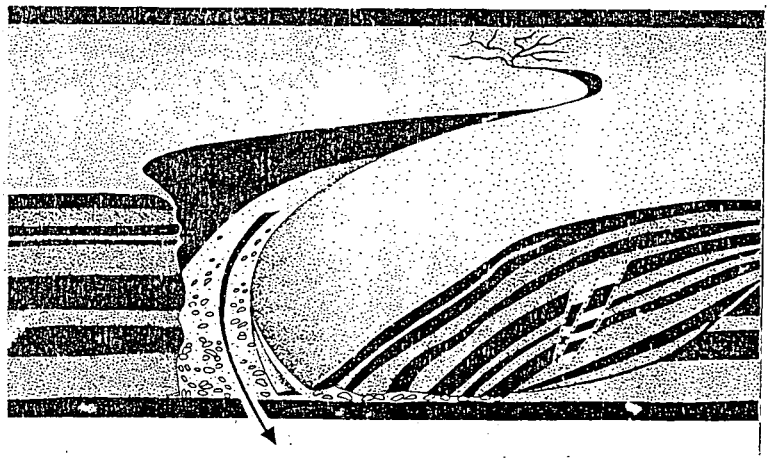

Fig. 2.6 Slumped structures in lateral accretion deposits of a tidal channel. Modified after Reineck and Singh (1980).

2.3.2.3 Chute/Scroll bar subfacies

Unit D (Fig. 2.5), which consists largely of tabular cross-bedded sandstone, is interpreted as a chute and/or scroll bar overlying point bar deposits. These sediments were deposited during high flood discharge following cutting of a chute channel across the point bar top with accumulation occuring at the down stream end of the point bar as depicted by Cant (1992). Bridge (1985) suggested that isolated sets of planar cross strata in upper point bar sediments may be a good indication of a chute/scroll bar. Such sediments may have occurred during flood stages, when part of the flow cut directly through the surface of the point bar, possibly resulting in a significant amount of bedload moving out of the main channel (Galloway, 1985 and Fig. 2.7). These deposits are thicker where downstream flow reinters the main channel and merges into a scroll bar further downstream (Galloway, 1985; Bridge *et al.* 1986). Tabular cross-bedding characterising chute and/or scroll bars always trends at an oblique angle to the palaeoflow direction of the main channel (Cant, 1978). Palaeocurrent data, if available, may have provided additional support for the above interpretation.

The upward decrease in grain size and the associated occurrence of fine ripples is probably an indication of decelerating low flow stage (Bridge *et al.* 1986).

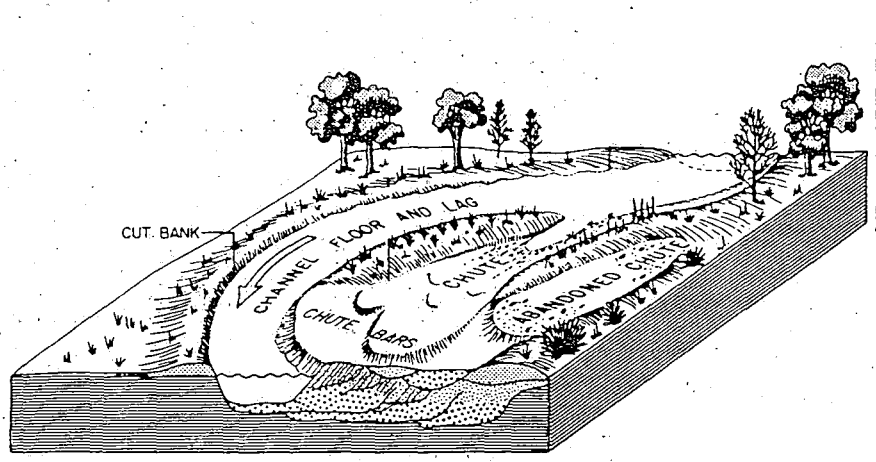

Fig. 2.7 Block diagram showing chute modified point bar. Modified from Galloway (1985).

2.3.2.4 Chute channel subfacies

The scour surface and the overlying clasts of unit E (Fig. 2.5) are critical evidence of channel incision. In addition, the identical composition of these clasts to the basal conglomerate (Unit A) further supports the interpretation of unit E as chute channel deposits cutting across the upper point bar surface. Galloway (1985) suggested that upstream parts of the chute channel commonly contain coarse lag material typically found in the main channel, which was introduced into the upstream end of the chute channel (Fig. 2.7). Cant (1992) claimed that chute channels are common in meandering rivers characterised by highly variable discharges.

The interpreted occurrence of chute channel and associated chute/scroll bar helps to support the interpretation of the underlying sequence as a point bar rather than a simple distributary channel fill which likewise may show an asymmetric fining-upward sequence similar to that of a point bar (Yinan *et al.* 1987).

Although the fine-grained featureless sandstone (Unit F), characterised by equally-spaced thin mudstone drapes, lacks evidences of exposure, it was probably deposited in an overbank, possibly levee environment of deposition. Upper point bars commonly merge upwards into levee deposits (Davis, 1992). However, Campbell and Hendry (1987) emphasized that inner accretionary bank deposits of a point bar are composed of fine to very fine-grained sandstone, siltstone and mudstone drapes. They stress that

inner accretionary bank deposits are almost impossible to identify in the ancient record unless they have a visible dip.

2.3.3 Mode of abandonment in high sinuosity channels

2.3.3.1 Gradually abandoned high sinuosity channel facies

Description: This channel facies is represented by the cored interval from 12674 ft to 12640 ft in well BD/44 (Appendix 5). The sequence is illustrated in detail in Fig. 2.8. The sequence erosively overlies a thick sandstone package which represents point bar and associated subfacies described in section 2.3.2. The scour surface is overlain by approximately 20 cm of conglomerate (Unit A from 12674 ft to 12673.2 ft). The clasts are quartzitic, poorly imbricated, light grey, subrounded to rounded and 1 to 2 cm long. Angular to sub angular grey to light grey mudstone intraformational clasts, 1 to 3 cm long, are common. Mud balls up to 10 cm in diameter are also present within unit A. A dark brown, poorly sorted, very coarse-grained sandstone package containing frequent floating pebbles (Unit B from 12673.2 ft to 12656 ft) overlies unit A. Scour surfaces are rare and probably define tabular cross-bedding set boundaries. Individual tabular cross-bedded sets within unit B are up to 30 cm thick, but this is difficult to see in the lower portion of the unit (Appendix 5 arrow). Unit B is in turn gradationally overlain by dark brown, medium-grained moderately sorted sandstone (Unit C from 12656 ft to 12650 ft) containing tabular cross-bedding in sets ranging from 5 to 10 cm thick. The tabular cross-bedding gradually passes upward into large-scale ripple cross-lamination which is generally confined to the uppermost part of the unit. Unit B is gradationally overlain by a light brown, moderately sorted, fine-grained sandstone (Unit D from 12650 ft to 12644.5 ft) which is mainly structureless, except for the possible presence of fluid escape features.

The whole of the sequence is sharply capped by a dark grey carbonaceous mudstone (Unit E from 12644.5 ft to 12640 ft) cut by a network of coalified fine plant roots. Rare coalified plant stems and impressions of plant debris occur within this mudstone unit, as well as small disseminated pyrite grains.

Individual sandstones within the sequence show an overall upward decrease in grain

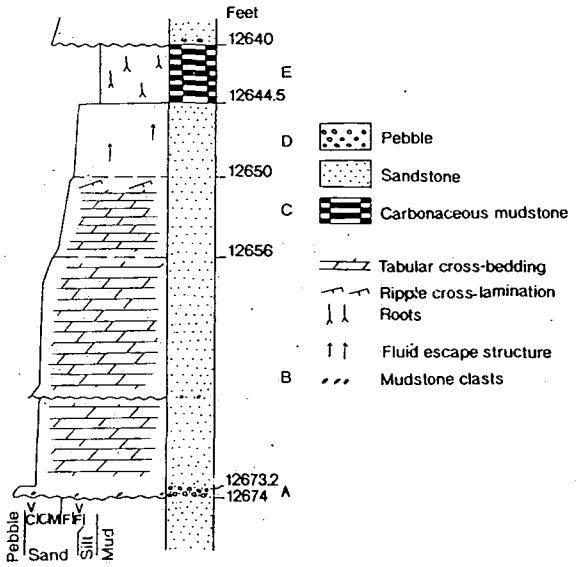

Fig. 2.8 Detail of section between 12674 ft and 12640 ft in well BD/44 core interval showing gradually abandoned high sinuosity channel facies.

size, whilst the sequence itself is erosively truncated by a coarse-grained, tabular cross-bedded sandstone unit.

Interpretation: The basal breccia is interpreted as a channel lag deposit resting on a scour surface. The abundance and predominantly angular shape of the mudstone rip-up clasts (Unit A) reflects the rapid depositional rate and limited distance of transport (Link, 1984). Abundance of intraclast material may further imply rapid channel shifting (Lawrence and Williams, 1987).

Throughout the sequence, an upward decrease in grain size together with a reduction in the scale of the sedimentary structures suggests a gradual waning of both flow depth and discharge (Galloway, 1985; Diemer and Belt, 1991). This is thought to result from partial abandonment of the channel possibly in response to chute cut-off (Allen, 1965). Bridge *et al.* (1986) suggested that initiation of chute cut-off is associated with change in flow alignment upstream during high discharges, particularly in bends of high sinuosity (Fig. 2.9a).

Allen (1965) described chute cut-off channel fill as being dominated by bedload sediments. This was attributed to streams continuing to flow for a long time through

the old channel thereby allowing bedload to continue to be deposited until closure is complete, after which filling is mainly due to suspension fines.

The successive planar cross-bedded sandstone (Units B and C) may have originated as avalanche sets of straight-crested, large, in-channel dune bedforms, with concomitant reduction in cross-bed set amplitude possibly reflecting reduced flow discharge and depth (Lawrence and Williams, 1987; Todd and Went, 1991).

Possible fluid escape structures in unit D may indicate pore fluid pressure and rapid dewatering possibly in response to change in river stage (Lawrence and Williams, 1987; Gersib and McCabe, 1981) or rapid deposition. Unit D is thought to represent the final deposits prior to channel abandonment. The final mudstone capping unit E suggests quiet water conditions (Link, 1984) with its dark grey colour attributed to persistent reducing conditions (Casshyap and Kumar, 1987). This is interpreted to represent the final fill of the channel and/or overbank fines.

In high sinuosity channels fining-upward sequences are deposited from point bar lateral accretion, channel shifting and vertical flood plain aggradation (Allen, 1965). Accordingly, the differences between gradually abandoned fining-upward channel fill deposits as in this example, and the one described previously are: (1) the predominance of trough cross-bedding in the previous example; (2) absence of

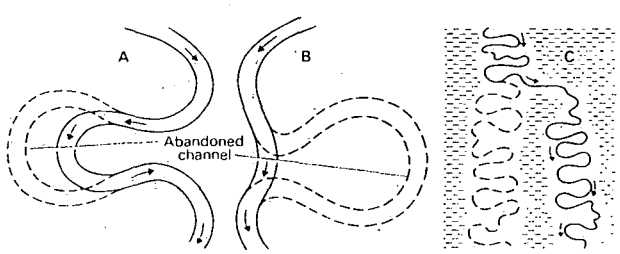

Fig. 2.9 Modes of channel shifting in meandering streams. (a) Chute cut-off, (b) neck cut-off, (c) development of a new meander belt following avalsion. Modified from Collinson (1991).

mudstone drapes in the abandoned channel fill of this example; (3) the lack of evidence of soft sediment deformation in this channel-fill sequence possibly because of lower depositional slopes; (4) the absence of chute modification in these channel-fill deposits; and (5) the lack of evidence of overbank sediments associated with the channel-fill

which favours vertical aggradation rather than lateral accretion (Casshyap and Kumar, 1987).

2.3.3.2 Abruptly abandoned high sinuosity channel facies

Description: A few abruptly abandoned channel facies have been recognised in cores in the study area. In well BD/44 (Appendix 6), for example, the deposits between 12614.8 ft and 12601.8 ft are thought to represent this facies which is reproduced in detail in Fig. 2.10. The sequence commences with a poorly imbricate, clast-supported pebble conglomerate (Unit A from 12614.8 ft to 12613.5 ft) resting on an irregular scour surface with 2 - 3 cm of relief cutting into very fine-grained ripple laminated sandstone. The clasts are quartzitic, light grey, subrounded to rounded, and range from 1 to 2 cm long. The conglomerate is sharply overlain by very fine-grained, light brown ripple laminated sandstone (Unit B from 12613.5 ft to 12613.3 ft), which is followed by a 4 m thick heterolithic unit (Unit C from 12613.3 ft to 12601.8 ft) consisting of light grey, very fine-grained horizontally laminated sandstone, siltstone, and dark grey to blackish, locally burrowed carbonaceous mudstone.

Thin coal seams, coalified plant roots, plant debris and impressions of plant leaves and stems are common in unit C (Swamp facies) which is described and interpreted in detail elsewhere in this chapter. The sequence is erosively capped by a medium-grained, tabular cross-bedded sandstone package.

Interpretation: Channel initiation and scouring into the underlying substrate is evidenced by the scour surface and overlying clasts of unit A. Shortly after channel initiation abrupt channel abandonment is thought to have taken place probably as a result of neck cut-off which is one of the major mechanisms of abandonment in high sinuosity channels (Allen, 1965 and Fig. 2.9b). Sudden abandonment of the channel segment may have abruptly prevented bedload influx and the channel was slowly filled by suspended load washed in from another nearby active channel (Galloway, 1985).

It has also been suggested by Gersib and McCabe (1981) that meander cut-off would produce a rapid decrease in flow causing mud to be deposited directly above the channel sequence.

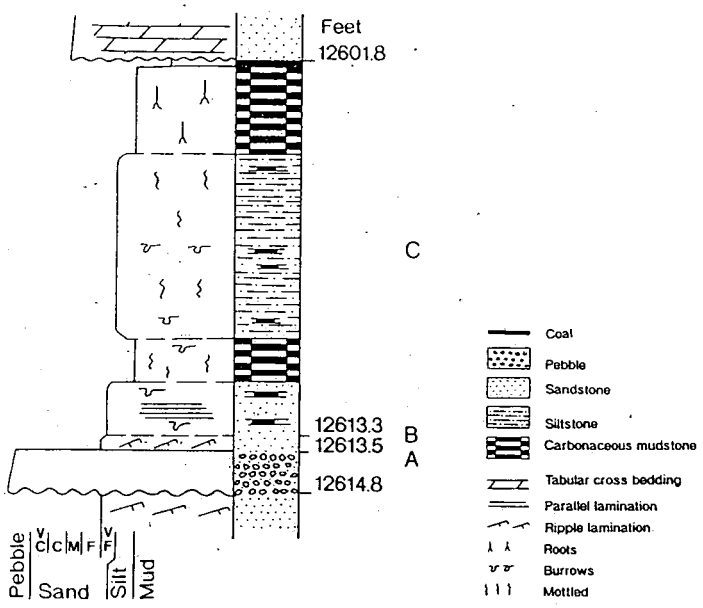

Fig. 2.10 Detailed section for the cored interval between 12614.8 ft and 12601.8 ft in well BD/44 illustrating abruptly abandoned high sinuosity channel facies.

The very fine-grained ripple-laminated sandstone (Unit B) is attributed to the final movement of bedload in the abandoned channel (Allen, 1965). The succeeding heterolithic, thick silty and muddy unit in C indicates the establishment of an ox-bow lake favouring plant colonisation and reducing conditions (Melvin, 1987). Ethridge *et al.* (1981) have pointed out that abandoned channel fill deposits are sometimes difficult to recognise in cores and they may include different types of deposits such as lacustrine, crevasse splays and poorly or well-drained swamp deposits. However, preserved channel plugs may provide good indicators of channel geometry.

2.3.4 Crevasse/ Minor channel facies

Description: This channel facies is illustrated in Fig. 2.11 and is represented by the cored interval from 12447.5 ft to 12440 ft in well BD/44 (Appendix 7). The sequence is composed of two nearly identical units, each of which occurs as a single storey showing a crude fining-upward trend. The lower unit A, from 12447.5 ft to 12444 ft,

rests erosively on the underlying dark grey carbonaceous mudstone. The sandstone above this scour surface is very coarse-grained, poorly sorted and dark brown in colour, fining upwards into very fine-grained, light brown sandstone. Convolute, parallel lamination and ripple lamination dominate the upper part of unit A. The overlying unit B from 12444 ft to 12440 ft also commences with an erosively-based, light brown, coarse-grained sandstone containing faint parallel bedding followed by poorly defined small-scale trough cross-bedding. Unit B also shows convolute and ripple lamination in the upper part which is in turn gradational with the overlying light grey, muddy siltstone.

Granule to small pebble-size clasts, occasionally associated with the basal scour surfaces, locally characterise the lower part of the units. Individual single storeys are locally penetrated in the top part by fine, *in situ* plant roots associated with disseminated minor plant debris.

Interpretation: The basal coarse-grained layers with rare intraclasts resting on the irregular scoured bases indicate scour by turbulent flows and subsequent filling (Rhee *et al.* 1993). Each discrete unit with crude fining-upward trend commences with a granule size conglomerate that fines up into rippled and parallel laminated very fine-

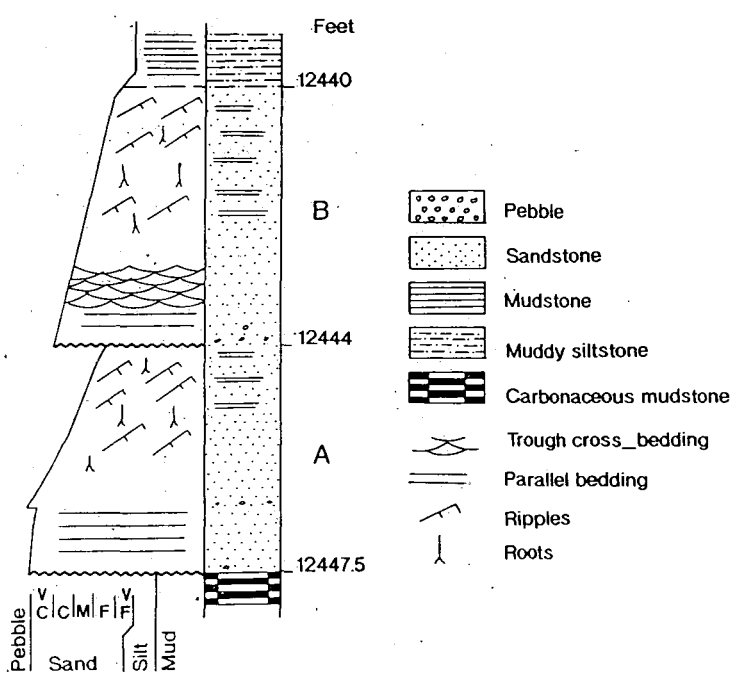

Fig. 2.11 Detail of section from 12447.5 ft to 12440 ft in well BD/44 showing multistorey crevasse/ minor channel deposits.

grained sandstone. This suggests channelised flow conditions with individual units representing crevasse channels formed by breaching of major channel banks (Fielding, 1986; Melvin, 1993). Parallel bedding in the lower unit A suggests initial deposition from broad relatively unconfined flows under upper flow regime conditions (Lawrence and Williams, 1987). By contrast the lower part of unit B displays faint trough cross-bedding associated with the plane bedding possibly due to rapid channel cutting and filling, mainly by vertical accretion of sinuous-crested dunes. The ripple lamination in both fining-upward units indicates lower flow regime traction dominated current deposits (McKee *et al.* 1967; Melvin, 1993). Convolute lamination is common, and is attributed to pore fluid expulsion generated during loading of the overlying sediments (Singh and Bhardwaj, 1991). *In situ* plant roots, locally associated with the upper parts of both units, suggests temporal variations in water level and/or palaeotopographically higher parts of the sequence (Melvin, 1987).

A direct interpretation of the classic fining-upward trend in both units, marked by a systematic variation in sedimentary structures may indicate waning flow velocity from an initial erosive phase (McKee *et al.* 1967; Collinson, 1991). The multistorey character of the entire sequence may be indicative of episodic filling (Fielding, 1986) or occupation several times by successive flood events of different magnitude.

Because crevasse channels are in topographically higher parts of the system they are greatly affected by river stage, and the long term maintenance of these channels may lead to the establishment of minor channels (Cant and Walker, 1978).

2.4 Overbank/floodbasin facies association

This facies association represents the accumulation of sediments deposited mainly from suspension during repeated overbank flooding (Allen, 1965; Flores, 1981). It also consists of sediments resulting from less confined traction currents restricted mainly to areas flanking major channels.

Siltstone, mudstone, carbonaceous mudstone and very thin, minor coals are the most common lithologies within the overbank facies association, which is marked, in many instances, with pedogenic and biogenic features. Fine to coarse-grained sandstone is

occasionally present and in most cases, confined to crevasse splays and levees, which contain ripple, parallel and wavy laminations, and rarely cross-stratification. Overbank and floodbasin fines in the core show an overall upward decrease in proportion to coarse-grained channel sandstones. Friend (1983) pointed out that the major factors controlling the geometry and distribution of overbank deposits include channel morphology, sediment supply, rate of subsidence and the avulsion behaviour of channels.

Seven facies have been identified within this facies association, and have been assigned to proximal and distal settings according to their interpreted distance from the channel.

2.4.1 Natural levee facies

Description: An example of this facies is illustrated in Appendix 8 in the core interval from 11136 ft to 11129.8 ft in well BD/36. The sequence starts with unit A from 11136 ft to 11132.5 ft (Fig. 2.12a). This unit consists of light grey, very fine-grained sandstone resting erosively on the underlying dark grey, carbonaceous mudstone. The erosional surface is characterized by a relief of up to 2 cm, with no preserved overlying coarse lag deposits. The sandstone is characterised by thin, dark grey streaky mudstone intercalations ranging from 0.5 to 1 cm thick. The mudstone intercalations, which display wavy and disturbed parallel lamination, appear to be less dominant towards the top of the sandstone unit. Sandstone unit A is gradationally overlain by a very fine-grained sandstone interval which is represented by unit B from 11132.5 ft to 11129.8 ft. This unit contains poorly defined, thin, possibly bioturbared mudstone in its upper part. The whole section (Units A and B) described above is sharply overlain by a grey to dark grey, thick, massive carbonaceous mudstone interval.

A similar example is illustrated in Appendix 9 from the cored interval 12389.5 ft to 12372 ft in well BD/44. A detailed section of the sequence is illustrated in Fig. 2.12b. The sequence is characterized by a variety of lithologic units including mudstone, muddy siltstone and dominant fine to very fine-grained sandstone. The section commences with an upward transition from the underlying muddy siltstone to very fine, grey to pale brownish-grey sandstone which is unit A, from 12389.5 ft to

12388 ft. The sandstone is disturbed and mottled, and probably bioturbated. It also exhibits a crude layering. This sandstone unit is gradationally overlain by unit B from 12388 ft to 12384.7 ft which consists of extensively bioturbated mainly vertically burrowed grey to light grey muddy siltstone displaying biogenically disturbed parallel lamination. This in turn fines up gradationally into grey to dark grey locally burrowed mudstone represented by unit C, from 12384.7 ft to 12383.5 ft. This mudstone unit is overlain by a sharply based, well cemented fine-grained, brownish-grey sandstone interval, represented by unit D from 12383.5 ft to 12379.8 ft, that lacks any obvious sedimentary structures. A dark grey mudstone interval, unit E from 12379.8 ft to 12378 ft, abruptly overlies the sandstone unit. The mudstone of unit E has rare preserved plant roots with red mottles of possible pedogenic origin, in the top part. Following this mudstone unit is a very fine, grey-greenish sandstone interval (unit F) from 12378 ft to 12376 ft. The sandstone shows no sedimentary structures apart from possible ripple cross-lamination in the basal part. This sandstone unit includes red, *in situ* diagenetic siderite grains with a diameter of < 1 mm. These have a spheroidal shape and a composition different from the host rock in which they occur (Scoffin, 1987). This sandstone unit is in turn sharply overlain by unit G, from 12376 ft to 12375 ft, which consists of a disturbed, reddish-grey mudstone with evidence of bioturbation, rootlets and pedogenesis. The entire sequence is sharply terminated by an interval of well cemented grey to light green, mottled very fine-grained sandstone (unit H) from 12375 ft to 12372 ft, that has abundant fine sideritic grains and well preserved plant rootlets. No sedimentary structures can be seen within this unit and the upper part of the sandstone gradationally merges into the overlying flood plain mudstone.

Interpretation: The overall fine-grained nature of the sediments described in the above two examples, the absence of coarse-grained sediments as well as the scarcity of scour surfaces suggests a predominantly low energy overbank environment of deposition (Miall, 1985b). The close spatial association of these sediments to the underlying coarse-grained channel sandstone suggests levee deposits flanking the main supply channels (Ethridge *et al.* 1981; Flores, 1981), deposited by sediment-laden waters spilling out over topographic lows along the channel banks (Coleman, 1969). The

prevailing fine to very fine-grained nature of the sediments may represent parts of a levee system (Elliott, 1974).

In the first example in well BD/36 (Appendix 8) the irregular lower surface and slight variation in relief on the underlying fine sediments, is considered to be a scour surface, which is a common phenomenon produced by high energy pulsatory over bank flood events (Galloway, 1981; Melvin, 1987). The gradual reduction in thickness, abundance of mud intercalations and the consequent upward thickening of the sandstone units may be indicative of levee progradation towards the flood plain and possible long term channel migration (Elliott, 1974; Miall, 1984; Collinson, 1991;

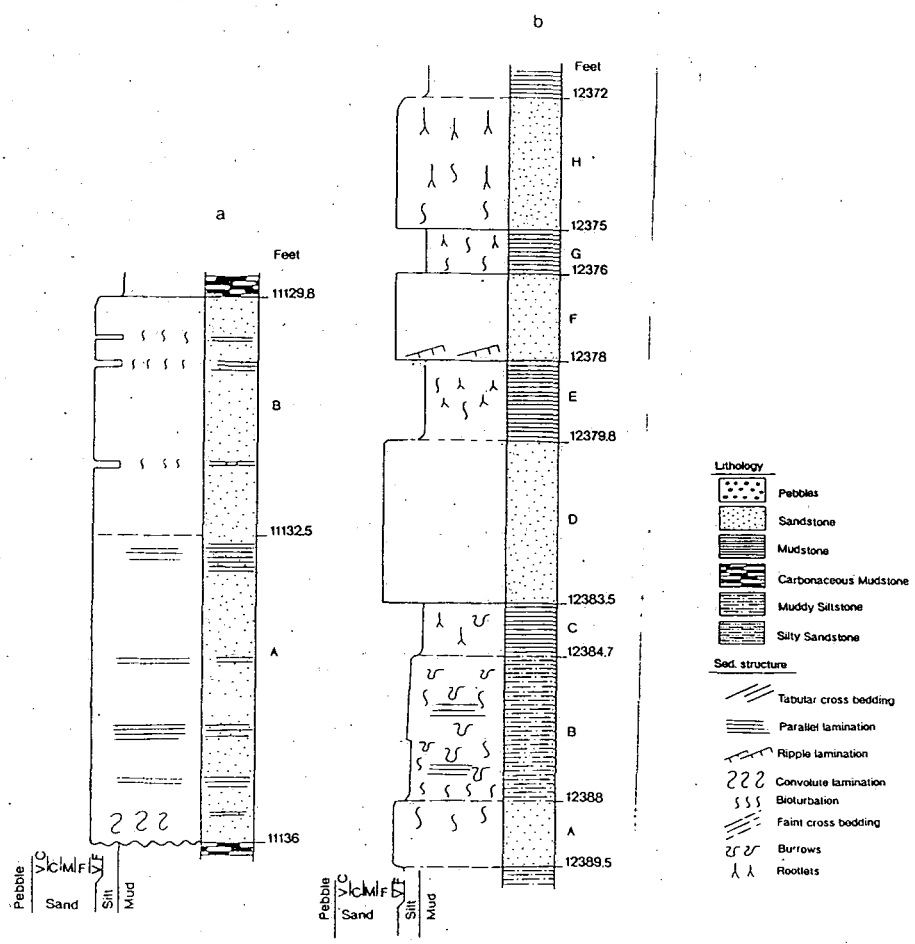

Fig. 2.12 Reproduced sections for the cored intervals between 11136 ft and 11129.8 ft in well BD/36 (a) and 12389.5 ft and 12372 ft in well BD/44 (b), representing natural levee deposits.

Melvin, 1993). The paucity of palaeosols within these sediments may be attributed to the submergence of the levee flanks and possibly levee crests (Fielding, 1986) or frequent flooding. The fine interbedding of the sandstone and mudstone in the lower

part is possibly an indication of fluctuating hydraulic conditions where sandstone is deposited during current activity and the mudstone during periods of quiet water (Casshyap and Kumar, 1987; Alexander and Gawthorpe, 1993). The relatively thick, mica-rich, very fine-grained sandstone unit at the top of the interval may represent a fairly rapid rate of deposition under suspension conditions (Singh and Bhardwaj, 1991). Applying the same criteria described above, the alternation of very fine sandstone, fine sandstone and mudstone in the sediments of the second example (Fig. 2.12b) may also reflect periodic fluctuations in flood discharge and deposition of sediments from multiple flood events (Galloway, 1981) with each unit interpreted as a discrete flood deposit in which the thicker sandstones indicate higher energy and deeper water flood events (Bridge, 1984; Fielding, 1986).

The abundance of roots, root mottling and red colouration (Units E, G) and the presence of siderite within the alternating sandstone (Units F, H) is probably attributed to sedimentation within topographically higher parts of the levee characterized by intermittent exposure (Galloway and Hobday, 1983; Melvin, 1987).

The mechanism by which siderite ($FeCO_3$) is formed, as part of early clastic diagenesis in organic-rich sediments, is the degradation of organic matter into water-soluble organic compounds (Curtis, 1987; Crossey and Larsen, 1992). In fresh waters with anoxic bottoms, anaerobic conditions prevail. With eccessive dissolved SO_4^{2-}, organic matter is degraded by sulphate-reducing bacteria producing two important products, H_2S and CO_2. Microbial processes, operating within distinctly stratified depth intervals, generate important water-soluble mineralizing agents, amongst them is HCO_3^- which normally increases in concentration in the vicinity of the water-sediment interface (Methanogenic environment or Me zone in the classification of Curtis, 1987), and favours the precipitation of iron carbonates in iron-rich sediments. Bahrig (1994) pointed out that precipitation of siderite is generally restricted to sedimentary environments characterised by: (1) sufficient availability of Fe^{2+}; (2) low sulphide concentration, because at high concentrations any iron will be precipitated as Fe-monosulphide (pyrite); and (3) a sufficient partial pressure of CO_2, which is commonly achieved in natural environment either by microbial activity or dissolution of less stable carbonates. In general, siderite in sediments can be used as an indicator of post-oxic environment characterised by strong anoxia coupled to a low rate of sulphide

reduction. The precipitation of siderite is favoured in a methanogenic environment, where the precipitation of siderite is coupled to processes of methane formation.

In the levee sediments described above, the interpretation of intermittent sediment exposure is strengthened by the alternation of rooted and red mottled sediments indicating exposure, and the siderite-bearing units reflecting anoxic conditions.

The lack of well defined sedimentary structures and the disturbed primary stratification of some units may be due to burrowing and intensive bioturbation.

Levee deposits have been described in the geological literature as sediments characterized by parallel beds of sandstone separated by mudstone partings. The sandstone is normally light grey in colour, fine to very fine-grained, generally silty and may contain plant debris, bioturbation, horizontal stratification and also carbonate concretions. Levee deposits are sometimes difficult to distinguish from upper point bar sediments, and are classified as levee deposits on the bases of their stratigraphic position adjacent to channel bodies (Link, 1984; Gasshyap and Kumar, 1987; Ghosh, 1987; Johnson and Pierce, 1990; Davis, 1992). This provides further support for the interpretation of the examples illustrated in Fig. 2.12 as levee deposits.

2.4.2 Crevasse splay facies

Description: An example of this facies is illustrated in cored section 12370 ft to 12358.5 ft in well BD/44 (Appendix 10). The section commences with unit A from 12370 ft to 12367 ft (Fig. 2.13a) which consists of fine-grained sandstone erosively overlying dark grey locally mottled mudstone. The erosive surface is characterized by local micro loadcasts and is followed by a 2 cm thick light grey, very coarse-grained pebbly sandstone that probably represents thin lag deposits. The succeeding fine-grained sandstone is light grey to brownish in colour, and locally micaceous near the base. It contains streaks and lenses of dark grey mudstone which grades up into convoluted and poorly defined ripple cross-lamination at the top. This sandstone is gradationally overlain by unit B from 12367 ft to 12366 ft which consists of pale, brownish-grey medium-grained sandstone with streaks of black carbonaceous mudstone. The sandstone displays tabular cross-bedding at the top. This sandstone interval is in turn sharply followed by unit C From 12366 ft to 12363.7 ft. This is

composed of reddish-brown, coarse-grained sandstone with medium to large-scale tabular cross-bedding with individual sets being about 30 cm thick, and individual foresets ranging in thickness from about 2 to 3 cm. Unit C is abruptly overlain by unit D from 12363.7 ft to 12360.3 ft which consists of reddish-brown, moderately sorted, very coarse-grained sandstone with subrounded to rounded grains, displaying poorly defined tabular cross-bedding. The entire coarsening-upward sequence is followed by a fining-upward section which commences with unit E, from 12360.3 ft to 12359 ft, consisting of reddish-brown, moderately sorted, medium-grained sandstone, containing parallel bedding at the bottom and less well defined cross-bedding at the top. This sandstone fines up into unit F, from 12359 ft to 12358.5 ft, which is composed of tan to light grey very fine-grained silty sandstone with no preserved sedimentary or biogenic structures, except possibly some bioturbation. Unit F is gradationally overlain by dark grey muddy siltstone. Individual sandstone units in the sequence are typically of uniform grain size and contain rare plant stems and plant roots.

A similar succession in the cored section of well BD/36 from 11192 ft to 11184 ft is shown in Appendix 11. The section starts with grey muddy siltstone (unit A) from 11192 ft to 11191 ft (Fig. 2.13b). Unit A gradationally overlies extensively burrowed, bioturbated and mottled mudstone. The muddy siltstone exhibits irregular to fine parallel lamination. This muddy siltstone unit is abruptly overlain by a heterolithic unit B from 11191 ft to 11189.5 ft that consists of thin interbeds of brownish, light grey, very fine sandstone with streaks of muddy siltstone that resembles the underlying unit. This heterolithic unit gradually changes upward into reddish-brown fine-grained and slightly micaceous sandstone, representing unit C from 11189.5 ft to 11187 ft, with very thin partings of dark grey to black mudstone. The sandstone exhibits bioturbation and burrows at the top. The sequence is gradually overlain by unit D from 11187 ft to 11184 ft, a one metre thick interval of grey to dark grey, locally red mottled and rooted micaceous muddy siltstone with parallel laminations.

Interpretation: The lithological characteristics and sedimentary structures of the sequence indicate a low energy environment, whilst the absence of internal scour surfaces within the sandstone units strongly suggests that the coarsening-upward

sequence followed by a fining-upward sequence in the first example is an overbank rather than a channel deposit (Rust and Jones, 1987).

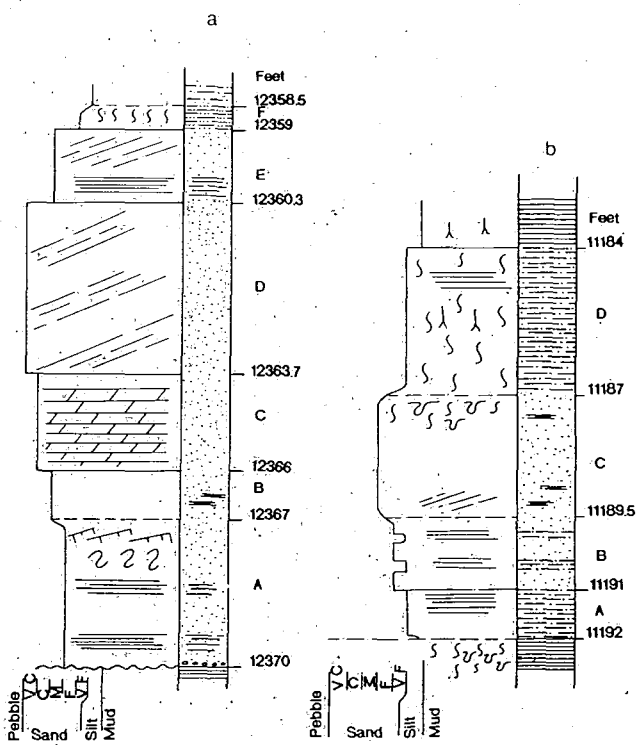

Fig. 2.13 Detail of sections from 12370 ft to 12358.5 ft in well BD/44 (a) and 11192 ft to 11184 ft in well BD/36 (b), illustrating progradation followed by retrogradation of crevasse splay deposits. See fig. 2.12 for index.

The isolation of such sediments within fine-grained floodplain deposits makes the interpretation of such sediments as overbank deposits more likely (Johnson and Pierce, 1990). The whole succession, in the first example, is interpreted as crevasse splay deposits.

The coarse-grained nature of the sandstone units may reflect proximity to the major feeder channel, with the coarsening-upward trend and concomitant increase in sandstone bed thickness reflecting progradation of the crevasse splay system into the laterally adjacent lower lying flood plain (Rust and Jones, 1987).

The scour surface and overlying pebbly sandstone at the base of the sequence in the first example (Fig. 2.13a) suggests that initially the unit might have been deposited under channelized conditions, possibly as part of a crevasse channel. The presence of microload casts can be considered to be a result of sedimentation before complete

dewatering of the underlying fine-grained substrate (Boggs, 1987). The fining-upward sequence that follows the coarsening-upward unit is interpreted as gradual crevasse splay retrogradation through decreased competency, sediment supply, and abandonment. The paucity of roots and root mottling, as well as burrowing activity throughout the interval implies fairly rapid rates of deposition and abandonment of the splay lobe. The fine mudstone laminations, ripple laminations and the mica-rich sediments within the lower sandy unit provides evidence of sediments being deposited under weak traction currents and rapid suspension fall out during waning flood waters (Singh and Bhardwaj, 1991). The presence of parallel lamination and thin mud partings suggest weak currents, possibly in the more distal parts of the system as described by Gersib and McCabe (1981). The abandonment of the splay lobe may be attributed either to the infilling of the crevasse channel or waning flow discharge in the river system (Gordon and Bridge, 1987). Similarly, the coarsening-upward followed by fining-upward sequences, as described above from well BD/36 (Fig. 2.13b), may likewise represent progradation and abandonment of a subaerial crevasse splay laid down on well drained flood plain deposits. The presence of bioturbation suggests prolonged periods of non-deposition during the evolution of the crevasse splay complex.

Crevasse splay deposits have been described and interpreted by several authors (e.g. Rienick and Singh, 1973; Ethridge *et al.* 1981; Flores, 1981; Galloway and Hobday, 1983; Galloway, 1985; Collinson, 1991; Davies *et al.* 1993) and others. Such sediments develop when flood waters are directed across and over the channel bank during exceptional flood events. They are normally coarser than the natural levee deposits (Rienick and Singh, 1973; Galloway and Hobday, 1983) and may lead to the diversion of the river course as the crevasse channel eventually enlarges to become a main destributary channel (Bridge, 1985).

Crevasse splay deposits have been described by Davies *et al.* (1993) as sediments that are muddier and finer than their channel counterpart sandstones. They may be red in colour due to a high ironoxide rich clay content and are usually laminated because of the sudden drop in flow velocity. They may also be destratified by bioturbation. Ethridge *et al.* (1981) showed that crevasse splay deposits fine and thin away from their feeder channel with progradation resulting in coarsening-upward sequences.

They added that in cores, crevasse splay deposits normally consist of fine to very fine sandstone with ripple cross- lamination, small-scale cross stratification, parallel lamination and scour and fill structures. The upper parts of the crevasse splay deposits can be rooted and possibly burrowed, and may contain pedogenic carbonate concretions and mottles. They normally grade up into well drained flood plain deposits. However, crevasse splay deposits can consist of coarser sediments that resemble the main stream bedload component as shown in the first example, especially in more proximal settings. In this case the crevasse channel feeding the splay lobe might have cut deep into the main channel bank, and as a result, it was able to tap coarser bedload sand and transport it into the adjacent flood plain (Oomkens, 1970; Galloway and Hobday, 1983). The siltstone and mudstone that overly the sandstone may represent sediments deposited mainly from suspension in the distal reaches of the splay lobe (Flores, 1981).

Coarsening-upward sequences in overbank sediments are not unique to crevasse splay progradation. Prograding levees can also produce coarsening-upward sequences similar to crevasse splays, but they are not attached to crevasse channels (Bridge, 1984; Collinson, 1991). Ethridge *et al.* (1981) suggested that lacustrine delta fill deposits are difficult to be distinguished from subaerial crevasse splay deposits in that they both tend to produce coarsening-upward trends, and thus the classification of the sediments described in the previous examples was mainly based on their stratigraphic position above unlaminated shallow water floodplain mudstones which was favourable for plant colonisation judging by the abundance of *in situ* plant rootlets. The lack of fresh water molluscs in the underlying deposits further supports the interpretation of these sandy units as prograding and retrograding subaerial crevasse splay deposits (Warwick and Flores, 1987). The presence of cross-stratification in the middle of the sandy unit in the first example, may indicate more confined flow (Rhee *et al.* 1993).

2.4.3 Lacustrine facies

Description: This is represented by the cored interval from 12336 ft to 12328.5 ft in well BD/44 (Appendix 12). A detailed section for the interval is illustrated in Fig. 2.14. The sequence starts with a sharply based medium to dark grey organic-rich

silty mudstone (unit A from 12336 ft to 12334.4 ft). The mudstone abruptly overlies a medium-grained, streaky to parallel laminated sandstone interval. The laminae range from a fraction of a centimetre to approximately 2 cm thick. Parallel and streaky laminations are less well defined and darker grey in colour in the lower 30 cm. The lamination becomes better defined in the overlying 20 cm thick grey mudstone which includes some rippled silty lenses. This is sharply succeeded by about 40 cm of finely laminated grey to red mudstone (Unit B from 12334.4 ft to 12333 ft) containing *in situ* plant rootlets and possibly root mottling. This distinctively red coloured section is in turn abruptly overlain by a one metre thick, flat laminated, dark grey silty mudstone with silty lenses (Unit C from 12333 ft to 12330.3 ft). Evidence of red colouration and plant rootlets are confined to the lowermost part of this unit. The entire sequence is capped by about 60 cm of dark grey, finely laminated organic rich mudstone (Unit D from 12330.3 ft to 12328.5 ft) erosively overlain by a very coarse pebbly sandstone package. The whole sequence described above lacks preserved biogenic features such as trace fossils and bioturbation apart from the root-mottled red mudstone middle section. Rare disseminated small pyrite grains can also be seen within the grey mudstone intervals.

A similar example from well BA/22 in the more proximal part of the field is illustrated in Appendix 13. The core interval 12387.7 ft to 12382 ft abruptly overlies a thick sandstone unit. It commences with a 10 cm thick coal seam (unit A) followed by about 30 cm of grey, possibly carbonaceous mudstone (Unit B) that exhibits poorly defined rippled silty lenses. It is sharply overlain by about 2 m thick interval of grey mudstone (Unit C) with irregular silty and sandy lenses possibly representing ripple structures. Some of the sandier lenses show local evidence of deformation. This is sharply overlain by a thick sandstone unit.

Interpretation: In the described examples, the fine-grained nature of the sediments, the dominant flat lamination and the scarcity of traction current-induced sedimentary structures suggests deposition of fine sediments predominantly from suspension fall-out in a stagnant water body, possibly a very shallow fresh water lake (Ethridge *et al.* 1981; Melvin, 1987). The absence of biogenic activity, paucity of plant rootlets and the lack of fresh water fauna, in addition to the presence of the pyrite grains further implies

that these sediments might have been deposited in a quiet, low energy anoxic environment, where clastic supply was restricted to fine mud beyond the direct influence of splays and other overbank flood events (Ethridge *et al.* 1981; Fielding, 1984; Allen and Collinson, 1991). The first example may initially represent an ox-bow lake generated by channel cut off as a result of rapid channel abandonment

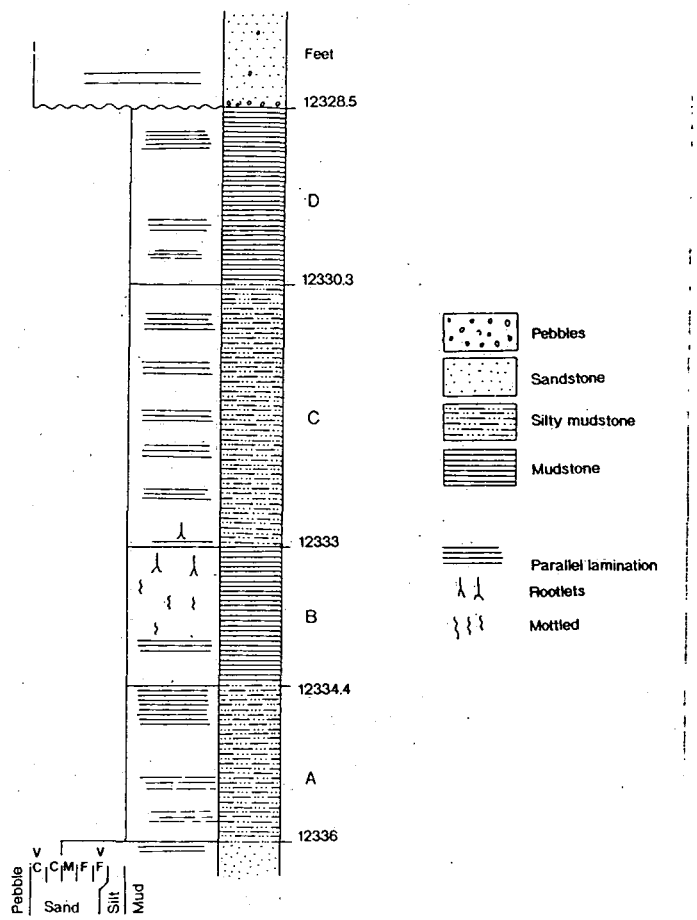

Fig. 2.14 Detail of section between 12336 ft and 12328.5 ft in the core section of well BD/44 showing lacustrine deposits.

(Gersib and McCabe, 1981; Groenewold *et al.* 1981; Melvin, 1993). Channel abandonment is also inferred from the sharp contact with the underlying sandstone unit interpreted as an active channel fill. Lake water depth shortly after the cut-off would be unfavourable for plant colonisation and hence may have inhibited the development of swampy conditions common in ox-bow lakes. In addition the dark grey colour of the mudstone at the bottom of the interval may represent a very slow rate of deposition within a sediment starved water column characterized by very little detrital input, in a reducing environment of deposition (Haszeldine, 1984). The dark grey colour of the

sediments may be attributed to the high organic content (Fielding, 1984). The proceeding silty unit which exhibits flaggy lamination marked by variation in grain size is common in laminated mudstone facies and possibly represents passive lake margin rather than lake floor setting, where silty laminae may represent sediments deposited by density currents (Ethridge *et al.* 1981; Farquharson, 1982). Melvin (1993) has described similar deposits as sediments cascading down lake margins in the form of sediment gravity flows, with ponding on the lake bottom leading to a distinctive interbedding of possible graded suspension siltstone and mudstone. Haszeldine (1984) has also identified similar deposits as rhythmite muds characterised by alternations of pale and dark layers with the dark layers having either erosive or flat bases. He considered them to be deposits of fine-grained turbid underflows in a body of fresh water. Unit B may represent the infilling of the lake to a level where plants could sustain a hold in the sediments, as inferred from the *in situ* plant roots and the root mottling. The associated red colour provides evidence of shallow water depths that might have allowed oxygenated water to produce iron oxides (Flores, 1981). Consequently the whole of the described section may represent steady lake level fall marked by a transition from lake floor to lake margin and eventually into lake infilling sediments. Farquharson (1982) attributed a similar succession to the progradation of a passive lake margin. Major lake drowning might have led to the re-establishment of dark grey, low energy lake floor sedimentation (Unit C) by fine suspension sediment fall-out. This contributed to the slow infilling of the lake to a level where currents and waves were capable of producing the uneven lamination. Another cycle of lake floor sedimentation followed, probably caused by a similar process of rising lake level and drowning (Unit D). The entire sequence was terminated by sedimentation of an active migrating channel. The alternation of drowning and shallowing of these small shallow lakes could have been due to fluctuations in the ground-water table (Galloway and Hobday, 1983).

The second described sequence (Appendix 13) represents sediments which have many characteristics in common with the previous example. The parallel and disturbed laminations (Unit C) may represent shallow lacustrine or marginal lacustrine deposits, as they sharply overly sediments interpreted as swamp deposits, as evidenced by the presence of the coal seam (Unit A) and the overlying black, highly carbonaceous

mudstone (Unit B). The swamp is also thought to have originated by abrupt channel cut off. Thus the whole sequence may represent a lacustrine facies slowly accumulating over a submergent backswamp (Gersib and McCabe, 1981).

Lacustrine facies in fluvial floodplain environments have been identified by Flores (1981), Gersib and McCabe (1981), Fielding (1984), Golia and Stewart (1984), Haszeldine (1984), Lawrence and Williams (1987), and Alexander and Gawthorpe (1993) among others. The sediments are characterised by well developed alternating laminations of dark grey organic-rich mudstone and siltstone of possible seasonal origin, commonly with no current generated sedimentary structures, reflecting low energy and a quiet reducing environment. Faunal remains and other biogenic features are rare to absent. Ethridge *et al.* (1981) suggested that fine lamination is the most important criteria for differentiating lacustrine from other overbank facies. Galloway and Hobday (1983) attributed the formation of some low relief alluvial plain lakes to the proximity of ground-water table level to the flood basin surface. They can also be induced by ox-bow lake cut off through channel abandonment.

Lacustrine facies in the core section of well BD/36 are entirely absent, and it comprises only a very subordinate amount (~ 3%) of the core section in well BD/44 and also in well BA/22 (~ 2%). Thus, volumetrically it comprises a very low percentage compared with other overbank facies which suggests that extensive and permanent deep lakes were not well developed throughout the depositional history of the formation, but were instead restricted to shallow, short-lived sites probably induced by submergence of cut-off ox-bow lakes rather than by major flood basin subsidence.

2.4.4 Swamp facies

Description: The sequence illustrated in Appendix 14 from the cored interval 12613.3 ft to 12601.8 ft in well BD/44 is an example of this facies. The interval is reproduced in detail in Fig. 2.15a. The sequence commences with unit A from 12613.3 ft to 12611.5 ft which consists of sharply based, whitish-grey, finely laminated very fine-grained silty sandstone, with intercalations of dark grey to black carbonaceous locally burrowed mudstone. This heterolithic unit is gradationally overlain by unit B from 12611.5 ft to 12610.2 ft which is composed of dark grey to black, mottled, and

possibly burrowed carbonaceous mudstone. This in turn is gradationally overlain by unit C from 12610.2 ft to 12604.6 ft consisting of light grey mottled siltstone with frequent thin layers of black, carbonaceous, locally mottled and possibly burrowed mudstone. The sequence is capped by unit D from 12604.6 ft to 12601.8 ft, represented by a 1 m thick, dark grey to black carbonaceous mudstone with a 10 cm thick coal seam at the very top. The coal is dull in luster and truncated by a medium-grained, erosively based cross-bedded sandstone. Throughout the entire sequence the carbonaceous mudstone contains plant debris, a coalified network of fine plant roots and impressions of plant stems.

Another example of this facies is shown in Appendix 15 in the cored section between 12495.5 ft and 12489.5 ft in well BD/44. The sequence commences with sharply based dark grey and brownish mudstone (Unit A) from 12495.5 ft to 12493.5 ft (Fig. 2.15b), overlying a thick, coarse-grained, cross-bedded sandstone unit. The mudstone is structureless, highly carbonaceous and contains abundant fine coalified plant roots and plant debris. Small disseminated pyrite nodules are present in the mudstone. This unit merges gradationally upward into unit B from 12493.5 ft to 12492 ft, which consists of light grey, silty, possibly mottled mudstone that lacks any sedimentary structures and is in turn gradationally overlain by unit (C) from 12492 ft to 12489.5 ft. This consists of a dark grey to brownish mudstone with preserved coalified plant debris and plant roots. Upward the unit becomes lighter in colour, and in the upper part it contains irregularly shaped, compacted, sand-filled mud cracks, ranging from 1 to 2 cm in width, and 10 to 15 cm deep. Unit C is erosively overlain by a thick package of horizontally bedded, very coarse-grained pebbly sandstone.

Interpretation: The predominantly dark grey colour of the sediments in the above sequences, abundance of plant stems, coalified plant debris, associated thin coal seams, presence of pyrite grains and lack of sedimentary structures suggests that the sediments were deposited within water-logged areas, possibly low energy swamps characterized by near-emergent surfaces of deposition (Howell and Ferm, 1980; Johnson and Pierce, 1990; Cant, 1992). The dark colour of the sediments reflects their high organic content, lack of drainage, and persistent reducing conditions due to the high water table level just above the depositional surface. The preservation of organic

debris suggests restricted circulation of the water environment (Melvin, 1987; Aslam, 1992) whilst the dominance of carbonaceous mudstone, and lack of thick coal seams indicates that these swamps may have been subjected to continuous inundations of fine terrigenous input that prevented the development of true peat and coal accumulations (Kirschbaum and McCabe, 1992). In Fig. 2.15a the swamp can be interpreted as being initiated by abrupt channel switching and abandonment, as

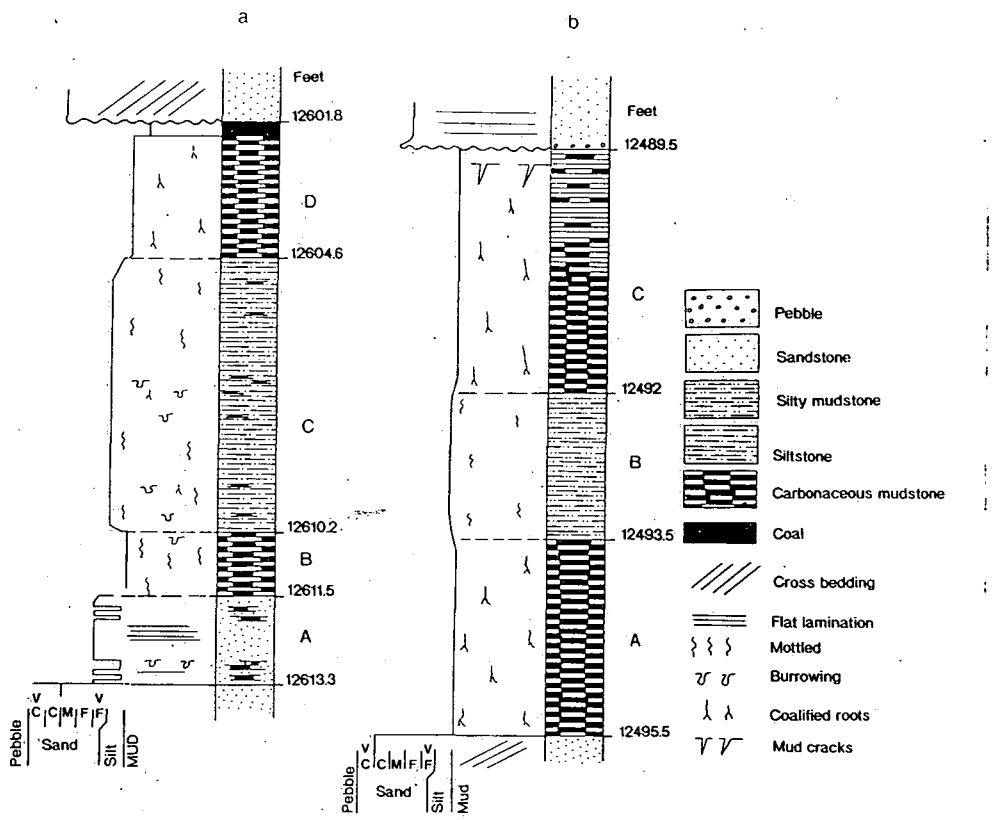

Fig. 2.15 Detail of core sections from 12613.3 ft to 12601.8 ft in well BD/44 (a) and from 12495.5 ft to 12489.5 ft in well BD/44 (b) illustrating swamp deposits.

evidenced by the sharp contact with the underlying coarse-grained sandstone unit interpreted as a channel deposit. Water depth in the abandoned channel shortly after cut off must have been favourable for the growth of vegetation and accordingly the establishment of swamp conditions enabling extensive humic sediments to accumulate (Fielding, 1984). The erosional contact with the overlying sandstone unit reflects the short-lived life of the swamp due to sediment washout and abrupt truncation by an active migrating channel. The interbedding of the carbonaceous mudstone with the light grey, fine-grained silty sandstone suggests frequent interruptions probably

caused by low energy overbank floods from a nearby active channel (Kirschbaum and McCabe, 1992). In the same sequence, an upward improvement in conditions favouring peat accumulation is thought to have developed, with consequent upward reduction in the intensity of detrital input, as evidenced by the higher carbonaceous content of the mudstone and the thin coal seam at the top possibly reflecting periodic upward shallowing of the swamp allowing denser vegetation to gradually occupy the sediment surface (Aslam, 1992).

In the sequence depicted in Fig. 2.15b the swamp conditions were similarly established by abrupt channel abandonment, but in this case the swamp is thought to have received more fine-grained clastic influx into the swamp and consequent emergence of the surface of deposition, as evidenced by the presence of irregularly shaped mud cracks (Appendix 15 Unit C). The occurrence of mud cracks normally indicates desiccation and reflects deposition within a subaerial fluvial environment (Todd and Went, 1991). The irregular shape of the mud cracks my be due to a shrinkage of the rooted mud and later compaction (Gersib and McCabe, 1981). The abundance of *in situ* plant roots in the above successions indicates the mainly autochthonous origin of the peat (Horne *et al.* 1978; Gersib and McCabe, 1981). Fielding (1985) suggested that autochthonous peats are more common in areas of flood basins characterized by emergent or near emergent surfaces of deposition. Primary sedimentary structures are rare in the carbonaceous units, probably in response to extensive root bioturbation (Ethridge *et al.* 1981).

The swamp facies comprises only a minor percentage of the overbank facies in the cored sections of well BD/44 and well BD/36. Coal accumulations throughout the entire formation are scarce, and when present they seldom exceed a few centimetres to a few decimetres in thickness. Factors discussed below may have contributed to the overall scarcity of thick coal and associated carbonaceous mudstone accumulations.

* McLean and Jerzykiewicz, (1978) suggested that preservation of peat requires a water table high enough to cover the depositional surface yet sufficiently low so that it does not drown the vegetation, and these conditions can only be found if the rate of subsidence/water level rise was equal to the vegetation accumulation rate. Such conditions were probably not common during alluvial plain sedimentation as we do not have thick coals preserved in the succession.

* Most of the carbonaceous mudstones and the associated thin coals deposited in back swamps resulted from channel abandonment and not in laterally extensive, subsidence induced flood basins that would have resulted in wide, low lying swamps. Thus, such sites were aerially restricted, ephemeral, and periodically deteriorated due to more frequent incursions of overbank fines from active channels (Diemer and Belt, 1991).
* Softness and rapid erodability of these sediments, in addition to the periodic autocyclic channel shifts, may have also resulted in the paucity of coal and carbonaceous mudstones (Casshyap and Kumar, 1987). Peats normally accumulate at very low rates of deposition (McCabe, 1984) and thus require depositional sites remote from active channels, under normal circumstances.
* In a similar case, Fielding (1984) noted that the extensive influence of the water table across an area, characterised by moderate subsidence, that promoted the establishment of swamp conditions was probably not common.
* Fielding (1985) suggested that coals and peat accumulations are generally less common in alluvial plains perhaps as a result of the tendency of the fluvial channels to migrate to the topographically low lying areas favourable for the accumulation of peat and coals.

2.4.5 Lacustrine delta facies

Description: The only documented sequence that represents this facies occurs in the cored section from 12569.6 ft to 12564 ft in well BD/44 and is illustrated in Appendix 16. A detailed section of the interval is shown in Fig. 2.16. The sequence begins with a sharply based, dark grey to brownish-grey, smooth-textured mudstone (Unit A from 12569.6 ft to 12569 ft). The mudstone commonly carries disseminated pyrite nodules ranging from 1 to 2 centimetres in diameter, as well as petrified plant roots and plant debris. Above this is a grey slightly silty mudstone (Unit B from 12569 ft to 12568.3 ft) that exhibits parallel to wavy parallel lamination, locally interrupted by 1 to 3 cm thick light grey silty streaks and lenses. Small pyrite nodules can also be seen in the lower part of the unit which is abruptly overlain by a dark grey mudstone interval (Unit C from 12568.3 ft to 12567 ft). This mudstone lacks preserved sedimentary structures or biogenic features and is in turn gradationally overlain by a grey to light grey muddy siltstone (Unit D from 12567 ft to 12565.2 ft). This muddy siltstone unit

contains very thin light grey silty streaks. The latter become thicker and more common towards the top of the unit, which shows local destruction of sedimentary structures probably due to bioturbation and burrowing.

The sequence is capped by a greenish-grey structureless siltstone (Unit E from 12565.2 ft to 12564 ft) which passes abruptly upwards into a thick, intensely rooted and bioturbated brownish-grey mudstone package.

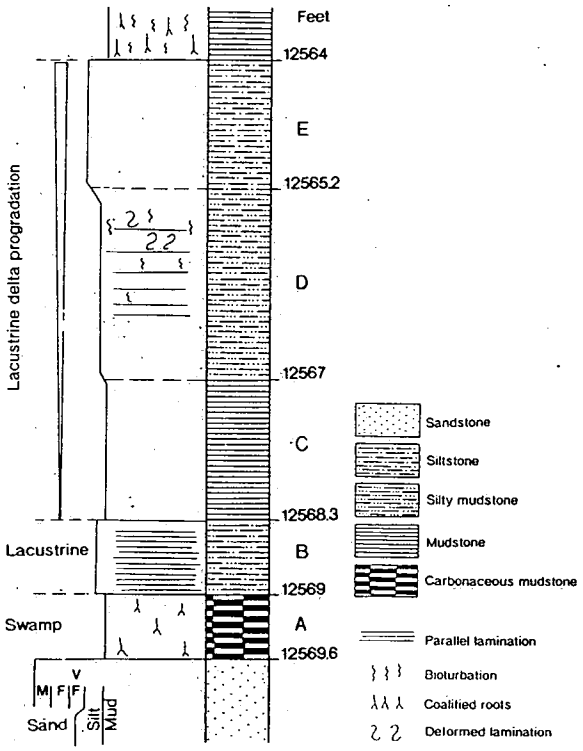

Fig. 2.16 Detail of core section between 12569.6 ft and 12564 ft in well BD/44 representing swamp, lacustrine and lacustrine delta fill deposits.

Interpretation: The sequence described above records the initiation of a swamp deposit which resulted from abrupt channel abandonment (Unit A). The swamp in turn is thought to have been abruptly terminated by sudden drowning (rise in base level) that led to the establishment of a lake and deposition of lacustrine sediments structured predominantly by parallel lamination (Unit B). The absence of biogenic features and presence of pyrite indicates that conditions within the lake were anoxic and not conducive to life. The minor coarsening-upward sequence, represented by the

stacked units C, D and E, may thus reflect silting-up of the shallow lake, prior to its filling and termination. Thus the section can be attributed to progradation of a small fluvio-lacustrine delta system (Oomkens, 1970), as described from the Coal Measures of NE England (Fielding, 1986). Such coarsening-upward sequences are thought to have developed as a result of crevasse splay progradation into a ponded water body or overspill material derived from an approaching active channel (Kelling, 1968). The advancing delta and concomitant filling of the depression eventually resulted in the emergence of the depositional surface, as evidenced by the thick rooted and pedogenically mottled brownish-grey mudstone package (Upper part of Fig. 2.16).

As mentioned elsewhere in this chapter, subaerial crevasse splay progradation also produces a similar coarsening-upward trend and in this example a subaqueous crevasse splay interpretation is mainly based on their stratigraphic position overlying lacustrine deposits (Picard and High, 1981). Cuevas Gozola and Martinius (1993) suggest that the most important differences between subaerial and subaqueous crevasse splays is that deltaic deposits infilling lakes usually consist of several layers separated by mud intervals due to different stages of progradation. They also noted differences such as the burrowing of the deltaic deposits and the absence of features such as carbonate palaeosols and mud cracks diagnostic of exposed sediments. Ethridge *et al.* (1981) suggested that lacustrine delta-fill deposits are characterised by high angle foreset beds that display soft sediment deformation and slump structures, and possibly small-scale structures such as ripples, and lenticular and wavy laminations. Sediment deformation may be the result of compaction and wave modification, or erosion during a fall in lake level (Golia and Stewart, 1984). It can also be explained as a result of decrease in flow velocity when crevasse splays enter ponded water (McKee *et al.* 1967). The criteria described above are probably applicable to the upper part of unit D.

The relatively small thickness of the coarsening-upward unit which represents the fluvio-lacustrine delta implies that the lake was shallow. However, differences in thickness and composition of fluvio-lacustrine sediments is a function of proximity to the source channel (Diemer and Belt, 1991). Kelling (1968) has identified a similar succession which he interpreted as an advancing fluvio-lacustrine delta system.

2.4.6 Well-drained flood plain facies

Description: Compared with other overbank facies, this facies comprises about 30 % of the cored section in well BD/44 and about 15 % in well BD/36. The cored section (Appendix 17) in well BD/44 illustrates an example of this facies. The sequence is characterised by an extensively colour mottled massive mudstone, ranging from earthy, reddish-brown to pale grey and greenish-grey. The mudstone is silty in parts and locally traversed by hairline networks of plant roots. Coalified organic debris is rare to absent. In general the mudstone is firm and crumbly, and in many cases it breaks along irregular smooth and shiny polished surfaces. Carbonate concretions are also common (Appendix 17 - arrow), occuring as either single or coalesced nodules ranging from 1 to more than 10 cm in diameter.

Interpretation: The section described above can be interpreted as a well-drained flood plain facies. This interpretation is based on the fine-grained nature of the sediments, colour mottling, abundance of plant roots, presence of carbonate concretions and the paucity of organic remains (Ethridge *et al.* 1981; Johnson, 1984; Melvin, 1987, 1993). The section may thus represent sedimentation from suspension fall-out of fine-grained sediments in areas of the flood plain remote from active channels.

The crumbly nature of the sediments and the ease with which the mudstone breaks along smooth polished surfaces. These resemble slickensides or internal tension surfaces of dislocation (pore-defining peds?) due to soil expansion and contraction in response to a seasonally fluctuating groundwater table. Gordon and Bridge (1987) and Melvin (1987) have attributed such features to the expansion of plant roots which are areas of low strength within the sediment pile. Within this facies, the original organic content has largely been destroyed by oxidation and faunal remains, if present, would be leached by fluctuations of the ground-water table (Johnson, 1984).

Carbonate concretions within fine sediments may reflect long periods of exposure consistent with aridity and long phases of channel inactivity (Turner, 1978; Lawrence and Williams, 1987). Moore and Nilsen (1984) have described similar successions extensively bioturbated by roots, exhibiting massive features, colour mottling and slickensides coupled with carbonate concretions forming stacked palaeosols, probably representing more proximal locations within the flood plain.

2.4.7 Poorly-drained flood plain facies

Description: This facies is less common than the well-drained flood plain deposits. The sequence, represented by the cored interval from 12457 ft to 12450.5 ft in well BD/44, is shown in Appendix 18. It consists of a firm, brownish-grey to grey mudstone (Unit A). The mudstone is slightly silty and locally traversed by networks of fine coalified plant roots, plant stems and other organic debris. Slickensides are also common but less dominant than in the well-drained flood plain facies. The mudstone merges gradually into blackish-grey, massive carbonaceous mudstone with frequent grains of pyrite (Unit B). The lower contact of the sequence with the underlying sediments is not well preserved in the core section.

Interpretation: Unit A is interpreted as poorly drained flood plain sediments deposited during episodic overbank flooding. Although roots normally represent exposure, the dominant grey colour of the sediments and the associated organic debris suggests a reducing environment which may indicate that the surface of deposition was continuously wet and saturated with water (Johnson and Pierce, 1990). The gradual merging of Unit A into the darker colour, pyritic and carbonaceous mudstone (Unit B) may imply the gradual submergence of the surface of deposition and the establishment of swampy conditions.

Poorly-drained flood plain facies seem to occur in alternation with their well-drained counterpart in the cored sections, suggesting oscillations of the ground-water table level. Relationship to the ground-water table may override climate in determining the nature of the flood plain (Galloway and Hobday, 1983). Moore and Nilsen (1984) suggest that red coloured and mottled shales represent deposition on higher parts of the flood plain (Proximal) whereas darker shales may be indicative of topographically lower and distal locations resulting in wetter hydromorphic soils.

2.5 Meander belt deposits

Description: The stacking of channel sequences from 12704.7 ft to 12532 ft in the core section of well BD/44 (Appendix 19) probably represents a fully preserved meander belt deposit. The base of the sequence is an erosional surface equivalent to

the fifth and sixth order bounding surfaces of Miall (1988a, b). The sequence consists of preserved point bar deposits and the fills of both abruptly and gradually abandoned channels, containing cross-stratification, horizontal lamination and ripple cross-lamination. Local erosion surfaces overlain by a basal breccia of mudstone rip-up clasts are also common. Some of the channel sequences show an incomplete fining-upward trend lacking passive channel fill deposits which could have been truncated by the succeeding channel segment. In the multistorey valley fill sandbody overbank fines are relatively minor and comprise < 10 % of the total preserved thickness.

Interpretation: The vertical stacking is interpreted to have evolved as a result of aggradation of a laterally migrating meander belt system possibly within an incised valley. Bridge (1985) suggested that within an aggrading channel belt the superposition of different channel fills and lateral accretion deposits is expected in all river types yielding a multi-storey character where each storey is a separate point bar or channel fill. The absence of such a multi-storey character in a meander belt is indicative of a low aggradation rate relative to channel migration. Diemer and Belt (1991) interpreted a multistorey sandbody as a result of channel belt development, where point bars and aggrading channel fills alternate and migrate successively down valley.

The scarcity of fine-grained sediments is attributed to the dominance of lateral channel migration over vertical aggradation (Bridge *et al.* 1986) or the fact that valley walls could have acted as a topographic threshold and consequently restricted the lateral migration of the channel belt giving no opportunity for overbank fine-grained sediments to be extensively preserved (Cuevas Gozola and Martinius, 1993). Collinson (1978) also claimed that preservation of overbank fines is a function of channel migration frequency which can be stabilised by clay plugs produced by channel cut-off events. It has also been suggested by Friend (1978) that within a valley fill deposit the presence of overbank fines may be explained in a number of ways such as high input of fine sediments and restriction of channel movement, but it is also favoured by lack of flood plain restriction by valley walls. Diemer and Belt (1991) suggested that avulsion in a meandering stream normally takes place during flood events and a river may comprise a low sinuosity course in the proximal part near the

proximal reaches of the avulsion (Fig. 2.9c). This may thus explain the low sinuosity channel sequence at the top of the meander belt deposits. Meander belts abandoned as a result of upstream avulsion may eventually become a topographic high on which back swamps, characterised by a high surface of deposition away from detrital input, may develop (Warwick and Flores, 1987).

The abandoned meander belt comprises a complex of elongate and laterally restricted sandstone bodies (Collinson, 1978). Meander belt width in this case can be predicted using the empirical formula of Collinson (1978) developed for high sinuosity streams.

Meander belt width (m) = $64.6 * (d)^{1.54}$ where 'd' is channel depth.

It has been suggested by Cuevas Gozola and Martinius (1993) that the preserved thickness of individual sandstone bodies within a channel complex does not have a direct relationship to the original thickness due to erosion of the upper part. Channel sandbody thickness therefore, is not equivalent to the channel depth with two exceptions: either the sandstone is an individual sandbody or the deposit is a meander lobe where the upper parts are preserved and possibly connected to overbank deposits. Accordingly channel depth, as previously estimated from a fully developed point bar, is approximately 4.5 m, with an estimated meander belt width of 655 m.

Chapter 3

Sedimentary facies analysis from wireline logs

3.1 Introduction

Traditionally subsurface lithology is determined from core or cutting analysis. It is however, often difficult to provide a continuous description of the formation from core data because very few holes are completely cored, and it is difficult to restore the components and the proper thickness of the lithological column from the second type. This is a function of the loss of some constituents (e.g. shale and siltstone), the influence of hole caving and other difficulties. Wireline logs, in contrast, give a continuous survey of the formations intersected by the well. It is also accepted that modern logging tools when used in combination, can give a good indication of the lithology (Schlumberger, 1989b; Rider, 1991). This is the basis of the concept of electrofacies. The term electrofacies has been defined as " *The set of log responses which characterises a bed and permits it to be distinguished from other beds* " (Serra and Abbott, 1980), and is considered to be analogous to the lithofacies (Delfiner *et al.* 1984) which represents a sedimentary rock unit deposited under certain environmental conditions. On the other hand, a set of vertically adjacent and genetically related electrofacies will give rise to the electrosequence (Schlumberger, 1989a). For instance, the bell and funnel shapes of gamma-ray logs correspond to typical forms of electrosequences.

Selley (1976) claimed that similar log patterns are sometimes produced by different environments. For this reason wireline log patterns should never be interpreted in isolation, and for better resolution it is necessary to compare core and log values.

In this chapter the interpretations are qualitative rather than quantitative based on wireline logs. The qualitative use defines not only the lithology but also the overall log patterns, curve shapes, trends, anomalies, contact relationships and base lines.

The purpose of this chapter is to review the use of wireline logs in facies analysis, and to define various characteristic motifs and integrate them with the sedimentary depositional environment (Appendices 22, 23, 24). A discussion of most common log types is represented in order to discuss their characteristics and limitations. However, the logs which will be used in this chapter are not capable of recording very thin beds. i.e. their bed resolution is limited.

3.1.1 Total gamma-ray log

The total gamma-ray log is a continuous record of the formations radioactivity which comes spontaneously from the three natural occurring radioactive elements thorium, uranium and potassium combined (Rider, 1991). The emission of gamma-rays is statistical (Doveton, 1986). Generally, natural radioactive minerals have a far greater concentration in mudstones than in most other sedimentary rocks (Table 3.1). Sedimentary rocks with high clay content will commonly emit higher gamma-ray than those with less clay content (Chamberlain, 1984; Rider, 1990). However, radioactive detrital grains may contribute significantly to the radioactivity of a sandstone and can obscure the general relationship between shaliness and gamma-ray log values. Accordingly, when interpreting the gamma-ray log shape of a sandstone difficulties arise because naturally radioactive silt- and sand-size detrital grains are mixed with the non-radioactive components. The commonly occuring natural radioactive detrital components include K-feldspar and rock fragments, when composed of mica (Doveton, 1986; Hurst, 1990). On the other hand, mudstones can not be considered as exclusively radioactive (Dybvik and Eriksen, 1983). For instance, illite is considered to be the main source of K emissions while chlorite contributes only a minor amount (Hurst, 1990). Consequently, any change in clay mineral composition will most likely entail a change in radioactivity (Rider, 1990). The presence of glauconite and heavy minerals e.g. zircon can give anomalously high gamma-ray readings (Selley, 1976). In addition authigenic and detrital forms of clay minerals may have different radioactivity (Humphreys and Lott, 1990). High organic content within sediments is often associated with high gamma-ray log values, due to the concentration of uranium adsorbed by organic matter (Schmoker, 1979, 1980). The primary relationship

Lithology/mineral	*Gamma-ray (API)*
Sandstone	*18 - 160*
Shale	*24 - 1000*
Limestone	*18 - 100*
Coal	*0 - 24*
Quartz	*0*
Muscovite	*140 - 270*
Biotite	*90 - 275*
Feldspar	*220 - 280*
Chlorite	*180 - 250*
Kaolinite	*80 - 130*
Smectite	*150 - 200*

Table 3.1 Gamma-ray logging-tool response values for common lithologies and minerals. (After Rider, 1991).

between grain size and the gamma-ray log can be additionally affected by the frequent occurrence of sandstone diagenesis e.g. the destruction of K-feldspar into illite. However, the effect of diagenesis is usually very difficult to asses (Rider, 1990).
The total gamma-ray log can be affected in the subsurface by borehole conditions such as hole enlargement and formation density i.e. the denser the formation the lesser the gamma-ray value (Rider, 1991). Bed resolution is about 30 cm for a logging speed of 30 cm/s.

3.1.2 Sedimentary environment interpretation from total gamma-ray logs

The most straightforward method of identifying facies and sedimentary environments from total gamma-ray logs is based on the relationship between grain-size and shale content (Schlumberger, 1989a; Rider, 1990, 1991). This relationship is disturbed primarily by two factors, one is compositional and the other is textural (Rider, 1990). As a general rule gamma-ray logs read low in sandstones and high in shales, and it is a matter of observation that clay content generally decreases with increasing grain-size

(Selley, 1976). Consequently, gamma-ray logs can be used as a continuous grain-size profile in clastic sections. Radioactivity is indirectly related to sediment grain- size but instead has a direct relationship to the amount of clay captured. The sedimentological interpretation of log shapes will in turn depend on the extent of the relationship between grain-size and clay content. The composition and texture of sedimentary rocks is greatly related to the hydraulic regime and energy of the environment of deposition (Davies and Ethridge, 1975; Myers and Bristow, 1984). In fluviatile environments, however, the relationship between grain-size and clay content is more consistent than actively winnowing marine environments where the clay fraction is more likely to be washed out from sediments of different grain-sizes (Rider, 1991). The most commonly cited gamma-ray log shapes are the bell, funnel and barrel shape as illustrated in Fig. 3.1. Gamma-ray log profiles may be applied in an analogous

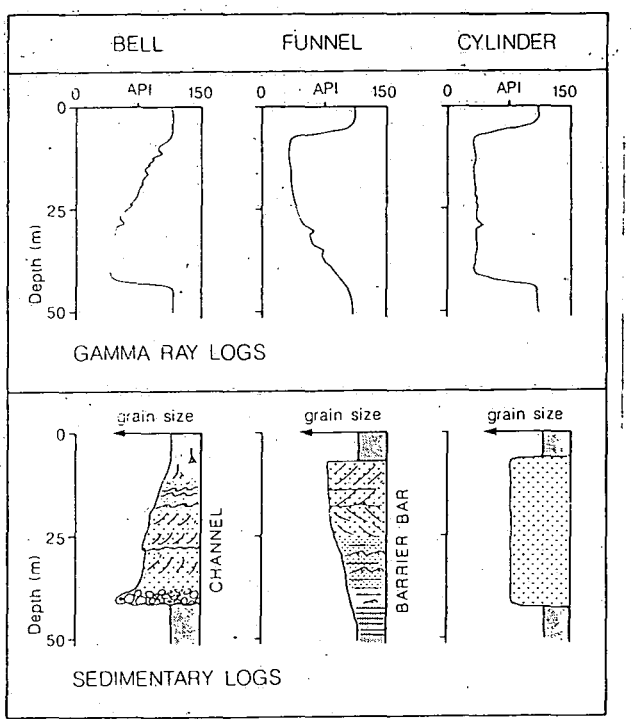

Fig. 3.1 The three principal gamma-ray log shapes and their corresponding sedimentary interpretation, after Rider (1990).

manner to the spontaneous potential log (SP) for the interpretation of sedimentary environments (Doveton, 1986). Thus, there is great diversity of gamma-ray log shape as illustrated in Fig. 3.2a. Selley (1976) advocated an approach using the gamma-ray log in conjunction with levels of glauconite and carbonaceous matter (Fig. 3.2b).

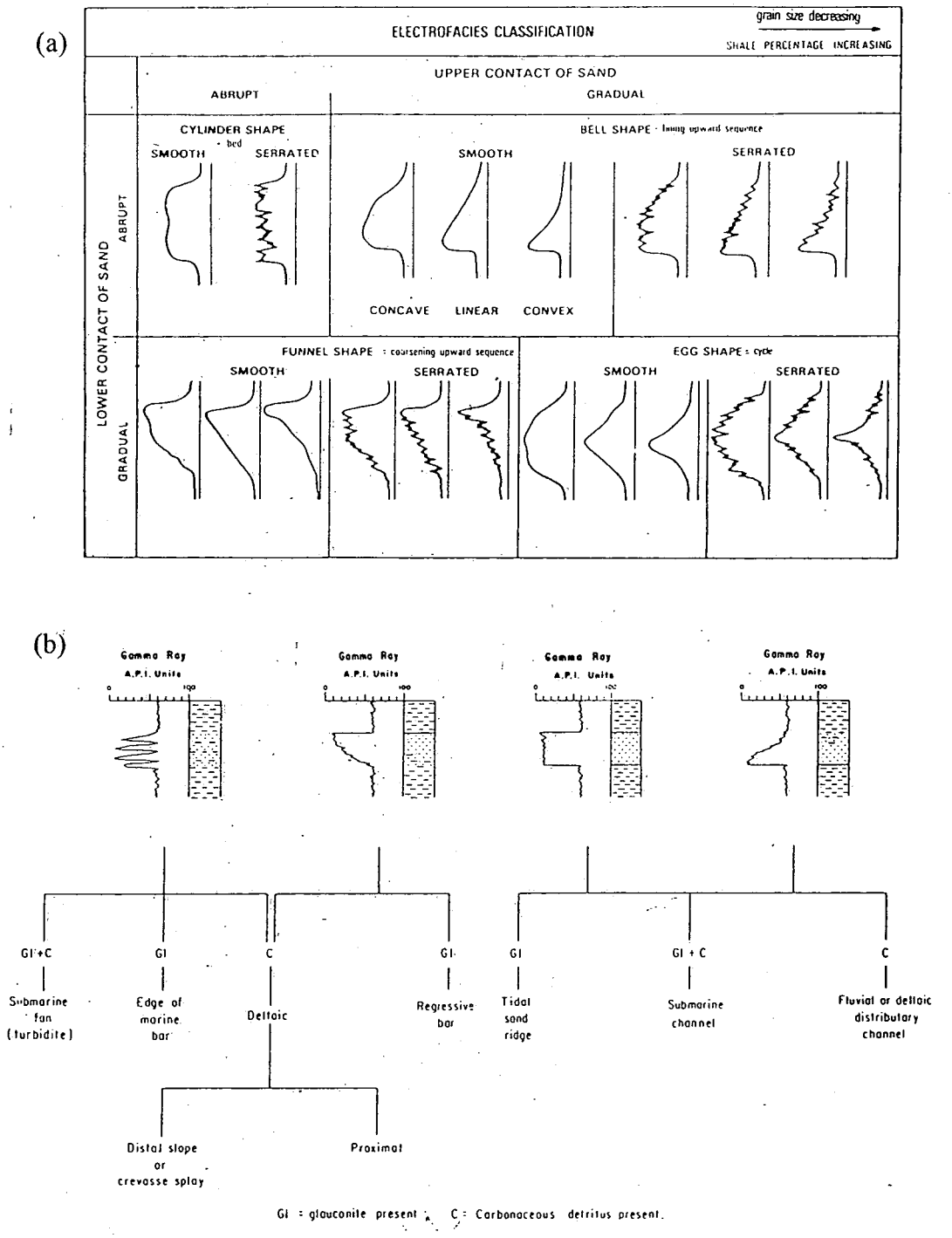

Fig. 3.2 Relationship between gamma-ray curve shape and grain-size or shaliness (a), after Schlumberger (1989a). Four characteristic gamma-ray log patterns in clastic sedimentary rocks (b), from left to right: thinly interbeded sand and shale, upward-coarsening profile, uniform sand with abrupt contacts, and fining-upward sequence with an abrupt base. (Modified from Selley, 1976).

Shale base lines can be drawn to estimate readings for normal shaliness. Similarly sand base lines for clean intervals can be plotted which coincide with the lowest readings. Gamma-ray log shape, however, can reflect an overall trend rather than just individual sediment bodies.

3.1.3 spectral gamma-ray log (NGS)

Several natural radioactive isotopes occur in sedimentary rocks. The main contributors of gamma-ray radiation are thorium, uranium and potassium (Adams and Weaver, 1958). Other radioactive isotopes are typically very modest contributors and may generally be disregarded (Dybvik and Eriksen, 1983). From the NGS log, the contributions of individual radioactive minerals are displayed separately which can then be used to map more subtle changes in lithology and sedimentary environment, identification of zones of heavy mineral concentrations, clay mineral fraction, distinction of mica and K-feldspar from clay minerals and identification of uranium-rich black shale (Doveton, 1986). Table 3.2 shows the concentration of these three radioactive components and their distribution. However, the distribution of the three elements is complex, involving the composition of the parent rock, sedimentary environment processes and the different geochemical properties of each element (Cowan and Myers, 1988) which sometimes leads to an ambiguous interpretation (Doveton, 1986).

Mineral	***Th(ppm)***	***U(ppm)***	***K(%)***
Illite	*10 - 25*	*1 - 5*	*3.5 - 8.3*
Kaolinite	*6 - 47*	*1 - 12*	*0 - 0.6*
Chlorite	*3 - 5*		*0 - 0.3*
Smectite	*6 - 44*	*1 - 21*	*0 - 1.5*
Muscovite	*0 - 25*	*2 - 8*	*7.8 - 9.8*
Biotite	*0.5 - 50*	*1 - 40*	*6.2 - 10*
K-feldspar	*3 - 12*	*0.2 - 3*	*10.5 - 16*

Table 3.2 Th, U and K concentrations for some typical sandstone minerals. (From Hurst, 1990).

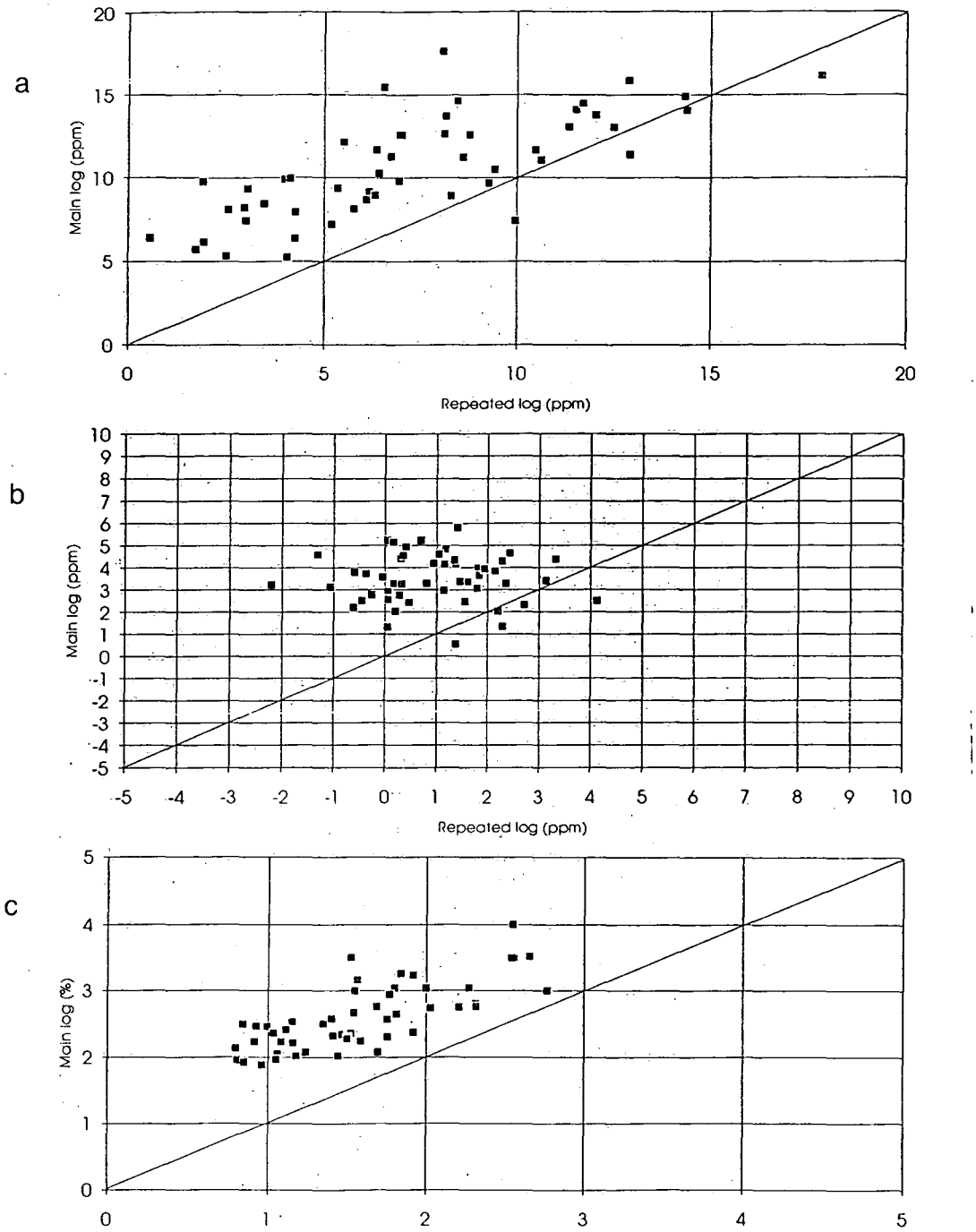

Fig. 3.3 Comparisons between main and repeated NGS log in well BD/44 from 13000 ft to 13100 ft illustrating thorium (a), uranium (b), and potassium (c). Note the shift of points above the 1-1 line probably due to statstical errors in log measurement.

As with the total gamma-ray log, the NGS log measurements are statistical and the measurement precision can vary from one log run to another (Hurst, 1990). Fig. 3.3 gives a favourable impression of the NGS log measurement accuracy by illustrating individual main log values for thorium, uranium and potassium plotted for repeated sections measured over the same depth intervals from 13000 ft to 13100 ft in well BD/44. The pronounced shift above the 1 to 1 line in both cross-plots inevitably reflects the random nature of radioactivity. The variation in precision is also aided by other factors such as log-depth matching accuracy and logging speed changes (Hurst, 1990). However, absolute measurements of radiation are not as important as the relative shifts (Chamberlain, 1984). Both total and NGS gamma-ray logs are used in conjunction with other log data in order to provide a realistic aid to environmental interpretation. Bed resolution is similar to the total gamma-ray log.

3.1.4 Sonic log

This log measures the acoustic velocity through the formation which is conventionally recorded as transit time (t) expressed in terms of microseconds per foot. It has to be considered that the transit time through a formation is not only a function of lithology but is also related to the pore fluid (Doveton, 1986; Schlumberger, 1989b). Table 3.3 illustrates different sonic log velocity and transit time ranges for various lithologies and minerals.

Lithology/mineral	*Tr. time (mic sec/ft)*	*Velocity (ft/sec)*
Sandstone	*55.5 - 51*	*18000 - 19500*
Quartz	*55.1*	*18150*
Limestone	*53 - 47.6*	*19000 - 23000*
Shale	*167 - 62.5*	*5000 - 16000*
Coal	*140 - 180*	*6500*
Organic matter	*180*	*5550*

Table 3.3 Average transit time and acoustic velocity ranges for some common lithologies and minerals. Modified from Stocks and Lawrence (1990) and Rider (1991).

The considerable amount of overlap in the velocity ranges indicates that the sonic log alone is seldom diagnostic of a certain lithology except for the case of rock types which are often close to a pure state, e.g. sandstone and coal which can be defined by narrow velocity ranges (Rider, 1991). Mudstone on the other hand, is a general term for a variety of clay mineral mixtures sometimes with accessory constituents such as organic matter. As a result mudstone transit time is drawn from the log itself in intervals indicated by other logs, e.g. gamma-ray (Doveton, 1986).

Because of its shallow depth of investigation, the sonic log can be affected by borehole irregularities. The bed resolution is about 2 feet and consequently thin beds may simply be disregarded.

3.1.5 Density log

This log is a continuous record of the formation bulk density expressed in terms of gm per cubic cm on a standard scale ranging from 1.95 to 2.95, which covers the actual density range of common rock types (Doveton, 1994). The measured density thus varies according to various lithologies. Table 3.4 portrays tool-derived densities of some common components with a considerable amount of overlap. Depth of investigation is very shallow (few cm), which means that the density log is affected by borehole irregularities. In contrast, bed resolution is acceptable (5-10 cm) compared to other macrodevice logs (Rider, 1991) making the log useful for drawing bed boundaries.

Lithology/mineral	*Bulk density (gm/cub. cm)*
Sandstone	*1.9 - 2.65*
Limestone	*2.2 - 2.7*
Shale	*1.8 - 2.75*
Organic shale	*1.8 - 2.4*
Coal	*1.15 - 1.7*
Pyrite	*4.8 - 5.17*

Table 3.4 Diagnostic log-measured lithology and mineral densities, after Rider (1991).

3.1.6 Neutron log

The basic significance of this tool is the indirect estimation of the formation porosity. The measured porosity actually reflects the hydrogen concentration (Schlumberger, 1989b). In most cases the cause of the hydrogen enrichment is the water contained in the sediment pore spaces (Doveton, 1994). Each mineral or lithology has its own diagnostic hydrogen richness which is translated by the neutron log into porosity values (Table 3.5). The neutron log has a slightly lower bed resolution than the density log. The best minimum resolution is about 1 m although true formation values may be obtained in beds down to 60 cm thick (Rider, 1991). When used in combination with the density log, the neutron log is an excellent lithology indicator.

Lithology/mineral	*Neutron porosity %*
Sandstone	*(-2) - 25*
Limestone	*(-1) - 30*
Shale	*25 - 75*
Coal	*38 - 52*
Quartz	*-2*

Table 3.5 Approximate ranges for neutron log porosity values for some common lithologies. Modified from Rider (1991).

3.2 Comparisons between core-derived facies and corresponding electrosequences

3.2.1 High sinuosity channel electrosequences

Fig. 3.4 (Units A, B and C) represents a point bar facies in well BD/44. This shows the close relationship between core-derived grain-size and the total gamma-ray log shape which corresponds to the bell shape of the typical fining-upward sequence (Fig. 3.1). The change in the level of radiation across the electrosequence reflects variations in clay content (Chamberlain, 1984). The electrosequence has an abrupt lower contact marked on various log patterns reflecting major incision into the underlying substrate. Electrofacies A (20 cm thick) is represented by a conglomeratic lag deposit composed

of matrix-supported quartzitic pebbles and mudstone clasts. Because of its small thickness, unit A has no distinctive log response apart from the slight shift in the neutron log which probably reflects the water content of the mudstone clasts (Table 3.5). Schlumberger (1989a) show that conglomerates can only be defined by their high resistivity values or by the dipmeter tool. The serrated nature of the gamma-ray log across electrofacies B1 corresponds to levels of contrasting grain size. These have been defined in the cored section as probably representing lateral accretion surfaces and reactivations caused by fluctuating discharge (Selley, 1976; Collinson, 1978, 1991; Galloway, 1981). Apparently, in electrofacies B1, the main source of radioactivity is thorium. In contrast, potassium remains almost unchanged across the entire sequence as can be seen from the NGS log response, reflecting minor changes in the sandstone composition. The density log also shows variations which are most probably related to textural changes (Rider,1990). Fig. 3.5a illustrates that chlorite/smectite (montmorillonite) is the dominant clay mineral type. Yet few scattered points of low thorium content are present and may indicate an illitic clay mineral and minor radioactive detrital grains. The potassium content of both smectite and chlorite are negligible (Eslinger and Pevear, 1988 and Table 3.2). However, the presence of heavy minerals in the sandstone as a source of thorium may preclude the application of thorium in clay mineral identification (Hurst, 1990). Accuracy is less important here as long as the exact composition of the sandstone is not a major goal.

The anomaly (Electrofacies B2) corresponds to a level of well-cemented sandstone. Both density and neutron logs show a considerable shift. The density log shows an increased average sandstone density from 2.3 to 2.45 gm/cc whilst the neutron porosity decreases from about 20 to approximately 11 %, accompanied by a change in the sonic log from about 90 to 70 mic sec/ft. This cementation causes a dramatic reduction in sandstone porosity from about 25% to almost 0%. In the sandstone of the Brent Group (Middle Jurassic), northern North Sea, authigenic kaolinite is one of the commonest and most abundant cement types (Humphreys and Lott, 1990) which, on purely mineralogical grounds, has a negligible inherent radioactivity (Cowan and Myers, 1988). Generally, in meandering river sediments kaolinitic cement is the most common (Schlumberger, 1989a).

Fig. 3.6 shows a comparison between the core-derived facies of a gradually abandoned high sinuosity channel and equivalent log response. Similar to the previous point bar electrosequence, this one corresponds to the bell shape of the typical fining-upward sequence. The thin basal lag (Electrofacies A, approximately 20 cm thick) can not be distinguished from the log response. Unit B which makes up most of the electrosequence is marked by the presence of three vertically stacked fining-upward sequences. These probably correspond to fluctuating flow discharge and low stage reactivations which are also reflected in the cored section by contrasting grain size and variations in the amplitude of the sandstone cross-bed sets. As in the previous example, electrofacies B1 and B3 correspond to levels of cemented sandstones. It is possible to estimate the type of cement from mineralogical compositions obtained from wireline logs (Schlumberger, 1989a), and in this example a siliceous/kaolinitic cement type is inferred from the low radioactivity. Electrofacies C is marked by a drastic variation in almost all log patterns, representing a marked change in litho-type from sandstone-dominated to mudstone-dominated electrofacies. Across the electrosequence, the overall upward increase in degree of shaliness is prominent on almost all log patterns. This is explained in the upward increase in radioactivity, neutron porosity and the slight upward increase in both transit time and formation density. However, comparing the two previous examples it is obvious that the fining-upward trend of the first example is more prominent than that of the gradually abandoned channel electrosequence. This is probably related to the higher degree of shaliness of the point bar sequence. Considering the variation between the log-derived porosity (ϕ) and the hydrocarbon-occupied porosity (ϕsh) (Fig. 3.4, 3.6), in the point bar electrosequence the isolation between the two porosity curves is more pronounced than that of the gradually abandoned channel, possibly reflecting the isolation of the point bar sequence in a host of fine-grained sediments after cut-off had taken place (?). Applying the Th/K cross-plot (Fig. 3.5) it is possible to predict the difference in lithological composition between the two electrosequences. As can be seen from the cross-plot the lithology of the gradually abandoned channel fill reflects less mature, less washed and winnowed sediments than the point bar sandstones. In the fluvial environment the most winnowed sediments are significantly enriched in quartz (Davies and Ethridge, 1975). Most of the points (Fig. 3.5b Series 1) fall within the

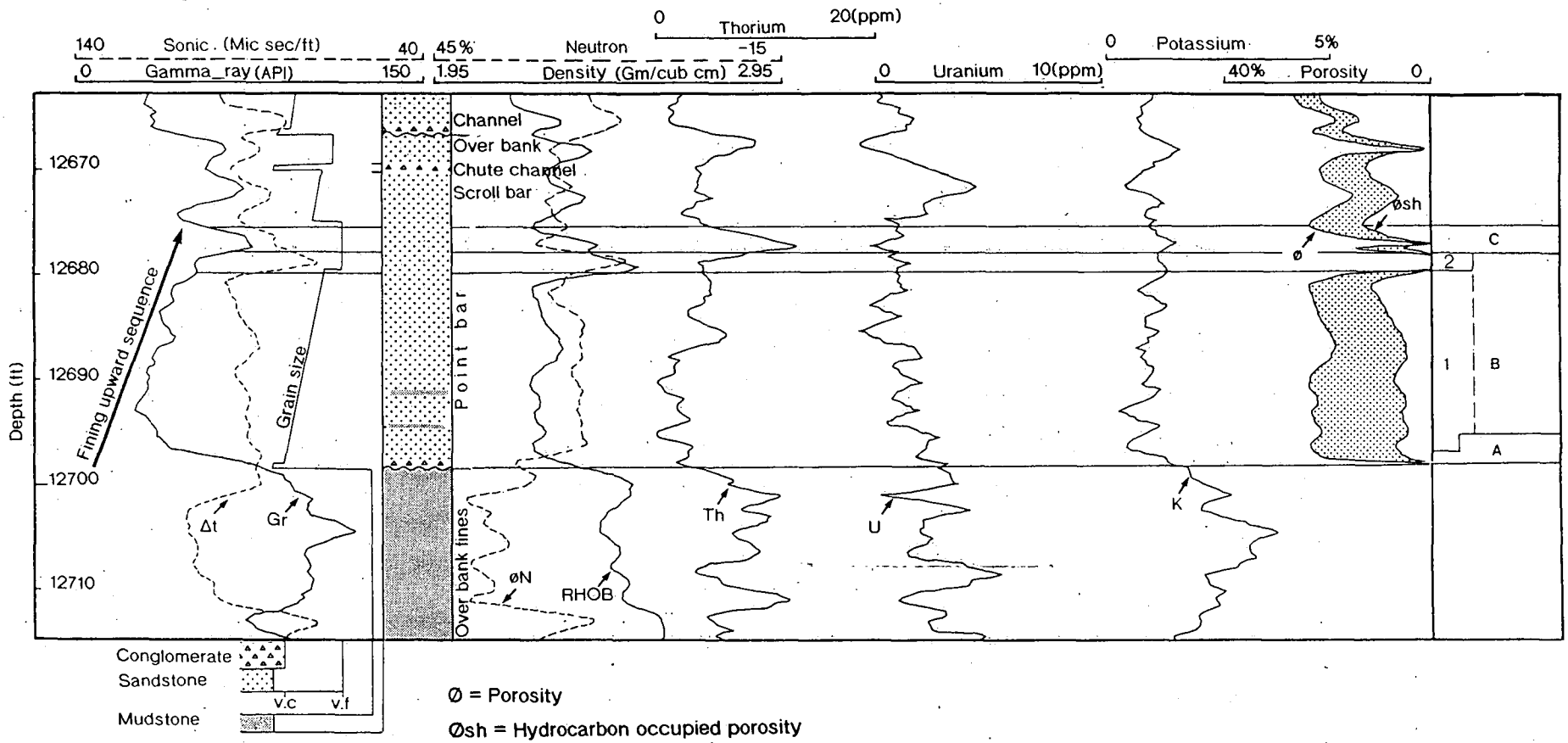

Fig. 3.4 Point bar sequence of a high sinuosity channel in well BD/44 illustrating comparison between core-derived lithology and log patterns. Gamma-ray log shows typical bell shape.

Th (ppm)
K (%)
0
4
8
12
16
20
0
1
2
3
4
5
6

Th (ppm)
K (%)
Series1
Series2
0
4
8
12
16
20
0
1
2
3
4
5
6

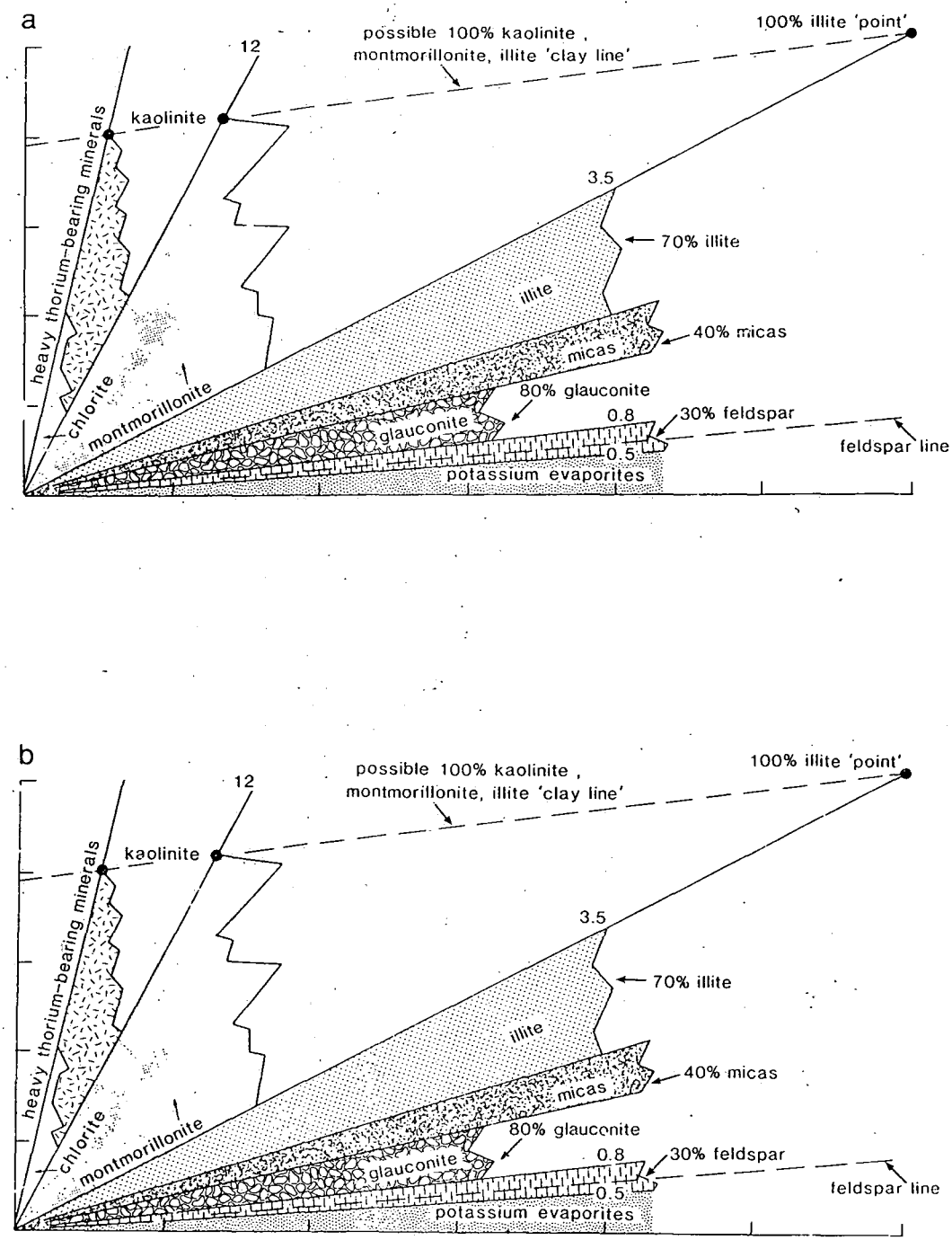

Fig. 3.5 Th/K cross-plots in well BD/44, in point bar sediments in the depth interval from 12700 ft to 12675 ft probably indicating mature sandstone (a). Similar Th/K cross-plot in well BD/44, in a high sinuosity channel sequence from 12668 ft to 12635 ft, probably represent less mature sandstone (b). Series1 represents Th/K cross-plot for channel sandstone sequence, and series2 represents Th/K cross-plot for channel abandonment sequence (See Fig. 3.4).

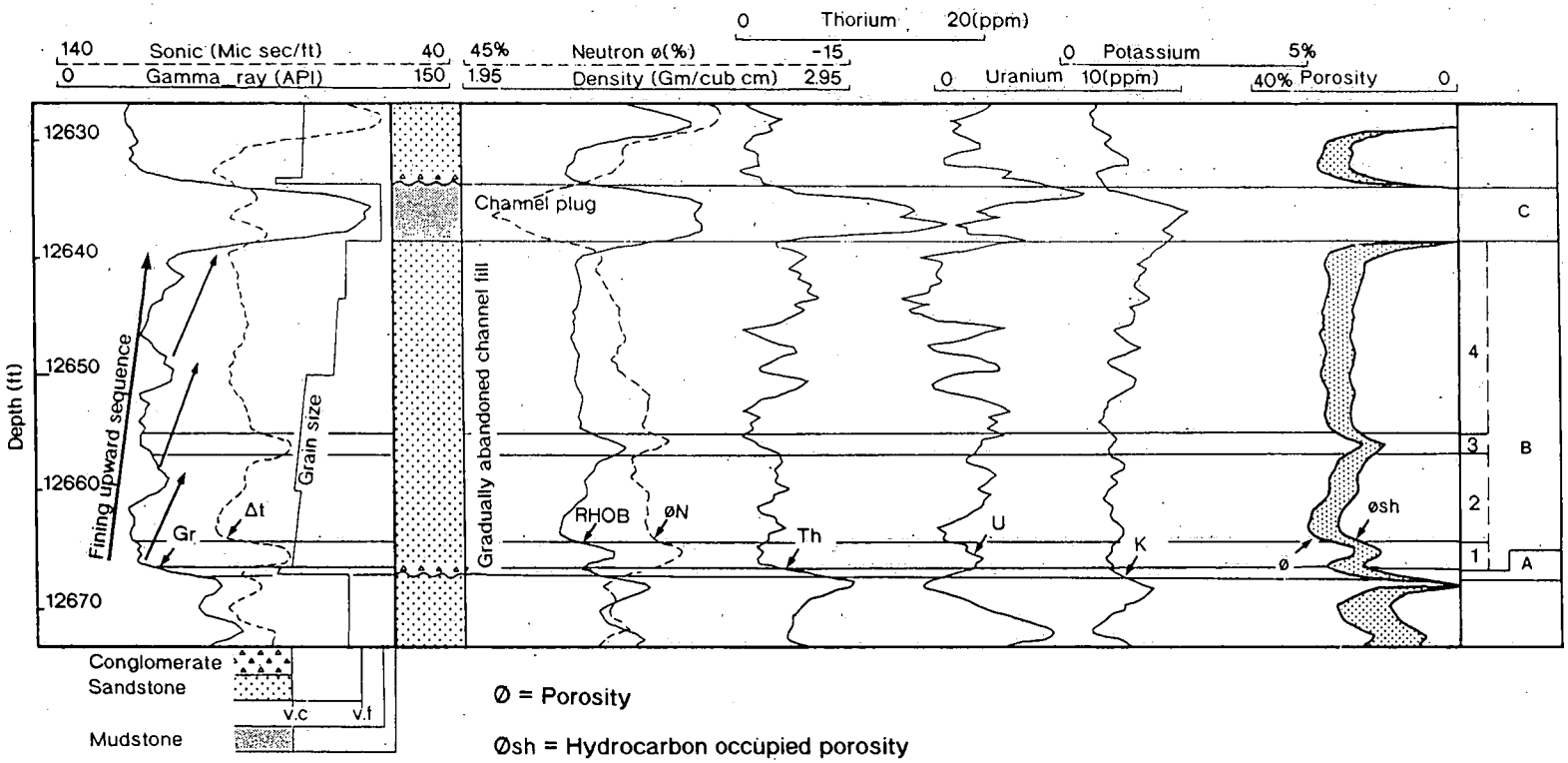

Fig. 3.6 Comparison between core-derived high sinuosity, gradually abandoned channel facies and the corresponding electrosequence in well BD/44 core section. The overall gamma-ray log shows the typical bell shape consisting of minor fining-upward sequences.

compositional range of illitic clay. However, the majority of points represent common radioactive detrital grains of k-feldspar and mica. Glauconite is always considered to be a marine indicator (Selley, 1976, 1985). Scattered points and points falling within the range of glauconite (Fig. 3.5b series 1) are probably attributed to statistical errors of the NGS log measurements (see section 3.1.3). Points corresponding to series 2 (Fig. 3.5b) represent mainly illitic clay mineral types of the channel plug electrofacies (c).

3.2.2 Low sinuosity channel electrosequence

The electrosequence (Fig. 3.7 electrofacies A, B) clearly matches the gamma-ray barrel log shape (Fig. 3.1), with abrupt upper and lower boundaries corresponding to abrupt incision and abandonment of a low sinuosity channel in well BD/44. The serrated shape of the gamma-ray log corresponds to contrasting grain size within the parallel stratification and cross-bedding of the poorly sorted, predominantly very coarse-grained sandstone. This has been attributed in the core-derived description to lateral and vertical accretion of straight to slightly sinuous-crested transverse tabular bars (Cant and Walker,1976, 1978). The effect is also manifest on both sonic, neutron and density log patterns. Distinction between minerals is problematic when logs are responding to several minerals simultaneously (Humphreys and Lott, 1990). Hence variations in log response within the electrosequence can also be linked at the same time to compositional changes in the sandstone. Fig. 3.8 (series 1) illustrates that the sandstone is enriched in radioactive detrital constituents (mica and k-feldspars) probably reflecting less washed and winnowed sediments. Texturally the clay mineral type is mainly dominated by illite/montmorrillonite. The dispersed points (Fig. 3.8 series 2) correspond to the illite/chlorite clay mineral type in the abandoned channel fill electrofacies. Electrofacies B2 (Fig. 3.7) corresponds to a well-cemented sandstone level, although no distinctive change in sandstone porosity can be seen. This is attributed to a malfunction in the density log starting from upper electrofacies B1. From the Th/K cross-plots (Fig. 3.5, 3.8) which is the most reliable way of estimating sandstone mineralogy from the NGS log (Hurst, 1990; Rider, 1991; Doveton, 1994), it is clear that a decrease in sandstone mineralogical maturity occurs with decreasing depth in well BD/44.

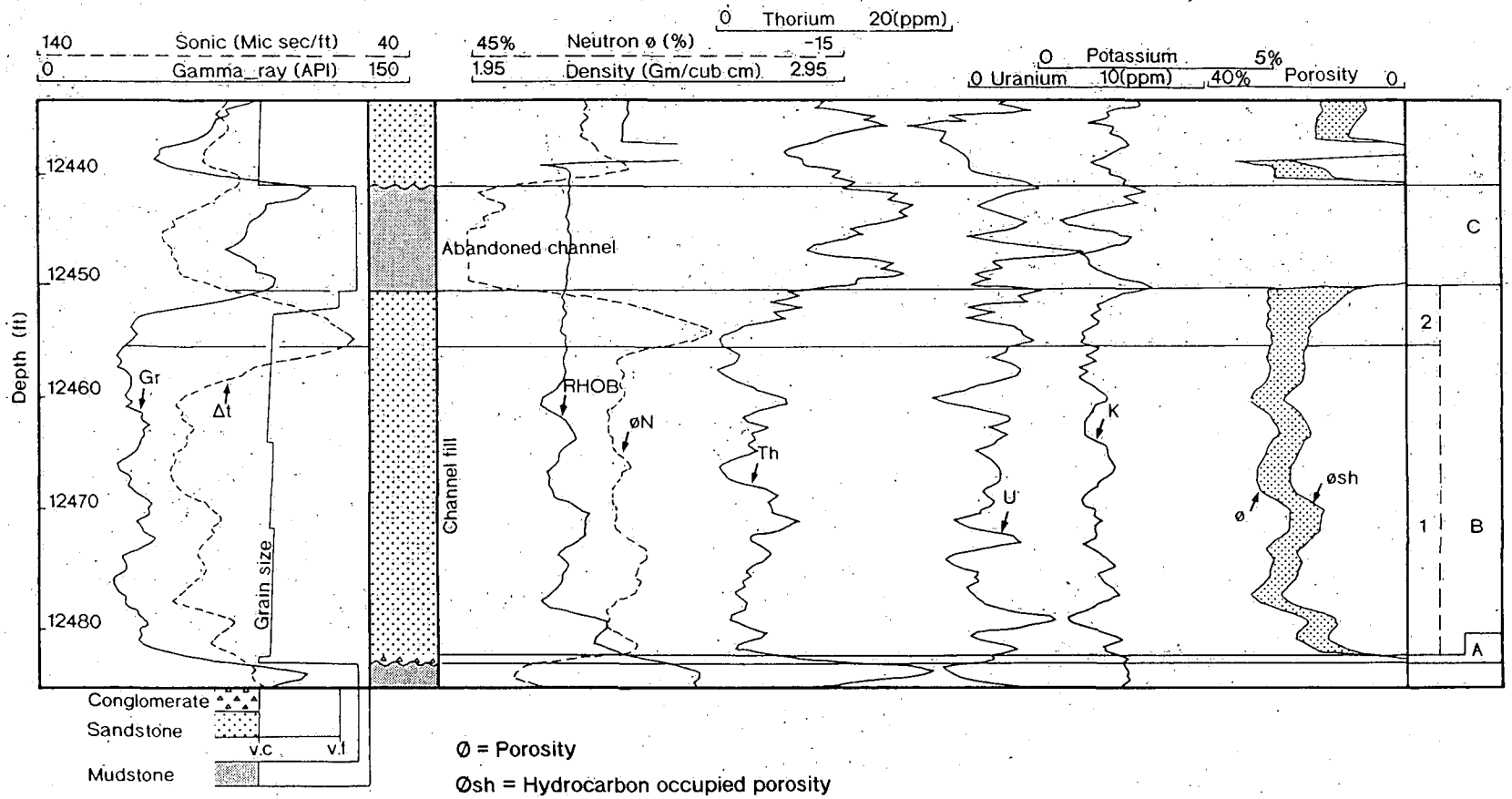

Fig. 3.7 Comparison between low sinuosity channel facies and the corresponding log responses in well BD/44. Gamma-ray log reflects the typical barrel shape.

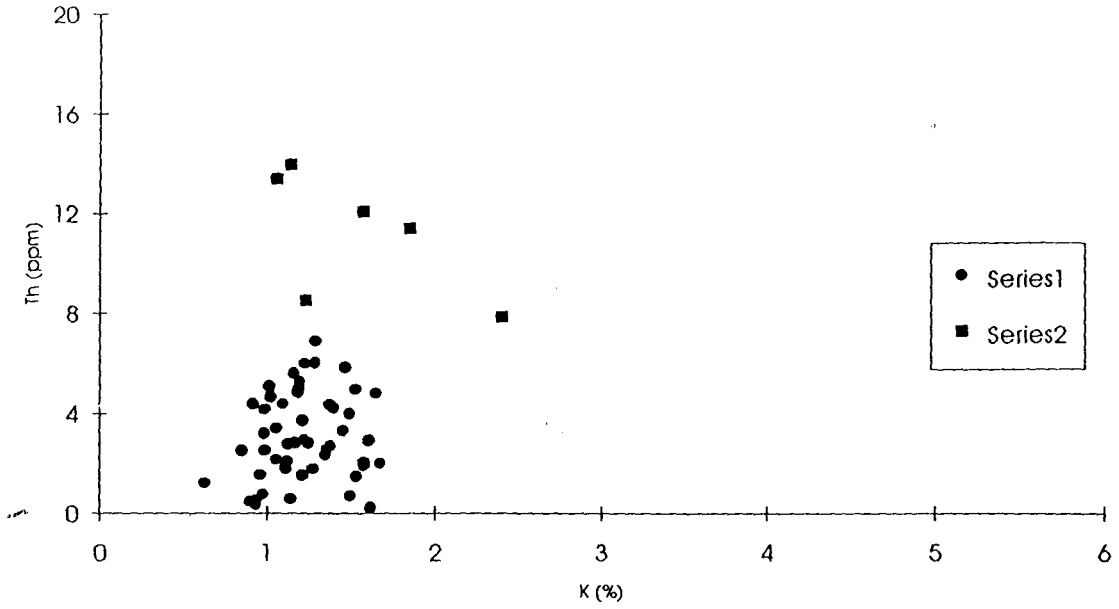
20
16
12
8
4
0
Th (ppm)
0
1
2
3
4
5
6
K (%)
Series1
Series2

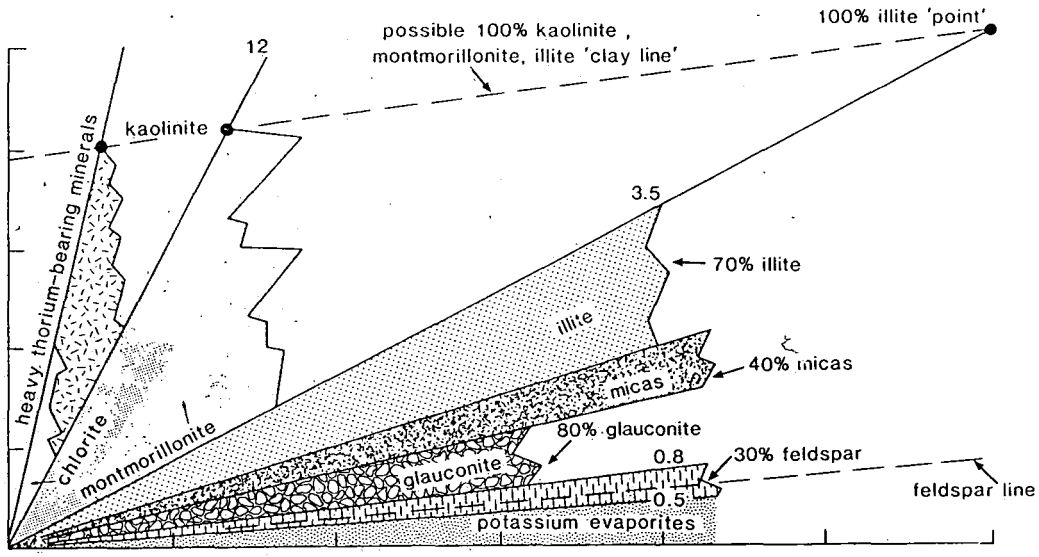

Fig. 3.8 Th/K cross-plot in a low sinuosity channel sequence from 12484 ft to 12442 ft in well BD/44 probably indicating poorly mature sandstone.

3.2.3 Crevasse splay /lacustrine delta electrosequences

These minor electrosequences are grouped together because of their close association in the fluvial environment. Both tend to produce coarsening-upward sequences and are difficult to differentiate on the basis of wireline logs unless enough pedogenic and biogenic evidence is available (See chapter 2 sections 2.4.2 and 2.4.5). Fig. 3.9 illustrates log patterns corresponding to a progradational followed by an abandonment crevasse splay facies in the cored section of well BD/44. The progradation is reflected in the typical funnel shape gamma-ray log (Fig. 3.1) in response to a gradual upward increase in grain size. Similarly the abandonment is reflected in the log pattern as a minor bell shaped gamma-ray log curve. The responses of the sonic and density log are similar.

Fig. 3.11a illustrates the correlation between core-derived lacustrine delta facies and the associated log patterns (See Fig. 2.16 for bed thicknesses and sequence). The

electrosequence produces the funnel shape of the gamma-ray log typically found in coarsening-upward sections (Fig. 3.1, 3.2). The minor electrosequence has a gradual lower contact and an ubrupt upper boundary reflecting gradual infilling and abrupt abandonment of a minor lake which forms the base of a thick flood plain sequence.

3.2.4 Swamp electrosequence

Fig. 3.10 represents log patterns in a swamp facies in the cored section of well BD/44. According to the core description this facies is dominated by very fine-grained organic-rich sediments resulting mainly from suspension fallout in stagnent water and a reducing environment of deposition. The log shapes characteristically reflect abrupt upper and lower boundaries indicating abrupt cut-off and termination of the swamp. The highest gamma-ray log values across the electrosequence clearly correspond to the organic-rich mudstones (Electrofacies B and D). High organic matter contents are often associated with high gamma-ray log values, and this is attributed to the concentration of uranium adsorbed by organic matter (Adams and Weaver, 1958; Schmoker, 1981). Typically, uranium is shown by irregular high peaks owing to the fact that it is commonly chemically combined and its continued solubility makes it susceptible to leaching and redeposition (Rider, 1991). Changes in organic content produce significant changes in mudstone density (Schmoker, 1979). Organic matter has low densities which contrast significantly with common rock matrix densities (Table 3.4), thus causing reduction in bulk density (Stocks and Lawrence, 1990). Pyrite, which is always associated with reducing environments has also a measurable effect on formation density (Table 3.4). In considering the effect of pyrite Schmoker (1979) derived the following empirical formula to estimate the organic content of a mudstone if variations from other causes are considered.

$$\text{øv} = (\sigma b - \sigma)/ 1.378$$

Where øv is the organic content by fractional volume, σb is defined as formation log density if no organic matter is contained, and σ is the log density at a given depth. In the swamp electrosequence (Fig. 3.10) the log density of the organic-rich mudstone

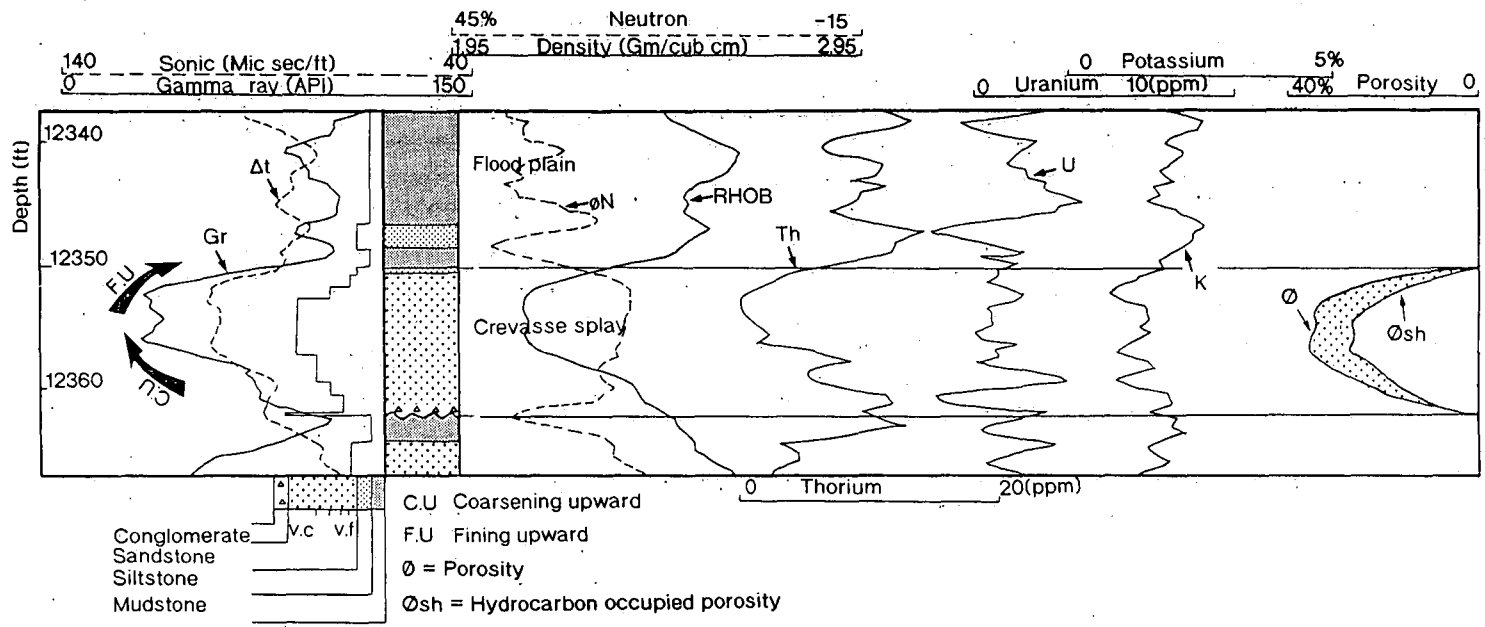

Fig. 3.9 Log patterns in response to a core-derived crevasse splay facies. The funnel shape of the gamma-ray log corresponds to a coarsening-upward trend of crevasse splay progradation. Similarly the upper part indicates a typical bell shape corresponding to the gradual abandonment of the splay lobe.

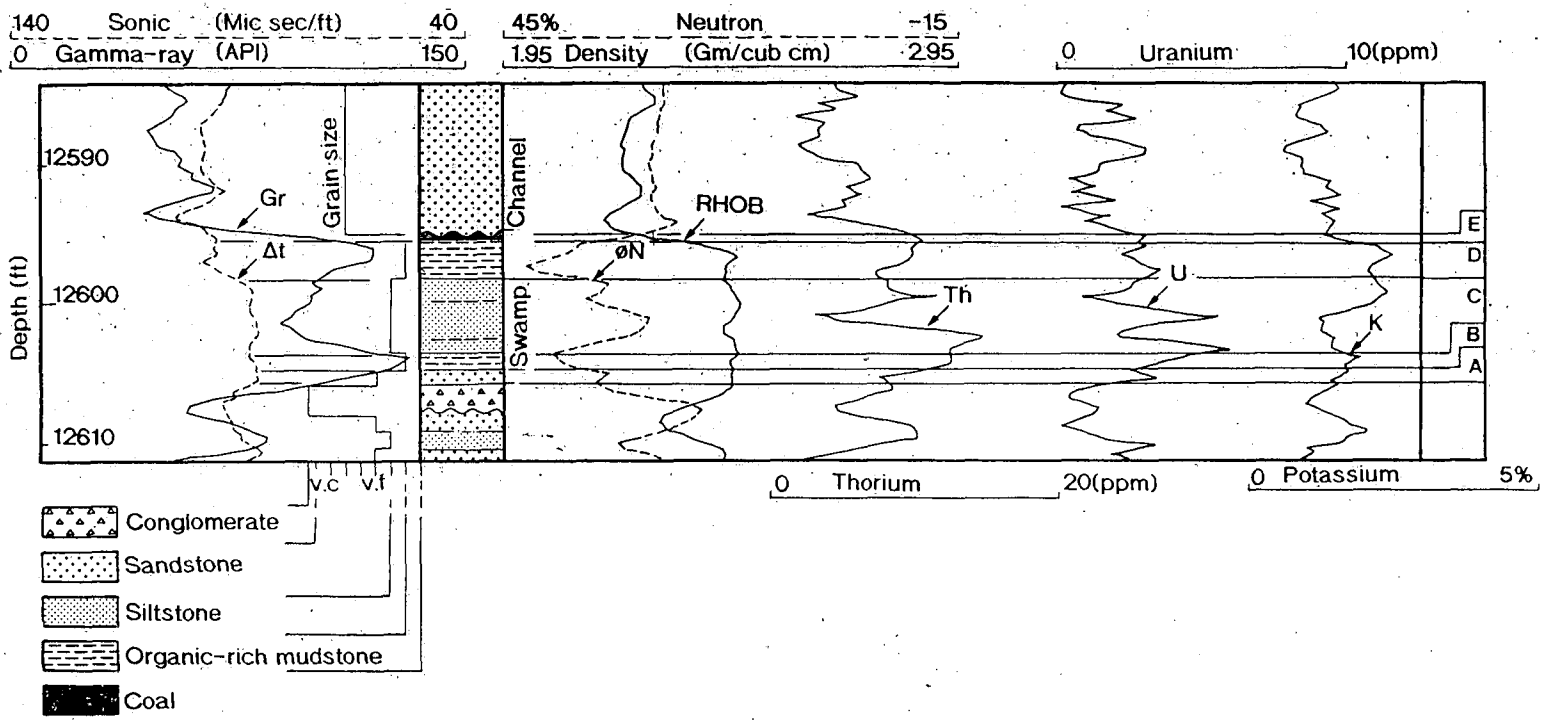

Fig. 3.10 Log responses in organic-rich sediments corresponding to a core-derived swamp facies in Well BD/44 core section.

(electrofacies B and D) is considered to be equal to 2.45 gm/cc and the average density of organic matter-free mudstone to be 2.70 gm/cc which is appropriate for many mudrocks (Myers and Jenkyns, 1992). The above equation indicates an organic content of 1.9 %, which is approximately on the margin between organic-rich (black shales) and barren (grey shales) (Shmoker, 1980). However, the main task of estimating organic content in this context is to convey information on depositional environment rather than the quantitative evaluation of a source rock. Electrofacies A and C are interpreted to have resulted from the detrital input brought into the swamp from an active adjacent channel. This resulted in a significant reduction in mudstone radioactivity as well as neutron porosity. The neutron log is sensitive to the additional quartz replacing clay. In addition, admixtures of organic matter cause an increase in the neutron log as they have higher hydrogen abundance (Rider, 1991). In contrast, sonic logs read relatively high, a normal phenomenon in organic-rich mudstones which can be used to qualitatively determine source rock (Meyers and Nederlof, 1984). Electrofacies E, which corresponds to a thin (10 cm) coal seam facies, has no marked effect on log patterns.This is attributed to the fact that such a small thickness is beyond the bed resolution of the typical logging macrodevices used (Schlumberger, 1989a). Coals often give very low radioactivity, very high sonic transit time and low bulk density (Tables 3.1, 3.3, 3.4). However, thick and laterally persistent coals are scarce across the entire formation (see chapter 2 section 2.4.4).

3.2.5 Floodplain electrosequences

The flood plain environment is the interchannel area which is characterized predominantly by the deposition of fine-grained sediment resulting mainly from suspension fallout of the over spilled sediments (Galloway and Hobday, 1983). The marked variation between these fine-grained sediments and the coarse-grained in-channel sediments makes the flood plain facies unique in its log character. Fig. 3.11b shows thick flood plain sediment accumulations in well BD/44 core section.

The electrosequence is characterized by slightly gradational lower and upper contacts marked on almost all log responses. The change from coarse-grained formation into flood plain fine-grained sediments reflects the dramatic shift in gamma-ray and density

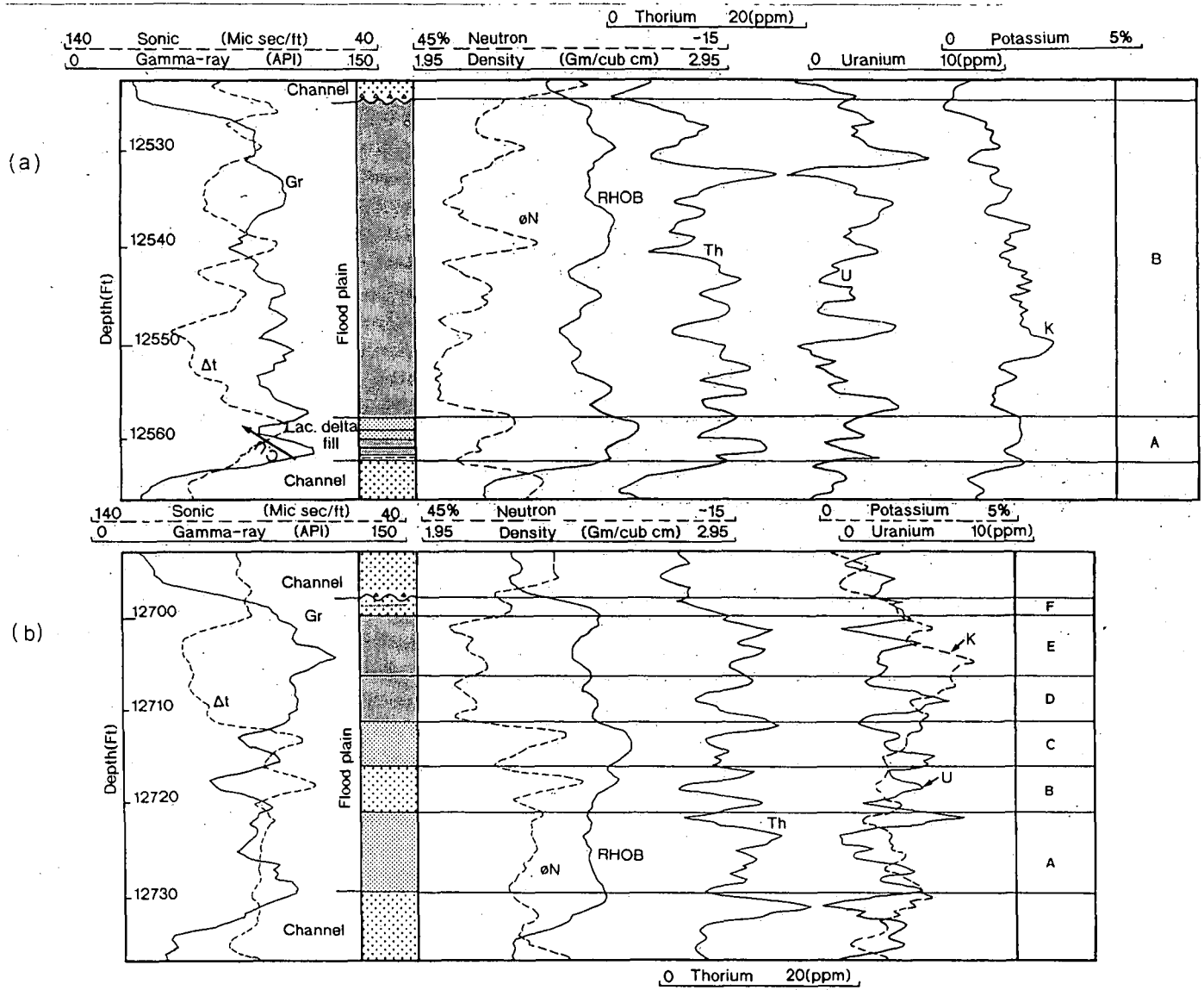

Fig. 3.11 Log patterns in flood plain sequences in well BD/44 (a) with minor funnel shape of gamma-ray log at the bottom corresponding to a lacustrine delta. See Fig. 3.9 for index.

logs which are puctuated by peaks usually correlated with changes in grain-size and facies. Electrofacies A corresponds to a core-derived facies of parallel laminated, micaceous muddy siltstone. The effect of mica is clear on both the potassium and density curve. Mica has a high specific gravity which normally affects the density log reading (Rider, 1991), and muscovite mica normally contributes significantly to the NGS log because of its high content of potassium (Table 3.2). Within the same electrofacies, the upward decrease in clay content is probably responsible for the upward reduction in neutron porosity and the concomitant increase in thorium content. The effect of the detrital input (Electrofacies B, C and F) is marked by the reduction of gamma-ray intensity, decrease in sonic transit time and neutron porosity. Electrofacies D and E clearly reflect an increase in gamma-ray intensity and a pronounced increase in both neutron porosity and sonic transit time combined with a slight reduction in mudstone density which is attributed to the organic content of these electrofacies (Schmoker, 1981). Is is now clear that mineralogical as well as textural changes in the mudstone significantly effect the inferred log pattern. Accessories such as organic matter and degree of compaction of the mudstone are also major factors controlling the physical properties of the mudstone. Across the electrosequence an upward increase in potassium content can be attributed to changes in clay mineral type, probably in relation to climatic changes.

3.3 Palaeoflow patterns from HDT log

The key design of the HDT (High Resolution Dipmeter Tool) is that four resistivity electrodes are mounted on two downhole pads measuring the resistivity of beds at each depth simultaneously in four different directions of the borehole. Side by side processing convert the results from adjacent resistivity electrodes to dip measurements including both dip magnitude and azimuth displayed as tadpoles. In this log format the head of a tadpole plotted at a given depth indicates the amount of dip according to a horizontal scale, while the tadpole tail points to the dip direction (e.g. Fig. 3.14). Results obtained from HDT log compared favourably with those from core and outcrop analysis (Herweijer *et al.* 1990; Cameron, 1992). Data selection has been applied to obtain meaningful dips. This process includes the selection of a maximum

cut-off value of 30° as indicating foreset dip magnitude. It was assumed by Cameron (1992) that taking 30° for maximum dip limits has the effect of focussing the analysis on those dips that are most likely to come from foresets. The spurious dip readings may originate from irregularities in the formation, from processing artefacts and post depositional destructional processes caused by dewatering and bioturbation, which normally have no directional implications (Höker *et al.* 1990).

It seemed, however, more rewarding to analyse data over trends, and for palaeoflow orientation it was assumed that foreset dips would occur only within the channel sandstone sequences, so the dipmeter log was zoned to identify likely channel intervals (Fig. 3.12). Palaeocurrent indicators in well 211/29-6 in the central part of the study area are summarised in Fig. 3.13.

Fig. 3.13a shows the palaeoflow pattern in a low sinousity channel system (Fig. 3.12 interval 1). The main cause of the pronounced dispersel of data is probably transverse bedforms oriented at high angles to the down current direction (Collinson, 1978; Kerr, 1984). Selley (1985) claimed that dipmeter motifs of braided deposits tend to be complex and dispersed, but foreset beds dipping at 20-25° may be present which dip downcurrent. Cross-bedding in braided channels tends to show a well-developed down current vector mode (Smith, 1972). However, other factors described earlier may have also contributed to the observed dispersel of data. The azimuth rose in Fig. 3.13a indicates a W-NW palaeoflow direction with a vector mean of 281. By contrast, in depth intervals interpreted as representing high sinuosity channel systems (Fig. 3.12 intervals 2, 3 and 4) palaeoflow patterns proved to be less dispersed (Fig. 3.13b, c and d).

Dipping surfaces measured within high sinuosity channels may include those of lateral accretion surfaces forming rather complex dip motifs. Lateral accretion surfaces draped with mudstone normally have low dips oriented at high angles to the more steeply dipping cross-bed foresets of the palaeochannel (Collinson, 1978, 1991). In point bars helical flow generates foresets whose down dip direction is oblique to the channel giving a bimodal azimuth fequency distribution in one point bar sequence (Schlumberger, 1989a). In the example (Fig. 3.13b) interpreted from log patterns as point bar sequence (Fig. 3.12 interval 2), the three readings from low angle (7, 8, 9°) lateral accretion surfaces indicate a direction of channel migration towards the NW,

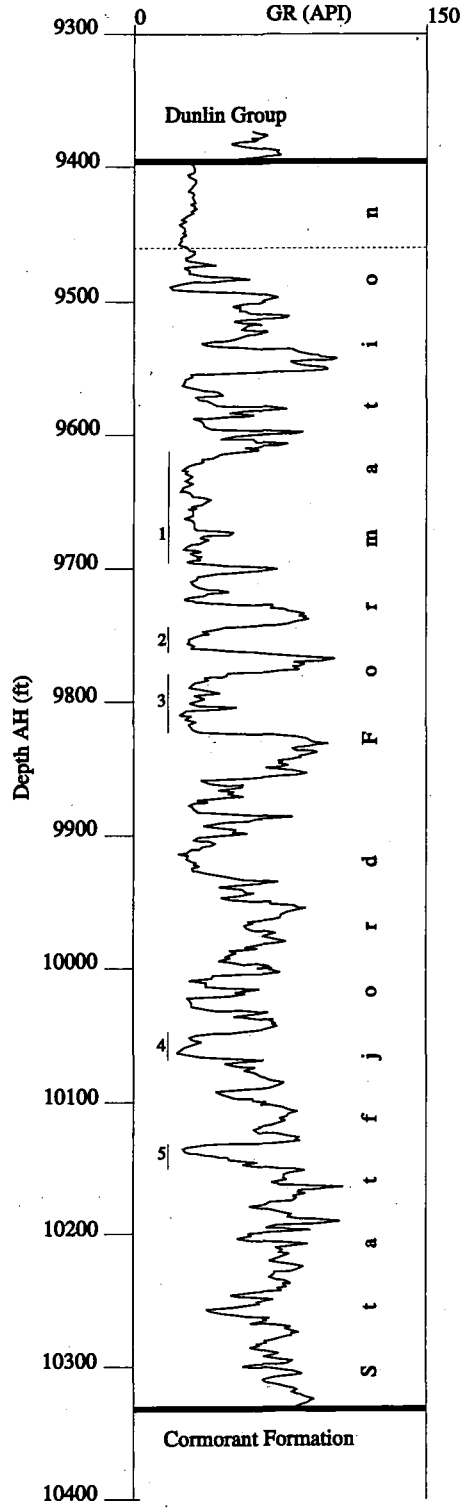

Fig. 3.12 Gamma-ray log versus actual hole depth in the deviated well 211/29-6 Brent Field with marked depth intervals representing low sinuosity channel sequence (1), high sinuosity channel sequences (2, 3 and 4) and prograding delta sequence (5).

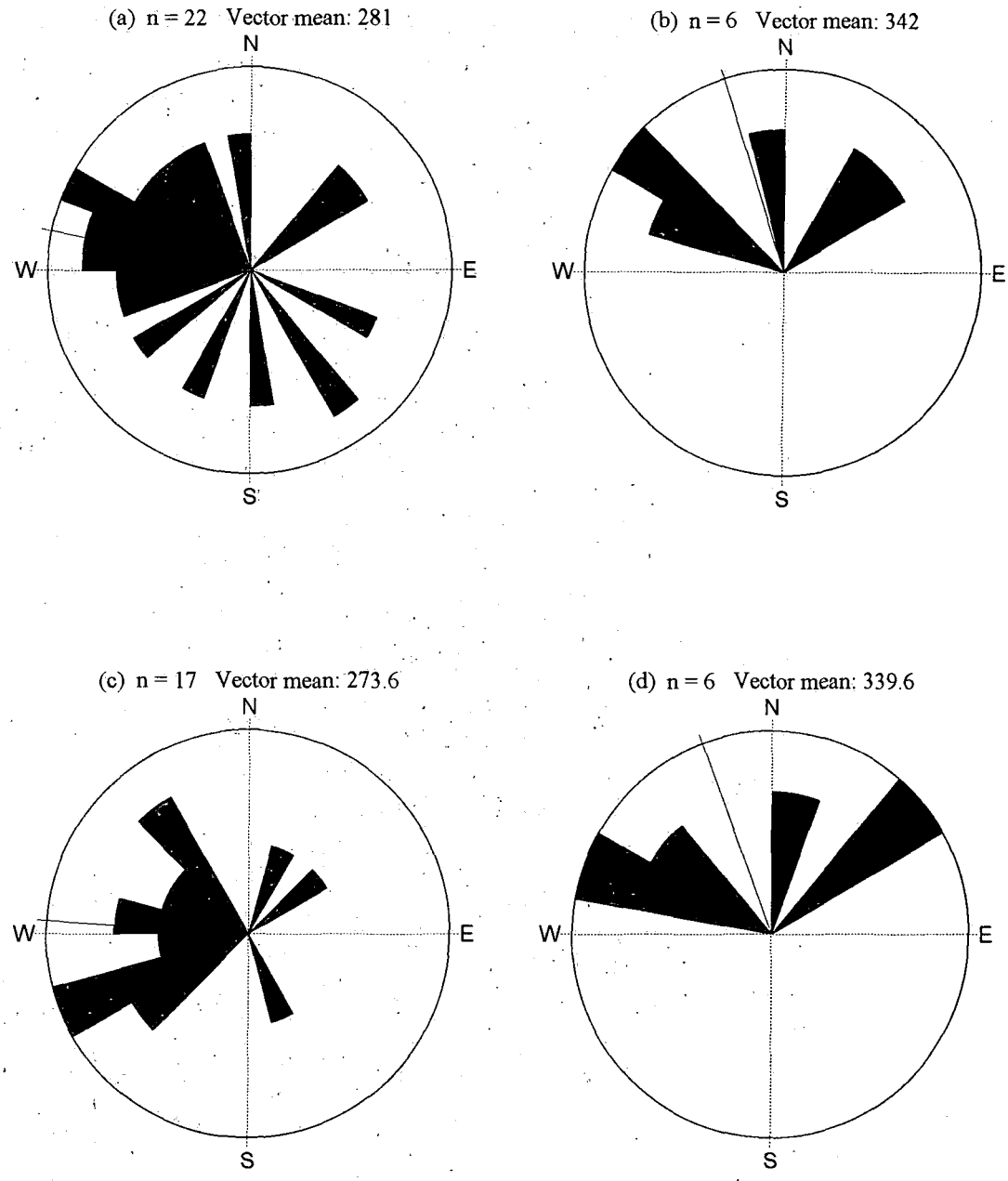

Fig. 3.13 Composite rose diagrams of azimuth distributions in channel sandstone sequences in well 211/29-6 representing low sinuosity channel sequence (a), high sinuosity channel sequence (c) and high sinuosity channel sequences including lateral accretion deposits (b, d). Solid line represents the vector mean.

with the inference that the channel belt having a SW-NE orientation. In interval 4 (Fig. 3.12) all the foreset dip readings are low, with one exception, suggesting that they may all represent lateral accretion foresets. The differences may represent different parts of the point bar surface within the meander, or different locations on the lateral accretion surface.

By contrast Fig. 3.13c shows the azimuth rose of a high sinuosity channel fill sequence (Fig. 3.12 interval 3). The pattern is different from the previous point bar sequences in that it has a poorly developed unimodal palaeoflow distribution. The computed vector mean of the vector means over the whole fluvial system is 310°, or to the NW.

The minor variations in the vector means (Fig. 3.13) may be attributed to different orientations of the meander belts cut by the well, or the rejuvenations of local minor source areas as a result of minor tectonic and/or climatic events during the evolution of the river system (cf Miall, 1984). However, the major fluvial channels in the axis of the basin are inferred to have transported sediments to the NW. Moreover, the overall consistency of the palaeoflow indicators coupled with the upward decrease in sandstone mineralogical maturity (see sections 3.2.1 and 3.2.2) proved to be adequate to indicate that no flow reversal occured during the evolution of the formation and that the entire sequence seemed to have been derived from southeasterly located terraces, probably the Fenno-Scandian Shield and the Horda Platform (Ziegler, 1990).

3.4 HDT log tadpoles in lobate sediments

Studies carried out on modern deltas reveal that rotational depositional dips occur on prograding sediment lobes. Selley (1989) proposed a technique for identifying rotational dip motifs of lobate sediments that tend to produce coarsening-upward sequences. The aim is to detect the apex of the lobe which is characterised by the highest sand/shale ratio, and to identify the direction and location of the source channel. The analysis has long been used to develop deltaic petroleum reservoirs, and can be extended to sediments of fluvial and submarine fan origin with a high degree of confidence (Williams, 1969). Lobate sediments such as those produced by crevasse splays and lacustrine deltas in fluvial environments typically yield coarsening-upward sequences as they prograde (Ethridge *et al.* 1981; Selley, 1985). Fig. 3.12 (interval 5)

reflects a coarsening-upward sequence (6m thick) in well 211/29-6, interpreted as a prograding lacustrine delta or a subaerial crevasse splay lobe (see section 3.2.3 for comparison). The tadpoles of the HDT log in the interval are portrayed in Fig. 3.14, and indicate an upward increase in dip value and a clockwise rotating azimuth.

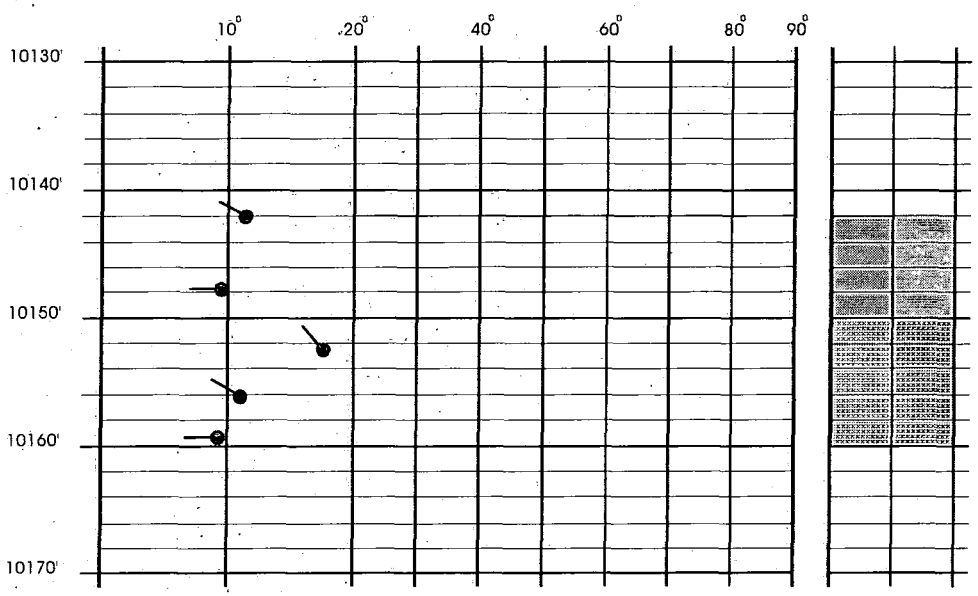

Fig. 3.14 HDT log tadpoles in the interval from 10142 ft to 10160 ft in the deviated well 211/29-6 showing an upward increase in dip value and a clockwise azimuth rotation.

The cycle is apparently symmetrically repeated across the interval, probably indicating two amalgamated delta lobes. Compared with Fig. 3.15a, the upward clockwise rotation pattern of the azimuths reflects the right hand side of a westward prograding lobe (Fig. 3.15b). This indicates that the main trunk stream feeding the outbuilding lobe is located to the east and that the delta lobe was intersected by the well on its northern flanks.

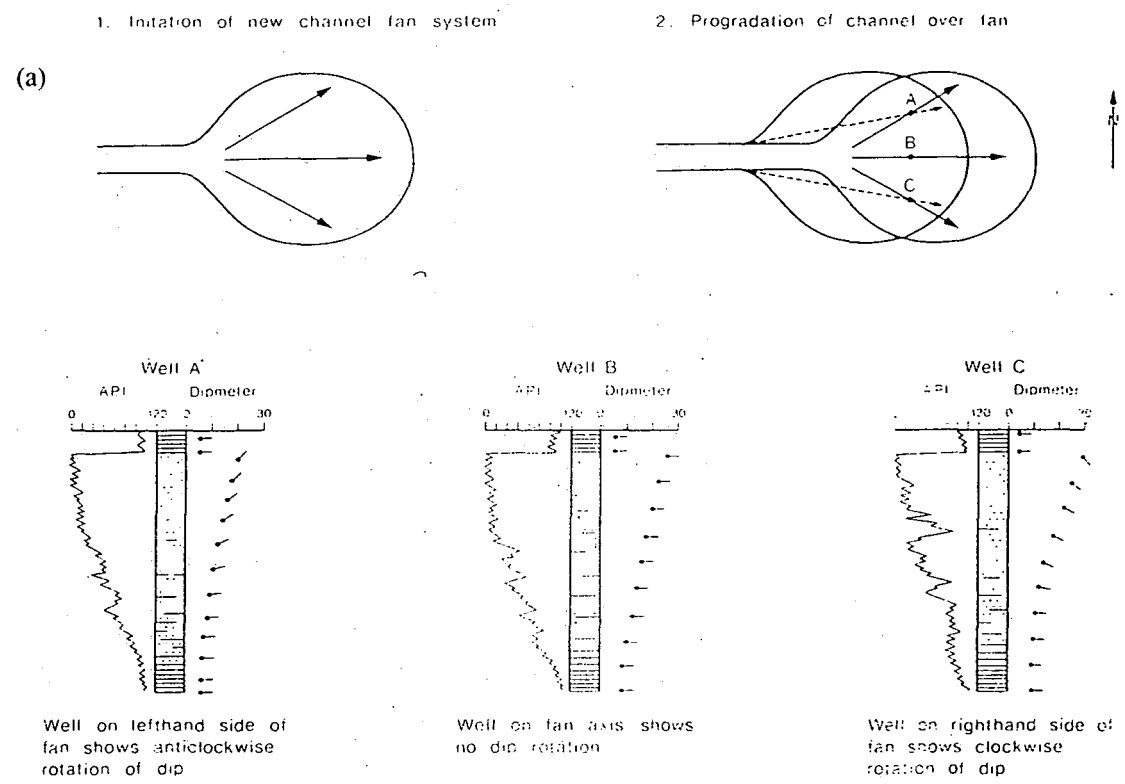

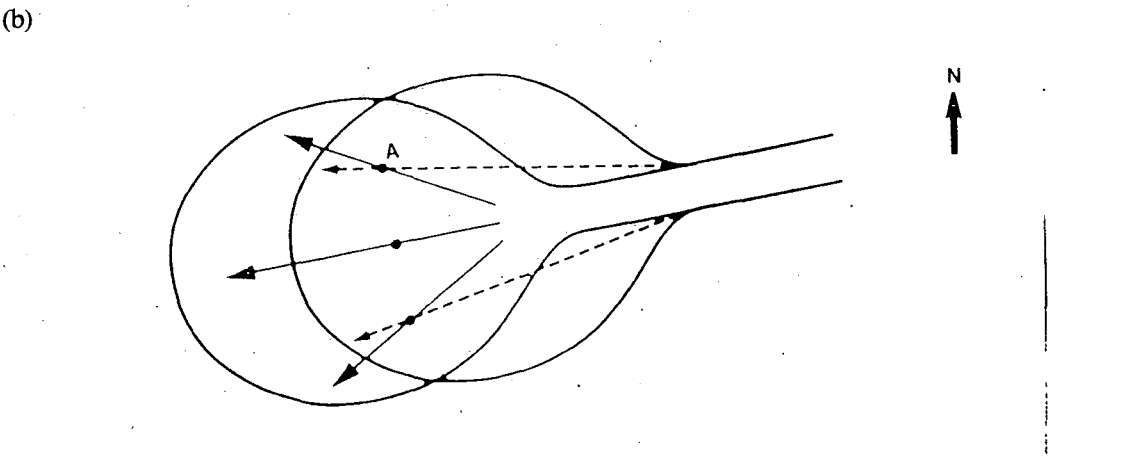

Fig. 3.15 (a) Schematic diagram illustrating the single genetic increment of a prograding sediment lobe: Note the anticlockwise and clockwise rotation of the slopes on the northern and southern flanks. The lower part shows gamma-ray and dipmeter logs for wells A, B and C (modified from Selley, 1989). (b) Schematic drawing showing the direction of the prograding lobe in well 211/29-6, (A shows location of the well).

Chapter 4

Sequence stratigraphic concepts and implications

4.1 Introduction

In recent years, sequence stratigraphy has proved itself to be a key element in recognizing stratal geometries. Sequence stratigraphic studies suggest that depositional facies are arranged in a predictable fashion within depositional sequences. The use of sequence stratigraphic concepts in conjunction with detailed facies analysis provides a greater degree of temporal resolution than is otherwise possible. It is a powerful predictive tool in petroleum exploration, extractive industries and basin analysis (Van Wagoner *et al.* 1990; Shanley and McCabe, 1993, 1994). Sequences and sequence boundaries divide sedimentary rocks into genetically related units bounded by surfaces with chronostratigraphic significance (Van Wagoner *et al.* 1988). Within the same framework, further subdivision of sedimentary units into parasequences, parasequence sets, and systems tracts has provided a powerful methodology for the analysis of time and rock relationships in the sedimentary record. Recognition and correlation of stacking patterns in terms of base level changes provide a model for better understanding the evolution and significance of changes in sedimentary architecture. This methodology, however, has been most successful in interpreting marine and coastal plain successions, but it has not been applied widely to non-marine successions (Posamentier and Weimer, 1993; Wright and Marriott, 1993; Surlyk *et al.* 1995). This is because non-marine depositional systems respond to a variety of both allocyclic processes such as climate, tectonics, and eustatic changes, and autocyclic processes such as channel avulsion. Among other difficulties are the poor biostratigraphic control, limited absolute age dating and numerous internal erosion surfaces (Shanley and McCabe, 1993). Nevertheless, it is well accepted that allocyclic processes are probably more significant on a regional basis. One key aspect of the conceptual models for geomorphic development of fluvial systems (e.g. Schumm, 1993; Wescott, 1993) is that areas in the same drainage basin or even along the same river system may not respond to extrinsic factors in the same way. Moreover, the rate of sediment supply

will have a pronounced effect on whether parts of systems tracts are developed. However, the application of sequence stratigraphy to continental strata is likely to result in the development of better correlation techniques and better prediction of the location, geometry and stacking of non-marine strata.

The main emphasis of this chapter, therefore, is to investigate the applicability of sequence stratigraphic methodology in a non-marine fluvial succession using variations in facies tracts and stacking patterns in relation to changes in base level. This approach assumes that the area during deposition was tectonically relatively quiescent, as deposition occurred during a post-rift thermal subsidence phase. Moreover, no significant climatic changes have been recorded throughout the depositional history of the formation (see chapter 1 sections 1.4, 1.6). However, because of the difficulty of describing each individual facies within a sequence stratigraphic framework it is more useful to deal with the systematic variations in processes such as changes in channel morphology that occur throughout a sequence during evolution of the depositional system. This large-scale variation is the subject of this chapter.

4.2 Sequence stratigraphic concepts of alluvial strata

There is a diversity of opinion concerning the impact that changes in relative sea level have in continental settings (Shanley and McCabe, 1994). Within coastal plain settings, the concept of a graded stream profile has been commonly used. Studying the concepts of near shore marine strata could link changes in relative sea level to patterns of fluvial aggradation or degradation. Posamentier and Vail (1988) suggested that in its natural course of development, a stream will strive to achieve a slope of maximum efficiency, wherein the 'slope' is delicately adjusted to provide, with available discharge and the prevailing channel characteristics, just the velocity required for transportation of all the load supplied from the source area. This state is referred to as a state of dynamic equilibrium at which streams are said to be graded or in a state of neither deposition nor erosion. However, grain-size distribution and depositional mode (e.g. braided or meandering) is a complex function of many factors such as climate, varying sediment source, vegetation and tectonics as well as accommodation space. Variations of

accommodation space as a function of sea level change will be the only factor common to all subaerial settings at any given time (Posamentier and Vail, 1988).

A stream at a state of equilibrium generally has a smoothly curved longitudinal profile (equilibrium profile). The elevation of each point on this profile is determined by the base level position at the downstream end of the profile (Posamentier and Vail, 1988; Schumm, 1993). Because the rate of base level change determines the rate at which accommodation space is created, changes in alluvial architecture may be interpreted in terms of changes of the rate of base level (Shanley and McCabe, 1993). This results in a better understanding of alluvial architecture, sand/mud ratio and sandstone interconnectedness. Controversy surrounds the effect of base level changes on river behaviour. First generation sequence stratigraphic models have dealt in a very rudimentary fashion with the response of fluvial systems to eustacy. Well-established geomorphic principles state that rivers may simply adjust to base level changes in other ways beside incision and aggradation by modifying their patterns and geometries (Schumm, 1993; Wescott, 1993). However, recent studies and studies carried out using flumes demonstrate that in large-scale fluvial drainage systems (e.g. Posamentier *et al.* 1992; Koss *et al.* 1994), when a river is affected by a base level rise or fall or by a horizontal shift of the river mouth, the river will probably respond by either aggradation or degradation to restore its equilibrium profile. After all, the channel must continue to carry its load of sediment with a given discharge and this requires a given gradient that can be restored by deposition (Fig. 4.1a, c) or by erosion (Fig. 4.1b). Profiles are generally graded at the point where they reach the sea. This point is regarded as the *bayline* which is defined as the demarcation line between fluvial and paralic sediments. In the absence of paralic sediment, the bayline coincides with the shoreline (Posamentier *et al.* 1988). Thus, sea level fluctuations will have a profound effect on the fluvial regime (Posamentier and Vail, 1988). Based on these assumptions, there must be a relationship that links the stacking patterns of alluvial and coeval marine strata as they both respond in the same way to sea level changes.

Relative sea level rise creates additional marine accommodation space and at the same time, shifts the position of the points to which stream equilibrium profiles are graded, thereby creating additional subaerial accommodation space. The subaerial

accommodation space has been defined by Posametier *et al.* (1988) as the space made available for sediments to fill between an old stream equilibrium profile and a

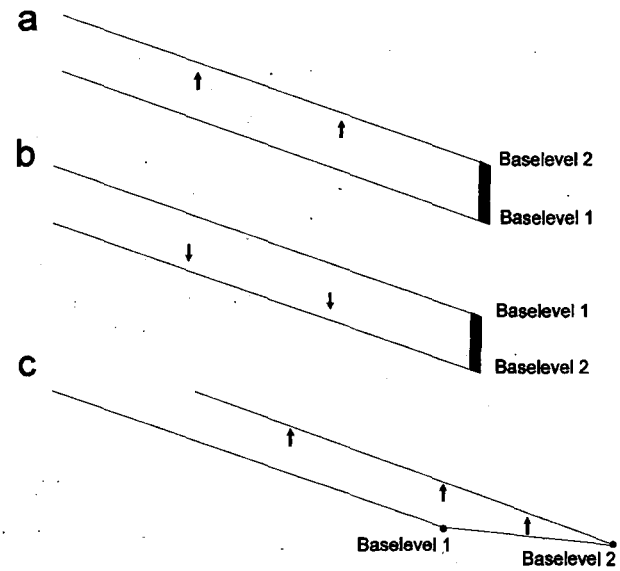

Fig. 4.1 Stream profile adjustment in response to base level changes. (a) base level rise from position 1 to 2, (b) base level fall from position 1 to 2, (c) Stream mouth shifts horizontally from position 1 to 2. Modified from Schumm (1993).

new higher one. The fundamental principle which governs sedimentation in fluvial environments (assuming constant sediment supply) is that a stream will aggrade if its equilibrium profile shifts basinward or upward and incise if its equilibrium profile shifts downward (Posamentier and Vail, 1988). The way these points move in response to eustatic change provides the key to understanding deposition and erosion in a subaerial environment. Posamentier and Vail (1988) assumed that during transgression an upward shift of the points to which streams are graded occurs along the same equilibrium profiles without a significant landward shift in position of these profiles. During a stillstand, the points to which profiles are graded shift basinward resulting in a constant basinward shift of the equilibrium profiles and thus producing subaerial accommodation space.

The extension of systems tracts into fluvial strata is an area of considerable interest and uncertainty. Shanley and McCabe (1993) introduced a model which purports to show how changes in fluvial sedimentology and geometry correlate to changes in marine and nearshore strata as a function of base level change (Fig. 4.2). A similar model (Fig. 4.3) has also been advocated by Wright and Marriott (1993). The model attempts

to relate changes in base level and accommodation space to alluvial architecture and

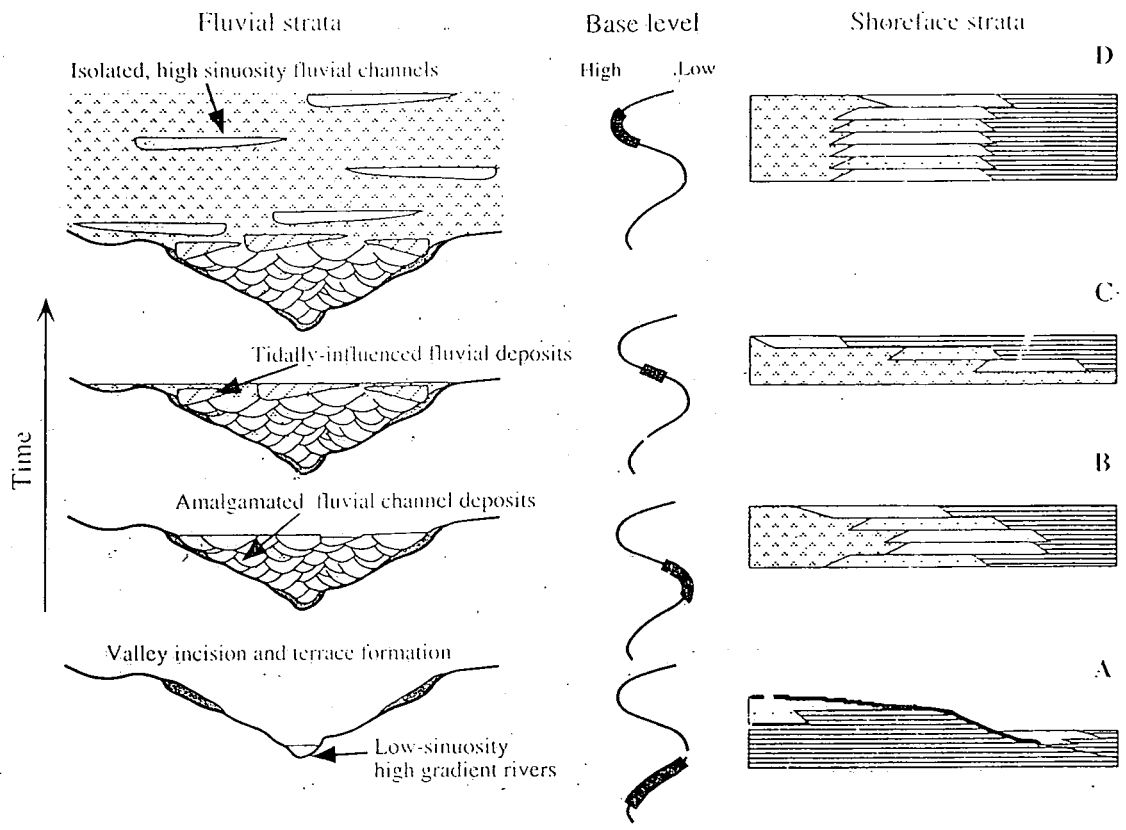

Fig. 4.2 Diagram showing the relationship between shoreface and fluvial architecture as a function of base level change. Slow rates of base level rise leading to base level fall (a), reduced rates of base level fall and slowly rising base level (b), increased rates of base level rise (c), and reduced rates of base level rise that are approximately balanced with rates of sedimentation (d). From Shanley and McCabe (1993).

soil development.

With increased overprinting by local factors, problems arise when applying sequence stratigraphic concepts to fluvial strata, i.e., how far inland can the effects of sea level change be observed (Posamentier and Weimer, 1993). This question, however, does not have a ready answer. Schumm (1993) suggested that base level changes affect the vertical position of a river to perhaps as much as 300 km inland giving as an example the Mississippi Valley. He further indicated that many variables appear to be significant including base level magnitude, rate and duration of base level change together with geological controls including lithology, structure and nature of valley alluvium in addition to geomorphic factors such as inclination of exposed surfaces. Large-scale flume studies of a model of a fluvial drainage basin carried out by Koss *et al.* (1994) show that base level changes significantly affect the shelf area but they have little

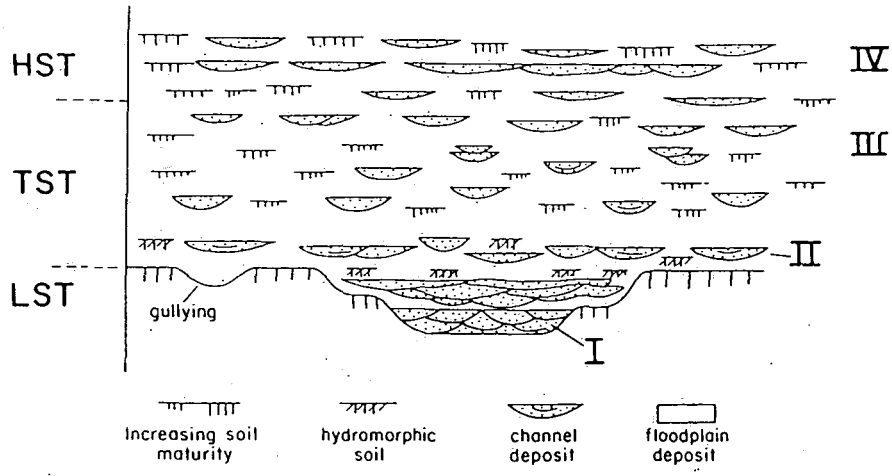

Fig. 4.3 Simple architectural/pedogenic fluvial model deposited during a third-order scale base-level fall-rise (type 1 sequence of Posamentier and Vail, 1988). LST= lowstand systems tract, TST= transgressive systems tract, and HST= highstand systems tract. From Wright and Marriott (1993).

effect on the fluvial drainage basin. Leopold *et al.* (1964) indicated that the effect on the depositional pattern of a river, as a result of base level changes, extends only for a short distance upstream. Hamilton (1995) also arrived at the same conclusion in that due to their proximity to the source area, non-marine sequences are effected by the interaction between sediment supply, local tectonics, climate and base level changes. Shanley and McCabe (1993) suggested that fluvial systems within perhaps 100-150 km, have the potential to be greatly affected by base level/relative sea level changes. Nonetheless, the systematic variation of systems tracts and the stacking patterns of the Statfjord Formation, that to a great extent match the eustatic curve, does strengthen the interpretation that these variations are at least partially related to base level fluctuations.

4.3 Sequence stratigraphic implications of the Statfjord Formation

The Statfjord Formation appears to be arranged in geometric patterns that can be related to two sequences (Fig. 4.4). Although the sequences are incompletely preserved, they possess all the attributes of depositional sequences described by Posamentier and Vail (1988), Posamentier *et al.* (1988) and Van Wagoner *et al.*

(1990). However, parasequences and parasequence sets are not identifiable. Identification of non-marine parasequences has yet to be reliably established and may well be impossible because the updip impact of marine transgression is minor and may be removed by subsequent allocyclic erosion of the fluvial system (Shanley and McCabe, 1994; Aitken and Flint, 1995; Surlyk *et al.* 1995). Nevertheless, it is possible to identify systems tracts on the basis of sequential position, facies association and systematic variations in architectural style and sediment body geometry. It is the geometric arrangement of these facies associations that characterize the architectural style of these strata and allows for comparison with marine strata.

4.3.1 Highstand systems tract

The highstand systems tract is deposited when the rate of relative sea-level rise gradually slows and eventually reverses (Wright and Marriott, 1993). On the basis of stacking patterns and facies geometry this systems tract is divided into early and late highstand stages.

4.3.1.1 Early highstand systems tract

The observed distinct sediment lobes, isolated channel deposits and the low sand/mud ratio of zone A (Fig. 4.4) may represent an early highstand systems tract. Wright and Marriott (1993) suggested that during early highstand, the accommodation space is added rapidly, and aggradation rates are rapid, resulting in a pattern of vertically stacked fluvial deposits with low lateral continuity. This conceptual model is in agreement with the predictive conceptual models of Posamentier and Vail (1988). These models postulate that following a basinward shift in the stream equilibrium profiles during a highstand, streams strive to re-establish their equilibrium through renewing sedimentation. Initially, sedimentation rates are high and deposition is characterized by rapid aggradation rates and a vertical stacking pattern. Shanley and McCabe (1991, 1994) postulated that alluvial strata with isolated meanderbelt sandstones and a significant amount of fine-grained overbank deposits are characteristic of highstand systems tracts associated with aggradational shoreface

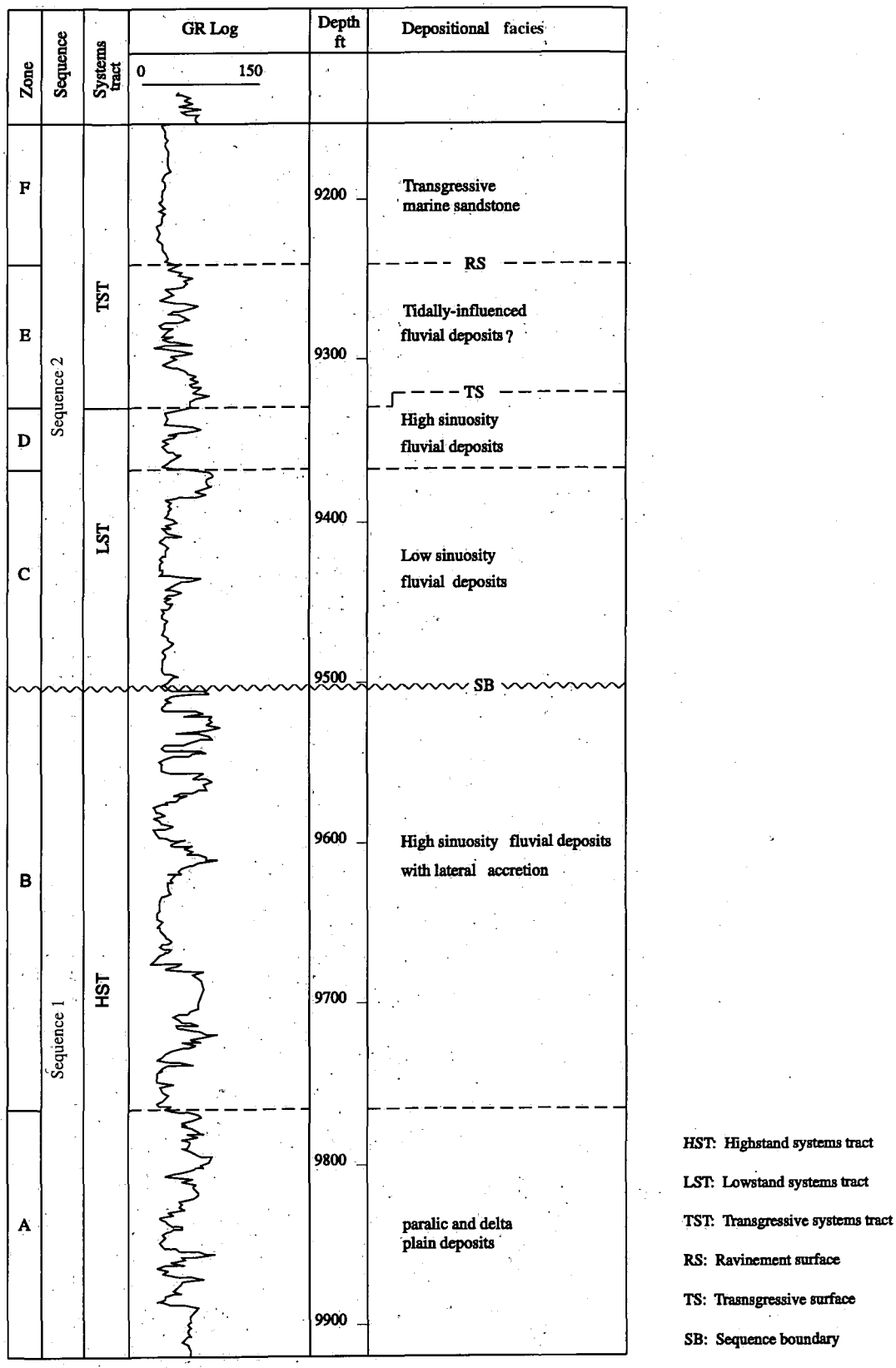

Fig. 4.4 Sequences and systems tracts of the Statfjord Formation. Classification based on stratal geometry and facies tracts. See page 121 for discussion of sequence boundary. Data from well BA/22.

parasequences, and reflect increased rates of accommodation that are balanced by rate of deposition (Fig.4.2d).

There is always a lag between the time the equilibrium profile reaches its maximum basinward position and the time fluvial deposition catches up with the equilibrium profile filling the space previously made available (Posamentier. *et al.* 1988).

The architecture of the early highstand systems tract is characterized by fine-grained floodbasin strata, isolated fluvial sandstones, and thin discontinuous coals and carbonaceous shales (zone A Fig. 4.4) which reflect the relatively rapid rates at which accommodation space is created relative to sediment supply (Shanley and McCabe, 1994). At the time when base level was kept constant, the experimental study of Koss *et al.* (1994) illustrated that sediments from the drainage basin form a delta which prograded basinward across the shelf. The observations of Dalrymple and Zaitlin (1994) suggested that highstand systems tracts are characterized by fluvio-deltaic systems. From the above discussion zone A (Fig. 4.4) may represent a delta plain environment of deposition, or more likely an upper delta plain away from direct marine inundation. Deposition is dominated by distinct amalgamated delta lobes (see Appendix 24, zone A, for further details of facies interpretation).

Deltaic deposition occurs when a stream encounters a standing water body as flow velocity abruptly decreases (McKee *et al.* 1967). The mouth of the stream is gradually displaced basinward and eventually because of the low gradient, channels become choked with sediment resulting in stream diversion and the formation of distinct lobes (Posamentier and Vail, 1988; Koss *et al.* 1994). At any time the delta front (bayline) represents the location of the points at which streams are adjusted, and separates fluvial from deltaic sediments. This point moves considerably basinward then abruptly landward in response to subsequent lobe abandonment. Similar deposits were interpreted by Feldman *et al.* (1995) as bay-head deltas formed in response to a shift in the balance between sediment supply and rising base level as deposition was confined to narrow tributary valleys.

The transition from the underlying transgressive systems tract is not preserved in the section. However, if present, it should reflect a change from amalgamated to isolated channel bodies and an increase in the degree of preservation of fine-grained sediment (Shanley and McCabe, 1991). According to Aitken and Flint (1995), thick and laterally

persistent coal seams are always associated with zones concomitant with maximum accommodation representing the maximum flooding, and hence, separating the transgressive from the highstand deposits. The best developed coals would be expected to occur during transgression at the time of maximum flooding. However, thick, laterally extensive coals can also occur in response to other flooding events not related to maximum marine flooding (Aitken, 1995). Aitken and Flint (1995) suggested that it would be difficult to distinguish highstand from the underlying transgressive deposits in relatively updip locations because both are represented by single-storey channel fills, high proportions of crevasse splays, coals, and thick flood plain successions. Thus, it would be more rewarding to identify a zone rather than a surface of maximum flooding. Channels within the transgressive system tract tend to be isolated and have a heterolithic fill, while those within the highstand are sandstone filled, and amalgamated. Moderate net to gross successions dominated by single story channel fills are thought to represent low rates of base level rise during the highstand (Aitken and Flint, 1995).

4.3.1.2 Late highstand systems tract

As the final position of the equilibrium profile is neared, during a stillstand, the rate of increase of subaerial accommodation space decreases and approaches zero. Vertical stacking grades into lateral migration, resulting in the development of sheet geometries with relatively high lateral continuity, and rivers tend to comb their flood plains reworking the existing sediments (Posamentier and Vail, 1988; Wright and Marriott, 1993). It is accepted that when accommodation space is zero during a stillstand, sediment bypass is more likely to occur (Shanley and McCabe, 1994). This probably marks the initiation of the late highstand systems tract (Zone B Fig. 4.4). The later geometry is thus characterized by a low rate of aggradation. Consequently, the conceptual models of Posamentier and Vail (1988) would suggest that correlation of the late highstand deposits is less problematic because of their greater lateral continuity. The stratigraphic models of Posamentier *et al.* (1988) suggest a widespread alluviation at this time.

On the basis of stratal geometry Shanley and McCabe (1993) highlighted the difference between early and late highstand deposits in that early highstand deposits are more

likely to be characterized by isolated channels, whilst late highstand deposits are laterally continuous. Additional sequence boundaries of higher frequencies may have punctuated this systems tract (cf Shanley and McCabe, 1993).

Because of the limited accommodation space Shanley and McCabe (1991) suggested that alluvial strata associated with this systems tract contain thin carbonaceous shales, discontinuous thin coals and localized channel sandstones. These are similar to observations from the Statfjord Formation (Fig. 4.4 Zone A, B). Late highstand systems tracts are characterized in the coeval shoreface by strongly progradational parasequences (Shanley and McCabe, 1991; Fig. 4.2d). Fig. 4.5 illustrates the stacking pattern and the transition from early to late highstand systems tracts in the coeval shoreface setting. Topsets show variation from predominantly aggradational during early highstand to predominantly progradational during the late highstand systems tract. The stratigraphic models of Posamentier *et al.* (1988) suggest either type 1 or type 2 unconformities separating the two stacking patterns.

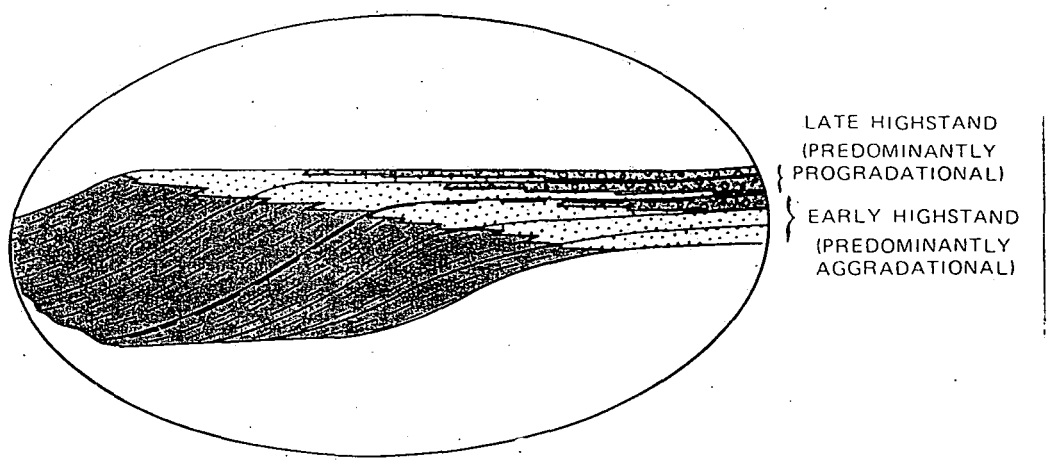

Fig. 4.5 Topset geometry of the highstand systems tract deposits in a shoreface setting. From Posamentier *et al.* (1988).

4.3.2 Lowstand systems tract

On the basis of channel geometry, stacking pattern and sand/mud ratio, this systems tract can be divided into two distinct end members: early lowstand wedge and late lowstand wedge.

4.3.2.1 Early lowstand wedge systems tract

The sandstones of zone C (Fig. 4.4), interpreted as the product of a braided river system, may represent sediments coeval to an early lowstand wedge systems tract. Lithologically these sandstones comprise several distinct bodies, each of which has a scoured base and generally fines upward from pebble-bearing sandstone with scattered conglomerates into medium-grained sandstone. Tabular cross-bedding is the dominant stratification type with some trough cross-bedding (see Chapter 2 section 2.3.1). These regionally extensive, multistorey sandstone bodies are interpreted, in many cases, (e.g. Allen and Posamentier, 1993; Aitken and Flint, 1995; Feldman *et al.* 1995) to overlie sequence boundaries associated with allocyclic processes. The multistorey geometry suggests that rates of floodplain and valley aggradation were relatively low (Bridge and Leeder, 1979). According to the observations of Shanley and McCabe (1994) multistory, multilateral channel units with a high relative proportion of interconnectedness and a high net to gross ratio are often thought to represent low rates of stratigraphic base level rise. The lack of evidence of lateral accretion surfaces and the scarcity of overbank deposits within zone C (Fig. 4.4) imply that infill was mainly by low sinuosity rivers (cf Aitken and Flint, 1995). The absence of fine-grained deposits form the upper parts of channel storeys also suggests preferential erosion due to low rates of fluvial aggradation and accommodation space (Shanley and McCabe, 1993). Similar coarse-grained, pebbly and amalgamated sandstones of braided streams have been interpreted by Shanley and McCabe (1993) and Surlyk *et al.* (1995) to have been deposited following a significant seaward shift in facies tracts. These deposits are temporally equivalent with shoreface deposits that initially prograde and subsequently begin to aggrade (Fig. 4.2b).

The early lowstand wedge deposits, that could represent an incised valley fill, are initiated during the resumption of a slow rise of relative sea level at the depositional shoreline break after cessation of stream incision (Posamentier and Vail, 1988). The coarse-grained nature of these sediments devoid of marine fauna merge with similar recent fluvial deposits landward of the bay line (e.g. Allen and Posamentier, 1993).

Fluvial aggradation initially takes place near the river mouth and progressively onlaps in a landward direction (Shanley and McCabe, 1993). Thus, the sedimentary fill within the incised valley may form a wedge that normally attains the maximum thickness in

the thalweg and thins both on the interfluve and landward in the vicinity of the bayline (Allen and Posamentier, 1993; Fig. 4.6). Because of the time lag between base level changes and subsequent fluvial response, little or no fluvial aggradation is expected to occur in the upstream segments of the incised valley unless lowstand conditions lasted a sufficiently long time . This may further strengthen the interpretation that the lowstand sediments would increase in thickness downstream and pinchout in the updip direction (cf Allen and Posamentier, 1993).

In considering the non-cohesive nature of the alluvium of the underlying highstand systems tract (Fig. 4.4 zone B), base level lowering may not have propagated inland for a considerable distance. Schumm (1993) postulated that experimental studies in low-cohesion sediment have shown that incision will not propagate indefinitely upstream. Unlike channels formed in low-cohesion sediment, channels in cohesive sediment incise further upstream.

In the case of type 2 unconformities these low sinuosity channel sediments are probably coeval to an early shelf margin systems tract instead of a lowstand wedge.

4.3.2.2 Late lowstand wedge systems tract

The increased preservation of discrete channel forms and higher proportion of fine-grained strata within the upper part of the incised valley fill is thought to reflect increased rate of additional subaerial accommodation space compared with rates of fluvial aggradation (Shanley and McCabe, 1993; Aitken and Flint, 1995). This may explain the isolated high sinuosity channel segments in the Statfjord Formation (zone D Fig. 4.4). Wright and Marriott (1993) claimed that when the rate of increase of accommodation space is relatively high, vertical accretion may be rapid resulting in isolated, confined channels with low interconnectedness. These are more likely coeval to aggradational shoreface parasequence sets during a time of equal rates of sediment supply and additional accommodation space, and are probably contemporaneous to a late lowstand wedge of the coeval shoreface. In a type 2 unconformity, these sediments are more likely equivalent to a late shelf margin systems tract.

Sequence stratigraphic interpretation of amalgamated fluvial channel deposits with little associated fine-grained overbank material overlying regionally extensive sequence

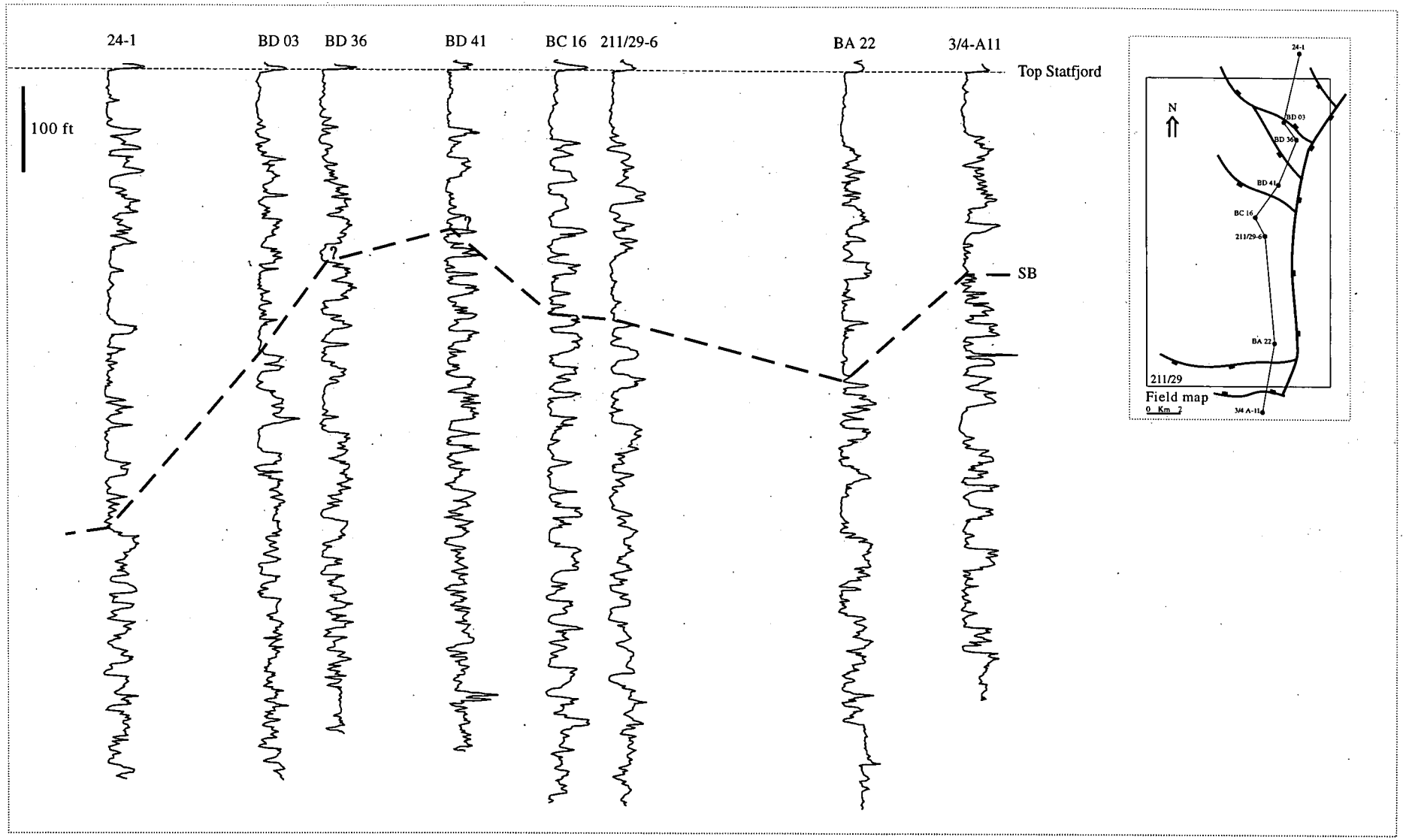

Fig. 4.6 Gamma-ray log correlation showing the regional extend of the sequence boundary (See page 114 for details).

boundaries, however, is a subject of considerable debate. In a similar case, Shanley and McCabe (1991) interpreted such sediments as representing a lowstand systems tract when viewed within a limited area, while on a regional scale, it is interpreted as the basal part of a transgressive systems tract. An alternative approach is to follow the EXXON terminology and regard all fluvial strata within the incised valley as lowstand deposits, and to assign the strata above the first 'local' flooding surface to the transgressive systems tract (e.g. Allen and Posamentier, 1993; Shanley and McCabe, 1993, 1994; Aitken and Flint, 1995). In a similar case, Allen and Posamentier (1993) put the boundary between the lowstand and transgressive systems tract at the change from fluvial to estuarine sedimentation. In the original definition however, (Van Wagoner *et al.* 1988, 1990) the transition from lowstand to transgressive systems tract was placed where the parasequence stacking pattern changed from progradational to retrogradational. The lowest evidence of marine flooding in the case of the Statfjord Formation is the widespread occurrence of the heterolithic (tidally influenced strata?) representing the upper boundary of the lowstand systems tract. However, the transition from lowstand to transgressive systems tract can not be identified precisely, because the transition from fluvial to tidally influenced deposits appears to be gradational.

4.3.3 Recognition of sequence boundary

Recognition of sequence boundaries in alluvial strata is difficult because basinward shifts in facies tracts and related incision can be hard to distinguish from local channel incision (Shanley and McCabe, 1993; Aitken and Flint, 1995). In this case, facies dislocation is interpreted on the basis of an abrupt contrast in facies tracts above and below the sequence boundary, and the change in the degree of fluvial channel sandstone amalgamation (cf Shanley and McCabe, 1993). The facies juxtaposition between zones B and C (Fig. 4.4), reflected in the marked contrast between the vertically stacked low sinuosity channel sandstone bodies, in which preservation of fining-upward stories is incomplete, and the underlying high sinuosity channel system which is dominated by lateral accretion suggests a sequence boundary unconformity. This variation probably represents a base level fall (cf Shanley and McCabe, 1989,

1991, 1993). This change can also be traced laterally from well log correlations (Fig. 4.6). Facies tract dislocations can only be used as an indication of sequence boundaries if the changes are of a regional extent (Aitken and Flint, 1995). Taking the above factors together, the interpretation of a sequence boundary in the Statfjord Formation within the study area is based on the combination of: (a) the degree of facies dislocation, (b) the marked contrast in grain-size above and below the surface, and (c) the regional mappable extent of the surface (Fig. 4.6) which indicates that fluvial incision was related to a significant fall in base level rather than simple channel switching. Shanley and McCabe (1993) suggested that the severity of facies dislocation may be used as a proxy of estimating the magnitude of base level change in a qualitative fashion. For instance, braided river sediments incised into marine shales reflect severe incision and greater base level change than where braided river sediments overly meandering deposits as in this example. According to the views of Posamentier and Vail (1988) as relative sea level falls the bayline drops below the shelf/slope break and stream equilibrium profiles are lowered causing incision and stream rejuvenation. Shoreface parasequences are truncated with a regional sequence boundary. At this time the stream sediment load is characterized by a high sand/mud ratio resulting from sediments being excavated by stream incision in addition to sediments being supplied by the drainage basin, while no sediments are left behind on the flood plain. As a result of increase in both fluvial gradient and sediment supply, sediments may bypass the alluvial realm and be redeposited in a more basinward position in the form of lowstand fan deposits (Shanley and McCabe, 1993). As relative sea level rises the bayline migrates landwards fan deposition ceases and lowstand wedge deposition resumes and continues until the bayline reaches the shelf surface and continues to migrate landward.

This sequence boundary may, therefore, represent a time hiatus coeval to the deposition of a lowstand fan during a rapid fall in relative sea level. The lack of subsurface data north of the study area precluded lowstand fan deposits being recognized. On the interfluve the sequence boundary is represented by subaerial exposure and the development of well-drained deeply weathered soils (Posamentier *et al.* 1992; Feldman *et al.* 1995).

4.3.4 Tidally influenced fluvial deposits in the Statfjord Formation

The core section of well BA/22 (Fig. 4.7) shows rhythmic lamination. Each cycle consists of a number of siltstone laminae each of which is capped by a mudstone drape which is normally a fraction of a mm thick. Individual siltstone laminae have an abrupt lower contact and gradually fine upwards into the overlying mudstone drape. Between the lower two arrows (Fig. 4.7) thin siltstone laminae, ranging from a fraction of a mm up to 2 mm thick, reveal gradual upward-thickening followed by subsequent thinning. This change in lamina thickness could be interpreted as flood periodicities or it may be interpreted as reflecting neap-spring-neap tidal current cyclicity of a half-lunar month (Kvale and Archer, 1990; Archer *et al.* 1995; D. Miller, pers. communication). Penecontemporaneous deformation and bioturbation partially preclude laminae identification. The thickest lamina (maxima) in the middle of the cycle is probably consistent with spring tides when solar and lunar tidal waves are coincident during new and full moon periods. The thinnest siltstone lamina (minima) is probably deposited within the thickest mudstone bundles (arrows) during neap tides at the time of the first and third moon quarters. Thick mud accumulation during the weaker neap tides formed because the threshold velocity for sand and silt transport was not exceeded, resulting in multiple periods of slackwater mud deposition (Kvale and Archer, 1990). Individual siltstone lamina are interpreted to reflect daily tidal events (Kvale *et al.* 1989), whilst mudstone drapes are interpreted to have deposited during a slackwater period following tidal deposition of the siltstone laminae. The gradual upward transition of individual siltstone lamina into mudstone indicates deposition during waning flow (Kvale and Archer, 1990). The number of laminae per cycle (14 or fewer) between zones of lamina minima indicate that subordinate tidal deposits do not exist or are not distinguishable from dominant tides. This further implies a diurnal palaeotidal regime where only one tide per day may have existed (cf Kvale *et al.* 1989).

Similar features attributed to tidal influences observed in rock record have been discussed by several authors (Allen and Posamentier, 1993; Shanley and McCabe, 1993; Aitken and Flint, 1995; Feldman *et al.* 1995). The studies of Shanley and McCabe (1994) have demonstrated that tidal influence can extend as far as 50 km inland of coeval shorelines. In an estuarine setting Allen and Posamentier (1993)

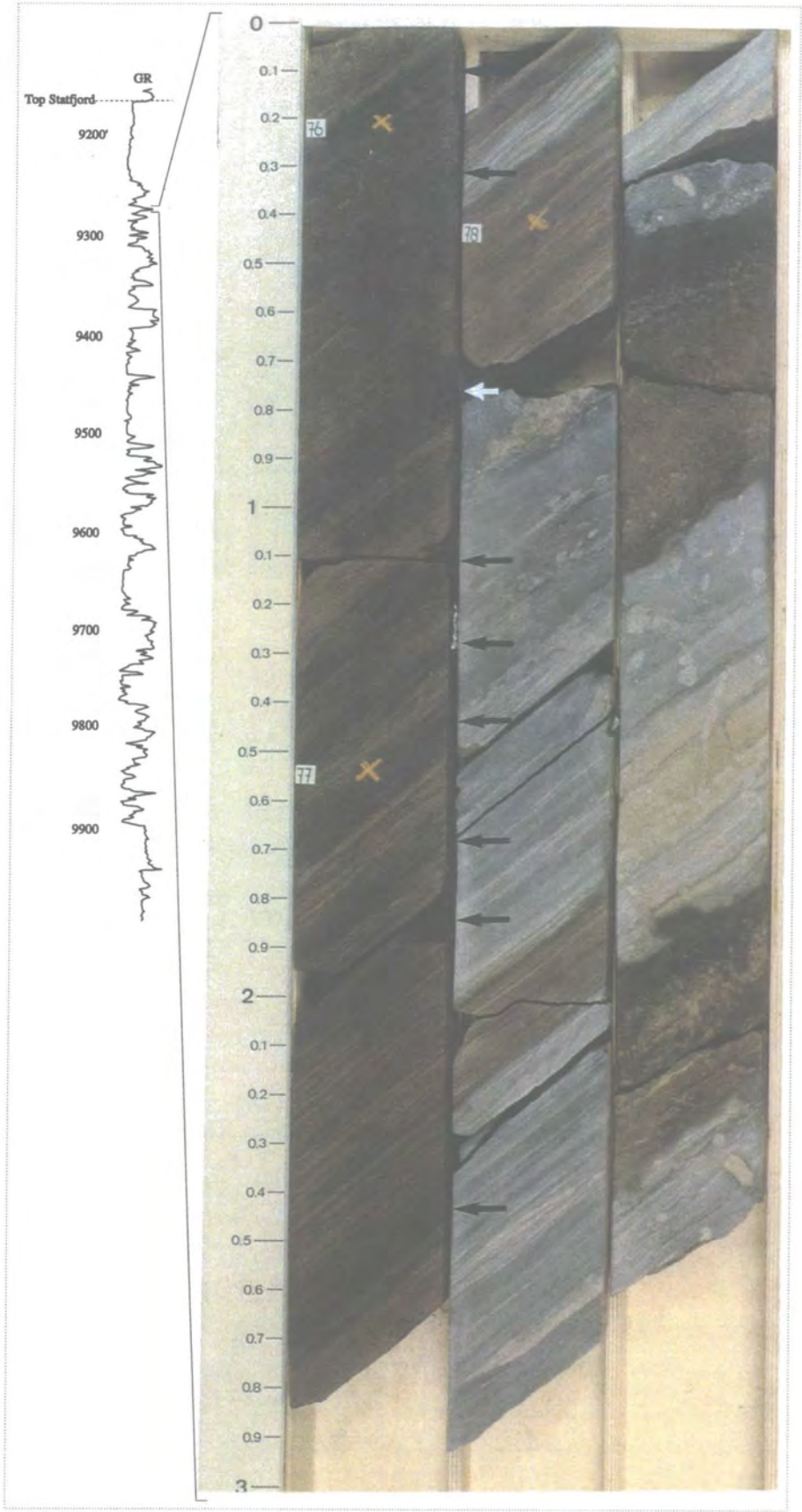

Fig. 4.7 Cyclical rhythmites probably indicating neap-spring-neap tidal cycles. Arrows are pointing to the position of lamina minima during neap tides. From Well BA/22 core section.

suggested that tidal influence may extend inland by as much as 115 km.

The existence of tidally influenced strata reflects the onset of a marine transgression (Allen and Posamentier, 1993) and tidal rhythmites have not been previously recorded from the Statfjord Formation.

4.3.5 Transgressive systems tract

In the coeval marine strata during the interval of lowstand wedge deposition, the rate of new shelf space added increases in response to a gradual increase in the rate of relative sea level rise. The rate of regression of the lowstand wedge gradually decreases until eventually the sediment supply can not keep pace with the rate at which the new shelf space is added, and a transgression at this time marks the end of the lowstand systems tract. Zone E in Fig. 4.4 may reflect tidally influenced fluvial strata that may relate to the higher rates of additional accommodation space and the initiation of a transgressive systems tract. Shanley and McCabe (1990, 1991) suggested that the highest rate of base level rise results in retrogradational shoreface parasequences and tidally influenced fluvial systems marking the initiation of a transgressive systems tract. The presence of tidal deposits overlying a fluvial section indicates that the eustatic rise was sufficiently rapid that increased accommodation space was greater than the fluvial sediment influx (Allen and Posamentier, 1993). Consequently, sediments supplied from upstream were deposited as aggrading, transgressive, tidally influenced facies that onlapped the lowstand fluvial profile. These isolated heterolithic deposits within an otherwise fluvial succession are correlated with the maximum flooding surfaces in the coeval marine realm. Shanley and McCabe (1994) suggested that the period of maximum flooding within alluvial strata is not represented by a condensed section but rather represented by the invasion of tidal processes in an area formally dominated by purely fluvial processes. This upward-deepening facies succession, reflected in the transition from amalgamated channel sandstones directly overlying a sequence boundary into isolated channel deposits and finally into tidally influenced strata, suggests coastal transgression and maximum marine incursion into the alluvial realm (Shanley and McCabe, 1993). Allen and Posamentier (1993) suggested that the shift from fluvial to tidally influenced strata clearly indicates that a marine transgression

occurred eliminating further fluvial contribution and accompanied by an accelerating shoreline transgression.

4.3.6 Recognition of transgressive surface

Posamentier and Vail (1988) indicated that a transgressive surface is typically observed at the upper boundary of the proximal lowstand wedge. As sea level rises gradually following a type 1 unconformity, the additional new space is initially restricted to the incised valleys since the shelf remains subaerially exposed. Consequently little new space is added until sea level rises above the pre-existing shelf surface. At this time abrupt additional accommodation space results in an abrupt landward shift of the depocentre generating a transgressive surface.

The interpretation of the transgressive surface is a debatable matter. Recently, it has become common to place the transgessive surface at the fluvial-estuarine transition (e.g. Posamentier *et al.* 1992; Allen and Posamentier 1993). Hence, in the Statfjord Formation the transgressive surface forms the base of the transgressive systems tract and separates the tidally influenced strata (zone E) from the underlying fluvial deposits (zones C, D Fig. 4.4). It represents the updip-migration position of the bayline and may be coincident with the sequence boundary in the upstream direction and on the interfluve where lowstand deposits are absent (Posamentier *et al.* 1992; Allen and Posamentier, 1993). Dalrymple and Zaitlin (1994) suggested that because fluvial deposition can continue throughout the transgression, the fluvial-tidal contact may be diachronous and lie above transgressive deposits. Thus, this contact may not be an appropriate choice for a transgressive surface.

4.3.7 Transgressive marine sandstone

Zone F (Fig. 4.4) consists of poorly-sorted very coarse-grained sandstone. Scattered well-rounded quartzitic pebbles up to 5 cm in diameter are present within this sandstone. The base of the sandstone is erosional with internal scour surfaces and poorly-defined sedimentary structures including flat bedding. Regionally the sandstone is mainly of a uniform thickness (25-30 m), and is interpreted as a marine sandstone

deposited during the subsequent shoreface transgression. Although no coarse-grained lag deposits were recognized the underlying surface may be interpreted as a wave ravinement surface. Van Wagoner *et al.* (1990) suggested that transgressive lags are rarely associated with flooding surfaces which are not coincident with sequence boundaries, and if noticed they are normally thin. When the rate of relative sea level rise is moderate to low the shoreline transgresses landward by shoreface erosion (Swift, 1975). As a result some part of the underlying deposits is reworked. This could describe a situation whereby a transgressive barrier/lagoon system initially aggrades and subsequently migrates landward in response to rising relative sea level (Arnott, 1995). Dalrymple and Zaitlin (1994) postulated that landward migration of the shoreline would have been accompanied by wave erosion and the formation of a wave ravinement surface seaward of a barrier island. Depending on the degree of subsequent marine reworking, some if not most of the transgressive barrier complex will be preserved (Arnott, 1995). Penland *et al.* (1988) developed the concept of transgressive submergence of the Holocene Mississippi River delta complex. According to these authors transgressive submergence is more effective on low gradient coastal plains. In their model, following an episode of delta lobe abandonment, sediments are reworked by shoreface erosion and spread laterally to form a barrier-island complex. With subsequent subsidence and consequent shoreline detachment, the barrier becomes progressively degraded and eventually submerged forming a subtidal shelf shoal several metres thick. A similar situation is envisaged for the upper part of the Statfjord Formation (Zone F Fig. 4.4).

In the case of an estuarine setting Allen and Posamentier (1993) described similar coarse-grained, well sorted sediments as estuary-mouth sands interpreted to have formed by longshore drift and flood tides. According to these authors the base of the sand is erosional with internal scour surfaces and sedimentary structures include flat bedding. The basal scour surface, deeply incised into the underlying estuarine sediments, is interpreted as a narrow tidal-inlet erosion surface. These sands were interpreted by Allen and Posamentier (1993) as forming a thick tidal-inlet deposits, separated from the underlying estuarine deposits by a tidal ravinement surface.

These sediments are assigned to part of the transgressive and not highstand systems tract because lithologically it would be difficult to detect the downlap surface (maximum flooding surface) separating the two (Allen and Posamentier, 1993).
The overlying, marine sandstones and shales of the Dunlin Group record continued marine transgressive inundation of the Brent Field.

4.4 Three-dimensional models

A simplified schematic illustration of the geological evolution of the Statfjord Formation in the study area in response to base level changes is portrayed in Fig. 4.8, models 1-7.

* Model 1 represents the deposition of zone A (Fig. 4.4) during an early highstand systems tract. The area was dominated by minor isolated channels and numerous stacked coarsening-upward successions most likely deposited within a delta plain environment representing stacked lacustrine delta lobes.

* Model 2 shows widespread alluviation and the deposition of zone B which is probably equivalent to a late highstand systems tract. Point bars and lateral accretion deposits dominate this zone probably reflecting reduced available subaerial accommodation space.

* Model 3 represents a time hiatus of nondeposition during a pronounced base level fall. Entrenched streams and incised valleys may have formed during this time. The base of the incised valleys represent a sequence boundary unconformity which is equivalent to subaerial exposure on the interfluve.

* Model 4 represents a slight rise in base level and the deposition of low sinuosity river deposits with a relatively high degree of channel interconnectedness. Thus, zone C may be coeval to an early lowstand wedge systems tract.

* Model 5 corresponds to the deposition of the isolated high sinuosity channel segments with a higher proportion of overbank fine-grained material of zone D which is interpreted as being equivalent to a late lowstand wedge systems tract. However, the global, eustatic-cycle and chronostratigraphic chart of Haq *et al.* (1988) (Fig. 4.9) dismisses the occurrence of lowstand fan deposition at this time which may suggest a type 2 unconformity separating sequence 1 from sequence 2 (Fig. 4.4). Based on this assumption Zones C and D (Fig. 4.4) may be alternatively interpreted as equivalent to early and late shelf margin instead of lowstand systems tracts.

* Model 6 shows the possible first 'local' major flooding and initiation of a transgressive systems tract, as reflected in the occurrence of the heterolithic, possibly tidally influenced strata of zone E. These are probably equivalent to a condensed section in the coeval marine realm.

* Model 7 illustrates continued transgression and deposition of the high energy marine sandstone of zone F which is probably separated from the underlying sediments by the occurrence of a wave ravinement surface indicating a landward migrating shoreline.

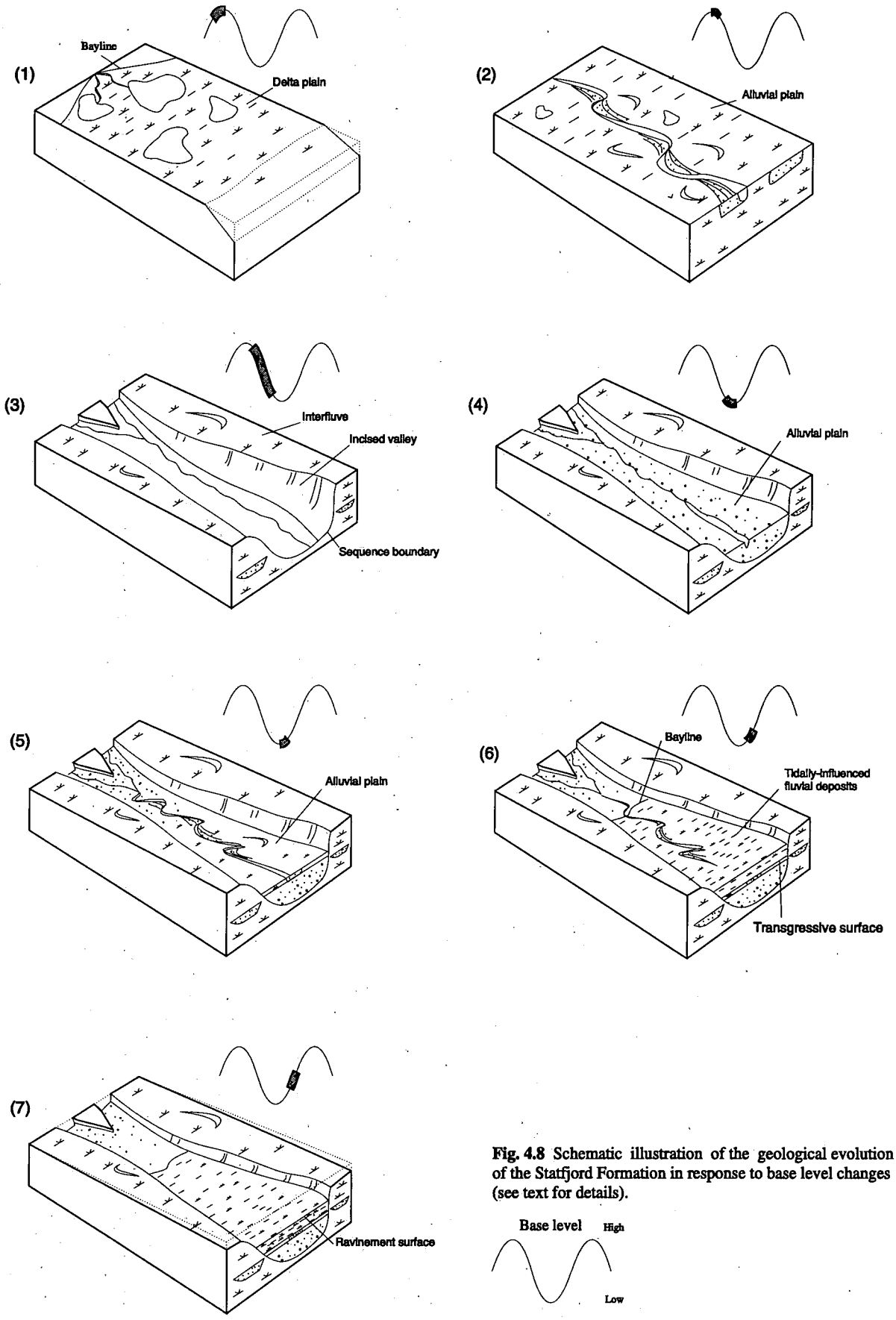

Fig. 4.8 Schematic illustration of the geological evolution of the Statfjord Formation in response to base level changes (see text for details).

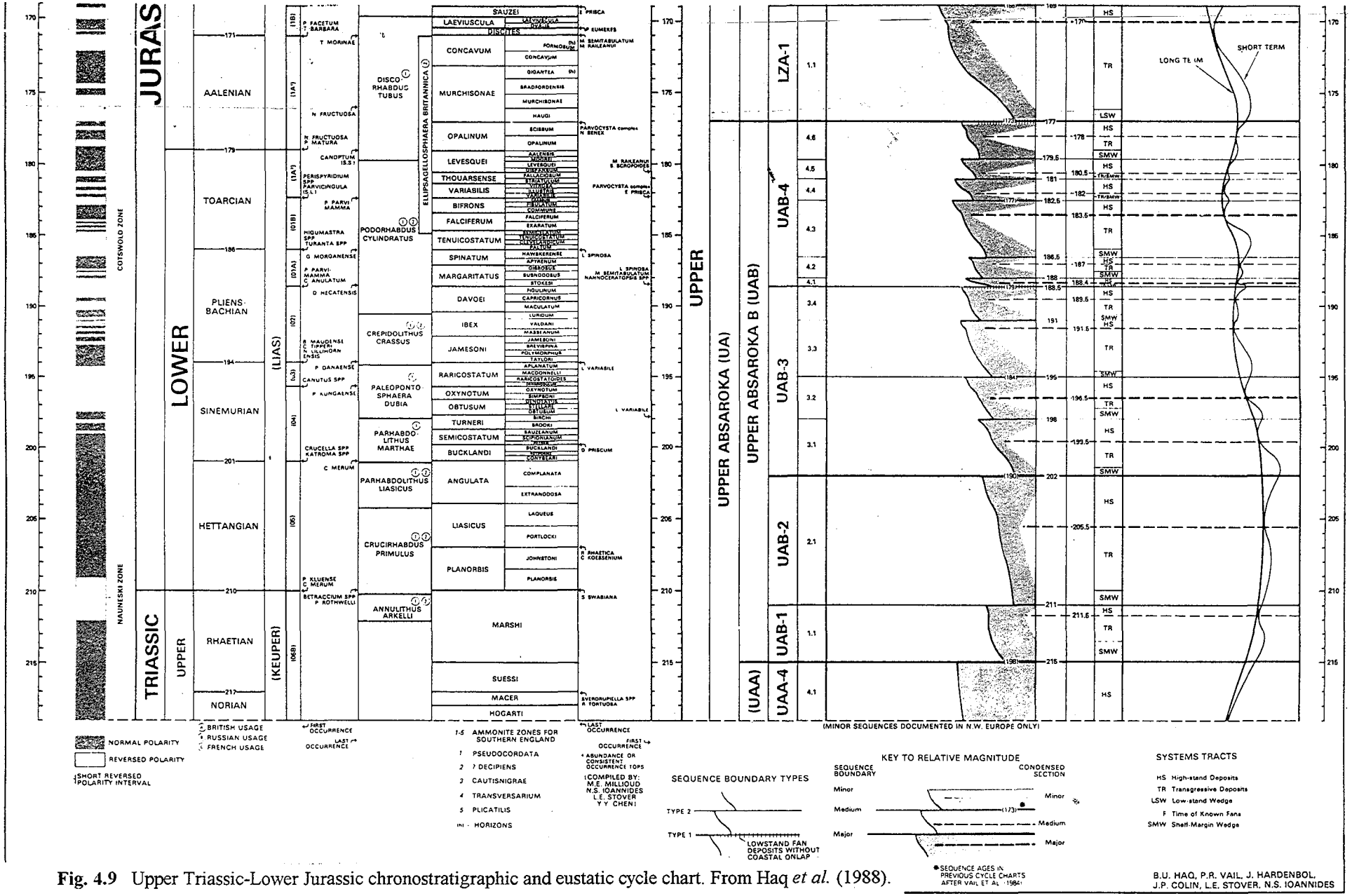

Fig. 4.9 Upper Triassic-Lower Jurassic chronostratigraphic and eustatic cycle chart. From Haq *et al.* (1988).

Chapter 5

General conclusions

In the Brent Field, northern North Sea, the Upper Triassic-Lower Jurassic Statfjord Formation is interpreted to have been deposited in a variety of sedimentary environments. These include delta plain, meandering rivers, braided rivers, tidally influenced fluvial systems and shallow, high energy marine environments. This study of the Statfjord Formation within the Brent Field provided an opportunity to examine sedimentary facies and environments, and has led to the following conclusions.

* Because of the low sand/mud ratio, and poor hydrocarbon potential, the lowermost part of the formation has not been extensively penetrated by cored boreholes. Hence, this part of the Statfjord Formation (which has been referred to in the previous chapters as zone A) is interpreted, based mainly on log data, to have been deposited within a delta plain environment. These deposits which are devoid of marine fauna, strengthen the interpretation of an upper delta plain setting away from direct marine inundation. Sedimentary facies are characterized by localized channel sandstone bodies, forming part of numerous stacked coarsening-upward sequences. The channels are minor, probably anastomosing distributaries with stable muddy banks. The coarsening-upward sequences may reflect stacked lacustrine deltas deposited as a result of distal river reaches depositing their fine-grained sediments into adjacent ponded waters.
Applying sequence stratigraphic principles, this zone is thought to have been deposited during an early highstand systems tract when the rate of addition of new subaerial accommodation space was gradually declining thereby providing the opportunity for the river system to build and prograde basinward. The rate of vertical accretion is relatively high at this time compared to the rate of lateral migration which provided an ideal setting for fine-grained sediments to be extensively stored. These sediments are probably equivalent to prograding to slightly aggrading parasequences in the coeval shoreface setting.

* Zone B consists predominantly of high sinuosity (meandering) river deposits. Evidence of lateral accretion surfaces in this zone has been documented within the core section of well BD/44. A diversity of sedimentary facies has been recognized within this zone, including point bar deposits, chute channels and chute modified point bars, gradually and abruptly abandoned high sinuosity channel facies in addition to a number of overbank facies including crevasse splays, swamp, and rare lacustrine and lacustrine deltas. Documented point bar sediments revealed that the bankfull channel depth of these high sinuosity rivers may have reached as much as 4.5 m. The lack of evidence of exposure of these in-channel sediments implies that the rivers were probably perennial. The overall sediment grain size within this zone ranges from very coarse-grained with scattered pebbles to very fine-grained sandstone, siltstone and mudstone.

In terms of base level change, this zone reflects the vertical change from the underlying vertically aggraded sediments to laterally migrating river deposits. This may be interpreted in the light of sequence stratigraphic principles as a change from an early highstand to a late highstand systems tract. Because of the lack of subaerial accommodation space at this time, rivers are interpreted to have migrated laterally combing the previously deposited fine-grained sediments. The sand/mud ratio is higher than the lower zone (A) and a characteristic shoe string geometry (terminology after Galloway, 1985) of the channel deposits predominates.

* A low sinuosity (braided) river system was the dominant depositional environment in zone C. Three distinct low sinuosity channel facies have been recognized within this zone: type 1, type 2 and type 3. Type 1 low sinuosity channel facies resembles the sandy braided Platte River facies model of Miall (1977), and is interpreted to have been deposited within a distal braidplain setting. Type 2 low sinuosity channel facies is characterised by numerous internal scour surfaces, very coarse-grained sediments and scattered pebble-size clasts. It is interpreted to have been deposited in a more proximal braided river system, and dominates the southern part of the study area. Type 3 low sinuosity channel facies matches the South Saskatchewan River model of Cant and Walker (1978) and is characterised by cyclic deposits dominated by trough cross-bedding and in many cases sand flat accumulations. This channel facies is interpreted as

an intermediate channel deposit between the proximal gravelly Donjek River and the sandy Platte River type models (Miall, 1977).

These low sinuosity river deposits are interpreted to have been deposited during a slightly rising base level following a significant base level fall. They overly a regional sequence boundary unconformity and are characterized by a high sand/mud ratio and high degree of channel sandstone amalgamation. These low sinuosity river deposits are interpreted as equivalent to an early lowstand wedge systems tract or an early shelf margin systems tract in the case of a type 2 unconformity. They are regarded as an incised valley fill which attains the maximum thickness in the channel thalweg and thins both in the interfluve and in a landward direction. The wedge like geometry of these incised valley fill deposits in addition to their high net/gross ratio and high lateral and vertical continuity provide an excellent hydrocarbon reservoir. The increased rate of rising base level during late lowstand resulted in isolated high sinuosity channel segments overlying the low sinuosity channel sandstones. These are interpreted as coeval to a late lowstand wedge or late shelf margin systems tract. In the previous chapters these isolated high sinuosity river deposits have been assigned to zone D.

* Evidence of tidal rhythmites, which may reflect the onset of a transgressive systems tract, has been documented in the core section of well BA/22 overlying the incised valley fill. These deposits, which are regarded as zone E in the previous chapters, are characterized by numerous thin siltstone laminae interbedded with thin mudstone drapes which form a cyclic periodicity. Each cycle with silty laminae normally less than 14 in number is interpreted to reflect a neap-spring-neap tidal cycle of a half lunar month in a diurnal palaeotidal regime. These deposits are probably equivalent to a condensed section in the coeval marine realm, and reflect the increased rate of addition of subaerial accommodation space marking the first 'local' major marine flooding.

* Continued shoreline transgression is reflected in the deposition of the high energy marine transgressive sandstone of zone F. These sediments are coarse- to very coarse-grained and contain scattered well-rounded quartzitic pebbles up to 5 cm in diameter. Poorly-defined flat bedding is the dominant stratification type in these sandstones. The overall uniform thickness of these sediments over the entire field indicate that a

pronounced marine transgression may have flooded both the incised valleys and the interfluves.

* Palaeocurrent indicators obtained from HDT log analysis reveal that the Statfjord Formation in the Brent Field has been deposited by a north to north-west flowing drainage system. The overall spacial and temporal consistency of these indicators throughout the formation further implies that no flow reversal occurred during the evolution of the Statfjord Formation.

* Sandstone mineralogical composition determined from NGS logs indicate that an overall decrease in sandstone mineralogical maturity occurs with decreasing depth across the Statfjord Formation. This may reflect a gradual upward decrease in the degree of reworking of sediments and/or decrease in the sediment transport distance.

* In considering the relative tectonic quiescence of the area during deposition of the Statfjord Formation, and the overall consistency of the palaeoflow patterns, it is possible to relate the changes in facies stacking patterns and facies tracts to oscillations in base level. This together with the close link between these changes and the eustatic curve further suggest that the Statfjord Formation in the Brent Field may have been deposited in a near shore setting.

REFERENCES

Adams, J. A. and Weaver, C. E. 1958. Thorium-uranium ratios as indicators of sedimentary processes: example of concept of geochemical facies. *American Association of Petroleum Geologists Bulletin,* 42, 387-430.

Aitken, J. F. 1995. Utility of coal seams as genetic stratigraphic sequence boundaries in nonmarine basins: an example from the Gunnedah Basin, Australia: Discussion. *American Association of Petroleum Geologists Bulletin,* 79, 1179-1181.

Aitken, J. F. and Flint, S. S. 1995. The application of high-resolution sequence stratigraphy to fluvial systems: a case study from the Upper Carboniferous Breathitt Group, eastern Kentucky, USA. *Sedimentology,* 42, 3-30.

Albright, W. A., Turner, W. L. and Williamson, K. R. 1980. Ninian Field, U. K. Sector, North Sea. *In:* Halbouty, M. T. (ed.) Giant Oil and Gas Fields of the Decade: 1968-1978. *American Association of Petroleum Geologists Memoir,* 30, 173-193.

Alexander, J. and Gawthorpe, R. I. 1993. The complex nature of a Jurassic multistorey, alluvial sandstone body, Whitby, North Yorkshire. *In:* North, C. P. and Prosser, D. J. (eds.) Characterization of fluvial and aeolian reservoirs. Geological Society Special Publication, 73, 123-142.

Allen, G. P. and Posamentier, H. W. 1993. Sequence stratigraphy and facies model of an incised valley fill: The Gironde Estuary, France. *Sedimentology,* 63, 378-391.

Allen, J. R. L. 1965. A review of the origin and characteristics of recent alluvial sediments. *Sedimentology,* 5, 89-191.

Allen, J. R. L. 1983. Studies in fluviatile sedimentation: bars, bar-complexes and sandstone sheets (low-sinuosity braided streams) in the Brownstones (Lower Devonian), Welsh Borders. *Sedimentary Geology,* 33, 237-293.

Allen, P. A. and Collinson, J. D. 1991. Lakes. *In:* Reading, H. G. (ed.) Sedimentary Environments and Facies. Blackwell Scientific Publications. 2nd edition. 63-94.

Archer, A. W., Kuecher, G. J. and Kvale, E. P. 1995. The role of tidal-velocity asymmetries in the deposition of silty tidal rhythmites (Carboniferous, Eastern Interior Coal Basin, U.S.A.). *Journal of Sedimentary Research,* 65, 408-416.

Arnott, R. W. C. 1995. The parasequence definition- are transgressive deposits inadequately addressed ?. *Journal of Sedimentary Research,* 65, 1-6.

Aslam, M. 1992. Delta plain coal deposits from the Than Formation of the Early Cretaceous Saurashtra Basin, Gujarat, Westren India. *Sedimentary Geology,* 81, 181-193.

Badley, M. E., Price, J. D., Rambech Dahl, C. and Agdestein, T. 1988. The structural evolution of the northern Viking Graben and its bearing upon extensional modes of basin formation. *Journal of the Geological Society of London,* 145, 455-472.

Bahrig, B. 1994. The formation of alternating chalk/siderite units during the Neogene in the Black Sea- an example of climatic control of early diagenetic processes. *In:* Wolf, K. H. and Chilingarian, G. V. (eds.) Diagenesis, IV. Developments in Sedimentology 51. Elsevier, 529pp.

Boggs, S. jr., 1987. Principles of sedimentology and stratigraphy. Macmillan Publishing Company, New York, 784pp.

Bowen, J. M. 1975. The Brent Oil Field. *In*: Woodland, A. W. (ed.) Petroleum and the Continental Shelf of North West Europe. Institute of Petroleum, London. 353-361.

Bridge, J. S. 1984. Large scale facies sequence in alluvial overbank deposits. *Journal of Sedimentary Petrology,* 54, 583-588.

Bridge, J. S. 1985. Palaeochannel pattern inferred from alluvial deposits: Critical Evolution. *Journal of Sedimentary Petrology,* 55, 579-589.

Bridge, J. S. 1993. Description and interpretation of fluvial deposits: a critical perspective. *Sedimentology,* 40, 801-810.

Bridge, J. S. and Leeder, M. R. 1979. A simulation model of alluvial stratigraphy. *Sedimentology,* 26, 617-644.

Bridge, J. S., Smith, N. D., Trent, F., Gabel, S. L. and Bernstein, P. 1986. Sedimentology and morphology of a low-sinuosity river, Calamus River, Nebraska Sand Hills. *Sedimentology,* 33, 851-870.

Brown, S. 1990. Jurassic. *In:* Glennie, K. W. (ed.) Introduction to the petroleum geology of the North Sea. Blackwell Scientific Publications, Oxford. 3rd edition, 219-254.

Brown, S., Richards, P. C. and Thomson, A. R. 1987. Patterns in the deposition of the Brent Group (Middle Jurassic) UK, North Sea. *In:* Brooks, J. and Glennie, K. (eds.) Petroleum geology of north west Europe. 899-915.

Cameron, G. I. F. 1992. Analysis of dipmeter data for sedimentary orientation. *In:* Hurst, A., Griffiths, C. M. and Worthington, P. F. (eds.) Geological applications of wireline logs II. Geological Society Special Publication, 65, 141-154.

Campbell, J. E. and Hendry, H. E. 1987. Anatomy of a gravelly meander lobe in the Saskatchewan River, Near Nipawin, Canada. *In:* Ethridge, F. G., Flores, R. M. and Harvey, M. D. (eds.) Recent developments in fluvial sedimentology. Contributions from the third international fluvial sedimentology conference. Society of Economic Paleontologists and Mineralogists Special Publication, 39, 179-189.

Cant, D. J. 1978. Development of a facies model for sandy braided river sedimentation: Comparison of the South Saskatchewan River and the Battery Point Formation. *In:* Miall, A. D. (ed.) Fluvial sedimentology. Canadian Society of Petroleum Geologists, Memoir, 5, 627-639.

Cant, D. J. 1992. Fluvial facies models and their applications. *In:* Scolle, P. A. and Spearing, D. (eds.) Sandstone Depositional Environments. *American Association of Petroleum Geologists,* Memoir. 31, 115-137.

Cant, D. J. and Walker, R. G. 1976. Development of a braided-fluvial facies model for the Devonian Battery Point Sandstone, Quebec. *Canadian Journal of Earth Sciences,* 13, 102-119.

Cant, D. J. and Walker, R. G. 1978. Fluvial processes and facies sequences in the sandy braided South Saskatchewan River, Canada. *Sedimentology,* 25, 625-648.

Casshyap, S. M. and Kumar, A. 1987. Fluvial architecture of the Upper Permian Raniganj Coal Measure in the Damodar Basin, Eastern India., *Sedimentary Geology,* 51, 181-213.

Chamberlain, A. 1984. Surface gamma-ray log: A correlation tool for Frontier Areas. *American Association of Petroleum Geologists Bulletin,* 68, 1040-1043.

Chauvin, A. L. and Valachi, L. Z. 1980. Sedimentology of the Brent and Statfjord Formations of Statfjord Field. *In:* The sedimentation of the North Sea reservoir rocks. Norwegian Petroleum Society. 1-17.

Coleman, J. M. 1969. Brahmaputra River: Channel processes and sedimentation. *Sedimentary Geology,* 3, 129-139.

Collinson, J. D. 1978. Vertical sequence and sand body shape in alluvial sequences. *In:* Miall, A. D. (ed.) Fluvial sedimentology. Canadian Society of Petroleum Geologists, Memoir, 5, 577-586.

Collinson, J. D. 1991. Alluvial sediments. *In:* Reading, H. G. (ed.) Sedimentary Environments and Facies. Blackwell Scientific Publications. 2nd edition. 20-62.

Cowan, D. R. and Myers, K. J. 1988. Surface gamma-ray logs: A correlation tool for Frontier Areas: Discussion. *American Association of Petroleum Geologists Bulletin,* 72, 634-636.

Crossey, L. J. and Larsen, D. 1992. Authigenic mineralogy of sandstones intercalated with organic-rich mudstones: intergrating diagenesis and burial history of the Mesaverde Group, Piceance Basin, NW Colorado. *In:* Houseknecht, D. W. and Pittman, E. D. (eds.) Origin, diagenesis, and petrophysics of clay minerals in sandstones. Society of Economic Paleontologists and Mineralogists Special Publication, 47, 125-144.

Cuevas Gozola, M. C. and Martinius, A. W. 1993. Outcrop data-base for the geological characterization of fluvial reservoirs: an example from distal fluvial fan deposits in the Lornca Basin, Spain. *In:* North, C. P. and Prosser, D. J. (eds.) Characterization of fluvial and aeolian reservoirs. Geological Society Special Publication, 73, 79-94.

Curtis, C. 1987. Mineralogical concequences of organic matter degradation in sediments: inorganic/organic diagenesis. *In:* Leggett, J. K. and Zuffa, G. G. (eds.) Marine clastic sedimentology. Graham and Trotman, London. 108-123.

Dalrymple, R. W. and Zaitlin, B. A. 1994. High-resolution sequence stratigraphy of a complex, incised valley succession, Cobequid Bay-Salmon River estuary, Bay of Fundy, Canada. *Sedimentology,* 41, 1069-1091.

Davies, D. K and Ethridge, F. G. 1975. Sandstone composition and depositional environment. *American Association of Petroleum Geologists Bulletin,* 59, 239-264.

Davies, D. K. Williams, B. P. J. and Vessel, R. K. 1993. Dimensions and quality of reservoirs originating in low and high sinuosity channel systems, Lower Cretaceous Travis Peak Formation, East Texas, USA. *In:* North, C. P. and Prosser, D. J. (eds.) Characterization of fluvial and aeolian reservoirs. Geological Society Special Publication, 73, 95-121.

Davis, Jr. R. A. 1992. Depositional systems: An introduction to sedimentology and stratigraphy. Prentice Hall, Englewood Cliffs. New Jersey. 2nd edition. 604pp.

Dawson, M. R. and Bryant, I. D. 1987. Three dimensional facies geometry in Pliestocene outwash sediments, Worcestershire, U. K. *In:* Ethridge, F. G., Flores, R. M. and Harvey, M. D. (eds.) Recent developments in fluvial sedimentology. Contributions to the Third International Fluvial Conference, Society of Economic Paleontologists and Mineralogists, Special Publication, 39, 191-196.

Deegan, C. E. and Scull, B. J. 1977. A proposed standard lithostratigraphic nomenclature for central and northern North Sea. Report of the Institute of Geological Sciences. 77/25. *Bulletin of the Norwegian Petroleum Directorate,* 1, 36pp.

Delfiner, P., Peyret, O. and Serra, O. 1984. Automatic determination of lithology from well logs. 59th ann. tech. Conf. SPE of AIME, Houston, Texas. Paper no. SPE 13290.

Diemer, J. A. and Belt, E. S. 1991. Sedimentology and paleohydroaulics of the meandering river systems of the Fort Union Formation, Southeastern Montana. *Sedimentary Geology,* 75, 85-108.

Doveton, J. H. 1986. Log analysis of subsurface geology, concepts and computer methods. New York, John Wiley& Sons. 273pp.

Doveton, J. H. 1994. Geological log interpretation: Reading the rocks from wireline logs. Society of Economic Paleaontologists and Mineralogists Short Course, 29, 169pp.

Dybvik, H. and Eriksen, D. 1983. Natural radioactivity of clastic sediments and the contribution of u, th, k. *Petroleum Geology,* 5, 409-416.

Elliott, T. 1974. Interdistributary bay sequences and their genesis. *Sedimentology,* 21, 611-622.

Eslinger, E. and Pevear, D. 1988. Clay minerals for petroleum geologists and engineers. Society of Economic Paleontologists and Mineralogists Short Course Notes. 22.

Ethridge, F. G., Jackson, T. J. and Yongberg, A. D. 1981. Flood basin sequence of a fine grained meander belt subsystem: The coal bearing lower Wasatch and Upper Fort Union Formation, South Powder River basin Wyoming. *In:* Ethridge, F. G. and Flores, R. M. (eds.) Recent and ancient non-marine depositional environments: Models for exploration. Society of Economic Paleontologists and Mineralogists Special Publication, 31, 191-209.

Feldman, H. R., Gibling, M. R., Archer, A. W., Wightman, W. C. and Lanier, W. P. 1995. Stratigraphic architecture of the Tonganoxie palaeovalley fill (Lower Virgilian) in northeasren Kansas. *American Association of Petroleum Geologists Bulletin,* 79, 1019-1043.

Fielding, C. R. 1984. Upper delta plain lacustrine and fluviolacustrine facies from the Westphalian of Durham Coalfield, NE England. *Sedimentology,* 31, 547-567.

Fielding, C. R. 1985. Coal depositional models and the distinction between alluvial and delta plain environments. *Sedimentary Geology,* 42, 41-48.

Fielding, C. R. 1986. Fluvial channel and overbank deposits from the Durham Coal Field, NE England. *Sedimentology,* 33, 119-140.

Fisher, M. J. and Mudge, D. C. 1990. Triassic. *In:* Glennie, K. W. (ed.) Introduction to the petroleum geology of the North Sea. Blackwell Scientific Publications, Oxford. 3rd edition, 191-218.

Flores, R. M. 1981. Coal deposition in fluvial paleoenvironments of the Paleocene Tunge River Member of the Fort Union Formation, Powder River area, Powder River basin, Wyoming and Montana. *In:* Ethridge, F. G. and Flores, R. M. (eds.) Recent and ancient non-marine depositional environments: Models for exploration. Society of Economic Paleontologists and Mineralogists Special Publication, 31, 169-190.

Farquharson, G. W. 1982. Lacustrine deltas in a Mesozioc alluvial sequence from Camp Hill, Antarctica. *Sedimentology,* 29, 717-725.

Friend, P. F. 1978. Distinctive features of some ancient river systems. *In:* Miall, A. D. (ed.) Fluvial sedimentology. Canadian Society of Petroleum Geologists Memoir, 5, 531-542.

Friend, P. F. 1983. Towards the field classification of alluvial architecture or sequence. *In:* Collinson, J. D. and Lewin, J. (eds.) Modern and ancient fluvial systems. International Association of Sedimentologists Special Publication, 6, 345-354.

Gabrielsen, R. H., Foerseth, R. B., Steel, R. J., Idil, S. and Klφvjan, O. S. 1990. Architectural styles of basin fill in the northern Viking Graben. *In:* Blundell, D. J. and Gibbs, A. D. (eds.) Tectonic Evolution of the North Sea Rifts. Oxford Science Publications. 158-179.

Galloway, W. E. 1981. Depositional architecture of Cenozoic Gulf Coastal Plain fluvial system. *In:* Ethridge, F. G. and Flores, R. M. (eds.) Recent and ancient non-marine depositional environments: Models for exploration. Society of Economic Paleontologists and Mineralogists Short Course, 19, 127-155.

Galloway, W. E. 1985. Meandering streams - Modern and ancient. *In:* Recognition of fluvial depositional systems and their resource potential. Society of Economic Paleontologists and Mineralogists Short Course, 19, 145-166.

Galloway, W. E. and Hobday, D. K. 1983. Terrigenous Clastic Depositional Systems. Springer-Verlag. New York. 423pp.

Gersib, G. A. and McCabe, P. J. 1981. Continental coal-bearing sediments of the Port Hood Formation (Carboniferous), Cape Linzee, Nova Scotia, Canada. *In:* Ethridge F. G. and Flores, R. M. (eds.) Recent and ancient non-marine depositional environments: Models for exploration. Society of Economic Paleontologists and Meniralogists Special Publication, 31, 95-108.

Ghosh, S. K. 1987. Cyclicity and facies characteristics of alluvial sediments in the Upper Paleozoic Monongahela- Dunkard Group, Central West Verginia. *In:* Ethridge, F. G., Flores, R. M. and Harvey, M. D. (eds.) Recent developments in fluvial sedimentology. Contributions to the Third International Fluvial Sedimentology Conference. Society of Economic Paleontologists and Mineralogists Special Publication, 39, 227-239.

Gibbs, A. D. 1990. Linked fault tectonics of the North Sea. *In:* Blundell, D. J. and Gibbs A. D. (eds.) Tectonic evolution of the North Sea Rifts. 145-157.

Glennie, K. W., 1990. Outline of North Sea history and structural framework. *In:* Glennie, K. W. (ed.) Intoduction to the petroleum geology of the North Sea. Blackwell Scientific Publications, Oxford. 3rd edition, 34-77.

Goff, J. C. 1983. Hydrocarbon generation and migration from Jurassic source rocks in the E. Shetland Basin and Viking Graben of the northern North Sea. *Journal of the Geological Society of London,* 140, 445-474.

Golia, R. T. and Stewart, J. H. 1984. Depositional environments and paleogeography of the Upper Miocene Wassuk Group, West-Central Nevada. *Sedimentary Geology,* 38, 159-180.

Gordon, E. A. and Bridge, J. S. 1987. Evolution of Catskill (Upper Devonian) river systems: Intra and Extra basinal controls. *Journal of Sedimentary Petrology,* 57, 234-249.

Groenewold, G. H., Rehm, B. W. and Cherry, J. A. 1981. Depositional setting and groundwater quality in Coal-bearing sediments and spoils in Western North Dakota. *In:* Ethridge, F. G. and Flores, R. M. (eds.) Resent and ancient non-marine depositional environments: Models for exploration. Society of Economic Paleontologists and Mineralogists Special Publication, 31, 157-167.

Höcker, C., Eastwood, K. M., Herwiejer, J. C. and Adams, J. T. 1990. Use of dipmeter data in clastic sedimentological studies. *American Association of Petroleum Geologists Bulletin,* 74, 105-118.

Hϕimyr, *ϕ*., Kleppe, A. and Nystuen, J. P. 1993. Effects of heterogeneities in a braided stream channel sandbody on the simulation of oil recovery: a case study from the Lower Jurassic Statfjord Formation, Snorre Field, North Sea. *In:* Ashton, M. (ed.) Advances in reservoir geology. Geological Society Special Publication, 69, 105-134.

Hamilton, D. S. 1995. Utility of coal seams as genetic stratigraphic sequence boundaries in nonmarine basins: an example from the Gunnedah Basin, Australia: Reply. *American Association of Petroleum Geologists Bulletin,* 79, 1182.

Haq, B. U., Hardenbol, J. and Vail, P. R. 1988. Mesozoic and Cenozoic chronostratigraphy and cycles of sea-level change. *In:* Wilgus, C. K., Hastings, B. S., Kendall, C. G. St. C., Posamentier, H. W., Ross, C. A. and Van Wagoner, C. J. (eds.) Sea-level changes: an integrated approach. Tusla. Society of Economic Paleontologists and Mineralogists Special Publication, 42, 71-108.

Haszeldine, R. S. 1984. Muddy deltas in fresh water lakes, and tectonism in the Upper Carboniferous Coalfield of NE England. *Sedimentology,* 31, 811-822.

Hein, F. J. and Walker, R. G. 1977. Bar evolution and development of stratification in the gravelly, braided Kicking Horse River, British Colombia. *Canadian Jornal of Earth Sciences,* 14, 562-570.

Herweijer, J. C., Höcker, C. F., Williams, W. H. and Eastwood, K. M. 1990. The relevance of dip profiles from outcrops as reference for the interpretation of SHDT dips. *In:* Hurst, A., Lovell, M. A. and Morton A. C. (eds.) Geological applications of wireline logs I. Geological Society Special Publications, 48, 39-43.

Horne, J. C., Ferm, J. C., Caruccio, F. T. and Baganz, B. P. 1978. Depositional models in coal exploration and mine planning in the Appalacian Region. *American Association of Petroleum Geologists Bulletin,* 62, 2379- 2411.

Hospers, J. and Ediriweera, K. K. 1991. Depth and Configuration of the crystalline basement in the Viking Graben area, northern North Sea. *Journal of the Geological Society of London,* 148, 261-265.

Howell, D. J. and Ferm, J. C. 1980. Exploration model for Pensylvanian upper delta plain coals, Southwest Virginia. *American Association of Petroleum Geologists Bulletin,* 64, 938-941.

Humphreys, B. and Lott, G. K. 1990. An investigation into nuclear log responses of North Sea Jurassic sandstones using mineralogical analysis. *In:* Hurst, A. Lovell, M. A. and Morton, A. C. (eds.) Geological applications of wireline logs I. Geological Society Special Publication, 48, 223-240.

Hurst, A. 1990. Natural gamma-ray spectrometry in hydrocarbon-bearing sandstones from the Norwegian contenental shelf. *In:* Hurst, A., Lovell, M. A. and Morton, A. C. (eds.) Geological applications of wireline logs I. Geological Society Special Publication, 48, 211-222.

Jackson, R. G. 1978. Preliminary evaluation of lithofacies models for meandering alluvial streams. *In:* Miall, A. D. (ed.) Fluvial sedimentology. Canadian Society of Petroleum Geologists Memoir, 5, 543-576.

Johnson, E. A. and Pierce, F. W. 1990. Variations in fluvial deposition on an alluvial plain: An example from the Tunge River Member of the Fort Union Formation (Paleocene), Southeastern Powder River Basin, Wyoming, U.S.A. *Sedimentary Geology,* 69, 21-36.

Johnson, H. D. and Krol, D. E. 1984. Geological modelling of a heterogeneous sandstone reservoir: Lower Jurassic Statfjord Formation, Brent Field: Society of Petroleum Engineers Paper 13050. 1-13.

Johnson, H. 1993. Structure, Pre-Permian, Upper Cretaceous, and Tertiary. *In:* The geology of the northern North Sea. United Kingdom Offshore Regional Report. British Geological Survey London.

Johnson, S. Y. 1984. Cyclic fluvial sedimentation in a rapidly subsiding basin, Northwest Washington. *Sedimentary Geology,* 38, 361-391.

Kelling, G. 1968. Patterns of sedimentation in the Rhondda beds. *American Association of Petroleum Geologists Bulletin,* 52, 2369-2382.

Kerr, D. R. 1984. Early Neogene continental sedimentation in the Vallecito and Fish Creek Mountains, western Salton Trough, California. *Sedimentary Geology,* 38, 217-146.

Kirk, R. H. 1980. Statfjord Field-A North Sea Giant. *In:* Halbouty, M. T. (ed.) Giant Oil and Gas Fields of the Decade: 1968-1978, *American Association of Petroleum Geologists Memoir,* 30, 95-116.

Kirschbaum, M. A. and McCabe, P. J. 1982. Controls on the accumulation of coal and on the development of anastomosed fluvial systems in the Cretaceous Dakota Formation of South Utah. *Sedimentology,* 39, 581-598.

Koss, J. E., Ethridge, F. G. and Schumm, S. A. 1994. An experimental study of the effects of base-level changes on fluvial, coastal plain and shelf systems. *Journal of Sedimentary Research,* 64, 90-98.

Kvale, E. P. and Archer, A. W. 1990. Tidal deposits associated with low-sulfur coals, Brazil Fm. (Lower Pennsylvanian), Indiana. *Journal of Sedimentary Petrology,* 60, 563-574.

Kvale, E. P., Archer, A. W. and Johnson, H. R. 1989. Daily, monthly, and yearly tidal cycles within laminated siltstones of the Mansfield Formation (Pennsylvanian) of Indiana. *Geology,* 17, 365-368.

Lawrence, D. A. and Williams, B. P. J. 1987. Evolution of drainage system in response to Acadian deformation: The Devonian Battery Point Formation, Eastern Canada. *In:* Ethridge, F. G., Flores, R. M. and Harvey, M. D. (eds.) Recent developments in fluvial sedimentology. Contribution to the Third International Fluvial Sedimentology Conference. Society of Economic Paleontologists and Mineralogists Spacial Publication, 39, 287-300.

Leopold, L. B., Wolman, M. G. and Miller, J. P. 1964. Fluvial processes in Geomorphology. Freeman, San Francisco. 522pp.

Lervik, K. S., Spencer, A. M. and Warrington, G. 1989. Outline of Triassic stratigraphy and structure in the central and northern North Sea. *In:* Collinson, J. D. (ed.) Correlation in hydrocarbon exploration. Graham and Trotman. London, 173-189.

Link, M. H. 1984. Fluvial facies of the Miocene Ridge Route Formation, Ridge Basin, California. *Sedimentary Geology,* 38, 263-285.

MacDonald, A. C. and Halland, E. K. 1993. Sedimentology and shale modeling of a sandstone-rich fluvial reservoir: Upper Statfjord Formation, Statfjord Field, northern North Sea. *American Association of Petroleum Geologists Bulletin,* 77, 1016-1040.

McCabe, P. J. 1984. Depositional environments of coal and coal-bearing strata. *In:* Rahmani, R. A. and Flores, R. M. (eds.) Sedimentology of coal and coal-bearing sequences. International Association of Sedimentologists Special Publication, 7, 13-42.

McKee, E. D., Crosby, E. J. and Berryhill, H. L. 1967. Flood deposits, Bijou Creek, Colorado. *Journal of Sedimentary petrology,* 37, 829-851.

McKenzie, D. P. 1978. Some remarks on the development of sedimentary basins. *Earth and Planetary Science Letters,* 40, 25-32.

McLean, J. R. and Jerzykiewicz, T. 1978. Cyclicity, Tectonics and coal: Some aspects of fluvial sedimentology in the Brazeau- Paskapoo Formation, Coal valley area

Alberta, Canada. *In:* Mial, A. D. (ed.) Fluvial sedimentology. Canadian Society of Petroleum Geologists Memoir 5, 441-468.

Melvin, J. 1987. Fluvio-Paludal deposits in the Lower Kekiktuk Formation (Mississippian), Endicott Field, Northeast Alaska. *In:* Ethridge, F. G., Flores, R. M. and Harvey, M. D. (eds.) Recent developments in fluvial sedimentology. Contributions to the Third International Fluvial Sedimentology Confernce. Society of Economic Paleontologists and Mineralogists Special Publication, 39, 343-352.

Melvin, J. 1993. Evolving fluvial style in the Kekiktuk Formation (Mississippian), Endicott Field Area, Alaska: Base level response to contemporaneous Tectonism. *American Association of Petroleum Geologists Bulletin,* 77, 1723-1744.

Meyer, B. L. and Nederlof, M. H. 1984. Identification of Source Rocks on Wireline Logs by Density/Resistivity and Sonic Transit Time/Resistivity Crossplots. *American Association of Petroleum Geologists Bulletin,* 68, 121-129.

Miall, A. D. 1977. A review of the braided-river depositional environment. *Earth Sciences,* 13, 1-62.

Miall, A. D. 1978. Lithofacies types and vertical profile models in braided river deposits: A summary. *In:* Miall, A. D. (ed.) Fluvial sedimentolgy. Canadian Society of Petroleum Geologists Memoir 5, 597-604.

Miall, A. D. 1984. Variations in fluvial style in the Cenozoic Synorogenic of the Lower Cenozoic Synorogenic of the Canadian Arctic Islands. *Sedimentary Geology,* 38, 499-523.

Miall, A. D. 1985a. Multiple-channel bedload rivers. *In:* Recognition of fluvial depositional systems and their resource potetial. Society of Economic Paleontologists and Mineralogists Short Course, 19, 83-100.

Miall, A. D. 1985b. Architectural-element analysis: A new method of facies ananlysis applied to Fluvial deposits. *In:* Recognition of fluvial depositional systems and their resource potential. Society of Economic Paleontologists and Mineralogists Short Course, 19, 33-81.

Miall, A. D. 1988a. Reservoir heterogeneties in fluvial sandstones: Lesson from outcrop studies. *American Association of Petroleum Geologists Bulletin,* 72, 682-697.

Miall, A. D. 1988b. Architectural elements and bounding surfaces in fluvial deposits: anatomy of the Kayenta Formation (Lower Jurassic), South West Colorado. *Sedimentary Geology,* 55, 233-266.

Moore, T. E. and Nilsen, T. H. 1984. Regional variations in the fluvial Upper Devonian and Lower Mississipian(?) Kanayut Conglomerate, Brooks Range, Alaska. *Sedimentary Geology,* 38, 465-497.

Myers, K. J. and Bristow, C. S. 1989. Detailed sedimentology and gamma-ray log characteristics of a Namurian deltaic succession: gamma-ray logging. *In:* Whateley, M. K. G. and Pickering, K. T. (eds.) Deltas: sites and trapes for fossil fuels. Geological Society Special Publication, 41, 81-88.

Myers, K. J. and Jenkyns, K. F. 1992. Determining total organic carbon contents from well logs: an interpretation GST* data and a new density log method. *In:* Hurst, A., Griffiths, C. M. and Worthington, P. F. (eds.) Geological applications of wireline logs II. Geological Society Special Publication, 65, 369-376.

Oomkens, E. 1970. Depositional sequences and sand distribution in the post-glacial Rhone delta complex. *In:* Morgan, J. P. and Shaver, R. H. (eds.) Deltaic sedimentation modern and ancient. Society of Economic Paleontologist and Mineralogists Special Publication, 15, 198-212.

Penland, S., Boyd, R. and Suter, J. R. 1988. Transgressive depositional systems of the Missisippi River delta plain: a model for barrier shoreline and shelf development. *Journal of Sedimentary petrology,* 58, 932-949.

Picard, M. D. and High, L. R. 1981. Physical stratigraphy of ancient lacustrine deposits. *In:* Ethridge, F. G. and Flores, R. M. (eds.) Recent and ancient non-marine depositional environments: Models for exploration. Society of Economic Paleontologists and Mineralogists Special Publication, 31, 233-259.

Posamentier, H. W. and Vail, P. R. 1988. Eustatic controls on clastic deposition II-sequence and systems tract models. *In:* Wilgus, C. K., Hastings, B. S., Kendall, C. G. St. C., Posamentier, H. W., Ross, C. A. and Van Wagoner, C. J. (eds.) Sea-level changes: an integrated approach. Society of Economic Paleontologists and Mineralogists Special Publication, 42, 125-154.

Posamentier, H. W., Jervey, M. T. and Vail, P. R. 1988. Eustatic controls on clastic deposition I-conceptual framework. *In:* Wilgus, C. K., Hastings, B. S., Kendall, C. G. St. C., Posamentier, H. W., Ross, C. A., and Van Wagoner, J. C. (eds.) Sea-level changes: an integrated approach. Society of Economic Paleontologists and Mineralogists Special Publication, 42, 109-124.

Posamentier, H. W., Allen, G. P. and James, D. P. 1992. High resolution sequence stratigraphy- the East Coulee delta, Alberta. *Journal of Sedimentary Petrology,* 62, 310-317.

Posamentier, H. W. and Weimer, P. 1993. Siliciclastic sequence stratigraphy and petroleum geology- Where to from here?. *American Association of Petroleum Geologists Bulletin,* 77, 731-742.

Potter, P. E. and Pettijohn, F. J. 1977. Paleocurrents and basin analysis. 2nd edition. Springer-Verlag. New York, 460pp.

Purvis, K. 1995. Diagenesis of Lower Jurassic sandstones, Block 211/13 (Penguin Area), UK northern North Sea. *Marine and Petroleum Geology,* 12, 219-228.

Rϕe, S. L. 1987. Cross-strata and bedforms of probable transitional dune to upper-stage plane-bed origin from a Late Precambrian fluvial sandstone, northern Norway. *Sedimentology,* 34, 89-101.

Rϕe, S. L. and Steel, R. J. 1985. Sedimentation, sea-level rise and tectonics at the Triassic-Jurassic boundary (Statfjord Formation), Tampen Spur, northern North Sea. *Journal of Petroleum Geology,* 8, 163-186.

Reineck, H. E. and Singh, I. B. 1973. Depositional sedimentary environments- with reference to terrigenous clastics. Springer- Verlag, Berlin, 439 pp.

Reineck, H. E. and Singh, I. B. 1980. Depositional sedimentary environments. 2nd edition. Springer-Verlag. New York, 549pp.

Rhee, C. W., Ryang, W. H. and Chough, S. K. 1993. Contrasting development patterns of crevasse channel deposits in Cretaceous alluvial successions, Korea. *In:* Fielding C. R. (ed.) Current research in fluvial sedimentology. *Sedimentary Geology,* 85, 401-410.

Richards, P. C. 1993. Permo-Triassic, Jurassic, Lower Cretaceous and Economic geology (hydrocarbon). *In:* The geology of the northern North Sea. United Kingdom Offshore Regional Report. British Geological Survey. London.

Rider, M. H. 1990. Gamma-ray log shape used as a facies indicator: Critical analysis of an oversimplified methodology. *In:* Hurst, A., Lovell, M. A. and Morton, A. C. (eds.) Geological applications of wireline logs I. Geological Society Special publication, 48, 27-37.

Rider, M. H. 1991. The geological interpretation of well logs. Revised eddition. Whittles Publishing, 175pp.

Rust, B. R. and Jones, B. G. 1987. The Hawkesbury Sandstone south of Sydney, Australia: Triassic analogue for the deposit of a large, braided river. *Journal of Sedimentary petrology,* 57, 222-233.

Schlumberger, 1989a. Sedimentary environments from wireline logs. ESF Marketing and Technique. 2nd edition. 243pp.

Schlumberger, 1989b. Log interpretation: Principles/Applications. Gulf Freeway, Houston, Texas.

Schmoker, J. W. 1979. Determination of organic content of Appalachian Devonian shales from formation density logs. *American Association of Petroleum Geologists Bulletin,* 63, 1504-1509.

Schmoker, J. W. 1980. Organic content of Devonian shale in Western Appalachian Basin. *American Association of Petroleum Geologists Bulletin,* 64, 2156-2165.

Schmoker, J. W. 1981. Determination of organic matter content of Appalachian Devonian shales from gamma-ray logs. *American Association of Petroleum Geologists Bulletin,* 65, 1285-1298.

Schumm, S. A. 1993. River response to base level change: implications for sequence stratigraphy. *Geology,* 101, 279-294.

Scoffin, T. P. 1987. An introduction to carbonate sediments and rocks. Blackie, Chapman & Hall, New York, USA. 274pp.

Scott, D. and Rosendahl, B. 1989. North Viking Graben: An East African Perspective, *American Association of Petroleum Geologists Bulletin,* 73, 155-165.

Selley, R. C. 1976. Subsurface environmental analysis of North Sea sediments. *American Association of Petroleum Geologists Bulletin,* 60, 184-195.

Selley, R. C. 1985. Ancient sedimentary environments. 3rd edition. Chapman and Hall, London. 317pp.

Selley, R. C. 1989. Deltaic reservoir prediction from rotational dipmeter pattern. *In:* Whateley, M. K. G. and Pickering, K. T. (eds.) Deltas: Sites and traps for fossil fuels. Geological Society Special Publication, 41, 89-95.

Serra, O. and Abbott, H. 1980. The contribution of logging data to sedimentology and stratigraphy. 55th Ann. Fall. Techn. Conf. SPE of AIME., Paper SPE 9270.

Shanley, K. W. and McCabe, P. J. 1989. Sequence stratigraphic relationships and facies architecture of Turonian-Campanian strata, Kaiparowits Plateau, south-central Utah. *American Association of Petroleum Geologists Bulletin,* 73, 410-411.

Shanley, K. W. and McCabe, P. J. 1990. Tidal influence in fluvial strata- a key element in high-resolution sequence stratigraphic correlation. *American Association of Petroleum Geologists Bulletin,* 74, 762.

Shanley, K. W. and McCabe, P. J. 1991. Predicting facies architecture thruogh sequence stratigraphy- An example from the Kaiparowits Plateau, Utah. *Geology,* 19, 742-745.

Shanley, K. W. and McCabe, P. J. 1993. Alluvial architecture in a sequence-stratigraphic framework: a case history from the Upper Cretaceous of southern Utah, USA. *In:* Flint, S. S. and Bryant, I. D. (eds.) The geological modelling of hydrocarbon reservoirs and outcrop analogues. International Association of Sedimentologists Special Publication, 15, 21-55.

Shanley, K. W. and McCabe, P. J. 1994. Perspectives on the sequence stratigraphy of continental strata. *American Association of Petroleum Geologists Bulletin,* 78, 544-568.

Singh, A. and Bhardwaj, B. D. 1991. Fluvial facies model of the Ganga River sediments, India. *Sedimentary Geology,* 72, 135-146.

Smith, N. D. 1972. Some sedimentological aspects of planar cross-stratification in a sandy braided river. *Sedimentary Geology,* 42, 624-634.

Steel, R. and Ryseth, A. 1990. The Triassic-Early Jurassic succession in the northern North Sea: megasequence stratigraphy and intra-Triassic tectonics. *In:* Hardman, R. F. P. and Brooks, J. (eds.) Tectonic events responsible for Britain's oil and gas reserves. Geological Society of London Special Publication, 55, 139-168.

Stocks, A. E. and Lawrence, S. R. 1990. Identification of source rocks from wireline logs. *In:* Hurst, A., Lovell, M. A. and Morton, A. C. (eds.) Geological applications of wireline logs I. Geological Society Special Publication, 48, 241-252.

Surlyk, F., Arndorff, L., Hamann, N. E., Hamberg, L., Johannessen, P. N., Koppelhus, E. B., Nielsen, L. H., Noe-Nygaard, N., Pedersen, G. K. and Petersen, H. I. 1995. High-resolution sequence stratigraphy of a Hettangian-Sinemurian paralic succession, Bornholm, Denmark. *Sedimentology,* 42, 323-354.

Swift, D. J. P. 1975. Barrier-island genesis: evidence from the central Atlantic Shelf, eastern U.S.A. *Sedimentary Geology,* 14, 1-43.

Todd, S. P. and Went, D. J. 1991. Lateral migration of sand bed rivers: examples from the Devonian Glashabeg Formation, SW Ireland and Combrian Alderney Sandstone Formation, Channel Islands. *Sedimentology,* 38, 997-1020.

Turner, B. R. and Monro, M. 1987. Channel formation and migration by mass flow processes in the Lower Carboniferous Fluviatile Fell Sandstone Group, North East England. *Sedimentology.* 34, 1107-1122.

Turner, B. R. 1978. Sedimentary patterns of uranium mineralization in the Beaufort Group of the Southern Karoo (Gondwana) basin, South Africa. *In:* Miall, A. D. (ed.) Fluvial sedimentology. Canadian Society of Petroleum Geologists Memoir 5, 831-848.

Van Wagoner, J. C., Posamentier, H. W., Mitchum, R. M., Vail, P. R., Sarg, J. F., Loutit, T. S. and Hardenbol, J. 1988. An overview of the fundamentals of sequence stratigraphy and key definitions. *In:* Wilgus, C. K., Hastings, B. S., Kendall, C. G. St. C., Posamentier, H. W., Ross, C. A. and Van Wagoner, J. C. (eds.) Sea-level changes: an integrated approach. Society of Economic Paleontologists and Mineralogists Special Publication, 42, 39-45.

Van Wagoner, J. C., Mitchum, R. M., Campion, K. M., and Rahmanian, V. D. 1990. Siliciclastic sequence stratigraphy in well logs, cores and outcrops. *American Association of Petroleum Geologists,* 55pp.

Vollset, J. and Dore', A. G. 1984. A revised Triassic and Jurassic lithostratigraphic nomenclature for the Norwegian North Sea. *Bulletin of the Norwegian Petroleum Directorate,* 3.

Walker, R. G. and Cant, D. J. 1984. Sandy fluvial systems. *In:* Walker, R. G. (ed.) Facies models, 2nd edition. Geological Association of Canada. 1, 71-89.

Warwick, P. D. and Flores, R. M. 1987. Evolution of fluvial styles in the Eocene Wasatch Formation, Powder River Basin, Wyoming. *In:* Ethridge, F. G., Flores, R. M. and Harvey, M. D. (eds.) Recent developments in fluvial sedimentology. Contributions to the Third International Fluvial Sedimentology Conference. Society of Economic Paleontologists and Mineralogists Special publication, 39, 303-310.

Wescott, W. A. 1993. Geomorphic thresholds and complex response of fluvial systems-Some implications to sequence stratigraphy. *American Association of Petroleum Geologists Bulletin,* 77, 1208-1218.

Williams, G. E. 1969. Characteristics and origin of a Precambrian pediment. *Geology,* 77, 183-207.

Wright, V. P. and Marriott, S. B. 1993. The sequence stratigraphy of fluvial depositional systems: the role of floodplain sediment storage. *Sedimentary Geology,* 86, 203-210.

Yinan, Q., Peihua, X. and Jingsiu, X. 1987. Fluvial sandstone bodies as hydrocarbon reservoir in Lake Basins. *In:* Ethridge, F. G., Flores, R. M. and Harvey, M. D. (eds.) Recent developments in fluvial sedimentology. Contributions to the Third International Fluvial Sedimentology Conference. Society of Economic Paleontologists and Mineralogists Special Publication, 39, 329-342.

Ziegler, P. A. 1975. North Sea basin history in the tectonic framework of North-Western Europe. *In:* Woodland, A. W. (ed.) Petroleum and the Continental Shelf of North West Europe. Applied Science Publishers Ltd. 131-149.

Ziegler, P. A., 1982. Geological atlas of Western and Central Europe. Elsevier, Amsterdam. 130pp.

Ziegler, P. A. 1988. Evolution of the Arctic-North Atlantic and Western Tethys. *American Association of Petroleum Geologists Memoir,* 43.

Ziegler, P. A. 1990. Tectonic and palaeogeographic development of the North Sea rift system. *In:* Blundell, D. J. and Gibbs, A. D. (eds.) Tectonic Evolution of the North Sea Rifts. Oxford Science Publications. 1-36.

Appendices 1-24

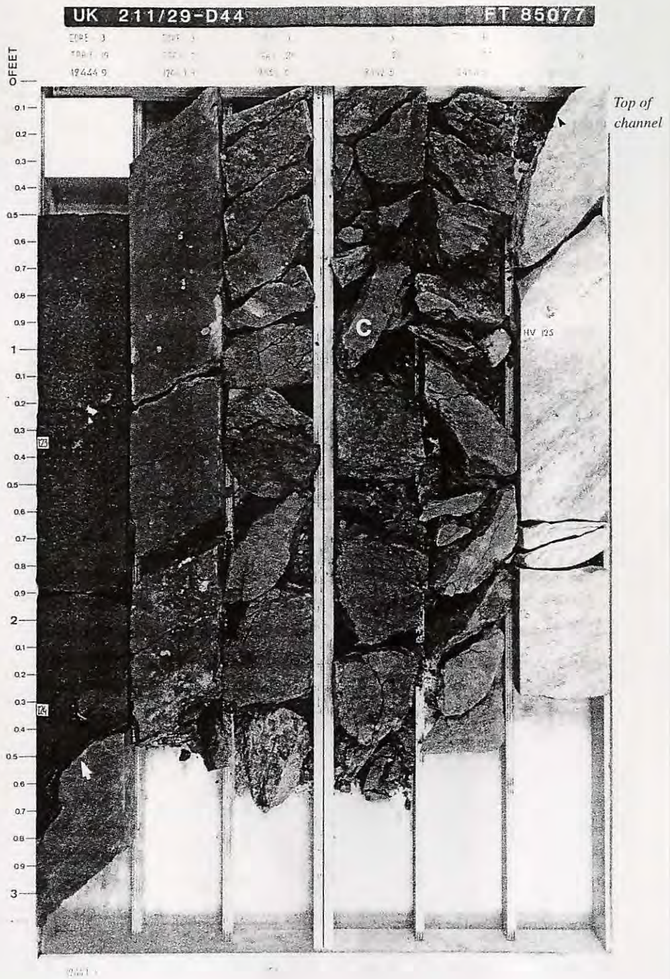

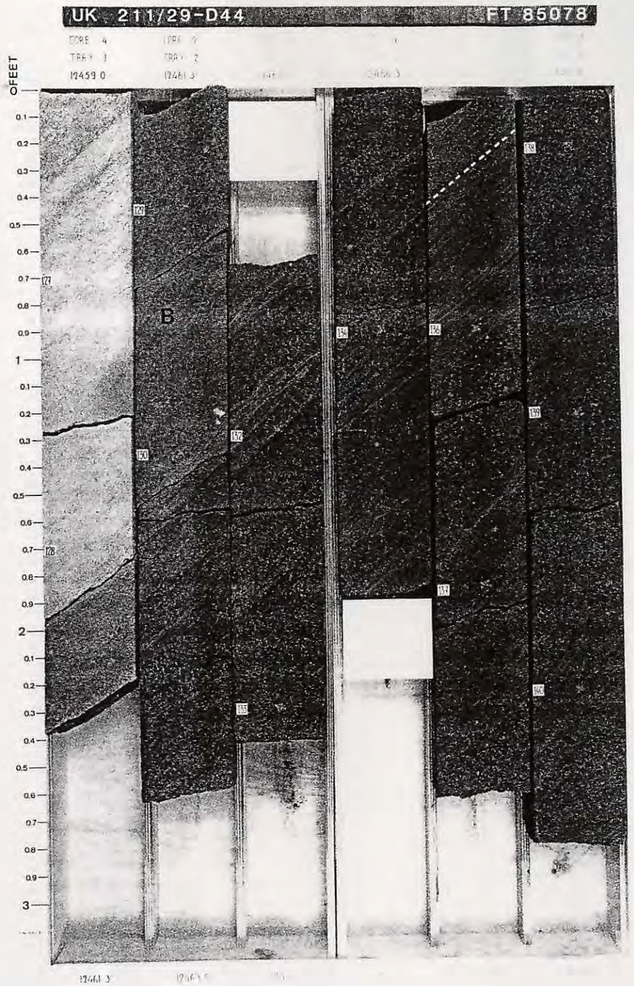

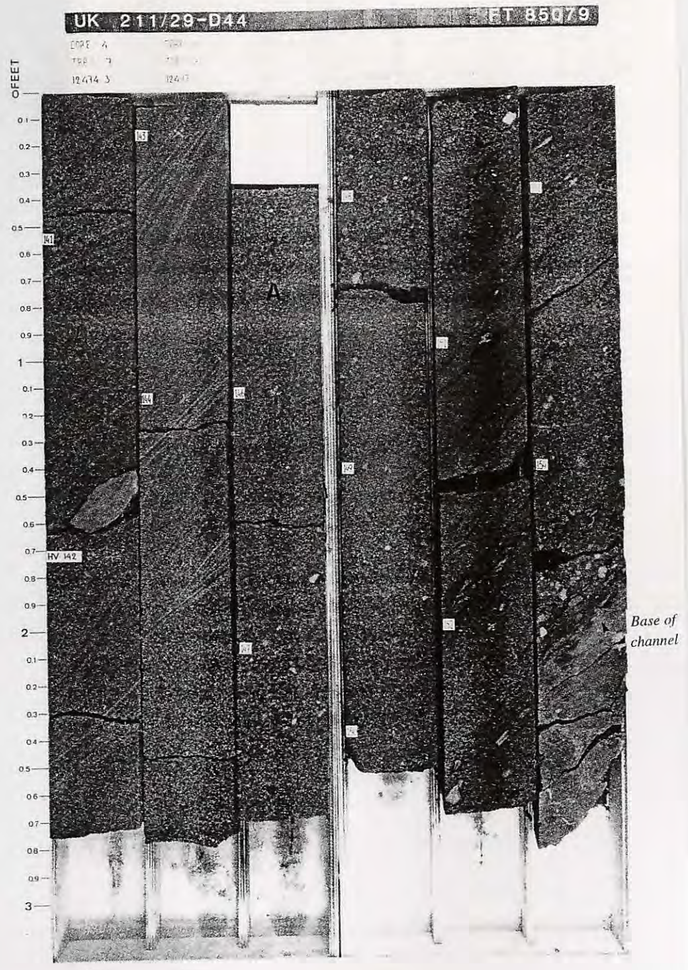

Appendix 1. Core photographs in well BD/44 showing type 1 low sinuosity channel facies from 12490 ft to 12457 ft. A, B and C refer to lithological units (See text for details). Unit C represents channel plug following abandonment.

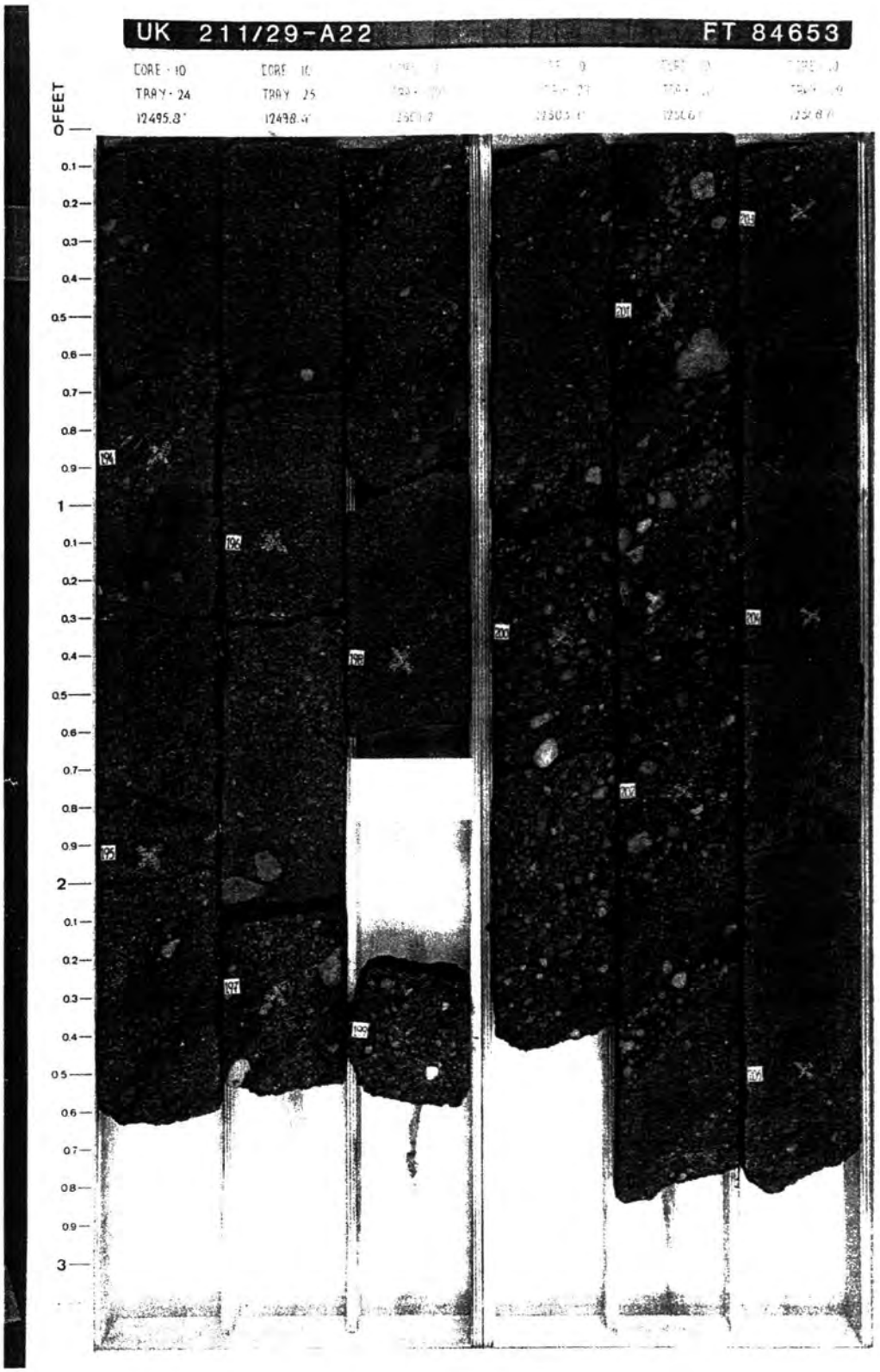

Appendix 2. Core photograph in well BA/22 illustrating part of a thick type 2 low sinuosity channel facies.

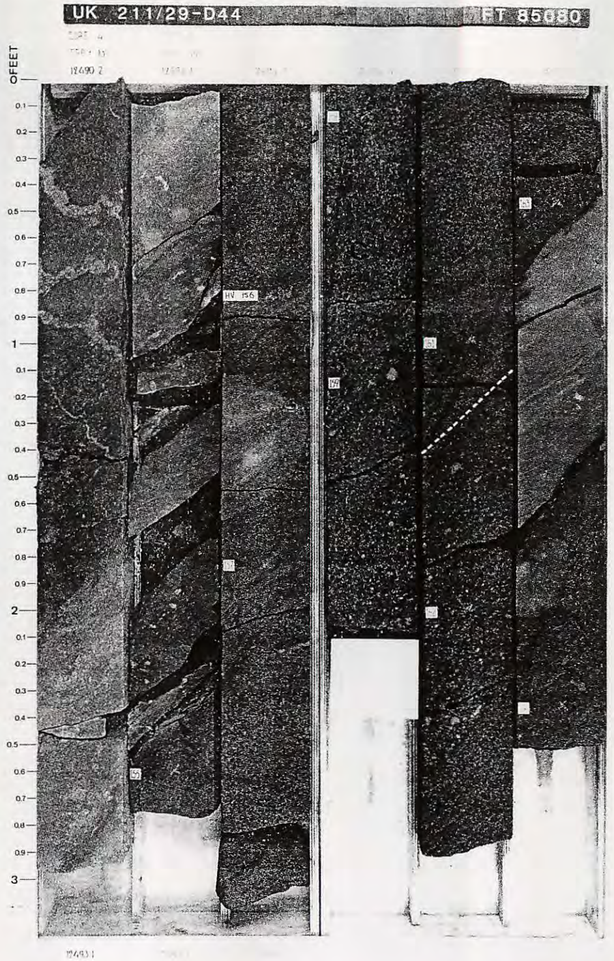

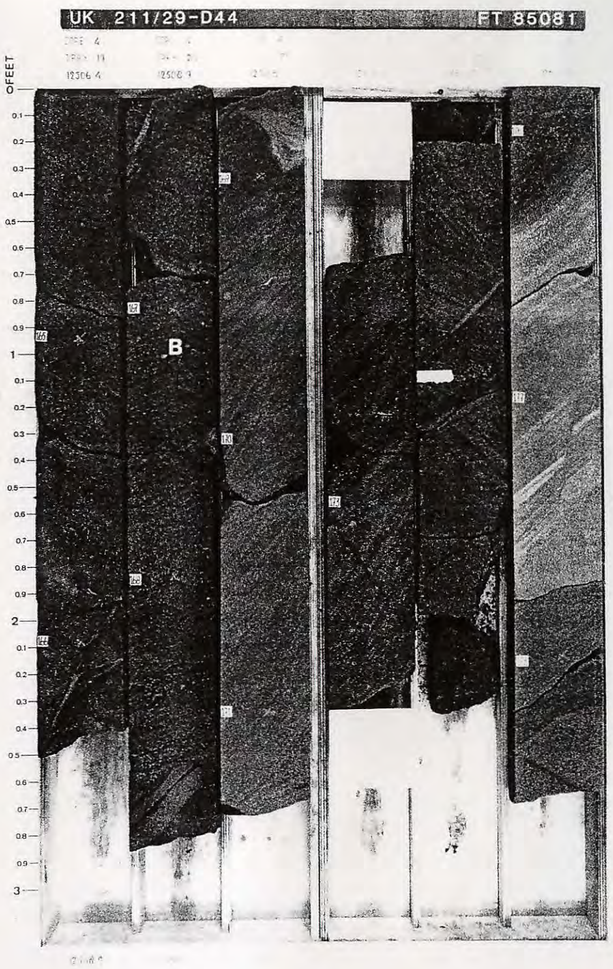

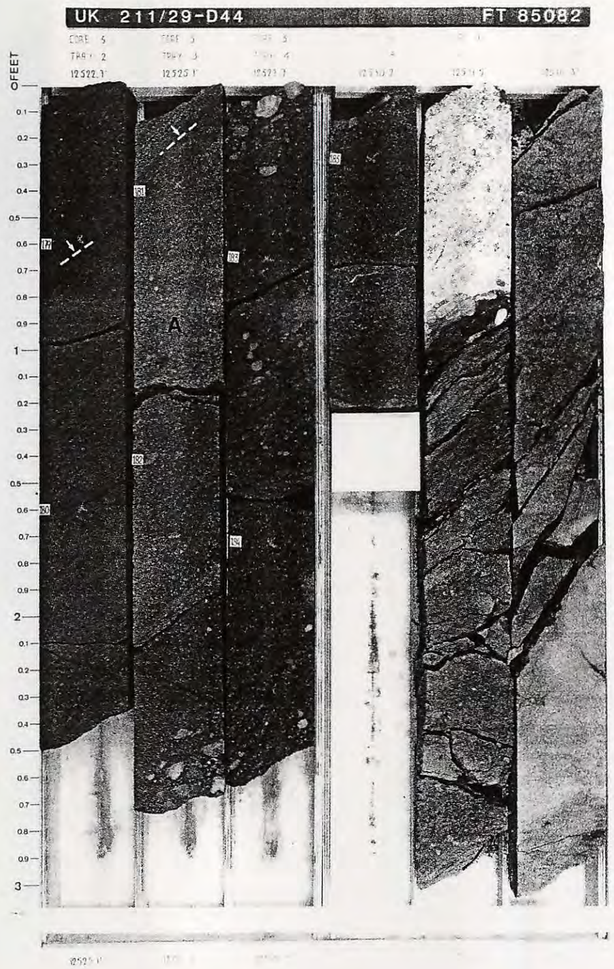

Appendix 3. Core photographs from 12532 ft to 12495.5 ft in well BD/44 illustrating type 3 low sinuosity channel facies. Dashed lines within unit A indicate set boundaries (See text for details).

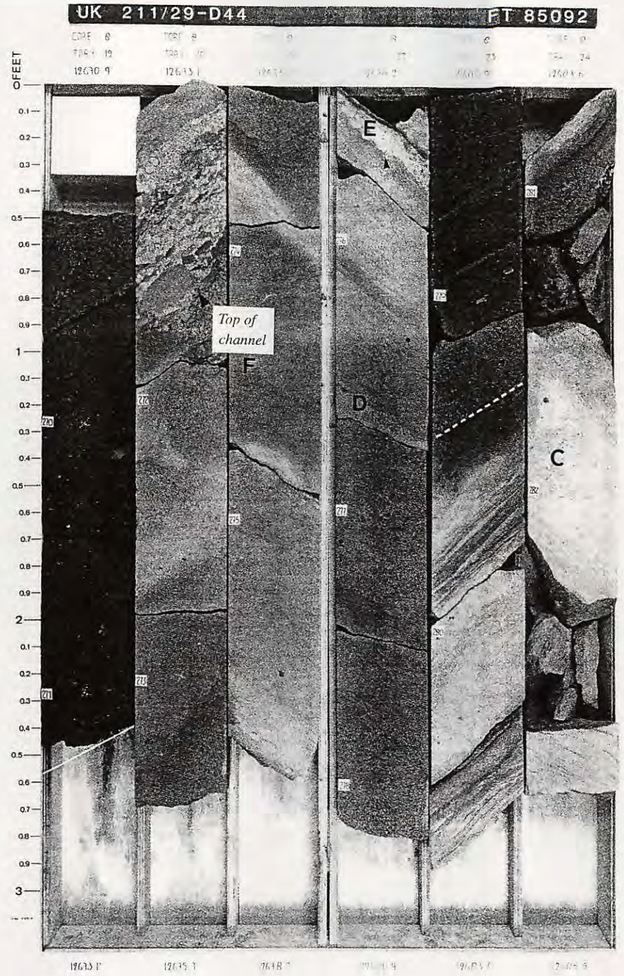

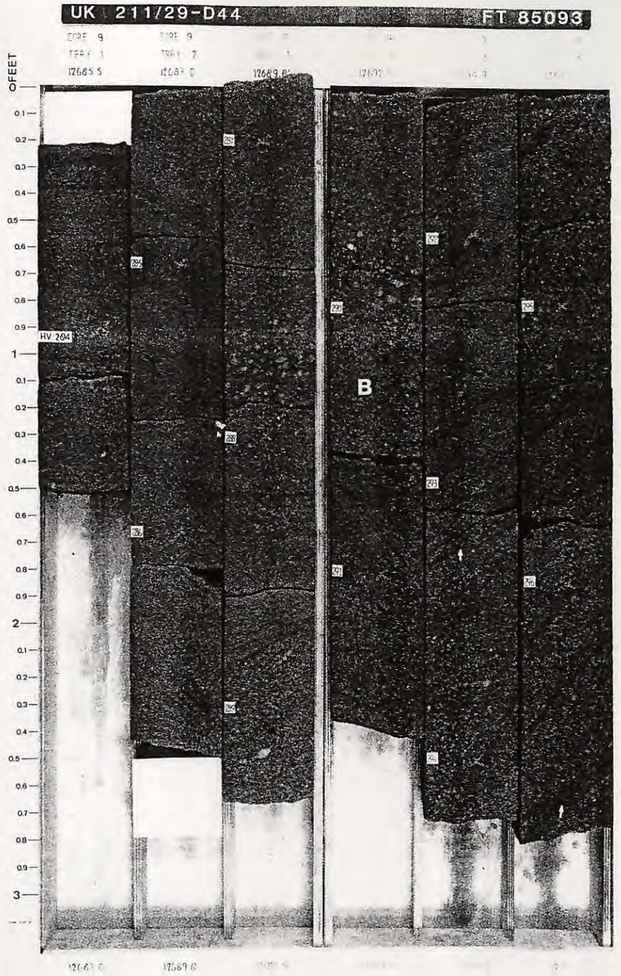

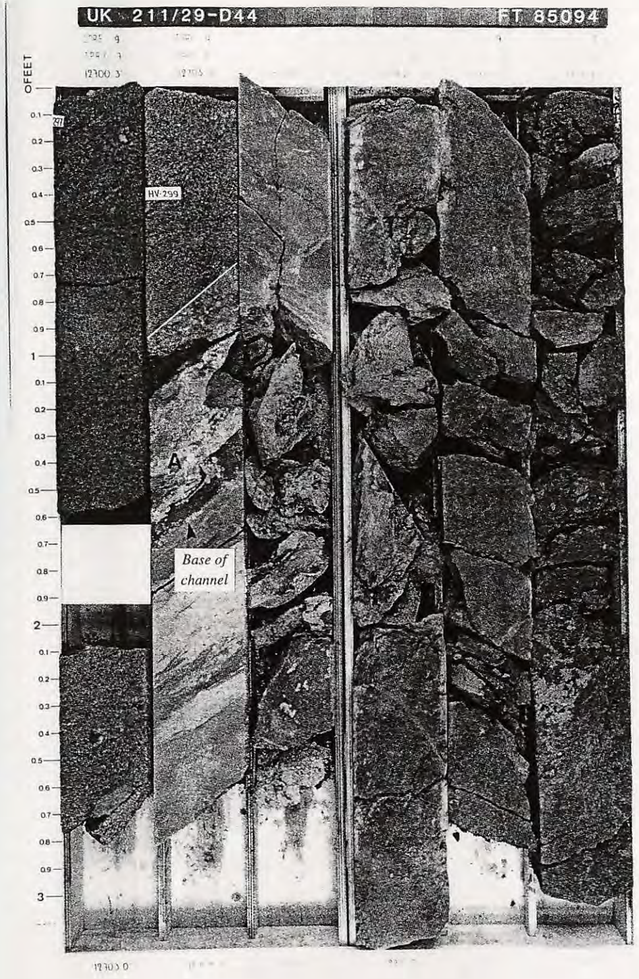

Appendix 4. Photographs of the core section of well BD/44 from 12704.7 ft to 12674 ft illustrating high sinuosity channel facies. Small white arrows within unit B point to minor syndepositional faults possibly in point bar sediments (See text for details).

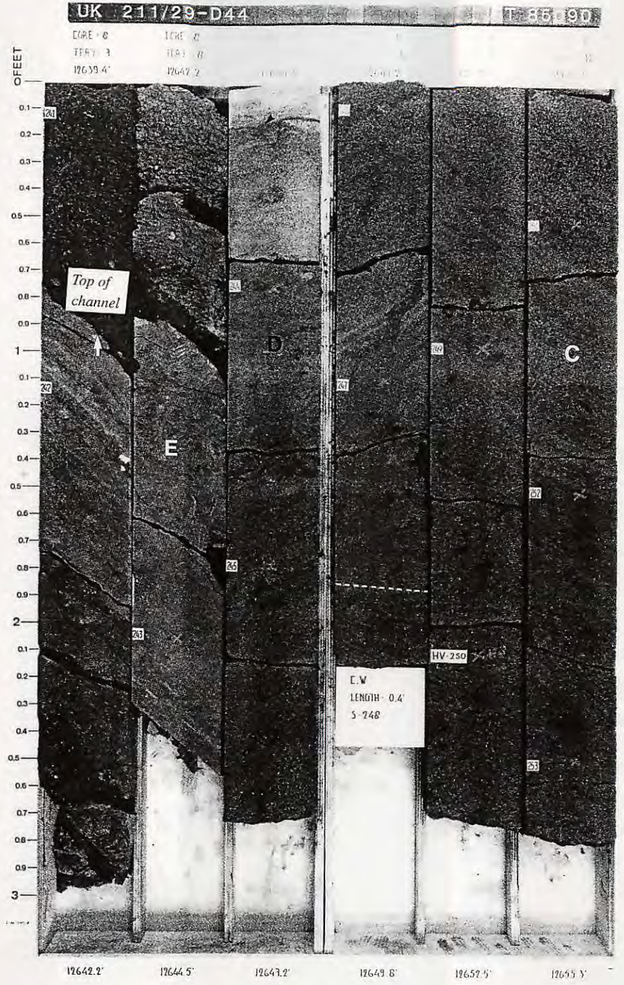

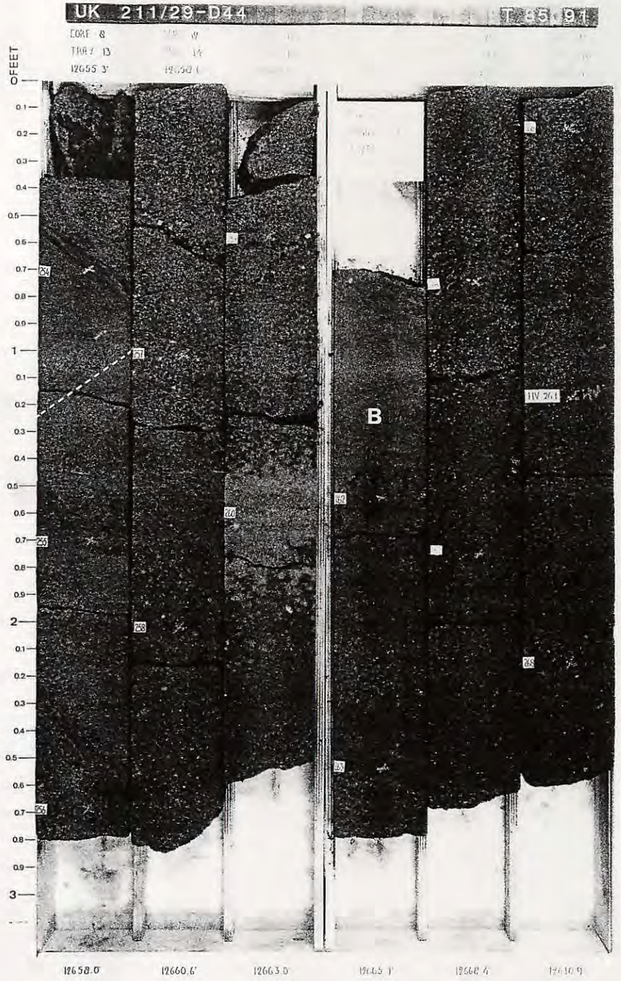

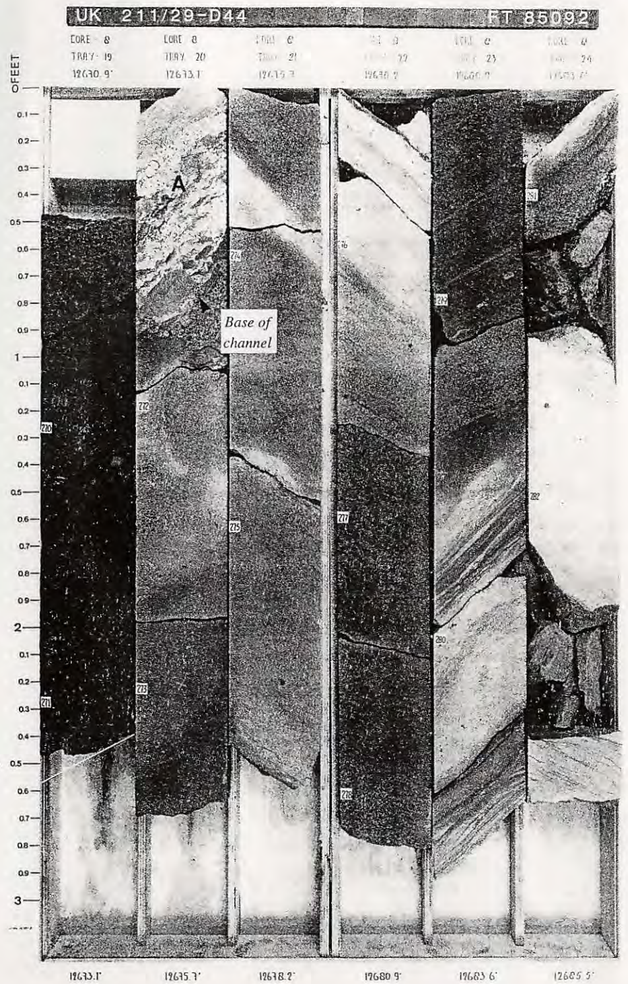

Appendix 5. Core photographs in the core section of well BD/44 from 12674 ft to 12640 ft showing gradually abandoned high sinuosity channel facies. (See text for details).

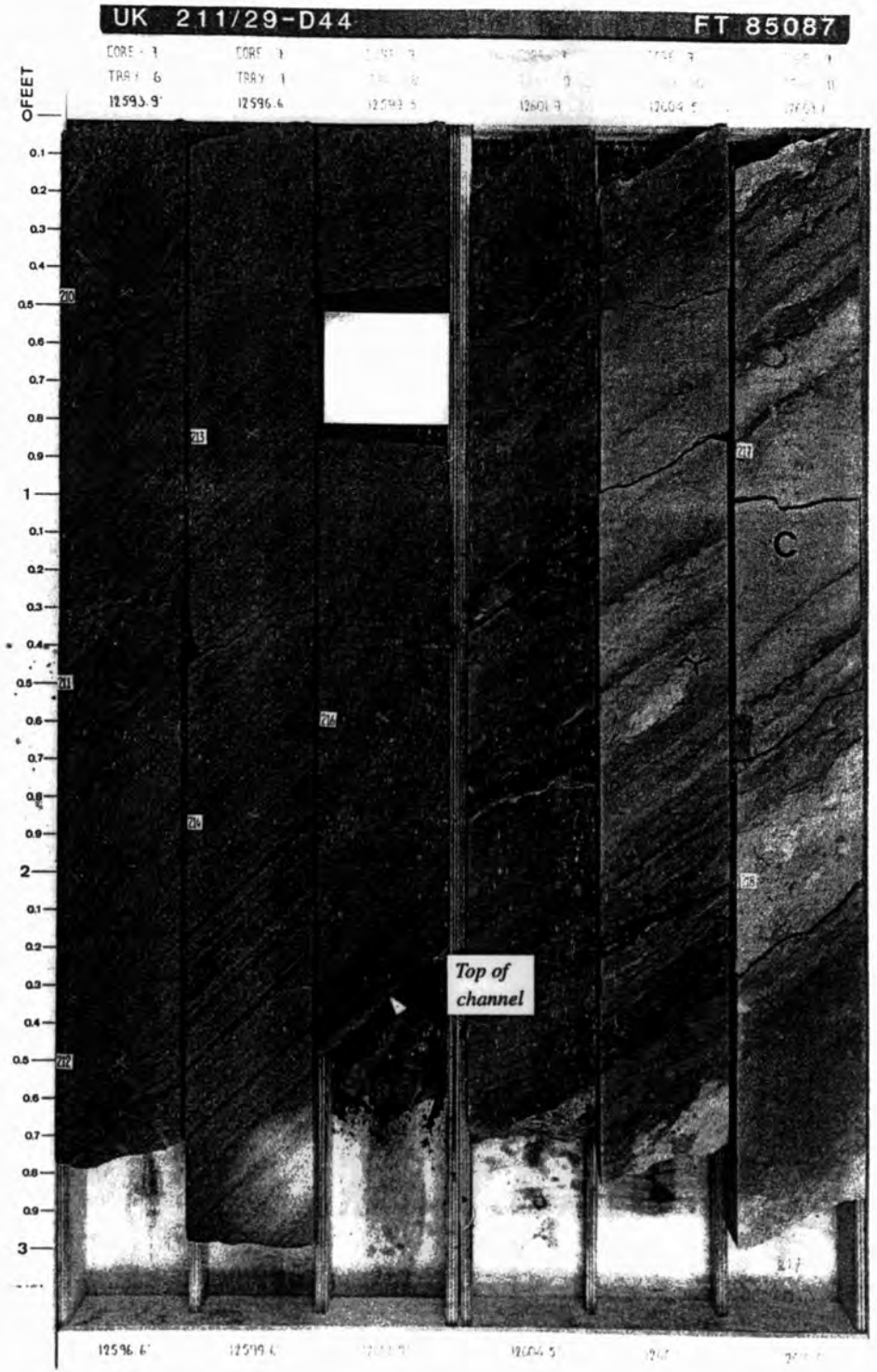
UK 211/29-D44
FT 85087
OFEET
Top of channel
C

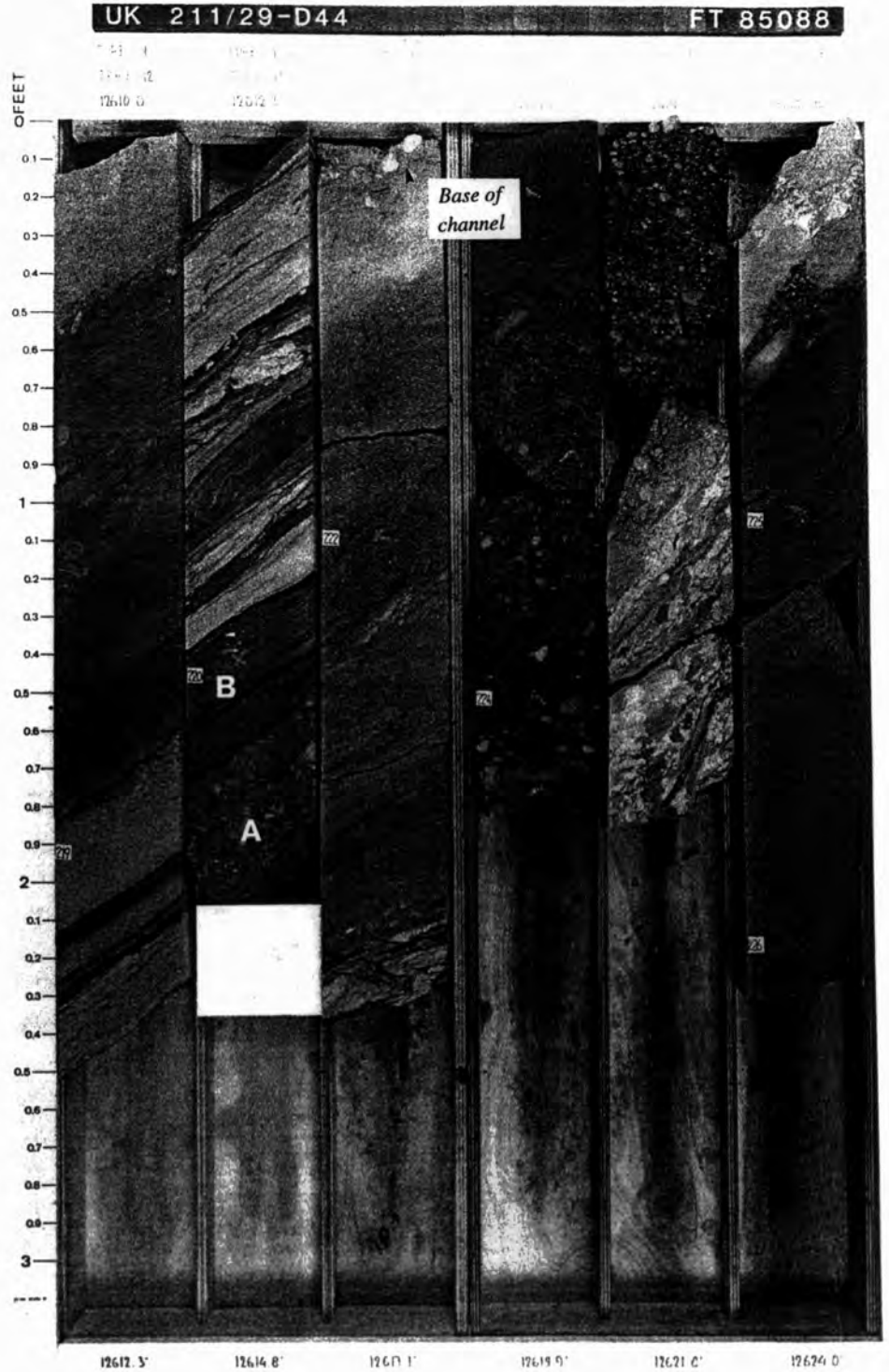
UK 211/29-D44
FT 85088
OFEET
Base of channel
B
A

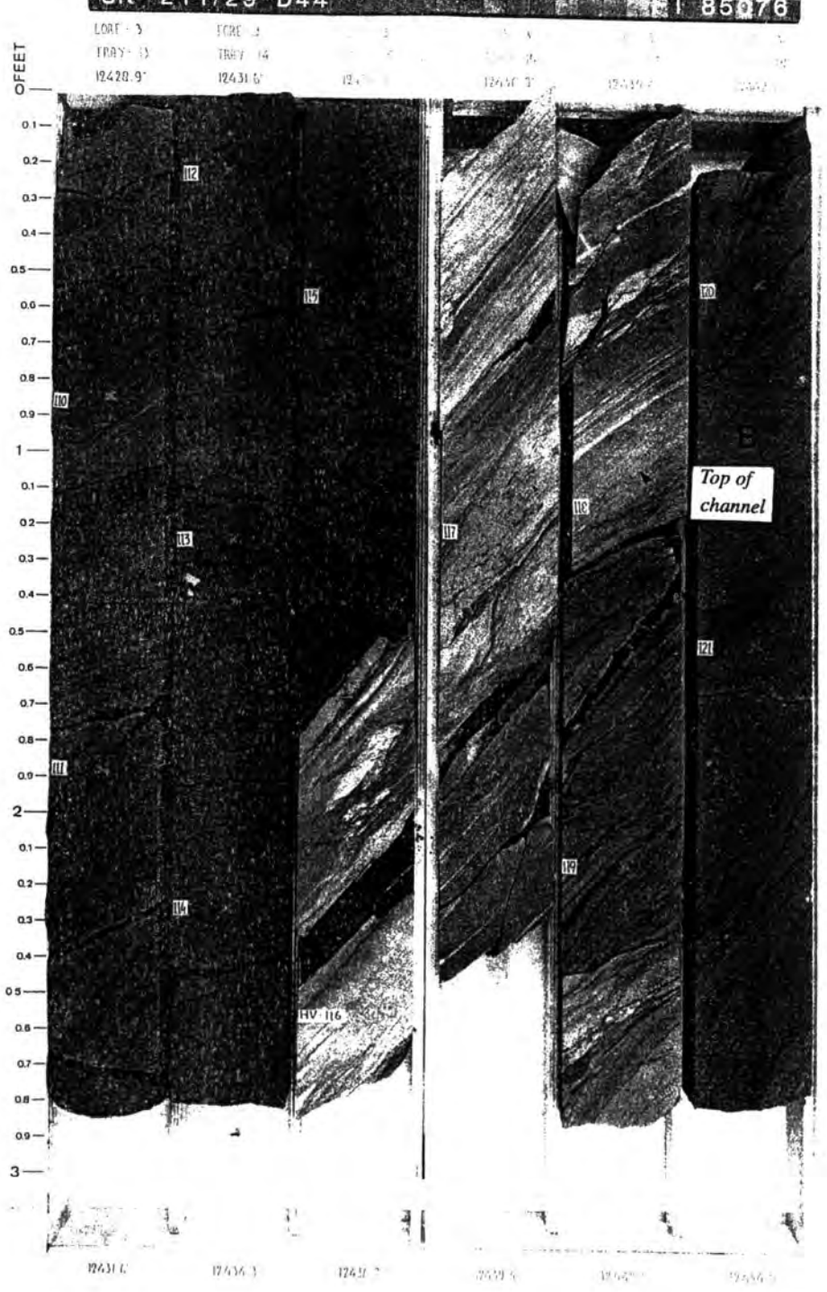

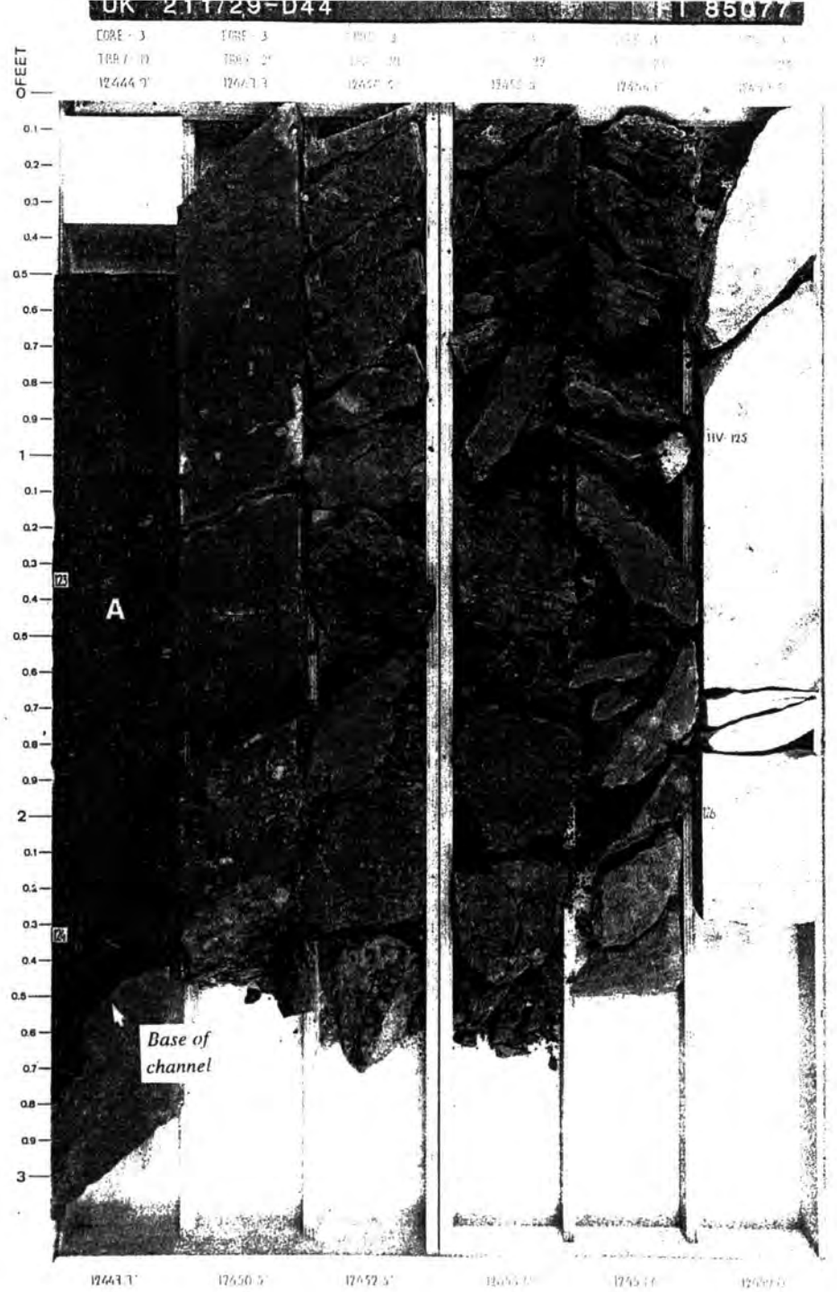

Appendix 7. Core photographs representing multistorey crevasse/minor channel facies from 12447.5 ft to 12440 ft in the core section of well BD/44.

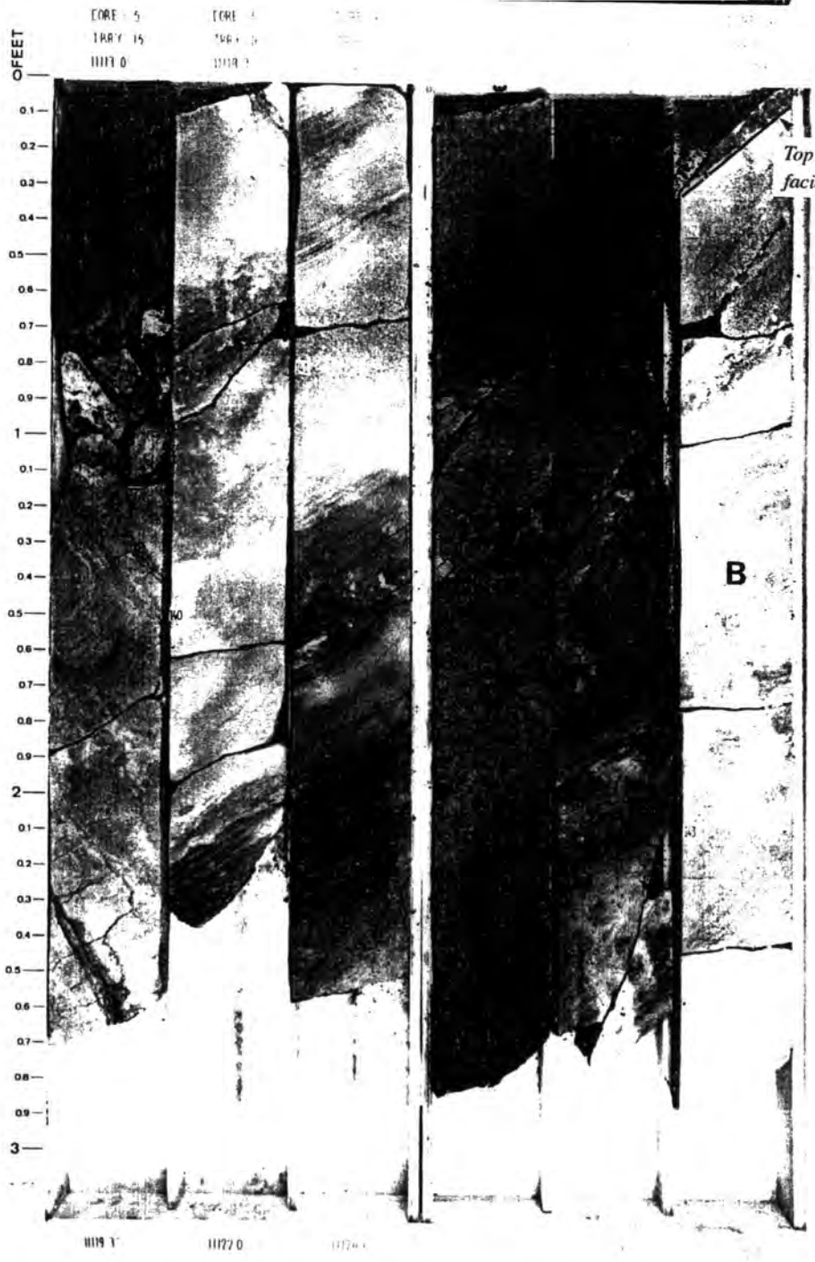

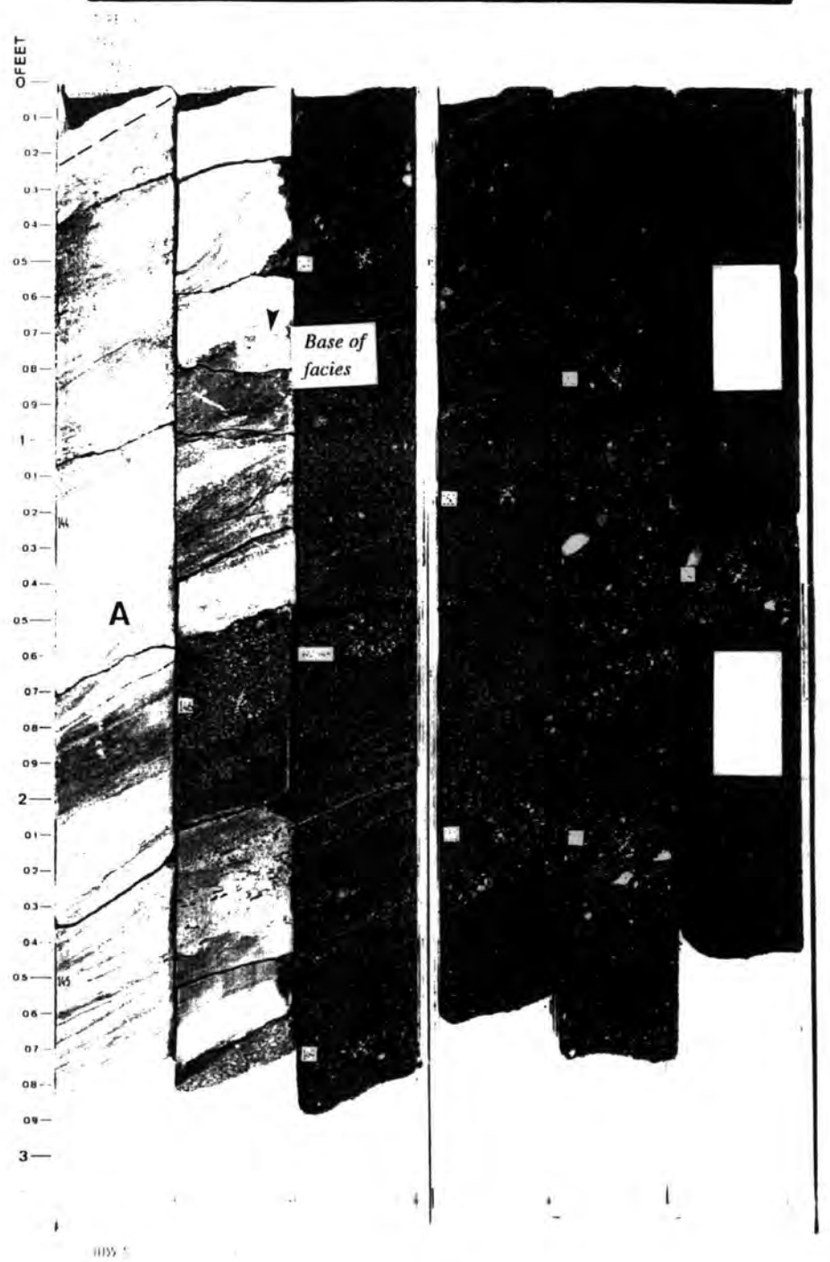

Appendix 8. Core photographs in the depth interval between 11136 ft and 11129.8 ft in well BD/36 showing an example of levee facies.

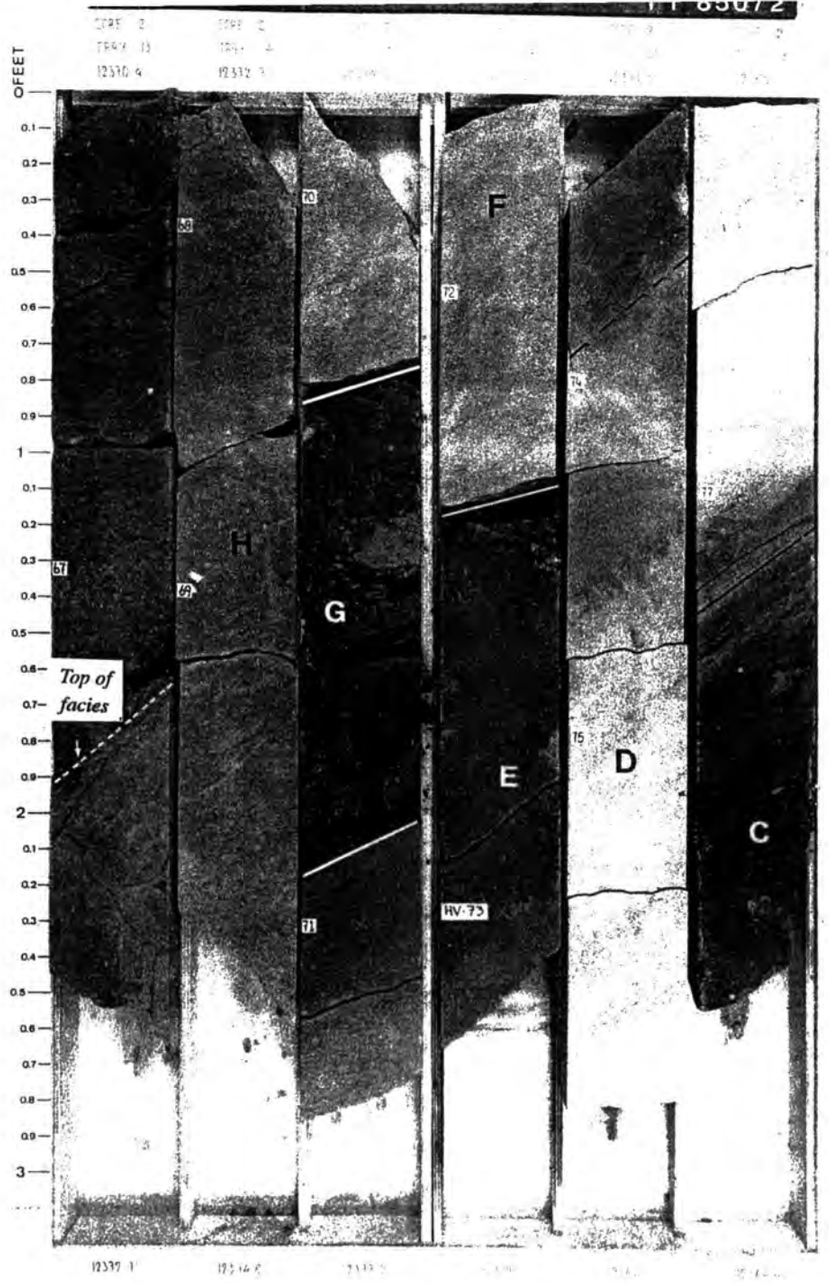

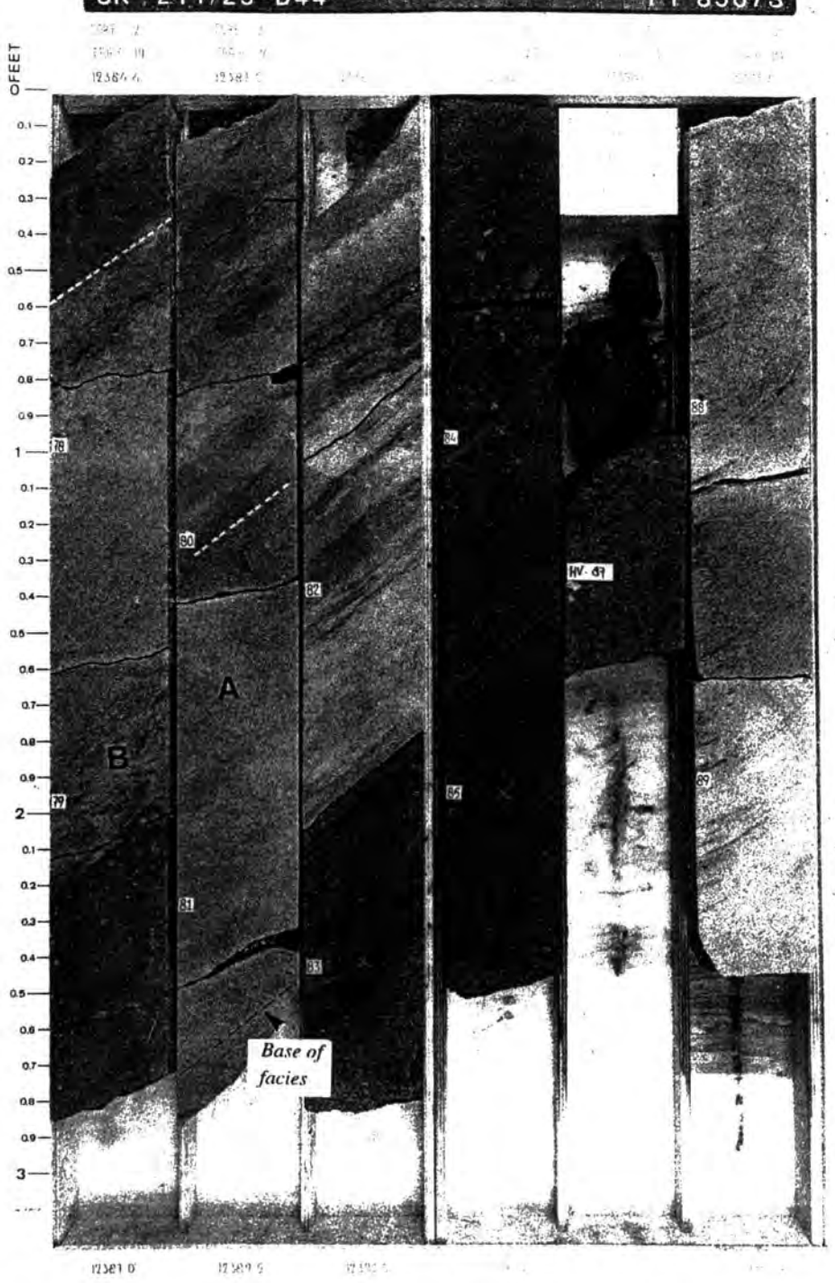

Appendix 9. Core photographs from 12389.5 ft to 12372 ft in the core section of well BD/44 illustrating a second example of levee facies (See text for details).

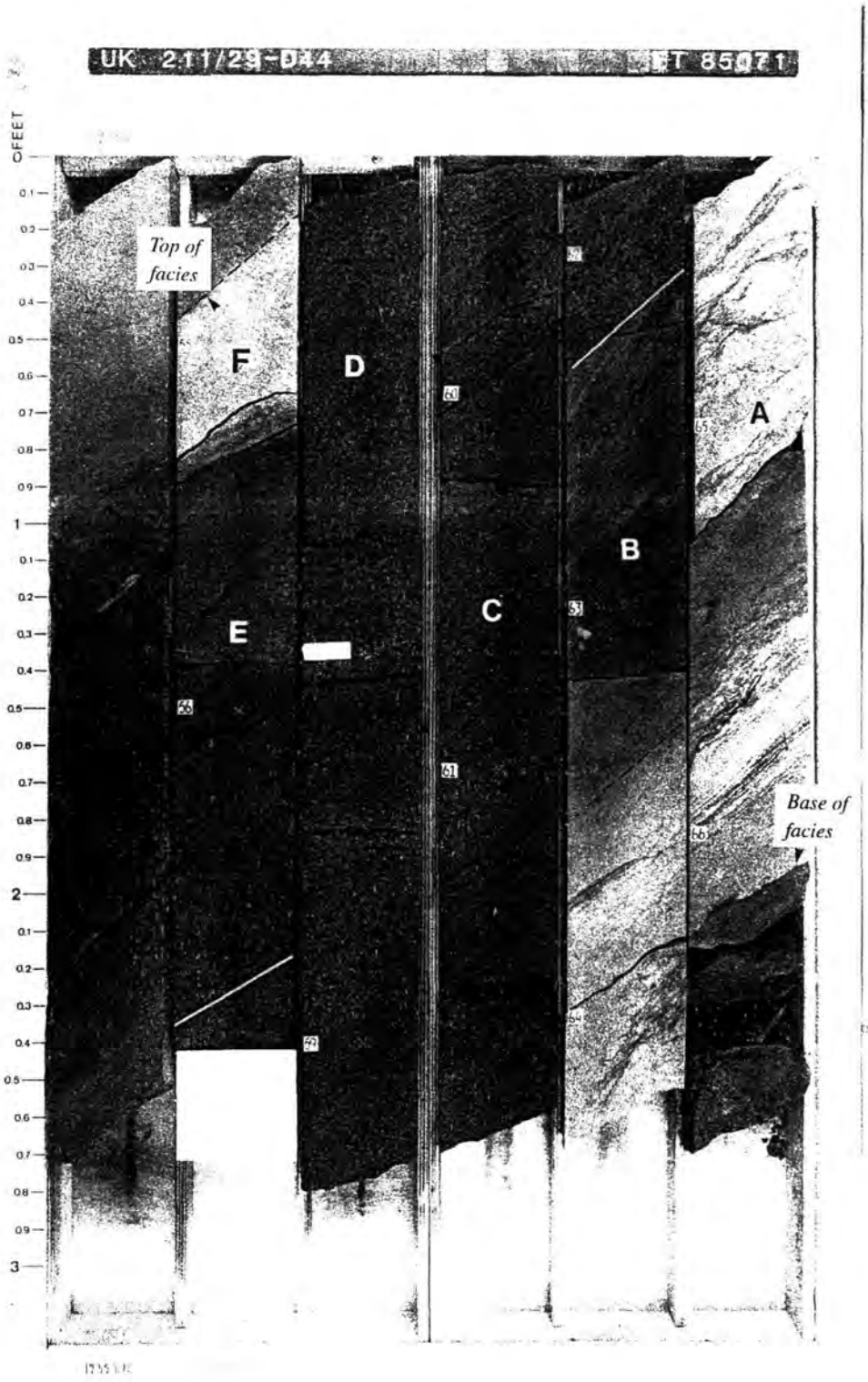

Appendix 10. Photograph in the cored section of well BD/44 in the depth interval from 12370 ft to 12358.5 ft illusrating an example of crevasse splay facies. Units A, B, C and D represent splay lobe progradation followed by gradual abandonment (units E and F). See text for details.

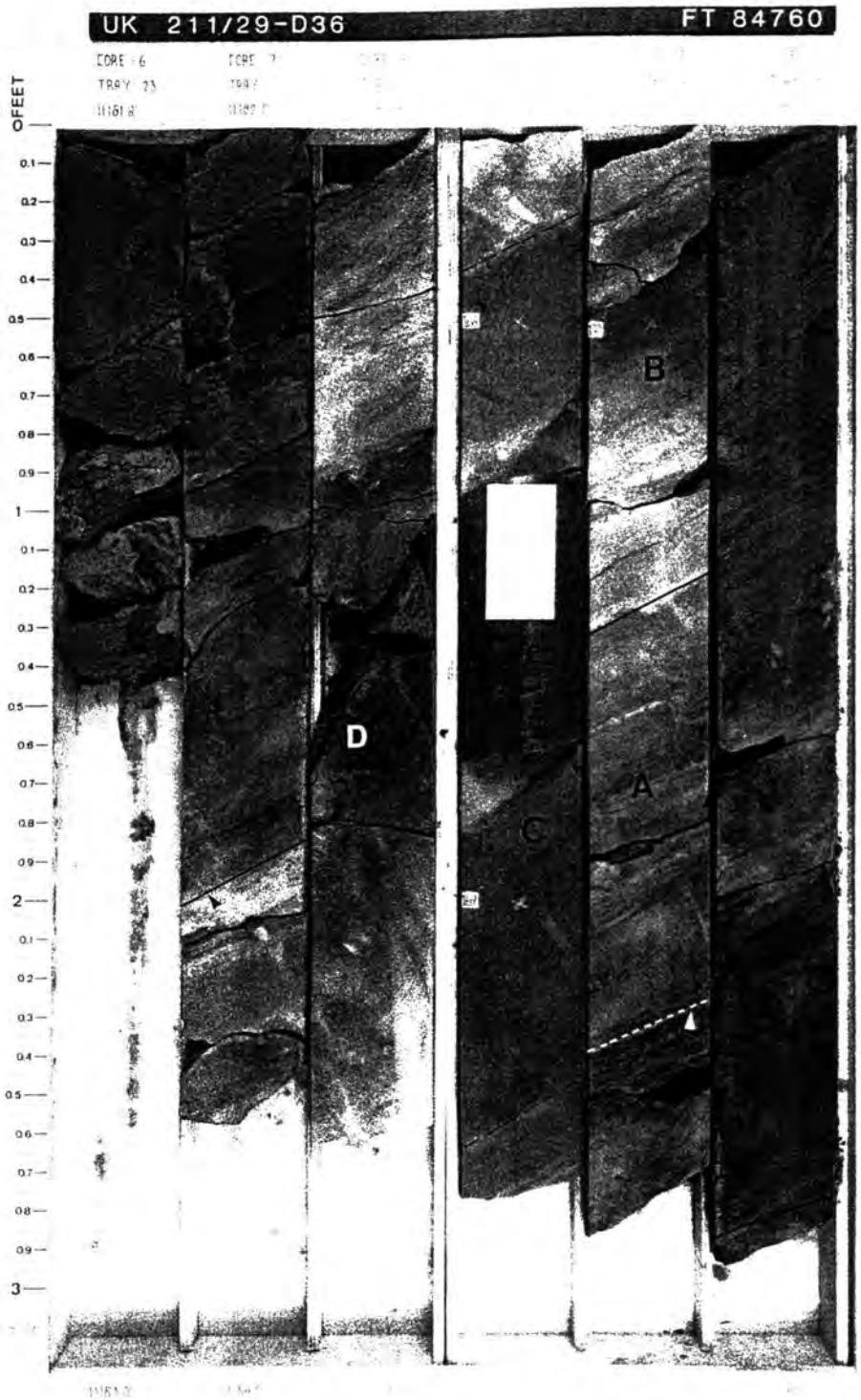

Appendix 11. Core photograph in well BD/36 cored section between 11192 ft and 11184 ft illustrating another example of crevasse splay facies.

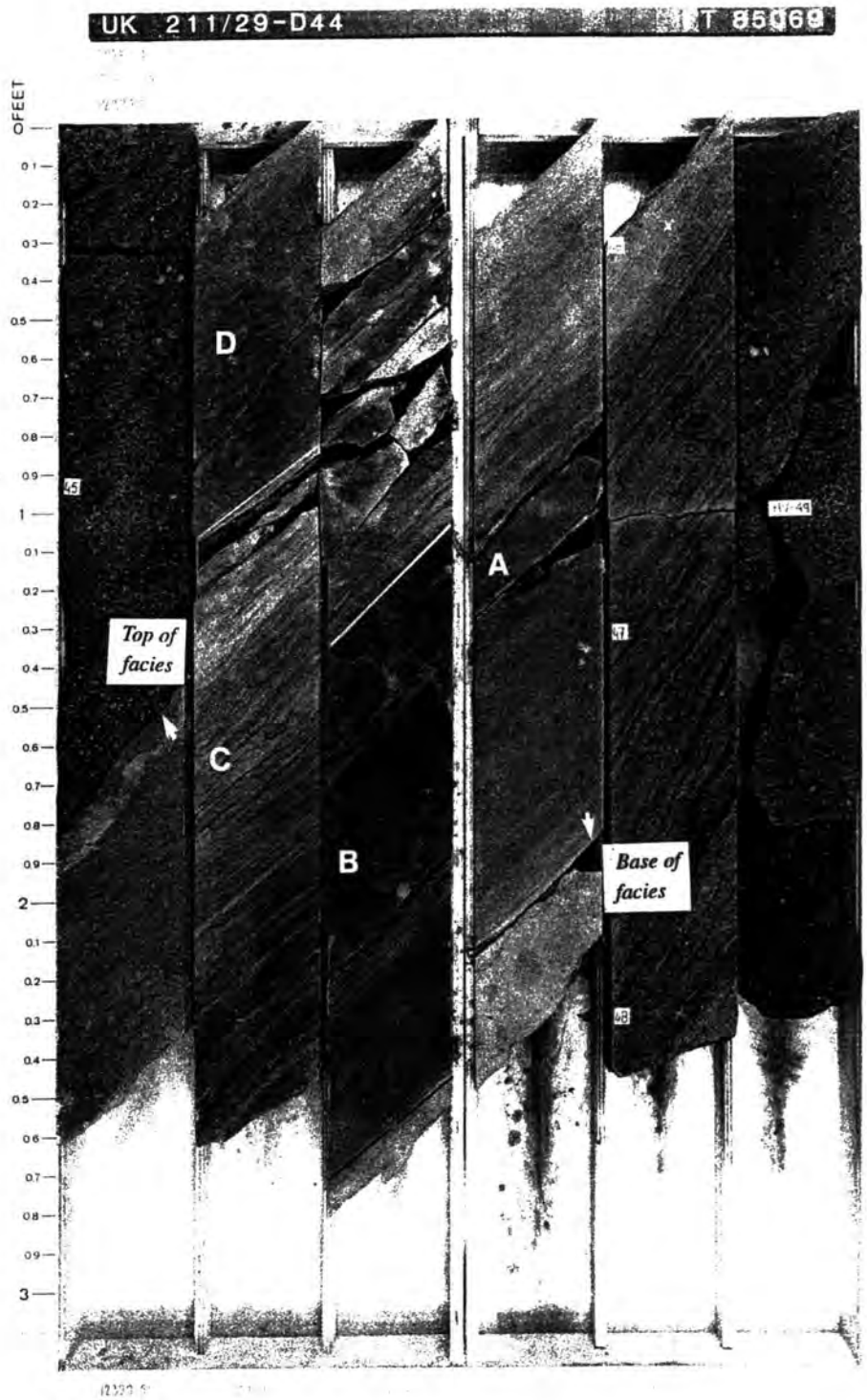

Appendix 12. Core photograph in well BD/44 from 12336 ft to 12328.5 ft illustrating an example of lacustrine facies. See text for details.

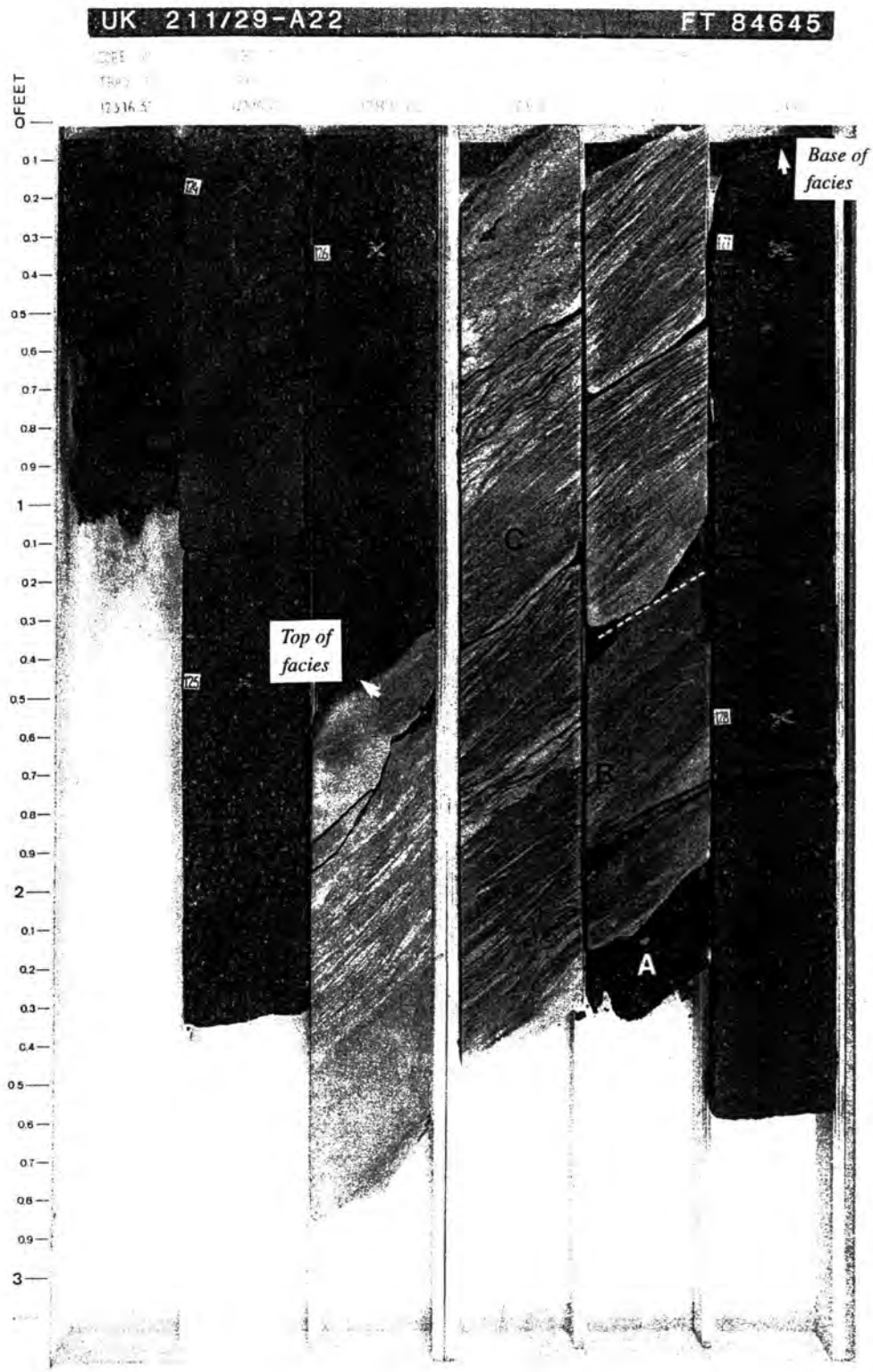

Appendix 13. Photograph in well BA/22 cored section from 12387.7 ft to 12382 ft illustrating another example of lacustrine facies. See text for details.

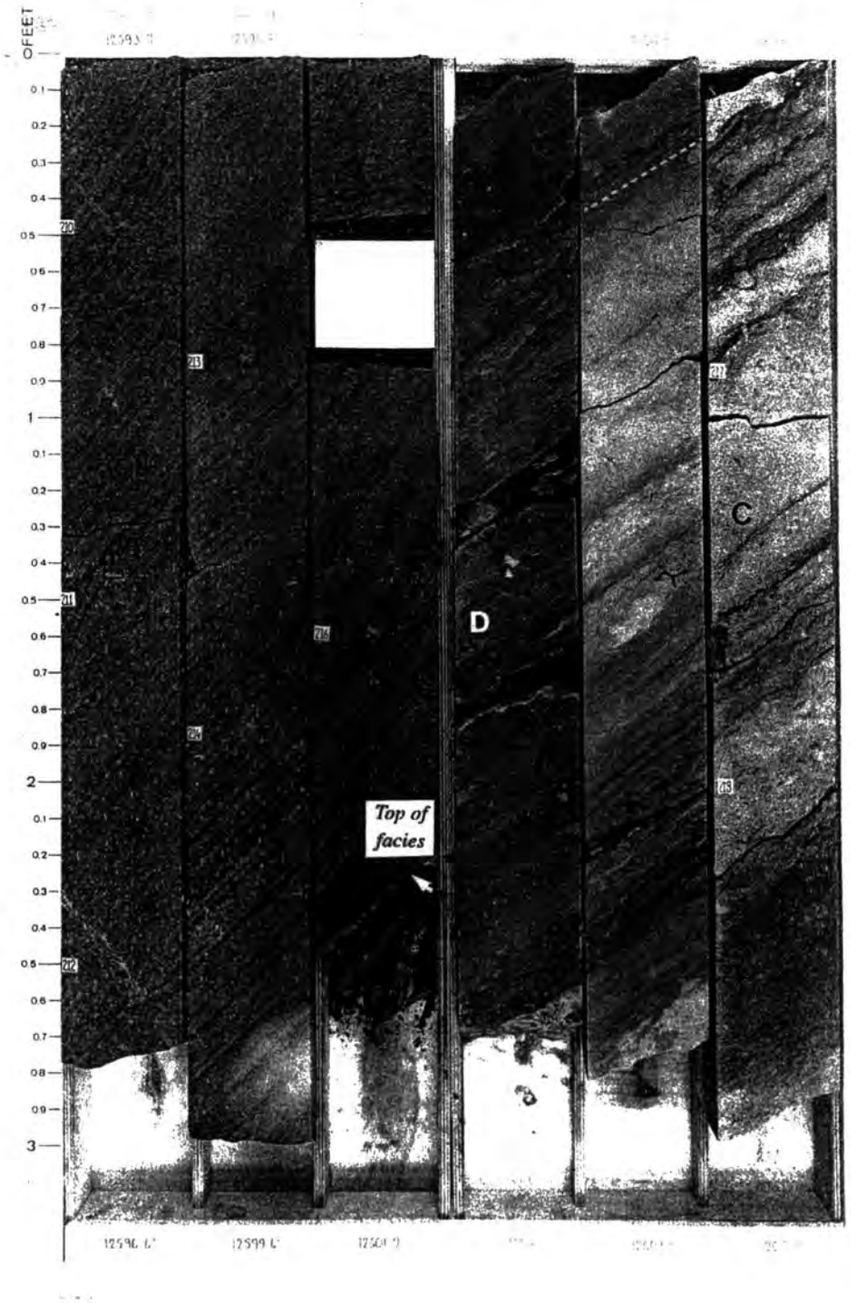

Appendix 14. Core photographs in the depth interval between 12613.3 ft and 12601.8 ft in well BD/44 showing swamp facies. See text for details.

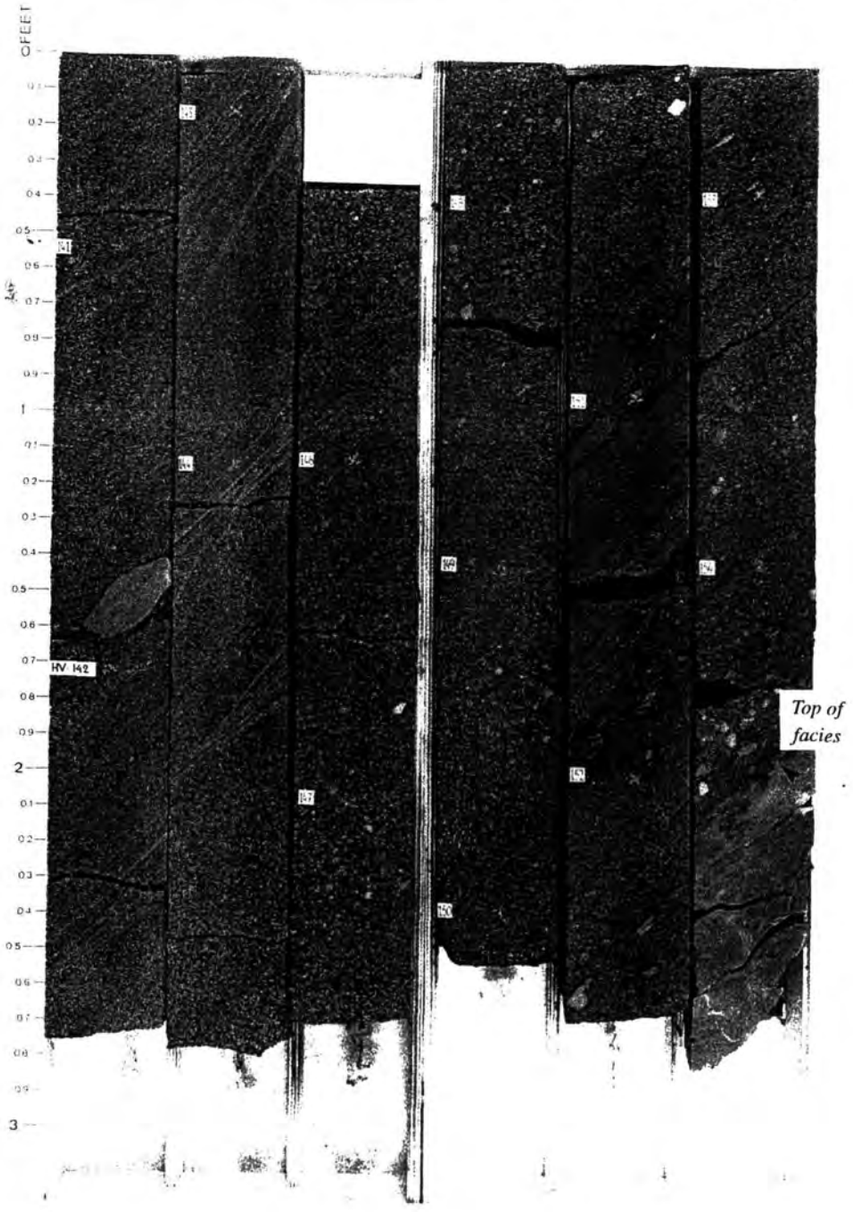

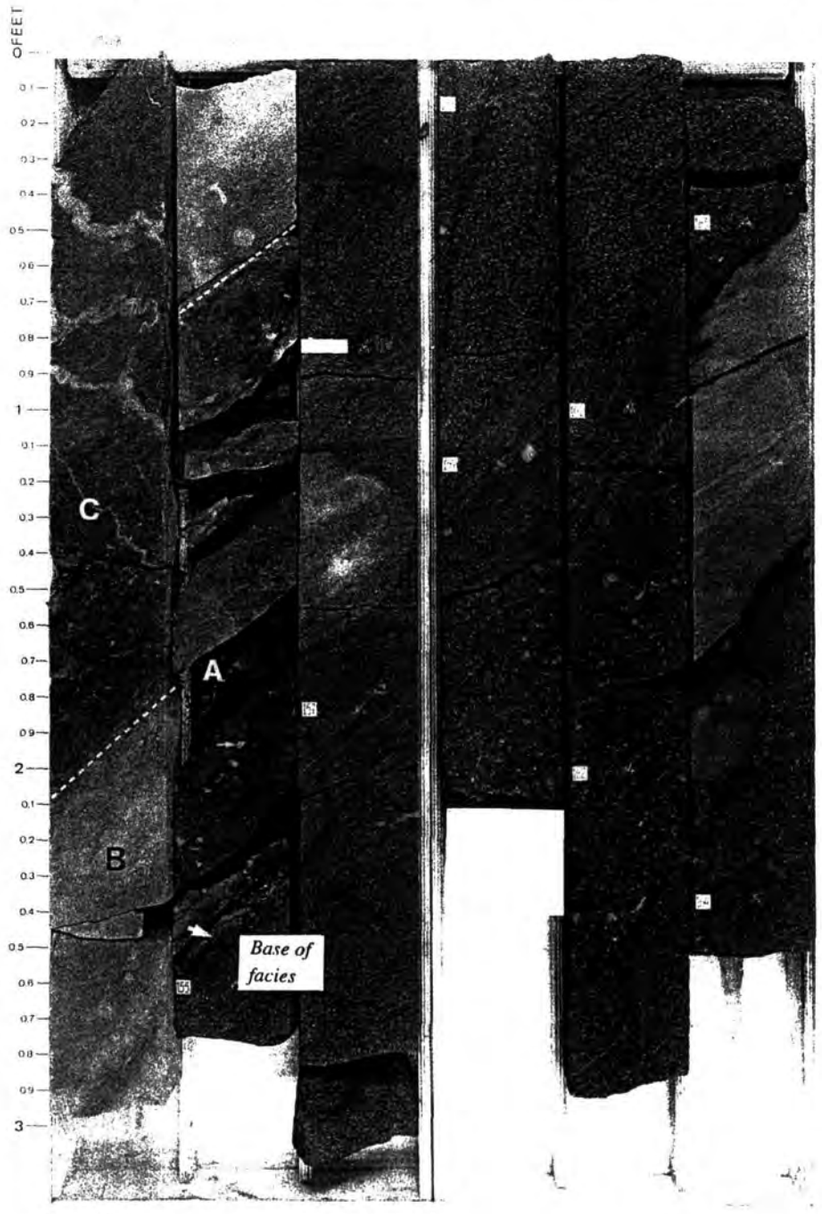

Appendix 15. Core photographs in well BD/44 from 12495.5 ft to 12489.5 ft illustrating a second example of swamp facies. See text for details.

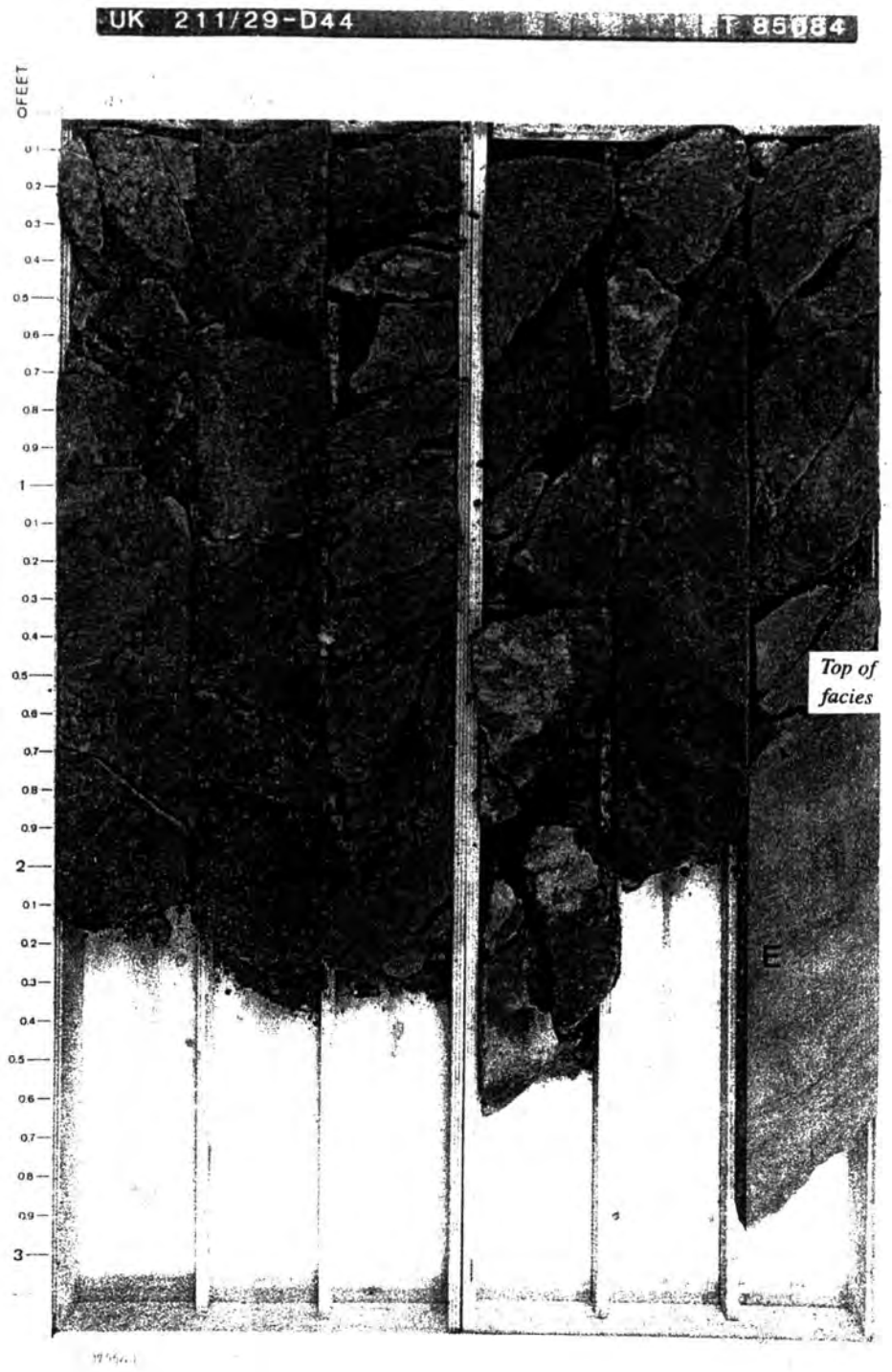

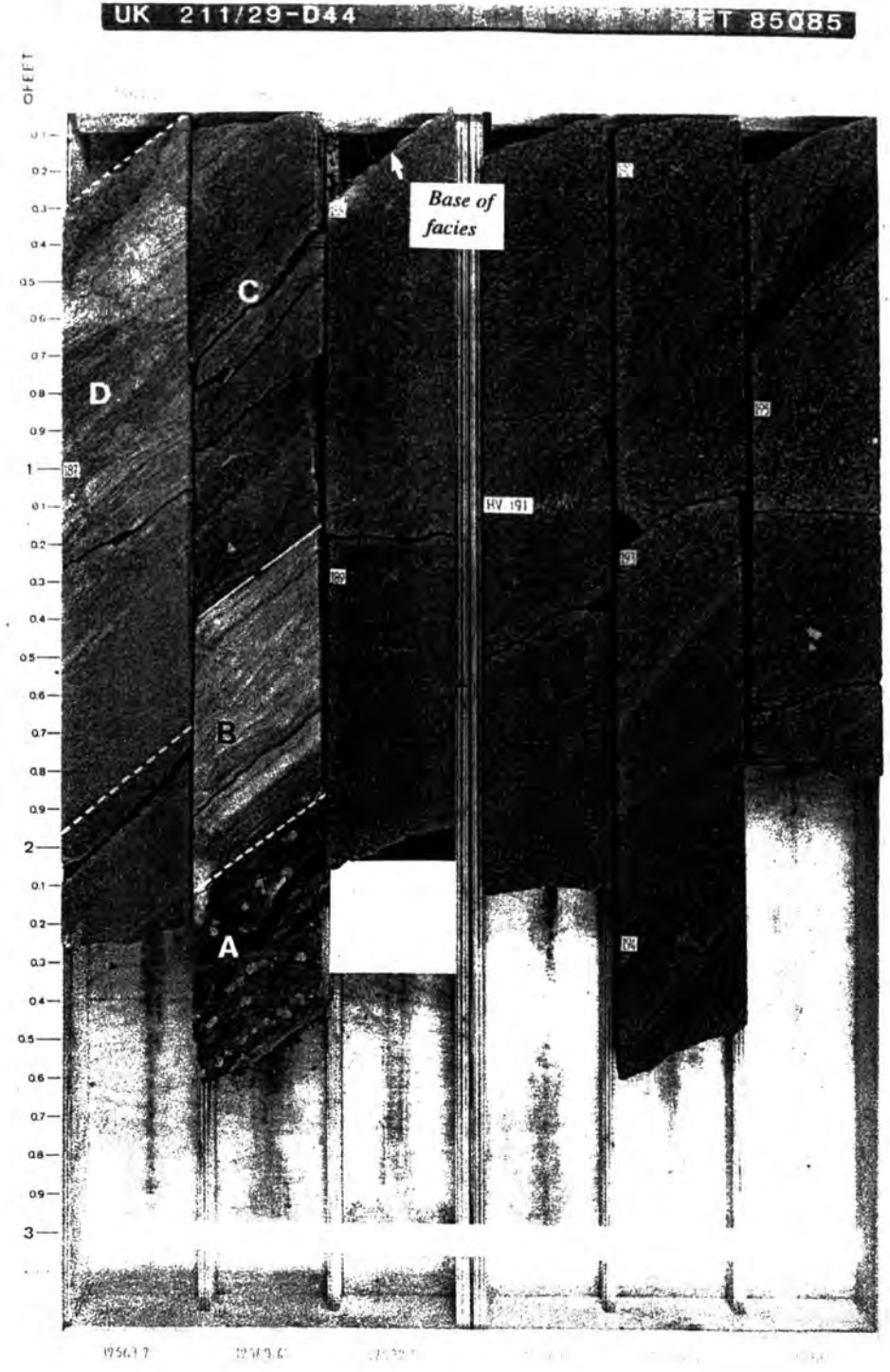

Appendix 16. Core photographs in the cored section of well BD/44

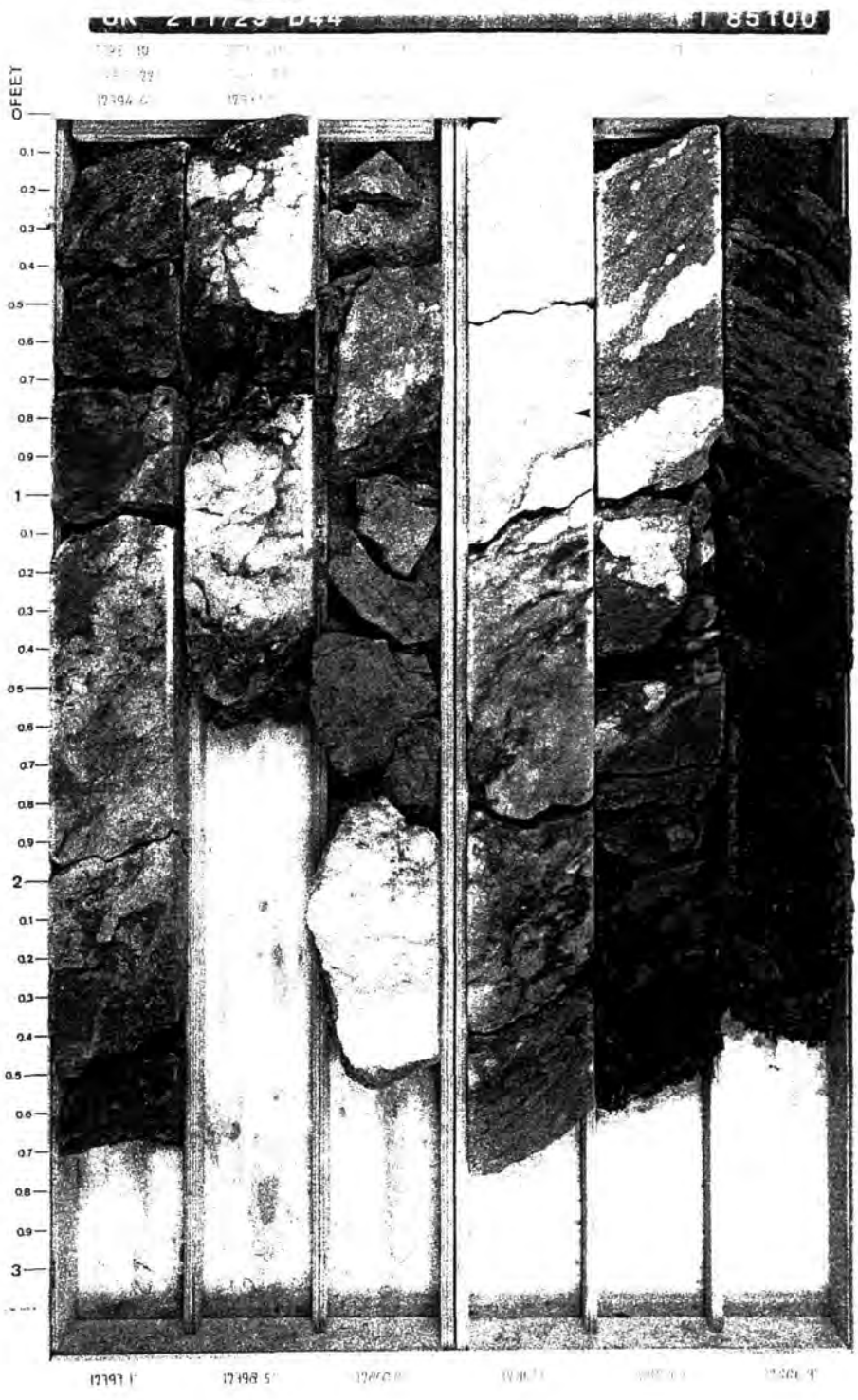

Appendix 17. Core photograph in the cored section of well BD/44 illustrating an example of well-drained flood plain facies. Arrow in the middle of the photo indicates carbonate concretion.

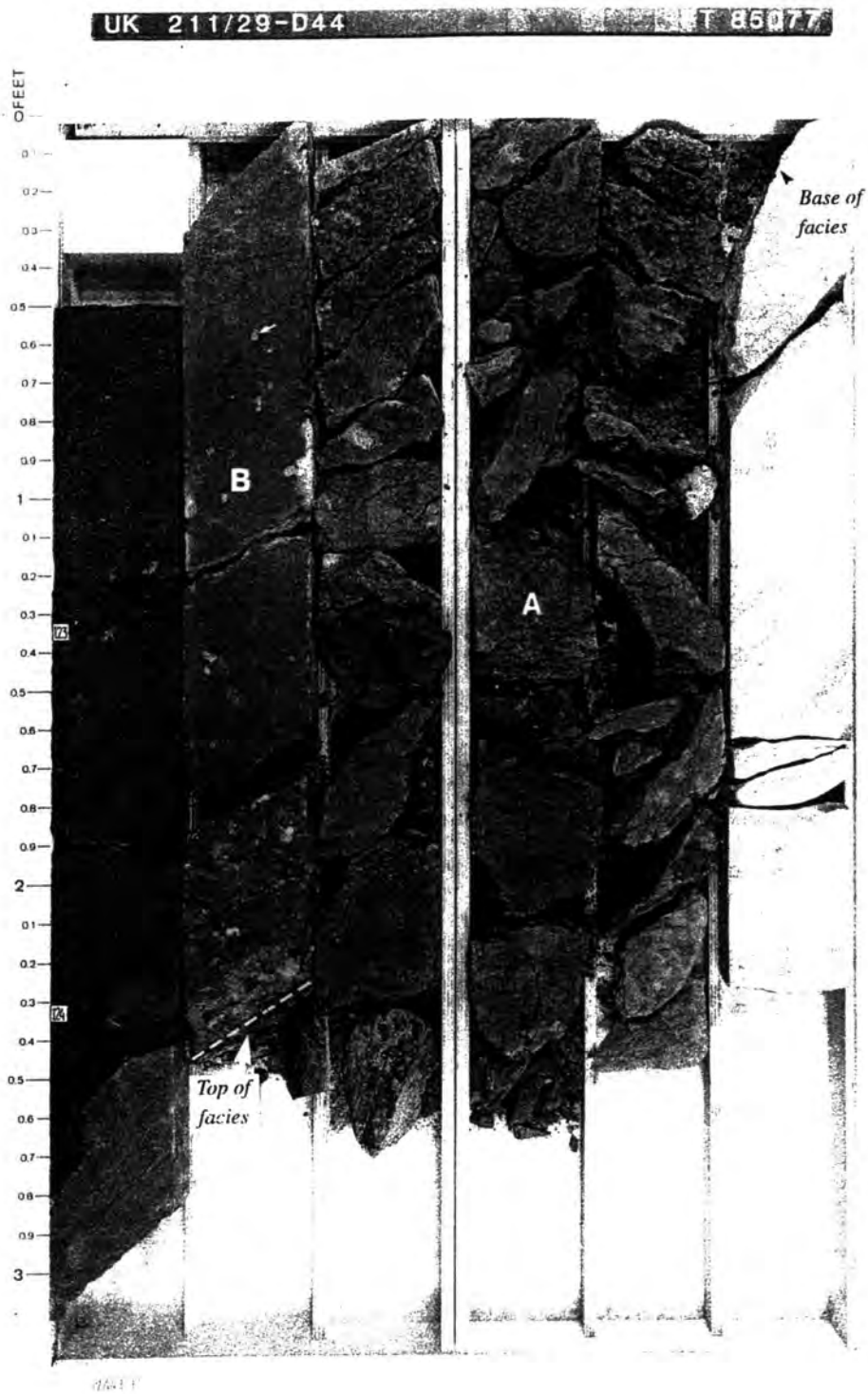

Appendix 18. Photograph in the cored section of well BD/44 showing an example of poorly-drained flood plain facies. See text for details.

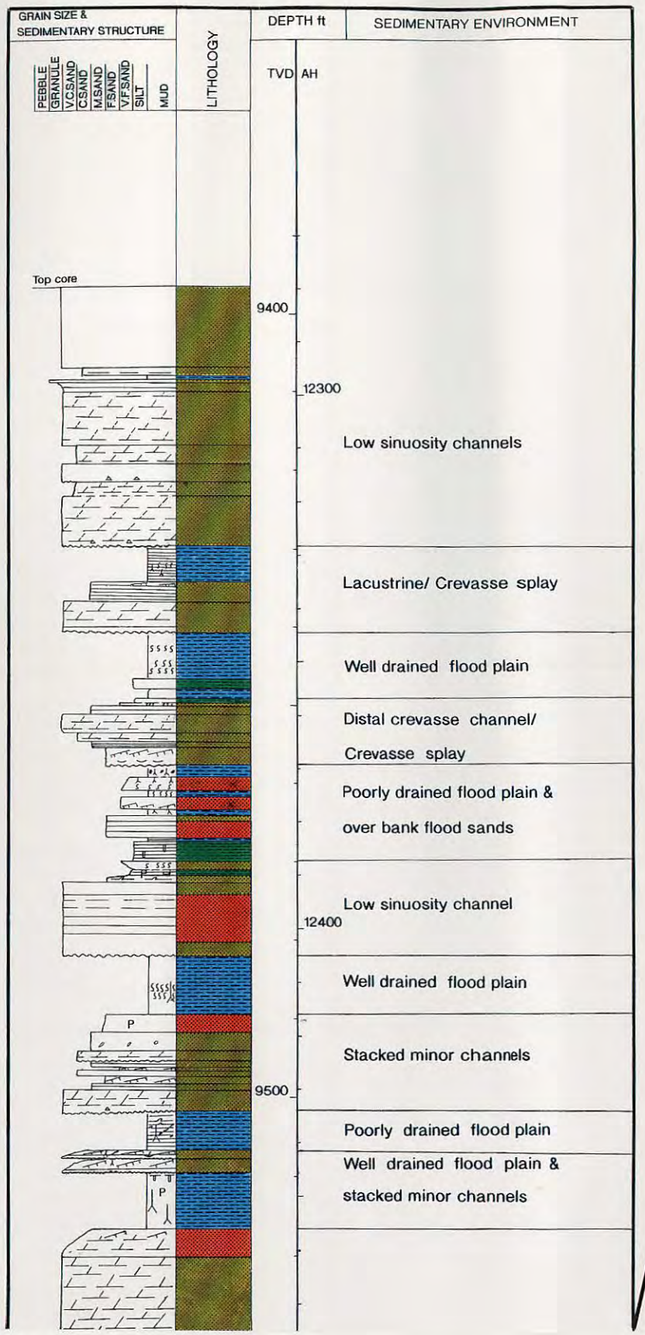

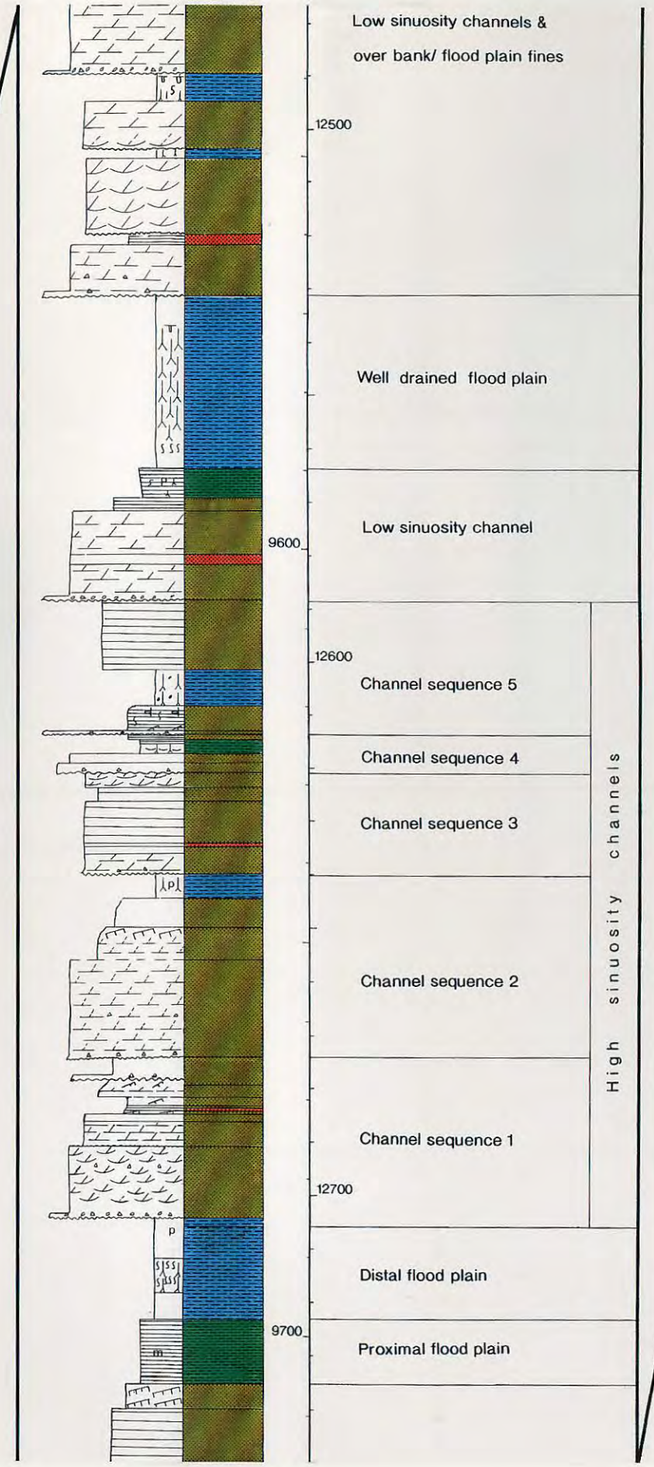

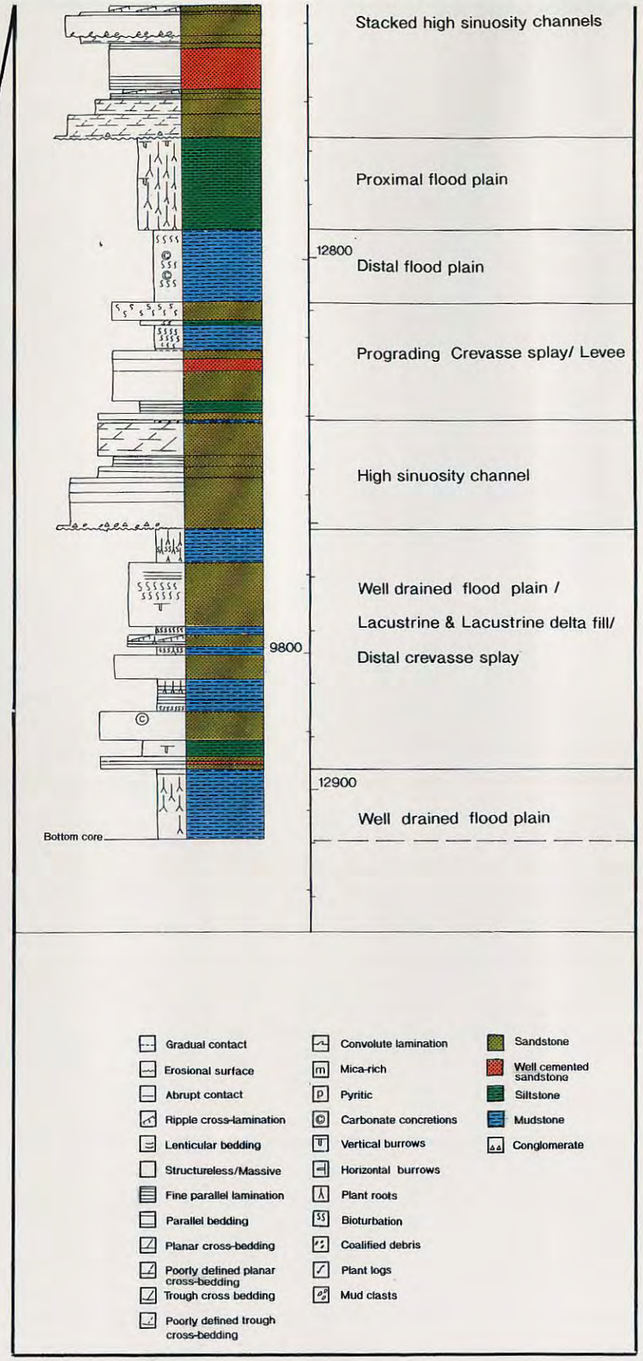

Appendix 19 Lithological log of the cored section of well BD/44, Brent Field.

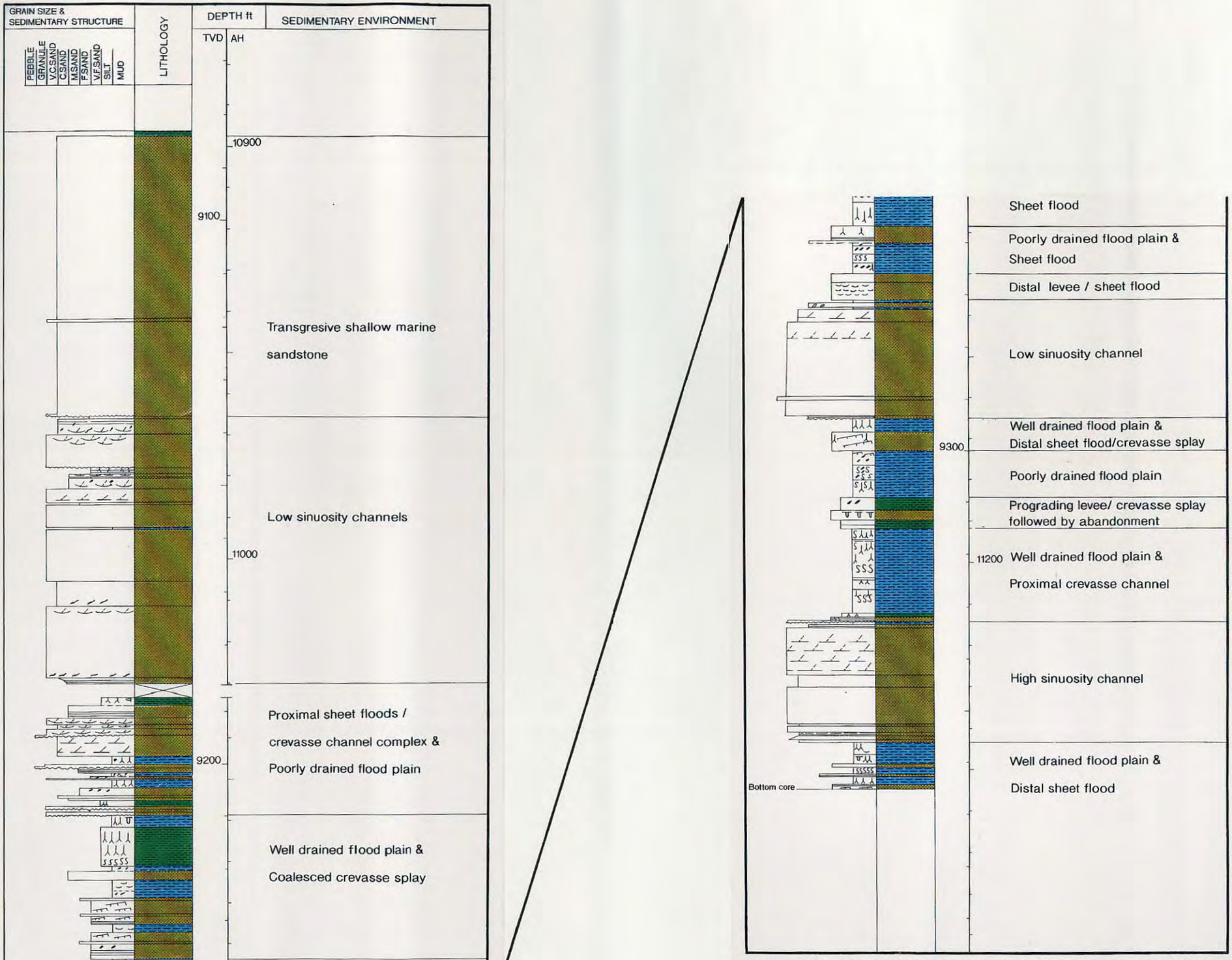

Appendix 20 Lithological log of the cored section of well BD/36. See Appendix 19 for index.

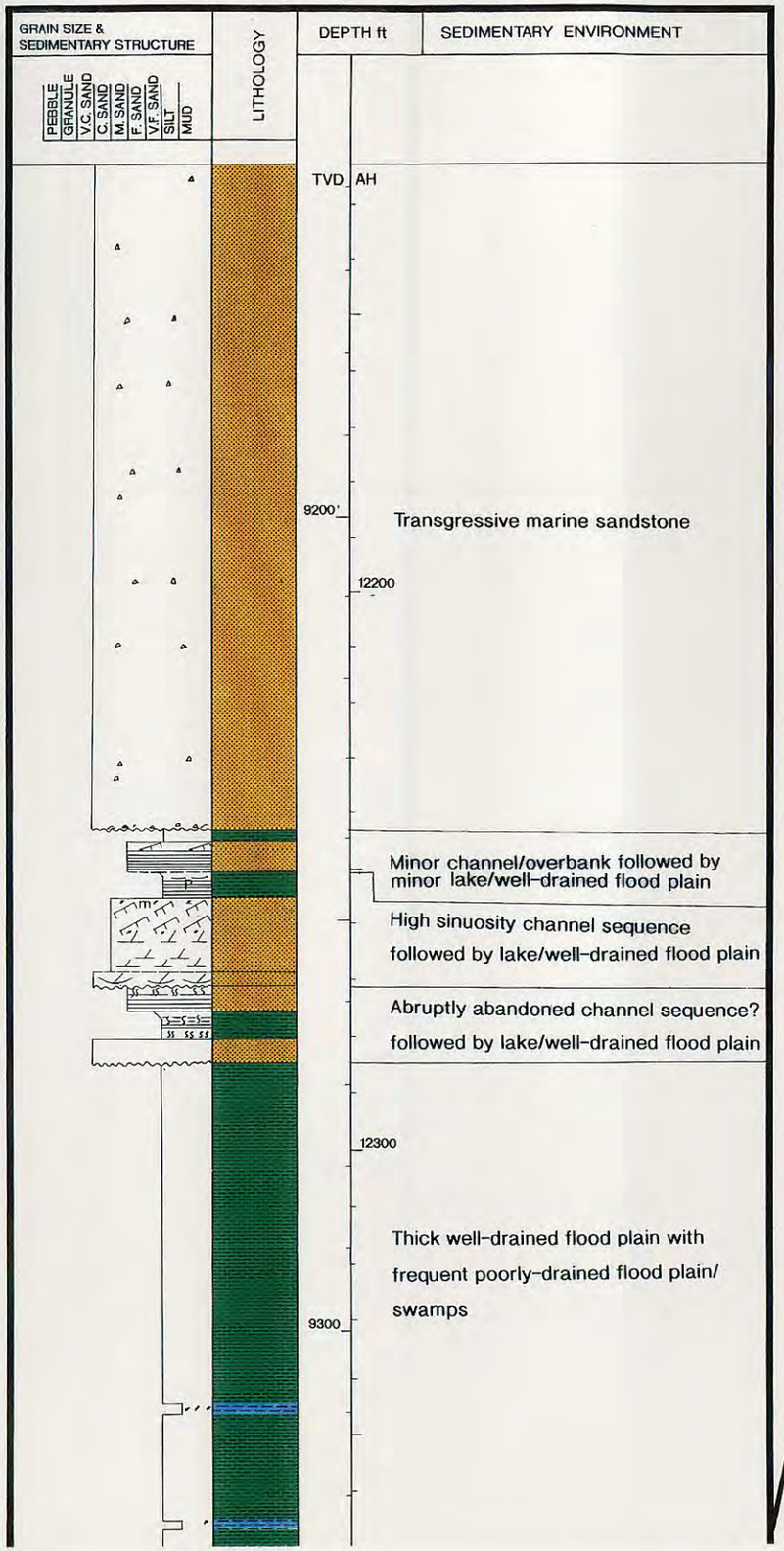

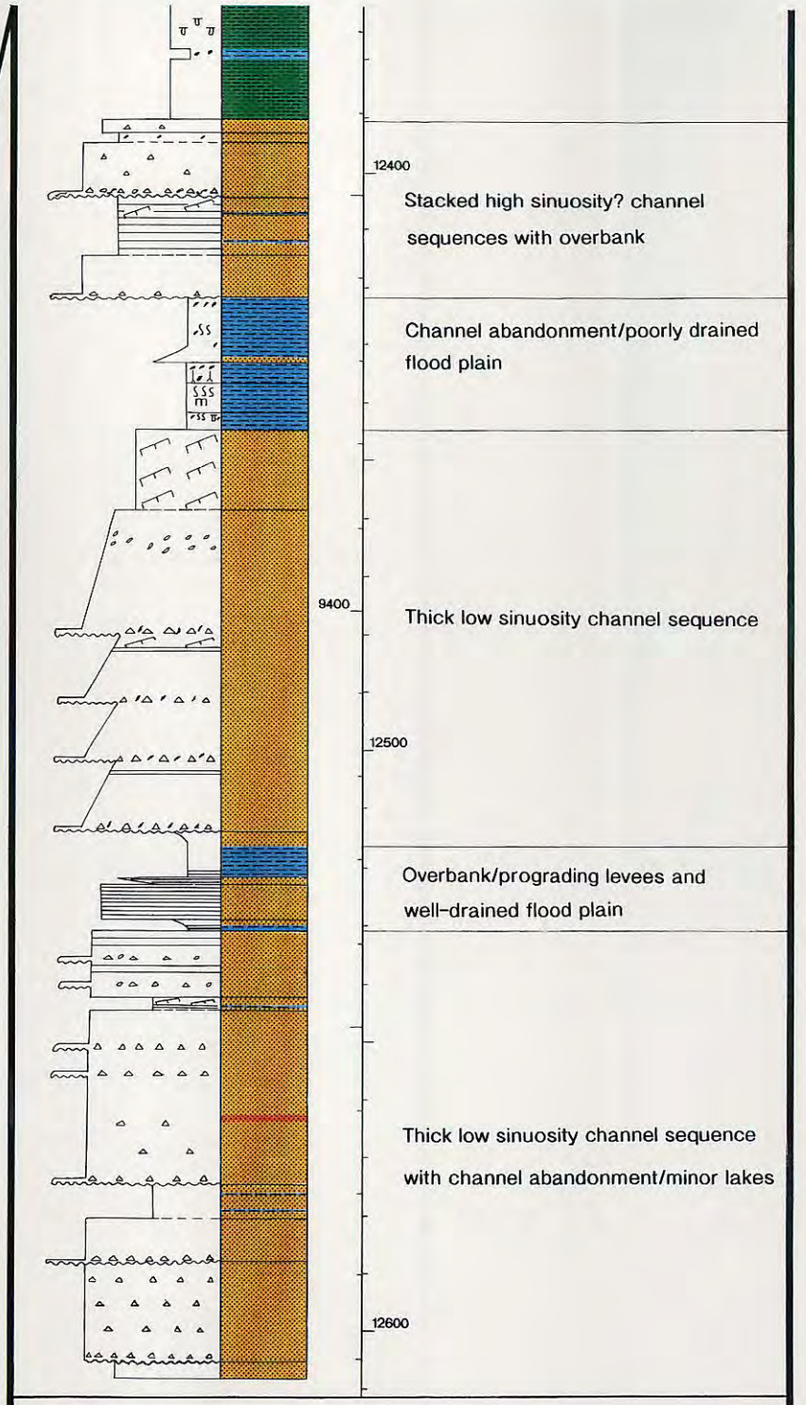

Appendix 21 Lithological log of the cored section of well BA/22. See Appendix 19 for index.

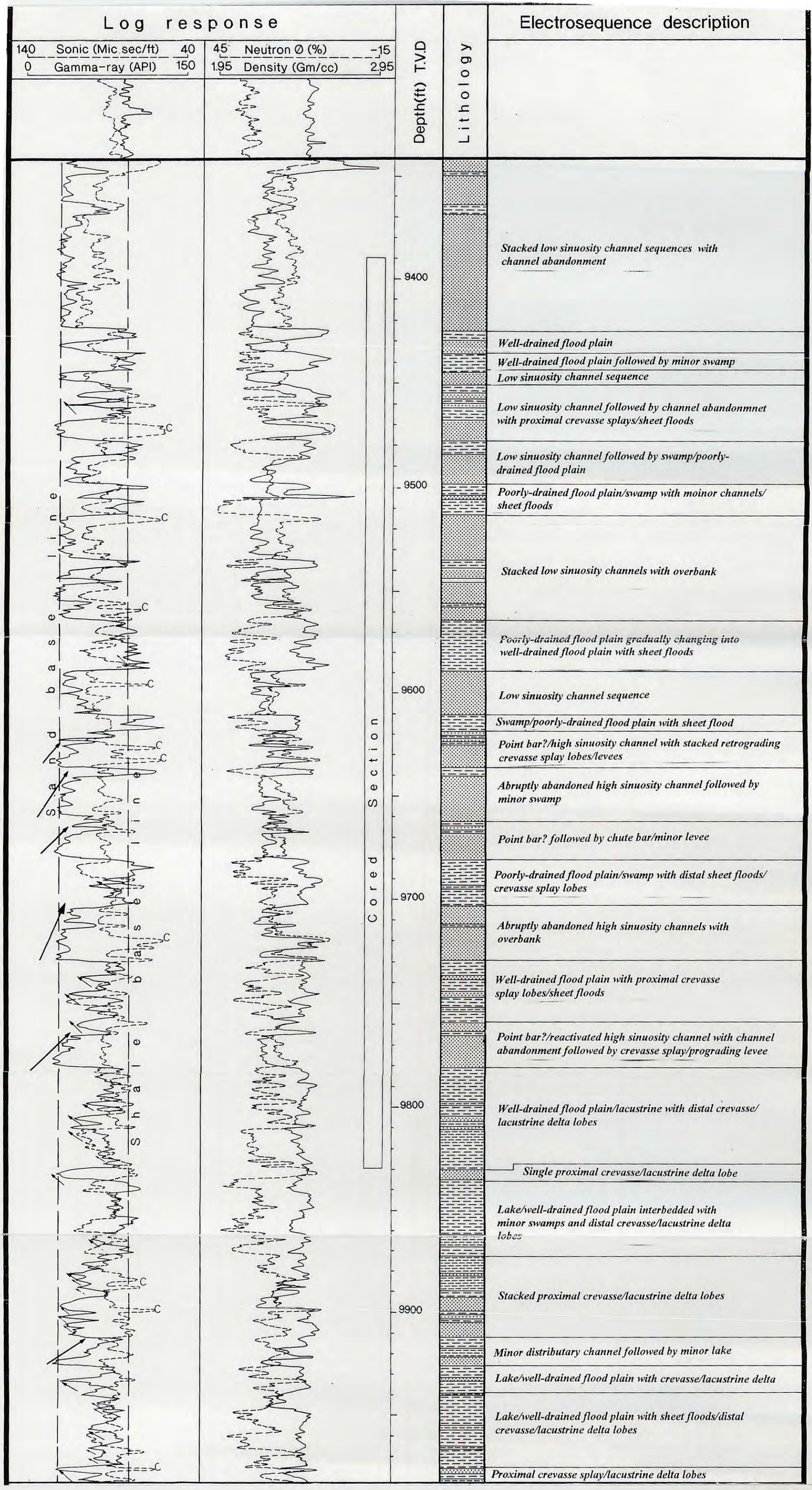

Index

Sandstone

Very fine sandstone/siltstone

Mudstone

C Well cemented sandstone

Coarsening-upward sequence

Fining-upward sequence

Appendix 22. Log-derived sedimentary facies interpretation of well BD/44 Brent Field.
Well cemented sandstone levels (c) have no sedimentological implications.

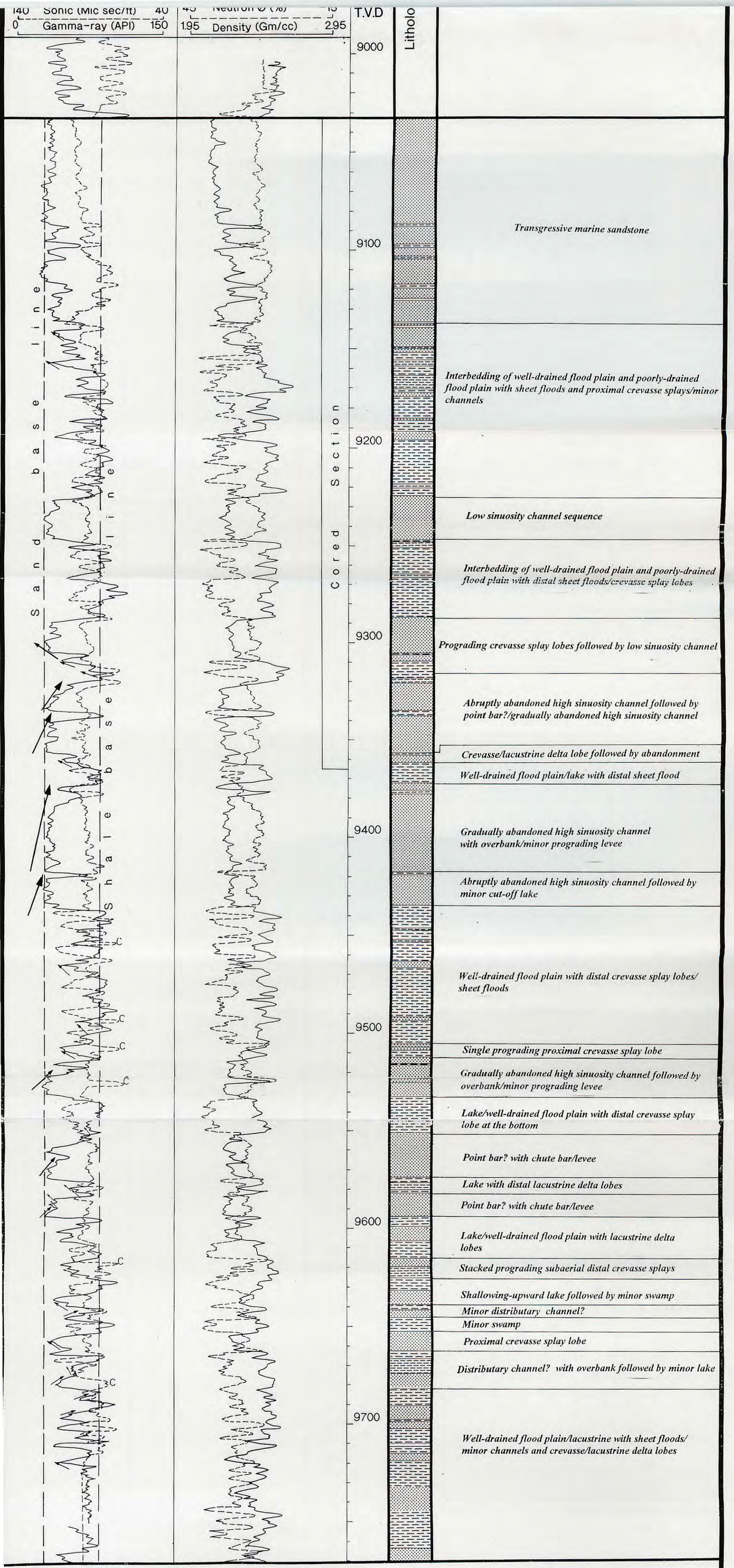

Appendix 23

Log-derived sedimentary facies interpretation of well BD/36. Well cemented sandstone levels (c) have no sedimentological implications. See Appendix 22 for index.

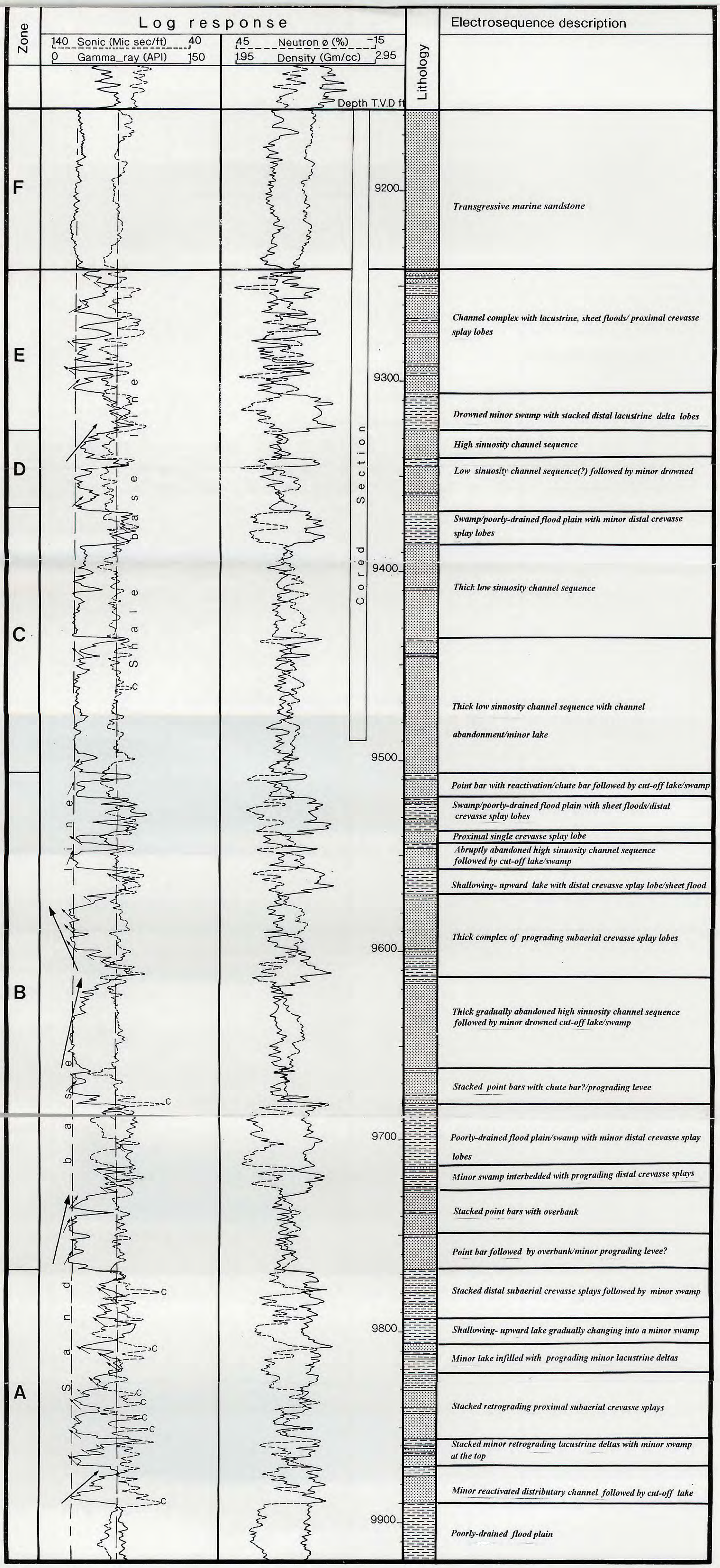

Appendix 24

Log-derived sedimentary facies interpretation of well BA/22. Well cemented sandstone levels (c) have no sedimentological implications, zones refer to systems tracts (See Chapter 4 for details). See Appendix 22 for index.